



National Library
of Canada

Acquisitions and
Bibliographic Services Branch

395 Wellington Street
Ottawa, Ontario
K1A 0N4

Bibliothèque nationale
du Canada

Direction des acquisitions et
des services bibliographiques

395, rue Wellington
Ottawa (Ontario)
K1A 0N4

Your file *Votre référence*

Our file *Notre référence*

NOTICE

The quality of this microform is heavily dependent upon the quality of the original thesis submitted for microfilming. Every effort has been made to ensure the highest quality of reproduction possible.

If pages are missing, contact the university which granted the degree.

Some pages may have indistinct print especially if the original pages were typed with a poor typewriter ribbon or if the university sent us an inferior photocopy.

Reproduction in full or in part of this microform is governed by the Canadian Copyright Act, R.S.C. 1970, c. C-30, and subsequent amendments.

AVIS

La qualité de cette microforme dépend grandement de la qualité de la thèse soumise au microfilmage. Nous avons tout fait pour assurer une qualité supérieure de reproduction.

S'il manque des pages, veuillez communiquer avec l'université qui a conféré le grade.

La qualité d'impression de certaines pages peut laisser à désirer, surtout si les pages originales ont été dactylographiées à l'aide d'un ruban usé ou si l'université nous a fait parvenir une photocopie de qualité inférieure.

La reproduction, même partielle, de cette microforme est soumise à la Loi canadienne sur le droit d'auteur, SRC 1970, c. C-30, et ses amendements subséquents.

Canada

**RECHARGE AND REGIONAL CIRCULATION OF THERMAL GROUNDWATER IN
NORTHERN JORDAN USING ISOTOPE GEOCHEMISTRY**

by

William T. Bajjali

A thesis submitted to the School of Graduate Studies and Research
in Partial fulfilment of the requirements for the degree of Ph.D., Earth Sciences

University of Ottawa

Ottawa-Carleton Geoscience Centre

Department of Geology

University of Ottawa



National Library
of Canada

Acquisitions and
Bibliographic Services Branch

395 Wellington Street
Ottawa, Ontario
K1A 0N4

Bibliothèque nationale
du Canada

Direction des acquisitions et
des services bibliographiques

395, rue Wellington
Ottawa (Ontario)
K1A 0N4

Your file *Votre référence*

Our file *Notre référence*

THE AUTHOR HAS GRANTED AN
IRREVOCABLE NON-EXCLUSIVE
LICENCE ALLOWING THE NATIONAL
LIBRARY OF CANADA TO
REPRODUCE, LOAN, DISTRIBUTE OR
SELL COPIES OF HIS/HER THESIS BY
ANY MEANS AND IN ANY FORM OR
FORMAT, MAKING THIS THESIS
AVAILABLE TO INTERESTED
PERSONS.

L'AUTEUR A ACCORDE UNE LICENCE
IRREVOCABLE ET NON EXCLUSIVE
PERMETTANT A LA BIBLIOTHEQUE
NATIONALE DU CANADA DE
REPRODUIRE, PRETER, DISTRIBUER
OU VENDRE DES COPIES DE SA
THESE DE QUELQUE MANIERE ET
SOUS QUELQUE FORME QUE CE SOIT
POUR METTRE DES EXEMPLAIRES DE
CETTE THESE A LA DISPOSITION DES
PERSONNE INTERESSEES.

THE AUTHOR RETAINS OWNERSHIP
OF THE COPYRIGHT IN HIS/HER
THESIS. NEITHER THE THESIS NOR
SUBSTANTIAL EXTRACTS FROM IT
MAY BE PRINTED OR OTHERWISE
REPRODUCED WITHOUT HIS/HER
PERMISSION.

L'AUTEUR CONSERVE LA PROPRIETE
DU DROIT D'AUTEUR QUI PROTEGE
SA THESE. NI LA THESE NI DES
EXTRAITS SUBSTANTIELS DE CELLE-
CI NE DOIVENT ETRE IMPRIMES OU
AUTREMENT REPRODUITS SANS SON
AUTORISATION.

ISBN 0-612-00575-5

Canada



UNIVERSITÉ D'OTTAWA
UNIVERSITY OF OTTAWA

ABSTRACT

The scarcity of water resources in Jordan poses difficulties for the development of the country and its relationship with its neighbours. Thermal groundwaters recently identified in the northern part of the country represent a 40 MCM/y resources for exploitation to meet the increasing demand for water. These thermal groundwaters are found in three well fields (Mukhebeh, JRV and Ramtha) and were investigated to determine their recharge origin, mean subsurface residence times, and the source of heat. They discharge in the northern part of Jordan Rift Valley and the rifted Yarmouk Valley, which are low elevation (50 to 150 m below sea level) zones of recent tectonism and volcanic activity. The range of temperatures is 30 and 56 °C and salinities vary between 500 and 2500 mg/l. Non-thermal groundwaters within the study area have also been studied. In particular shallow groundwater in adjacent highlands region (Ajloun Mountains) are examined to determine their role in recharge to those regional flow systems.

The principal aquifer is the Upper Cretaceous B2/A7 group, a package of carbonate formations with high kerogen content at depth. This aquifer outcrops in the Ajloun Mountains and flanking regions and is confined by overlying marls in the down gradient regions. A deeper sandstone aquifer underlies the study area and hosts thermal groundwater which was sampled in the Ramtha area.

The major geochemical processes in the subsurface have generated various geochemical facies in the thermal waters. These include carbonate dissolution to calcite saturation in the recharge areas. The thermal groundwater in Mukhebeh and JRV well fields are found to be chemically similar to the carbonate groundwater from Ajloun mountains recharge area. All

thermal waters are characterized by sulphate reduction, driven by oxidation of kerogen. Sulphate is of marine evaporite origin dissolved from within the aquifer with a component of volcanogenic sulphur. Some thermal waters have also Na-Cl salinity component related to evaporite dissolution.

The thermal waters are of meteoric provenance, originating as rain falling over the carbonate highlands in Jordan and Syria. The $\delta^{18}\text{O}$ and δD isotopic data show that all thermal groundwaters are largely associated with Eastern Mediterranean Meteoric Water Line, signifying recharge under the climate regime which dominates today in Jordan. The exception is groundwater from the deep sandstone aquifer which is associated with Global Meteoric Water Line, signifying recharge during Pleistocene time. The isotopic composition of groundwater suggests two distinct recharge areas for the Mukhebeh well field: Ajloun Mountains (Jordan) and Mount Hermon (Syria).

The thermal waters are untritiated and have low ^{14}C values of dissolve inorganic carbon (3 to 22 pmc). The ^{14}C values are affected by the subsurface geochemical evolution including (i) carbonate dissolution (ii) sulphate reduction and (iii) incorporation of mantle CO_2 in the rift zone. A sequential geochemical model was developed to correct the initial ^{14}C value for these processes. Age estimates so corrected fall in a range between 5 and 17 Ka B.P. These values are in agreement with the stable isotope ($^{18}\text{O}/^2\text{H}$) data which indicate dominantly Holocene recharge. The ^{36}Cl supports the ^{14}C data that the circulation time for some thermal waters is relatively short.

In Mukhebeh, isothermal groundwater discharging from different depths suggests a strongly fault controlled discharge zone. Local variation in temperature may be attributable to variation in the geothermal gradient related to local igneous activity. The water temperature in the Ramtha and JRV well fields are dictated by the regional geothermal gradient.

ACKNOWLEDGMENTS

Great thanks and appreciation to my supervisors Dr. Ian Clark and Dr. Peter Fritz for their invaluable guidance, encouragement, and critical assessment of all written work. Financial support for this study was provided by Dr. Clark and by a Graduate Scholarship from the University of Ottawa. Special thanks to Dr. Andre Lalonde for his help in extending this scholarship. I am grateful to Mr. George Milton for his patience in reading and editing drafts of my thesis.

I would like to thank the Ministry of Water and Irrigation in Jordan that made this exciting project possible through their support for sampling analysis. My thanks are also extended to my colleagues in the WAJ and Laboratory and Environmental Control in Water Authority of Jordan, Dr. Raja Gedeon, Hassan Amro, Mohamad Al-Momani, Suzan Kilani, Faisal Rsheidat, Jamal Jawawdeh, and Hani Attar, for their excellent services for analyses. Special thanks to Gilles St-Jean, Natalie Morisset, John Loop, Jean-Francois Tardif and Edward Hearn at the isotope, chemical and computer laboratories at the University of Ottawa for their help and guidance.

Special thanks for my friends Mark Mihalasky, Yousef Al-Mouji, Bahram Daneshfar, Robert Philips and Morcire Sylla for contributing their artistic talent and good company. Final thanks to my wife Hala, who continuously encouraged and supported our family, and my children Tawfiq and Luai for their love.

**This Thesis is dedicated to my family,
my wife Hala and my children Tawfiq and Luai**

Table of Contents

	page
Abstract	i
Acknowledgments	iii
Dedication	iv
Table of Contents	v
List of Figures	x
List of Tables	xii
Chapter I The Strategic Importance of Groundwater	1
I-1 Introduction	1
I-2 Previous Studies	7
I-3 Objectives of the Research	14
Chapter II Approach to Solve the Problems	15
II-1 Methodology	15
II-2 Field Sampling Program	15
II-3 Analytical Methods	16
II-4 General Review of Environmental Isotopes	19
II-4.1 Stable Environmental Isotopes	19
II-4.2 Radioactive Environmental Isotopes	22
II-5 Radiocarbon Correction Techniques	25

Chapter III Geology and Hydrogeology of the Study Area	29
III-1 Physiography and Drainage	29
III-2 Climate	31
III-3 Soil Types and Vegetation	35
III-4 Geology and Groundwater Flow Systems	36
III-4.1 Aptian-Albian (Kurnub)	38
III-4.2 Cenomanian to Toronian - Ajloun Group	42
III-4.3 Santonian to Eocene - Balqa Group	44
III-4.4 The B2/A7 Aquifer	46
III-4.5 Oligocene to Helocene	47
III-5 Structural Geology	49
III-5.1 Jordan Rift Valley	49
III-5.2 Ajloun Dome	51
III-5.3 Ramtha - Wadi Sarhan Fault	52
Chapter IV Precipitation and Surface Water	53
IV-1 Precipitation	53
IV-1.1 Chemical Composition of Precipitation	54
IV-1.2 Isotopic Composition of Precipitation	56
IV-1.3 Tritium Concentration in Precipitation	66
IV-2 Surface Water	67
IV-2.1 Isotopic and chemical characteristic of Yarmouk River	68

Chapter V Non-Thermal Groundwater	73
V-1 Nualmeh Area	74
V-1.1 Recharge Estimation	78
V-1.2 Hydrochemistry of Groundwater	78
V-1.3 Isotopic Composition of Groundwater	83
V-1.4 Radioactive Isotope of Groundwater	85
V-2 Side Wadies Area	88
V-2.1 Phreatic aquifer	90
V-2.1.1 Hydrochemistry of Groundwater	90
V-2.1.2 Isotopic Composition of Groundwater	93
V-2.1.3 Radioactive Isotope of Groundwater	95
V-2.2 Confined Aquifer: (Wadi Al-Arab Well Field)	98
V-2.2.1 Hydrochemistry of Groundwater	99
V-2.2.2 Isotopic Composition of Groundwater	103
V-2.2.3 Radioactive Isotopes of Groundwater	105
V-3 Adasyfa Area	107
V-3.1 Hydrochemistry of Groundwater	108
V-3.2 Isotopic Composition of Groundwater	111
V-3.3 Tritium in the Groundwater	114
V-4 Ramtha area	116
V-4.2 Hydrochemistry of Groundwater	118
V-4.3 Isotopic Composition of Groundwater	125

V-4.1	Radioactive Isotope of Groundwater	127
V-5	North-East Desert	130
V-5.1	Hydrochemistry of Groundwater	132
V-5.2	Isotopic Composition of Groundwater	137
V-5.3	Radioactive Isotope of Groundwater	139
V-6	Summary of non-thermal groundwater	140
Chapter VI Thermal Water		141
VI-1	Geothermal Setting in Northern Jordan	141
VI-1.1	Location and Development of Thermal Waters	141
VI-1.2	Groundwater Temperature and Geothermal Gradients	148
VI-1.3	Tectonic Environment	155
VI-2	Hydrochemistry of the Thermal Water	157
VI-2.1	Geochemistry of Mukhebeh Area Groundwater	159
VI-2.1.1	Mukhebeh Wells (No.1 to 7)	161
VI-2.1.2	JRV1 Well and Maqla Spring	161
VI-2.1.3	Redox Conditions	165
VI-2.1.4	Balsam and Hammat Gader - Mixed System	167
VI-2.2	Geochemistry of JRV Area Groundwater	168
VI-2.3	Geochemistry of Ramtha Area Groundwater	170
VI-2.4	General Discussion	170
VI-2.5	Temperature Calculation by Different Geothermometers	173

VI-3	Origin of the Recharge of the Thermal Waters	178
VI-3.1	Stable Isotope of Thermal Waters	178
VI-3.1.1	Mukhebeh and JRV Groundwater	178
VI-3.1.1.1	Recharge Elevations and Regions	180
VI-3.1.2	Palaeowater for the Ramtha Area	185
VI-4	Origin of Salinity and Sulphate Reduction	187
VI-5	Mean Residence Time of Groundwater	194
VI-5.1	Tritium	194
VI-5.2	Carbon-14	195
VI-5.2.1	Radioactive Dating-Controls on the Input Function (A_0)	198
VI-5.2.2	Radiocarbon Activities in Recharge Waters	199
VI-5.3	Radiocarbon Ages of Thermal Groundwaters	203
VI-5.3.1	^{14}C Activity and $\delta^{13}\text{C}$ in the Thermal Waters	203
VI-5.3.2	Subsequent and ^{14}C Age Correction in Thermal Waters - q_1 and q_2	207
VI-6	Chloride-36 (^{36}Cl)	213
Chapter VII Summary, Conclusions and Recommendations		217
References		223
Appendix A		245
Appendix 1		246
Appendix 2		248
Appendix 3		250

List of Figures

I-1	Location Map of Jordan	2
I-2	Location Map of the Study Area	6
I-3	Flow System for the B2/A7 Aquifer of the Study Area	10
III-1	Major Physiographic and Surface Drainage	29
III-2	Rainfall Distribution in Jordan mm/y (Average 50 Years)	33
III-3	Simplified Geological Map of the Northern Part of the Study Area	39
III-3A	Cross Sections Between Zarqa and Yarmouk Rivers	40
III-4	Cross Section for Kurnub Between Jordan and Iraq	41
III-5	Major Structural Features in the Study Area	50
IV-1	$\delta^{18}\text{O}$ - δD Diagram for Precipitation	57
IV-2	Altitude Effect	64
IV-3	$\delta^{18}\text{O}$ - δD Diagram for Yarmouk River	70
IV-4	Chloride - Oxygen-18 Relationship for Yarmouk River	72
V-1.1	Location Map of the Nuaimh Well Field	76
V-1.2	Water Level Fluctuation in Yarmoon Observation Well	77
V-1.3	Fingerprint Diagram for Nuaimh Well Field	80
V-1.4	$\delta^{18}\text{O}$ - δD Diagram for Nuaimh Well Field	84
V-1.5	TDS versus Tritium for Nuaimh Well Field	87
V-2.1	Location Map of the Side Wadies Well Fields	89
V-2.2	Water Level Fluctuation in Kufr Assad Well	91
V-2.3	Fingerprint Diagram for Side Wadies Well Field	94

V-2.4	$\delta^{18}\text{O}$ - δD Diagram for Side Wadies Well Field	96
V-2.5	TDS Versus Chloride of Wadi Al-Arab Well Field	100
V-2.6	$\delta^{18}\text{O}$ - δD Diagram of Wadi Al-Arab Well Field	104
V-3.1	Location Map of the Wells in Adasyia Area	107
V-3.2	Fingerprint Diagram for Adasyia Area	109
V-3.3	$\delta^{18}\text{O}$ - δD Diagram for Adasyia Well Field	113
V-4.1	Location Map of the Wells in Ramtha Area	117
V-4.2	Na^+ - Cl^- Relationship for Ramtha Groundwater	120
V-4.3	$\delta^{18}\text{O}$ - δD Diagram for Ramtha area	126
V-4.4	$\delta^{18}\text{O}$ - TDS for Ramtha area	128
V-5.1	Location Map of the Well Field in NE Desert	130
V-5.2	Water Level Fluctuation in Baej well	133
V-5.3	Na^+ - Cl^- Diagram for NE Desert	135
V-5.4	$\delta^{18}\text{O}$ - δD Diagram for NE Desert	138
VI-1	Location Map of Mukhebeh Area	143
VI-2	Water Level Fluctuation in JRV1 Well	146
VI-3	Depth Versus the Temperature of the Thermal Wells	151
VI-4	Geothermal Gradient Map of Jordan	153
VI-5	Composition Diagram of Thermal Well Fields	160
VI-6	Sodium Versus Chloride (meq/l) of thermal Waters	172
VI-7	$\delta^{18}\text{O}$ - $\delta^2\text{H}$ Diagram for the Thermal Waters	179
VI-8	$\delta^{18}\text{O}$ - $\delta^2\text{H}$ Diagram for Mukhebeh and JRV Well Fields	181

VI-9	Geological Cross Section Between Zarqa River and Hermon Mountains	184
VI-10A	$\delta^{34}\text{SO}_4$ Versus SO_4^{2-}	191
VI-10B	$\delta^{18}\text{O}$ Isotope of SO_4^{2-} Versus $\delta^{18}\text{O}$ of H_2O .	191
VI-11	$\delta^{34}\text{SO}_4^{2-}$ Versus $\delta^{18}\text{SO}_4^{2-}$	193
VI-12	Comparison Between Different Geochemical Models	212

List of Tables

III-1	Average Amount of Rain for the Period 86/92	35
III-2	Litho-Stratigraphic Unit of the Study Area	38
IV-1	Chemical Analyses of Precipitation	55
IV-2	Weighted Mean Value of the Precipitation Isotope	59
IV-3	Regression Line Between $\delta^{18}\text{-}\delta\text{D}$, T vs. $\delta^{18}\text{O}$, and P vs. $\delta^{18}\text{O}$	60
IV-4	Statistical Treatment of the Rainfall Stable Isotope	62
IV-5	Isotope and Chemistry of Yarmouk River and Some Springs	69
V-1.1	Average Chemical Composition of the Groundwater in Nuaimh	79
V-1.2	Ionic Strength, Ratio and Saturation Indexes for Nuaimh Well Field	81
V-2.1	Average Chemical Composition of the Side Wadies Groundwater	92
V-2.2	Ionic Strength and Saturation Indexes of the Side Wadies Groundwater	93
V-2.3	Chemical Average of Wadi-Al-Arab Well Field	101
V-2.4	Chemical Ratios, Ionic Strength, $\text{Log}_{\text{PCO}_2}$ and Saturation Indexes	102
V-3.1	Average Chemical Composition of the Groundwater	110
V-3.2	Chemical Ratios, Ionic Strength, $\text{Log}_{\text{PCO}_2}$ and Saturation Indexes	111

V-4.1	Average Chemical Composition for Ramtha Groundwater	119
V-4.2	Ionic Ratios for Ramtha Groundwater	121
V-4.3	Mixed Ratio Between B2/A7 and B4 Aquifer in Ramtha Area	122
V-4.4	Ionic Strength and Saturation Indexes for Ramtha Groundwaters	124
V-5.1	Average Chemical Composition of the Groundwater	134
V-5.2	Chemical Ratios and Type of Water	136
VI-1	General Hydrogeological Information About the Thermal Wells	145
VI-2	Temperature Fluctuation of Some Thermal Wells	150
VI-3	Average Chemical Parameters and Type of Water	158
VI-4	Ionic Ratios, Saturated Indexes and P_{CO_2} of Thermal Waters	162
VI-5	Matrix Correlation Coefficient Between the Ions of Groundwater	164
VI-6	Eh, pH, HS^- , and SO_4^{2-} of Thermal Waters	166
VI-7	Calculation the Mixing Water in Balsam Spring	168
VI-8	Chemical and Isotopic Geothermometer Temperature	175
VI-9	The Average and Standard Deviation of Mukhebeh and JRV Well Fields	183
VI-10	$\delta^{34}S$ ‰ Variations in Sulphate from Different Materials	188
VI-11	$\delta^{34}SO_4$, $\delta^{18}O$ of SO_4^{2-} , $H_2^{18}O$, HS^- , Eh, SO_4^{2-} , and Cl^-	190
VI-12	TOC, Tritium, ^{14}C and ^{13}C Data of the Thermal Water	196
VI-13	^{14}C Correction by Sulphide	209
VI-14	Chloride Concentration and Isotope Ratios in Some Thermal Waters	215

Chapter One

The Strategic Importance of Groundwater

I.1-Introduction

Since biblical times, securing fresh water supplies in the Middle East have attracted man's energies and ingenuity. The region is arid and surface water both scarce and usually ephemeral. As a consequence, groundwater resources have played the lead role in underpinning social and economic growth. However, the role of sustainable development of these groundwaters requires an understanding of their provenance and renewability.

This thesis attempts to develop this understanding for Jordanian groundwater in the highly strategic northern border region with Syria, the Golan Heights and Israel.

Jordan, shares its borders with Syria in the north, Iraq in the east, Saudi Arabia in the south, and The West Bank and Israel in the west (Fig.I-1). It was created in 1921, and received independence from the British in 1964. The political regime is a monarchy with an elected parliament. The territory of Jordan is approximately 92000 km² and its population in 1991 was estimated to be 3.8 million.

Jordan is not an oil producer and depends on phosphate and potash production for its major revenue source. Other components of the economy include light industry, agriculture and tourism.

Agriculture is very important to Jordan's economy, but the limited water resources restricts significant growth and necessitates the import of the majority of the food sources.

Jordan is considered an arid area, lying within the Mediterranean bioclimate

region. An essential feature of this region is a concentration of rainfall during the winter season (October to April) and a very marked summer drought. Average precipitation in Jordan is estimated to be less than 100 mm/y in the desert. The desert makes up approximately 90 % of the Jordan territory.

Water resources are very scarce due to the aridity of the country and the limited amount of rain. The surface water resources include the Yarmouk River and springs. The flow of surface water is estimated to be 750 Million Cubic Meter per year (MCM/y). The majority is lost during the winter period due to flood flashing and consequently only 320 MCM/y is available for use (Bilbeisi, 1992). The largest source of surface water is the Yarmouk River.

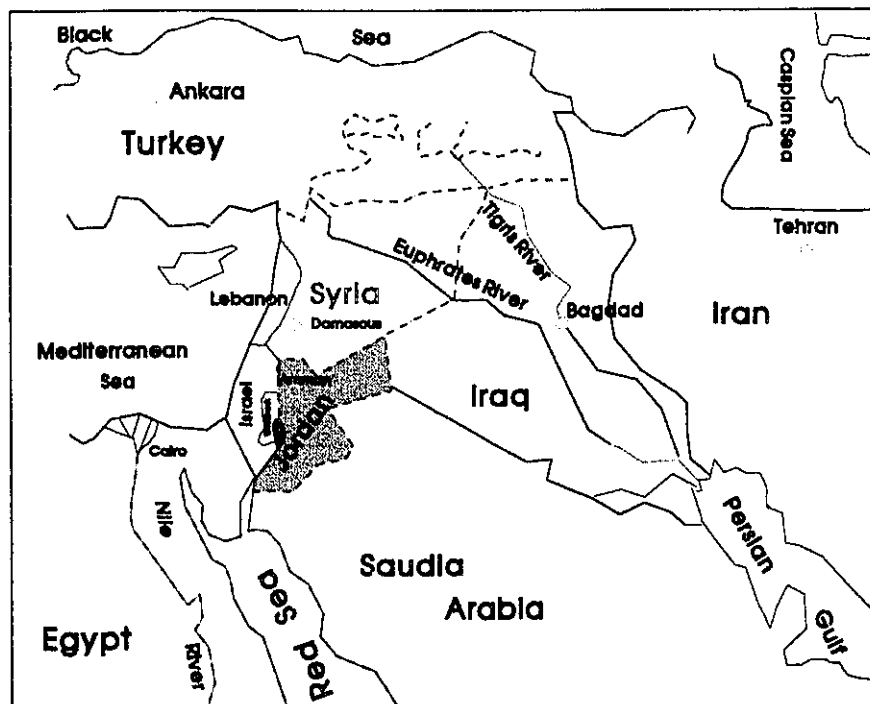


Fig.I-1 Location Map of Jordan

Groundwater is considered the major water resource in many areas in the country. It is comprised of both renewable and nonrenewable resources. The estimated renewable groundwater is 300 MCM/y and the non-renewable is 100 MCM/y (Ministry of Water and Irrigation and UNDP, 1992).

The demand for water has increased tremendously in the last 5 years due to the increase in population, and expansion of agricultural and industrial activities. To satisfy the increased need for water, abstraction from groundwater sources has increased beyond the safe yield for the majority of the basins. This exploitation pattern has caused a decrease in water level and deterioration of the groundwater quality. For example, the safe yield of groundwater in the Yarmouk Basin is estimated to be 40 MCM/y. The total abstraction in 1991 was estimated 72 MCM, exceeding the safe yield by 75% (Ministry of Water and Irrigation and UNDP, 1992). Only 22 MCM is used for municipal demand, while the remaining 50 MCM is used for irrigation.

Recommendations by the Water Authority of Jordan (WAJ) to meet the increased needs of water in the country are (i) to build surface reservoirs (dams); (ii) the exploitation of new aquifers (iii) treat and reuse waste-water; and (iv) change the irrigation pattern. These items are seen to be the most appropriate projects in order to provide more water resources for the various purposes.

In the study area the Wehdeh dam was proposed to be built at the Yarmouk River to provide Jordan with approximately 100 MCM fresh water per year. Unfortunately for economic, financial and political reasons, this project remains uncompleted.

The Yarmouk River (YR) is one of the main tributaries of the Jordan River (JR),

originating from springs that discharge in Syria. The contribution of the YR to the JR is approximately 400 MCM/y, based on an average for the period of 1963-1991 (WAJ-Files). There are three riparian countries along the Yarmouk River (Jordan, Syria and Israel) who continue to contest resource appropriation. The dispute over water in this area began in the 1920's when the British and French agreed in 1924 to discuss the water issue of the Jordan and Yarmouk Rivers and use these resources for irrigation and hydroelectricity (Kally, 1991). In 1953-1955, Eric Johnson, USA representative of President Eisenhower to the Middle East, worked out a two year water sharing agreement plan between the riparian countries of the Jordan River (Naff and Matson, 1984).

The Johnson Plan allocation for Jordan is 100 MCM/y of a total of 1370 MCM/y from the Jordan River and 377 MCM/y of a total of 400 MCM/y from the Yarmouk River. The actual amount of water from the YR that is accessible to Jordan is approximately 100 MCM/y. This water is taken from the YR through King Abdallah Canal and is much less than its allocation from the Johnson Plan. Since the 1950's, Jordan has endeavoured to build the 100 MCM capacity Wehdeh dam on the YR at Maqaren area in order to gain it's allocation of the Johnson negotiations. Technical studies were completed, but the project was halted due to Israel's claim for political modifications of the Johnson negotiations with the concept of " water security" (Wolf, 1993). Israel claims that its allocation from the Yarmouk River should be greater. With the Wehdeh dam, Jordan will benefit from 90% of its water and Syria will benefit from 75 % of its hydroelectric potential. The water will be used for irrigation and domestic uses, this will go along with resolving Jordan's water crisis.

In 1964 Israel diverted the Jordan River from North Tiberia Lake to the Naqab Desert by the National Water Carrier, denying Jordan its rightful allocation of 100 MCM/Y.

In view of the political difficulties inherent in the use of the surface water resources, groundwaters became a critical option in the Yarmouk basin.

In addition to available fresh groundwater resources, deeper, thermal groundwater resources have become increasingly attractive. Such resources are restricted mainly to the Jordan Rift Zone between the southern end of the Dead Sea and Lake Tiberia.

A drilling program in the early 1980's was initiated in North Jordan, mainly in the Yarmouk basin and JRV. The wells drilled in the Mukhebeh and in JRV area encountered hot water with a temperature range between 30 and 56 °C. The wells struck an artesian aquifer bringing water to the surface at a tremendous flow rate ranging between 200 and 6000 m³/h. The Mukhebeh well No.1 drilled in 1982, was the greatest artesian flow recorded to date in the world. The total discharge was estimated to be 6000 m³/h.

The quality of these thermal waters is generally very good, with TDS content below 1000 mg/l. The tremendous discharge of these thermal wells attracted the Water Authority to use these resources for irrigation and domestic use. This is in addition to their traditional use for curative purposes.

This study will focus on three thermal well fields within the Yarmouk Basin and the northern JRV: (i) Mukhebeh, in the western Yarmouk River Valley (ii) Northern JRV and (iii) the Ramtha area in the Eastern Yarmouk Basin (Fig.I-2). The study area covers an area of approximately 3500 km². The thermal sources comprise 14 drilled boreholes

and 2 springs. The springs (Maqla and Balsam) issue some 500 m from the Yarmouk River in the Mukhebeh area. The Mukhebeh and JRV areas are located at an elevation lower than 200 m below sea level (bsl), while the Ramtha area is around 400 m above sea level (asl). These sources are described in detail in section (VI-2), and the hydrogeological information can be found in appendix 2.

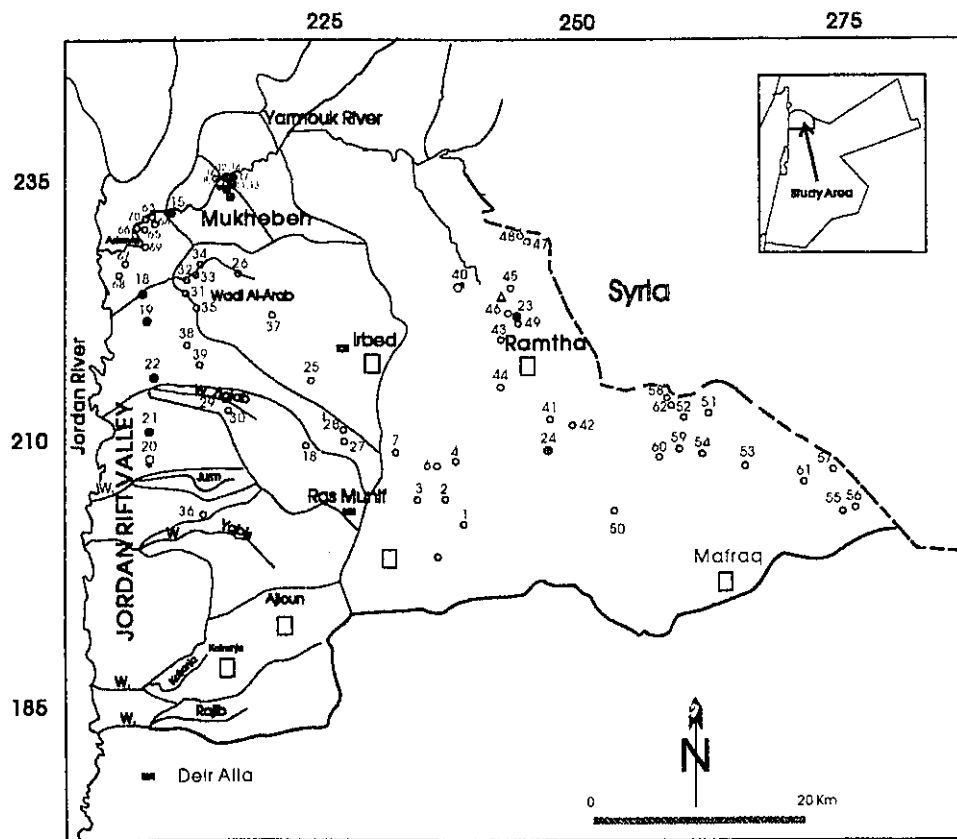


Fig.I-2 Location Map of the Study Area

The thermal waters and the non-thermal waters together are examined in this study. The aquifers from which all the groundwaters issue are found in the Upper Cretaceous, Turonian-Campanian strata. The exception is the S-90 well, which develops water from the lower Cretaceous (Albian-Aptian) strata.

These tremendous groundwater resources find themselves in a dramatic hydrogeological setting. These thermal springs and wells of Mukhebeh and JRV areas are located in karstic terrain at a fault junction over 200 m bsl, essentially the lowest datum possible, with nearby highlands rising to 2200 m asl (Hermon Mountains, Golan heights to the north and Ajloun Mountains to the south). A huge natural discharge is taking place not only in the Jordanian territory but also down hill of the Golan Heights (Hammat Gader springs).

Previous groundwater studies which had been carried out before and after drilling the wells have paid little attention to the origin of these thermal groundwaters in this study area. The source of heat, recharge history, regional flow path and gradients and the age of the water remain poorly understood.

I-2 Previous Studies

This section reviews the previous studies that dealt with hydrogeology of the study area. In addition, it summarizes the most important thermal studies which have been conducted in Jordan. The conclusions of these various thermal studies will be briefly discussed below as they are relevant to the thermal water in this study.

The most important studies which dealt with the hydrogeology of North Jordan

include:

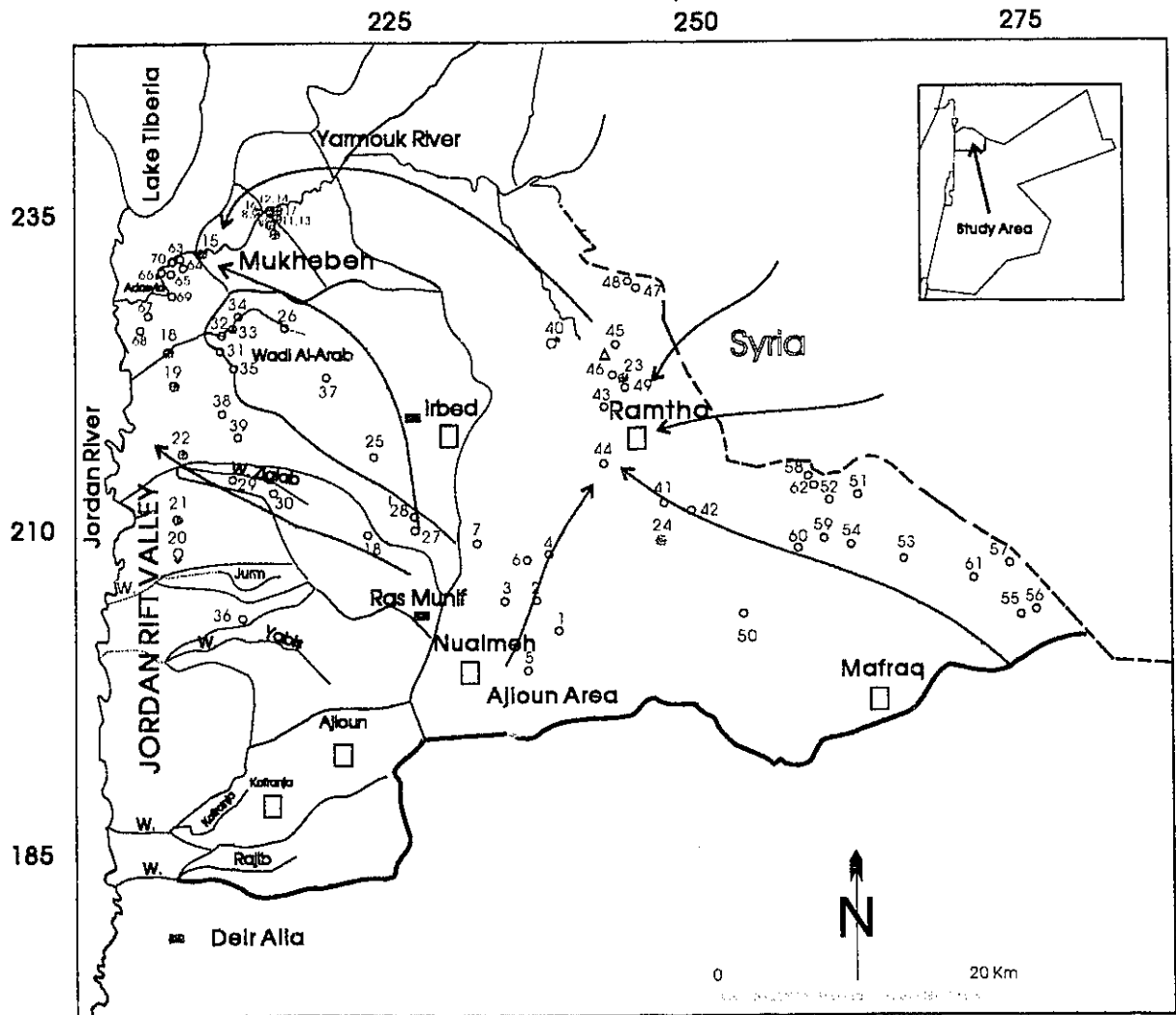
Parker, D. H., 1969. The author described in detail the aquifer systems in Jordan. He classified the water bearing formations, recharge and groundwater movement, hydrochemistry and potential water development. Concerning the study area he estimated the recharge to the Ajloun-Irbid area to be 110 MCM/Y. He describes the flow system as being from the Ajloun dome to the Jordan and the Yarmouk valleys.

Hirzallah, B (1973). His study about the groundwater in the Jordan Rift Valley concluded that recharge is derived locally from the precipitation falling above the escarpment. The Upper Cretaceous aquifer is the main potential producing aquifer. The alluvium, interfingering Lisan marl and the underlying older rock units are the water bearing formation in the Jordan Rift Valley. The good quality water is associated with the alluvium and Upper Cretaceous aquifer, while poor quality water is associated with the Lisan marl and the deeper aquifer (Zarqa).

Joudeh, O., 1983. This author conducted a detailed study for the Mukhebeh and Wadi Al-Arab area. In the study an evaluation of the Upper Cretaceous aquifer recharge was carried out. The flow system is described as radiating from the northern flanks of Ajloun mountains toward the north, north west and west. The springs in the Yarmouk Valley in Mukhebeh area are described as the discharge area for the flow system coming from Ajloun Highlands. The formations from Cenomanian to Campanian were found to form one aquifer unit. A hydrogeological map for the area was prepared. In addition, the quality of the groundwater was characterized.

The North Jordan Water Resources Investigation Project Staff (NIWRIPS), (1989). The authors of this study evaluated the water resource potential in the Yarmouk Basin and the side catchments of the valley in the northern Jordan Rift. The flow system is affected by the tectonic environment of the Rift Zone. Five aquifer systems were defined within the study area. The flow system from the recharge area to the discharge area of the Turonian-Campanian aquifer was discussed. The available groundwater resource for each water bearing formation was calculated. The hydrogeological map of Joudeh, (1983) was slightly modified. The modification is based on new hydrogeological investigation. The flow system is described as radiating from the Ajloun Highlands toward the north and north west to discharge in the JRV and Mukhebeh area. Second flow comes from Syria in NE toward the North-East Desert via Ramtha to Mukhebeh area. Third flow is coming as subsurface flow from Amman Zarqa basin (Fig.I-3). The hydrochemistry of the basin and the type of water in the different aquifer systems was also discussed.

El-Naser H. (1991). This study dealt with the hydrodynamic flow system and developed a hydrochemical model. The author's conclusion about the flow system coincided with the previous two studies. The author described that in the study area there are two major aquifers. The Kurnub sandstone (Lower Cretaceous) and the carbonate B2/A7 (Upper Cretaceous). The former has a potentiometric surface higher than that of the latter, therefore a considerable amount of water is lost from the lower aquifer to the upper aquifer as upward leakage. The continuous pumping from Mukhebeh and Wadi Al-Arab areas will decrease the potentiometric surface of the Upper aquifer, and will cause increased upward leakage from the Kurnub to the B2/A7. The model also showed that the



Legend

- | | | | |
|---|------------------|---|-------------------------------|
| ☉ | Rainfall Station | □ | Town |
| ⊙ | Thermal Water | △ | Treatment Plant |
| ○ | Cold Water | → | Flow System For B2/A7 Aquifer |
| ⊙ | Spring | | |

Fig.I-3 Flow System for the B2/A7 aquifer of the study area as proposed by earlier studies (NJWRIPS, 1989)

Mukhebeh and Wadi Al Arab affect each other by pumping. Hydrogeochemical models indicated that the Mukhebeh and Wadi Al-Arab areas are a mixing between two end members, the B2/A7 and the Kurnub. The mixing ratio from the Kurnub water is in the range between 3 and 39%.

These various studies however, fall short of addressing the origin of the recharge, direction of the flow systems, residence time and the origin of heat of the groundwaters.

In terms of thermal waters several investigations of geothermal energy in Jordan have taken place over the last twenty years within the Natural Resources Authority (NRA). Sunna', (1992), reviewed in an internal report the thermal groundwater projects that have taken place within the NRA. The occurrence of hot springs along the JRV has focused attention on the origin of heat, in order to use it as a source of energy, especially for electricity, tourism, industry and other applications. The top priority was given to Ma'in and Zara springs, some 1 to 2 km east and north east to the Dead Sea. They were considered to be the most promising sources due to their tremendous total discharge (1943 m³/h) and their highest observed temperature in the country (63 °C) (Department of Water Resources Development, 1987).

These studies of the Ma'in and Zara springs proposed two possible hydrogeological-thermal processes: (i) deep circulation of the recharge water facilitated by deep faults associated with the Jordan Rift Zone is responsible for the heat; (ii) the hot groundwater is simply associated with recent volcanism.

Bender (1974), This work observed that the majority of thermal water in Jordan is restricted to the Jordan Rift Zone. He suggested that these hot springs, especially Ma'in

springs, are associated with the Middle Pleistocene or younger basalt volcanism that accompanied the formation of the Rift.

McNitt (1976), reviewed the chemical data, collected by the NRA, and made a recommendation to carry out work project in the Zarqa Ma'in area.

Marinilli G. (1977), conducted research on the various hot springs and the outcropping volcanic rocks. His conclusion was that the most important geothermal area is the Zarqa Ma'in area.

Truesdell (1979), concluded from the geochemical evidence that the source of heat for Ma'in and Zara Springs is deep circulation in a normal geothermal gradient. The study showed that the heat at depth is no more than 110 °C. Thus, mixing with cooler water is the only process that could produce the observed surface temperature from high subsurface temperatures.

Abu-Ajamieh (1980), reported that the thermal groundwaters suggest the existence of a geothermal field in the subsurface of the Wadi Zarqa Ma'in and Zara areas. The local basaltic eruptions render the area favourable for the occurrence of geothermal fields. The author observed that the springs closer to volcanic plugs have higher temperatures.

Galanis, et al., (1986), conducted a study to measure the surface pattern of heat flow in different parts of Jordan. After comparing the distribution of heat flow values with the geologic structures, they divided Jordan into three groups. The highest heat flow was found at Zarqa Ma'in ranging from 91 to 472 milli watt per square meter (mW/m^2), followed by the Azraq area ranging from 70 to 135 mW/m^2 and the regional one, which range from 42 to 65 mW/m^2 . The area of high heat flow is associated with the fault zone

of the Dead Sea or Zarqa Ma'in fault. The conclusion is that water heated by deep circulation, is the source of heat.

Rimawi, O. and Salameh, E. (1988), studied the chemistry of the Zarqa Ma'in thermal system from the recharge area to discharge sites of thermal water east of the Dead Sea. The reservoir temperature was estimated to be 73-82 °C. The calculated geothermal gradient found to be 7.6 °C/100m in the Zara area and 3.6 °C/100m in the Zarqa Ma'in area. They suggested that the presence of a thermal insulating layer in the form of unsaturated sandstone and/or shales results in the accumulation of thermal energy which raises the temperature of the water below this layer.

Bajjali, W. (1988), analyzed several thermal and non-thermal springs from different parts of the country for chemical and isotopic composition. The study indicated that the springs of Ma'in and Zara are of meteoric origin, circulating deep within the aquifer. Due to this deep circulation the $\delta^{18}\text{O}$ became enriched due to oxygen exchange with the matrix. That suggests the temperature of the reservoir is greater than 100 °C.

Williams, H. H. et al., (1990), prepared a geothermal gradient map of Jordan using all available temperature data from geophysical logs from drilled wells. A depth-temperature profile was constructed for each well and an average geothermal gradient calculated for each profile. They found a considerable range in geothermal gradient from 2.1 to 5.0 °C/100m. The highest geothermal gradients were found in the Risha area east of Jordan due to the thickness of Silurian shale which is around 2170 m in RH-3 well.

The geothermal gradient in the Dead Sea - Jordan Valley Rift was found to vary between 2.2 and 3.7 °C/100m. The authors quotes Michelson (1985), to have reported geothermal

gradients on the order of 4.5 °C/100m in shallow boreholes in the Yarmouk River area.

I-3 Objectives of the Research

In the light of these previous studies, there is a gap of knowledge with respect to the thermal waters in Northern Jordan. Considering the strategic importance of the thermal and non-thermal groundwater resources in the region, this thesis has focused on the following main objectives:

1- Determine the recharge origin the thermal waters on the basis of new geochemical and isotope data together with hydrogeological information, and to re-evaluate existing flow models.

2- Constrain the subsurface residence time of the thermal waters and to establish:

a - if recharge occur under the modern climate, or

b - whether the thermal waters were recharged under a different paleoclimate.

3- To understand the mechanism of heating and the geothermal gradients which control the temperature of the thermal water.

Chapter Two

Approach to Solve the Problems

II-1 Methodology

Hydrochemistry and environmental isotope hydrology have become fundamental tools of hydrogeological studies. Geochemistry and isotopes are nonetheless, tools to complement classical hydrological methods including geology and aquifer delineation, transmissivity, piezometric surface contouring and discharge measurements. However, geochemical and isotopic techniques are particularly well suited as groundwater and process tracers over regional-scale dimensions where classical methods become less tenable. The geochemistry of a groundwater is a reflection of soil and vegetation conditions in the recharge area and subsequent rock-water interaction and geological conditions along the flow path.

Environmental isotopes (^{18}O , ^2H) are generally not affected by such geochemical processes, and can act as a tracer of recharge origin and recharge processes. The stable isotope contents in groundwaters reflect the climate prevailing at the time of recharges as well as the elevation of the recharge area. Radioisotopes shed light on groundwater subsurface mean residence time.

Here, geochemical and hydrogeological approaches are used, based on complementary hydrogeological data generated in the course of this and earlier studies.

II-2 Field Sampling Program

Monthly water samples of precipitation were collected from three rainfall stations

in the study area since 1989 (Fig.I-2). Published precipitation data (Bajjali, 1990a) were also used in this study. Groundwater was sampled from several wells during the period of 1987 to 1993. The sampling campaign was done during work in Water Authority of Jordan (WAJ) and during the study period in Ottawa. Data of sampling are given in Appendix 1 and 3 with each analysis.

Stable isotope analyses of oxygen-18 and deuterium in addition to radioactive tritium were carried out for the precipitation and the groundwater. Carbon-14 was performed for several cold and thermal water wells. Seven and five thermal wells were sampled for ^{34}S and ^{36}Cl respectively. Chemical analyses were also carried out for all the groundwater and the precipitation if the amount of rain was enough for such analyses. The environmental isotope and chemical analyses were carried out in Water Authority of Jordan (WAJ). Some samples especially the oxygen-18, deuterium, carbon-13 and the ^{34}S were analyzed at the University of Ottawa (OU). The ^{36}Cl were analyzed at AECL, Chalk River Laboratories. The analyses can be found in Appendix (1 and 3).

II-3 Analytical Methods

Tritium (^3H): Enriched tritium in water sample was done by electrolyses. The tritium content of the samples was measured in a Liquid Scintillation Spectrometer (Packard 3255). The detection limit of the equipment used is 1 Tritium Unit (TU). The analytical accuracy was around 1 TU (1 TU correspond to 0.118 Bq/Kg).

Carbon-14 (^{14}C): For carbon isotope analyses of DIC, groundwater samples were collected in 60 liter plastic containers, the pH was raised to above 11 with carbonate free NaOH

solution. The DIC was precipitated as BaCO_3 with $\text{BaCl}_2 \cdot 2\text{H}_2\text{O}$. The BaCO_3 was converted to CO_2 by acidification and benzene. The ^{14}C was synthesized in the liquid scintillation spectrometer with an analytical precision better than 2 pmc.

Carbon-13 (^{13}C): The isotopic composition of dissolved inorganic carbon (DIC) in water is determined by the analyses of CO_2 generated by reaction with phosphoric acid. The CO_2 is analyzed on a triple collector VG SIRA 12 mass spectrometer.

Chlorine-36: Dissolved chloride was stripped from 1L samples and converted to AgCl targets for ^{36}Cl analysis. Analyses were performed on the Atomic Energy of Canada Ltd. particle accelerator facility at Chalk River, Ontario, Canada.

Deuterium: The water converted to hydrogen gas by reduction on zinc. The H_2 gas is analyzed on an automated double collector VG 602D mass spectrometer at (UO) and by Delta-E Finnigan Mass Spectrometer at (WJ). The results are normalized to V-SMOW (WJ). The results are normalized to SMOW. The accuracy of measurement is around 1.3 ‰.

Oxygen-18 (WJ): An automatic preparation line is connected directly to the Mass Spectrometer. The CO_2 gas equilibrated with 3 ml of water sample was used for measurements. The analytical accuracy was around 0.2 ‰.

Oxygen-18 (OU): The oxygen isotopic composition of water is determined by CO_2 -water equilibration at 25 °C using an automated system. The CO_2 is analyzed in a triple collector VG SIRA 12 mass spectrometer. The analytical accuracy on the analyses is 0.15 ‰.

^{34}S of SO_4^{2-} and ^{18}O of SO_4^{2-} : Water samples for dissolved sulphate were collected in 1

litre bottles, Cadmium acetate was added during sample collection as the water is not sulphide-free. This precipitates out cadmium sulphide CdS, which can then be collected on a 45 μ filter, prior to conversion to silver sulphide. The silver sulphide sample is converted to sulphur dioxide gas for mass spectrometric analysis. The fluid remaining after the initial extraction of CdS is retained and barium chloride ($\text{BaCl}_2 \cdot 2\text{H}_2\text{O}$) is then added to precipitate out the sulphate fraction as BaSO_4 . This was converted to (SO_2) for analyses of ^{34}S by high temperature reaction in the presence of copper oxide at the University of Ottawa, and to CO_2 for analyses of ^{18}O by high temperature reaction with graphite at the University of Waterloo.

Chemical Analyses:

The following chemical parameters were determined in (WAJ) using several procedures given in each case:

-Electrical Conductivity (EC) PW 9505 Conductivity Meter.

-pH: Bekman Model 3560 digital pH meter.

- Ca^{+2} : Titration with 0.2 N EDTA, indicator murexide.

- Mg^{+2} : Titration with 0.2 N EDTA, indicator Eriochrome Black T.

- Na^+ and K^+ : Flame Emission Photometric Method.

- SO_4^{2-} : Titration with 0.2 N EDTA, indicator Eriochrome T.

-Cl: Titration with 0.01 N AgNO_3 , indicator potassium chromate.

- HCO_3^- : Titration with 0.02 N H_2SO_4 , indicator of bromcresol green and methylred solution.

- NO_3^- : Spectrophotometer (Perkin-Elmer) Lambda 9. Screen Method HCl 1 N.

-F, Br: Ion selective electrode. Fisher titration Model 465.

- SiO₂: Spectrophotometer, Calorimetric method. (lambda 9).

At (OU), some cations (Ca²⁺, Mg²⁺, Na⁺, K⁺) were analyzed by Thermo Jarrel Ash Inductively Coupled Argon Plasma Atomic Emission Sequential Spectrometer (ICAP).

II-4 General Review of Environmental Isotopes

The isotope can be defined as atoms whose nuclei contain the same number of protons but different number of neutrons. Isotope hydrology since the 1960's became a successful and advanced tool in hydrogeological by acting as natural tracers of flow system and geochemical processes and indicators of age.

II-4.1 Stable Environmental Isotopes

The terrestrial abundance of stable isotopes have remained essentially unchanged during geologic times. However, their distribution within the geosphere and hydrosphere are a function of the various reactions in these systems. The environmental isotopes then became tracers of reaction and mass movement through these systems. The most important isotopes participating in the hydrological cycle are (¹⁸O, ²H, and ¹³C).

Oxygen-18 (¹⁸O) and Deuterium (²H)

Oxygen-18 and deuterium are fundamental tracers of groundwater origin and movement as both isotopes are incorporated into water molecules and thus are an integral part of any water mass. The oxygen atom has three stable isotopes ¹⁶O, ¹⁷O, and ¹⁸O with abundances of 99.763 %, 0.035 %, and 0.1995 % respectively (Nier, 1950). Hydrogen has

two stable isotopes ^1H , and ^2H (D), with an abundance of about 99.984 % and 0.0156 % and a ratio $^2\text{H}/^1\text{H} = 0.000015$ (Urey et al., 1932).

The primary reference standard for the $^{18}\text{O}/^{16}\text{O}$ and $^2\text{H}/^1\text{H}$ is Standard Mean Ocean Water (SMOW). Therefore, an isotope abundance is generally reported as the deviation of the isotope ratio of a given sample (A) relative to that of a standard (S):

$$\delta_{(A)} = \frac{R_{(A)} - R_{(S)}}{R_{(S)}} \times 1000 \text{ ‰} \quad \text{II-1}$$

$$\text{e.g. } \delta^{18}\text{O} = \frac{{}^{18}\text{O}/{}^{16}\text{O}_{(\text{sample})} - {}^{18}\text{O}/{}^{16}\text{O}_{(\text{standard})}}{{}^{18}\text{O}/{}^{16}\text{O}_{(\text{standard})}} \times 1000 \text{ ‰}$$

The results are expressed as part per thousand (permil, ‰) difference from the reference. The isotopic composition of the Standard Mean Ocean Water (SMOW) is very close to the average isotopic composition of the ocean.

Throughout the natural circulation process of water in the hydrogeological cycle, isotopes are redistributed during phase changes. Fractionation resulting from evaporation and distillation during sequential condensation (rainout) is the major cause of the variation of the stable isotope composition of natural waters. Thus, the most important parameter affecting the degree of isotopic depletion is the temperature which decrease during rainout, giving rise to various effects (altitude, latitude, distance from ocean, etc.) of practical importance for the hydrological applications (Dansgaard, 1964). Accordingly ^2H and ^{18}O are used in water resources to clarify the origin of groundwater, by using the variation of δ value of precipitation in order to establish the time and place of

groundwater recharge.

Carbon-13 (^{13}C)

The chemical element carbon has two stable isotopes, ^{12}C and ^{13}C . Their abundance is about 98.89 % and 1.11 %, so that the $^{13}\text{C}/^{12}\text{C}$ ratio is about 0.011 ‰ (Nier, 1950). As a result of the kinetic as well as the equilibrium fractionation the isotopic ratio shows a very large variation. The abundance of ^{13}C in a sample is expressed with respect to an "average marine carbonate" or PDB standard. The PDB is the carbonate from a certain (marine) belemnite found in the Cretaceous Pee Dee Formation of North America. Atmospheric CO_2 has a $\delta^{13}\text{C} = -7$ ‰. The vast majority of plants have $\delta^{13}\text{C}$ values between -10 to -30 ‰. Soil CO_2 has ^{13}C contents close to those of the vegetation. Marine carbonate has $\delta^{13}\text{C} = 0 \pm 2$ ‰ controlled by exchange with atmospheric CO_2 .

Sulphur-34 and Oxygen-18 in Sulphate

Dissolved sulphur is common in natural groundwater. It can exist as SO_4^{2-} (oxidizing condition) and as H_2S or HS^- (reducing condition). Isotope analyses on aqueous sulphur can provide an insight into recharge environments, flow path and can suggest the source of the dissolved species, in addition can provide information on reduction - oxidation reactions. The $\delta^{18}\text{O}$ of SO_4^{2-} provides information about the source of the sulphate species, and about the geochemical environment of the groundwater in which the SO_4^{2-} is found (Pearson and Richtmire, 1980).

Sulphur has four stable isotopes, ^{32}S (95 %), ^{33}S (0.76 %), ^{34}S (4.22 %) and ^{36}S (0.014 %). Stable isotope compositions are reported as δ -value in per thousand enrichment relative to standard. The standard for the sulphur isotope is troilite (FeS) from the Canyon

Diablo iron meteoric (CD).

II-4.2 Radioactive Environmental Isotopes

If a nucleus contains too great an excess of neutrons or protons, it will disintegrate to form a stable isotope. The fundamental law of radioactive decay is based on the fact that it is a purely statistical process so that the decay probability is equal for any atomic nucleus of a certain isotope and remains equal in time. The radioactivity of a compound is defined as the number of disintegrations per unit of time.

$$A = A_0 e^{-(\ln 2/T_{1/2} \cdot t)} \quad \text{II-2}$$

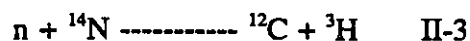
Where A =measured ^{14}C activity and A_0 =initial ^{14}C activity, $T_{1/2}$ is the half-life defined as the time required to decay to $A/A_0 = 1/2$ and $t = -8267 \ln A/A_0$.

The interest in use of ^{14}C and ^3H in isotope hydrology comes from the nature of their input and their respective half-life. ^{14}C and ^3H input functions to the groundwater means the estimation of their concentration in recharge water. This measurement can help us to estimate the groundwater residence time (age), flow dynamics, replenishment process, surface groundwater relationship, groundwater stratification, interrelation between different aquifer strata (leakage), and mixing and/or interconnection between thermal waters with present hydrological cycle.

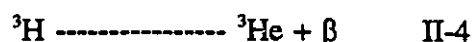
Tritium

Tritium (T) is a radioactive isotope of hydrogen (^3H), has a half-life of 12.43 ± 0.03 years and decays by the emission of β^- particles with a maximum energy of 18 Kev (Jacobs, 1968).

Its natural abundance is usually expressed in Tritium Units (TU) ($1 \text{ TU} = 1 \text{ }^3\text{H}/10^{18}$ hydrogen atom). Tritium is produced in the atmosphere by the interaction of cosmic ray produced particles with the nuclei of atmospheric gases, principally by proton and neutron induced reactions (Allen, et al., 1966).



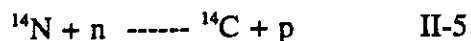
When the tritium decays it changes to helium by the reaction:



Tritium is produced in the upper stratosphere and is oxidized to H_2O and gradually transported into the lower troposphere to reach the Earth's surface as tritiated water in rainwater, snow and atmospheric moisture. Due to thermonuclear testing since 1953, the tritium content of the atmosphere has increased greatly. Maximum levels of this tracer recorded up to 10,000 T.U. in Ottawa (Canada) in the northern Hemisphere, following extensive testing in 1961-1962. Tritium concentration has decreased since in the atmosphere since this era. Tritium remains a good indicator of the presence of recently infiltrated water. Tritium, can be used to trace the movement of meteoric waters throughout the hydrological cycle (Eriksson, 1967; Carmi and Gat, 1973). The tritium content has been utilized in different hydrological applications, successful dating of groundwater e.g. (Eriksson, 1967, Clark, et al., 1987), measuring the degree of mixing of two or more water sources (Dincer et al., 1974), and other applications.

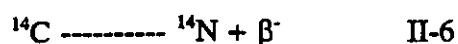
Carbon-14 (${}^{14}\text{C}$)

Carbon ${}^{14}\text{C}$ is naturally formed in the transitional region between the stratosphere and troposphere about 12 Km above the earth surface through the nuclear reaction:



^{14}C thus formed oxidizes to $^{14}\text{CO}_2$, which mixes with inactive atmospheric CO_2 . Accordingly ^{14}C is then introduced into the biosphere by photosynthesis and into the hydrosphere by dissolution of CO_2 from plant respiration and decay, by direct incorporation of atmospheric CO_2 , or by dissolution of organic carbon.

^{14}C decays according to the following law:



with a maximum β^- energy of 156 Kev and a half-life of 5730 ± 40 years. Pure oxalic acid, distributed by the US National Bureau of standards, is used as a primary reference standard .

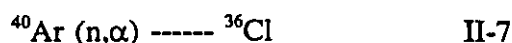
^{14}C is not an isotopic tracer of water molecules, but of the various species of inorganic dissolved carbon or dissolved organic carbon.

Since the industrial revolution in the last century, large amounts of ^{14}C free CO_2 from fossil fuels were introduced into the atmosphere and caused a drop in the ^{14}C by about 10 %. An increase took place in the ^{14}C in the atmosphere and in plants after the era of thermonuclear bomb testing (Tamers and Scharpenseel, 1970). Carbon-14 is potentially useful in dating water infiltrated during the last 30,000 years.

Chlorine-36 (^{36}Cl)

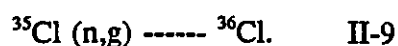
Chloride is generally considered to be an excellent tracer in groundwater studies. It is highly soluble and has a simple geochemistry. ^{36}Cl has many advantages as a dating tool for very old groundwater. The half life is 3.01×10^5 years giving a potential dating range of more than 2 million years.

Chloride-36 is primarily produced in the upper atmosphere through the bombardment of argon gas by cosmic radiation, according to the following two reactions:



where n = neutron, α = alpha particle, p = proton.

Common ^{35}Cl in the atmosphere can be irradiated by cosmic flux to produce ^{36}Cl .



where g = gamma radiation.

Providing that the system after recharge and ^{36}Cl input remains closed with respect to other sources, radioactive decay should reflect the subsurface residence time of the host groundwater. Despite the uncertainties, recent work has shown its great potential for hydrogeology both as a dating tool and in recharge studies. Time estimates based on ^{36}Cl decay are depend upon a knowledge of the cosmic input (initial activity) and on the contribution of additional dissolved chloride sources along the flow path of the groundwater (Andrews and Fontes, 1992). The sources of the chloride can come from

- (i) chloride diffusion from higher salinity solutions contained within the aquifer,
- (ii) dissolution of evaporite within the aquifer or its aquitards.

II-5 Radiocarbon Correction Techniques

The complexities associated with aging the groundwater are well recognized and discussed in various works (Geyh, 1972; Fritz, et al., 1979a; Fontes and Garnier, 1979). This section will review and summarize some of the most important methods, that have

been used in this study to determine the residence time of the groundwater. The majority of these ^{14}C models are based mainly on dissolution of calcite in closed system condition. However, numerous studies also show that in many groundwaters considerably greater dilution occurs. Processes responsible for this may be (i) carbonate dissolution by bacterial CO_2 (Barker et al., 1987), or (ii) carbon originating from the oxidation of organic matter (Winograd and Farlekaes, 1974) and addition of (iii) volcanic CO_2 (Fritz, et al., 1979b). The (ii) and (iii) items will be discussed in detail in section (VI-5).

Groundwater dating was first introduced 37 years ago by Munnich (1957). Since then several attempts have been made to correct the ^{14}C based on the geochemical processes that can control the geochemical evolution of a groundwater in carbonate aquifer.

Vogel (1970), following several soil measurements in Germany he adapted an initial ^{14}C to be 85 ± 5 pmc irrespective of climate condition. This procedure is based on a black box model and does not account for the isotope exchange reactions which occur beneath the water table.

Geyh, (1972), proposed an exponential model where he found that the initial ^{14}C can drop from 65 to 75% in karst systems. His assumption was based on two carbon sources, the Soil CO_2 which provides the modern carbon component and limestone with "dead" carbon.

Tamers (1975), his model is based on the chemistry of the groundwater.

$$A_o = \frac{m\text{CO}_2 + 0.5m\text{HCO}_3^-}{m\text{CO}_2 + m\text{HCO}_3^-} A_g \quad \text{II-10}$$

Where m stands for molalities; A_g is the ^{14}C activity of soil CO_2 . The limitation of the model is that it assume closed system conditions for CO_2 and does not consider any possible isotope exchange.

Pearson et al., (1972) introduced a correction model based on variations in the $\delta^{13}\text{C}$ abundances: any process that alter the ^{14}C value will affect the ^{13}C . The A_o obtained from a carbon/isotope-mass balance where:

$$A_o = \frac{\delta^{13}\text{C}_{\text{DIC}} - \delta^{13}\text{C}_{\text{Carb}}}{\delta^{13}\text{C}_{\text{Soil}} - \delta^{13}\text{C}_{\text{Carb}}} \quad \text{II-11}$$

This model, like the above, assumes that these reactions occur under closed system conditions precluding isotope exchange with the gas reservoir. For the sake of calculation the $\delta^{13}\text{C}_{\text{Carb}}$ value of the solid carbonates in the aquifer are assumed to be zero, as they are of marine origin. The $\delta^{13}\text{C}_{\text{Soil}}$ values of the soil are fairly well documented and will vary between about -20 to -25 ‰.

Nevertheless the above equation is only correct if the soil CO_2 is taken up by the water without significant fractionation effect. This is the case in low pH environment where minor isotope fractionation effects occur during the transition from $\text{CO}_{2(g)}$ to carbonic acid (H_2CO_3) (Fritz, et al., 1979a). Such low pH is not dominated in the recharge area of this study, therefore the $\delta^{13}\text{C}_{\text{Soil}}$ replaced by initial $\delta^{13}\text{C}$ ($\delta^{13}\text{C}_{\text{IN}}$) defined as :

$$(\delta^{13}\text{C}_{\text{IN}}) = \delta^{13}\text{C}_{\text{Soil}} + \varepsilon \quad \text{II-12}$$

where "ε" is the temperature dependence, the $\delta^{13}\text{C}_{\text{IN}}$ is dependent on the $\delta^{13}\text{C}_{\text{Soil}}$ and the isotopic enrichment factor between soil $\delta^{13}\text{C}$ and the carbonate species at higher pH in an open system.

Pearson and Hanshaw (1970), Suggested that the initial carbonate content of groundwater that should be determined, which together with dead carbon added under closed system conditions, gives the final amount of DIC in the groundwater. Then the q factor is defined as follow:

$$q = \text{initial}_{\text{DIC}}/\text{final}_{\text{DIC}} \quad \text{II-13}$$

The initial DIC should be calculated by assuming value of the P_{CO_2} and pH close to the condition in the recharge area. The final DIC is measured alkalinity of the sample.

Fontes and Garnier (1979), this approach is based upon chemical consideration for estimating the amounts of inactive and active carbon and on an isotopic reaction to estimate further exchange within the aquifer. They assumed that several component could added to the groundwater (a) dissolution of sulphate minerals (gypsum or anhydride), (b) cation exchange may substitute alkaline earth ions for alkali ions in solution. Their ^{14}C correction model was a geochemical algorithm to account for such additions, and an isotope mass balance approach based on carbon exchange with either CO_2 or CaCO_3 .

Reardon and Fritz (1978), added an isotope model to the computer program WATEQF, to calculate the carbon isotopic composition of groundwater. They adjust initial parameters (P_{CO_2} , temperature and $\delta^{13}\text{C}_{\text{soil}}$) at reasonable values to account for final conditions and compute A_0 . Thus calculation require pH and temperature as measured chemical parameters. The concentration of the total dissolved carbon and the aqueous CO_2 can be evaluated from first and second dissociation constant of carbonic acid. In addition the model may be used to compute age differences between pairs of water samples along the flow path using congruent and incongruent carbonate dissolution models.

Chapter Three

Geology and Hydrogeology of the Study area

III-1 Physiography and Drainage

Jordan is a land lying on the north-western edge of the Arabian Peninsula, which is bordered by the Mediterranean Sea, Red Sea, Indian Ocean and the Persian Gulf. Seven important physiographic regions are recognised in the country (Bender, 1974), and are presented in (Fig.III-1).

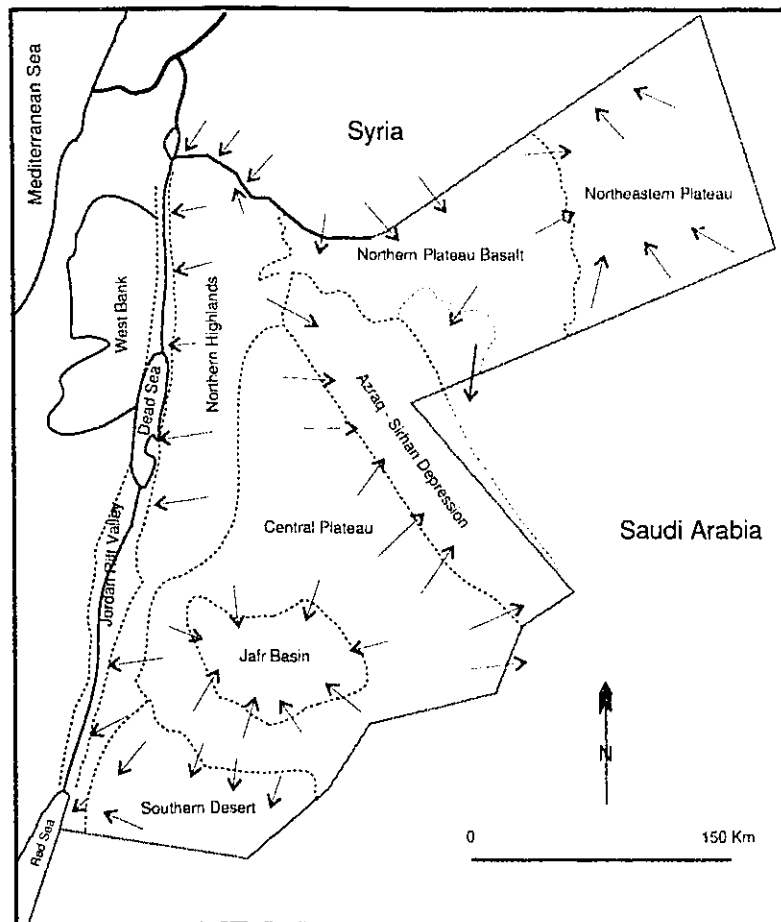


Fig.III-1 Major Physiographic and Surface Drainage Trends (Modified from Wilkinson, 1992)

The study area is located in the northern part of Jordan, and comprises the Yarmouk basin and the northern part of the JRV. About 75% of the Yarmouk Basin is inside the Syrian Territory and the rest is in Jordan. The area is bounded by the Jordan River to the west and the Yarmouk River to the north. The topographic relief of the area ranges in elevation from 200 m bsl in the JRV up to 1235 m asl in the northern highlands.

Three distinctly different physiographic provinces can be found in the study area (Fig.III-1):

1-Jordan Rift Valley. (JRV). The JRV extends from the Red Sea in the south to Lake Tiberia in the north a distance of about 360 km. The Dead Sea is located in this depression, which is the lowest land surface in the world at 402 m bsl.

2-Northern Highlands. These highlands represent the uplifting eastern JRV margin sloping gently toward the east, and sloping very steeply toward the JRV. The highest elevation in Jordan was recorded in these highlands at 1800 m asl (west of Maan, in the south). Ajloun Mountains form the northernmost part of these highlands.

3-Northern Plateau Basalt. This region is considered to be the southern edge of the great Tertiary Basalt flows of the Hauran Plain and Druze mountains in Syria (Quennell, 1959). This area is known as the North-Eastern Desert of Jordan, where the basalt flows cover approximately 11,000 km². The altitude decreases from 1100 m asl in the northern border of Jordan with Syria to about 550 in the vicinity of the Azraq Depression.

Three major features control the drainage of the study area; the JRV in the west, the Yarmouk River in the north and north-west and internally draining basins (Fig.III-1).

The Northern Highlands is breached by a number of westward drainage valleys in the area between the Yarmouk River and the southern end of the Dead Sea (Fig.III-5). The overall trend of the wadies is more or less east-west, with minor north-south. The largest of these are, from north to south, the Yarmouk River, Wadi Al-Arab, and Wadi Ziglab. The last two are bounded with dams. The Yarmouk River has a drainage basin that lies in both Jordan and Syria and is considered the only significant surface water resources in the country.

III-2 Climate

Jordan lies within the Mediterranean bioclimatic region which, as an essential feature, has a concentration of rainfall during the cool winter season and very marked summer drought. Over most of Jordan an arid desert climate exists dominated by low precipitation and high potential evapotranspiration. There are two major atmospheric circulation patterns in the country. In winter the area is within the sphere of influence of the temperate latitude climatic belt, and cool, moist air moves from the Mediterranean Sea. In the summer months, the area lies within the subtropical high pressure belt of dry air; temperature is high and no rainfall occurs.

The main source of the precipitation that occurs over the area are the *frontal* and *non-frontal* precipitation. The frontal precipitation results from the lifting of warm air on one side of a frontal surface over colder and dense air on the other side (Sa'ad, 1986).

The nonfrontal precipitation is caused by reasons unrelated to fronts, where the

most important ones are:

1-Orographic precipitation, which results from mechanical lifting of an air mass over mountain barriers. This happens when a moist air mass moves toward a mountain, and then is deflected upward by the mountain. The upward motion will cause cooling below the saturation temperature (dew point) and the precipitation occurs. Such type of rain is observed in Ajloun mountains.

2-Convective precipitation, this type takes place by the late afternoon thunderstorms which develop from day long heating of moist air. The rising warmer lighter air in the colder denser surroundings will create an instability into the air, and this may cause an increase in the speed of the upward and downward motions followed by rapid saturation. This type of rainfall usually occurs during the warmer months of the season, like October, November, April and May.

The air masses over Jordan come from different sources. In Autumn/Spring, rains are associated with Mediterranean air, originating from the Atlantic. In winter, rains are associated with continental polar air masses originating from Siberia (Russia) and Europe. Vapour is generated over the Mediterranean Sea before entering the area.

The 50-year average annual rainfall intensities range from 600 mm in the northwest to less than 50 mm in the eastern and southern desert (Fig.III-2).

The highest mean annual rainfall occurs along the Northern Highlands in the Ajloun mountains in the study area. The average annual precipitation decreases rapidly into the JRV and eastward. The monthly rainfall is extremely variable from year to year. Jordan's average rainfall amounts to about 8,419 MCM/year, varying between 6,000 and

10,205 MCM/year for the period of 85/91 (WAJ, 1991). North east of the study area (Yarmouk Basin and side wadies), this amount was 735 MCM (8.77 % of the total amount of rain in the country), for the year of 90/91. Approximately 92.2% of the rainfall evaporates, while 5.4 % recharges the groundwater and the rest flows in the rivers and wadis (Bilbeisi, 1992).

Maximum summer temperatures average 32 in the Northern Highland to 38 °C in the JRV and Desert. Maximum winter temperatures average 14 °C in the highlands and 17-21 °C in the desert and JRV.

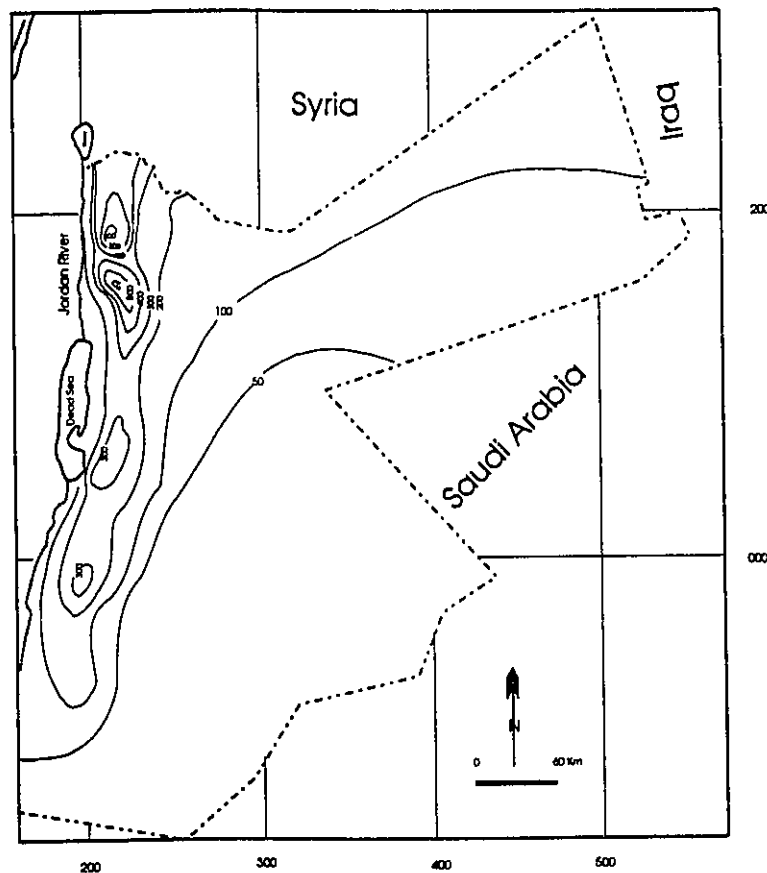


Fig.III-2 Rainfall distribution in Jordan mm/y (average 50 years)

In the study area the temperatures are highest along the JRV and coolest in the Northern Highlands. The long term average temperature in Ras Munif in Ajloun Mountains ranges between 16.8 to 21.3 °C in Summer and 5.4 to 18.2 °C in Winter. While in the JRV in the Deir Alla Station is between 19.1 to 33 °C in Winter and 33.8 and 38.7 °C in Summer (Meteorological Department, 1988).

During the winter months the relative humidity is generally above 55 % and in January and February, it may be above 90 % for much of the rainy days (Meteorological Department, 1988). In Summer months the relative humidity is low, but there is a wide range, especially between day and night. The highest potential evaporation occurs during the hottest months and the months with the lowest evaporation are December to February.

The study area is covered with a network of rainfall stations distributed in strategic locations. There are 45 daily rainfall stations and 15 automatic stations. In addition, rainfall data from the Syrian portion of the Yarmouk Basin is also monitored to give detailed information about the rainfall distribution in the whole basin (NJWRIPS, 1989). Table III-1 represents the average rainfall distribution for 6 years (1985/1992), in seven rainfall stations from different locations in the study area.

The table indicates that there is a significant seasonal variation in rainfall over the area. The highest average was recorded in Ras Munif in the Ajloun Mountains which is considered as one of the recharge areas to the groundwater. The lowest amount of rain is in Um-Jmal area (North-East Desert) and Deir Alla (JRV). The rainfall is characterized by its irregularity, varying from year to year, with occasional snowfall on

the Ajloun Mountains.

Table III-1 Average amount of rain for the period 1986/1992 in mm

Station	86/87	87/88	88/89	89/90	90/91	91/92	Avg.
Ras Munif	670.1	691.4	449.3	532.5	495.1	1151.4	633.5
Irbed	602.5	562.5	297.5	453.7	434.3	908.9	515.6
Deir Alla	344.2	350.6	255.6	303.7	252.3	599.6	334.5
Ramtha	308.9	328.6	189.3	334.9	260.7	479.7	294.5
Maqaren	537.9	491.5	220.7	270.1	244.7	846.5	415.6
Samar	596.8	539.6	273.1	458.5	388.7	900.8	502.4
Um-Jmal	148.2	219.7	101.5	117.9	114.7	191.4	134.3

The average yearly rainfall at the Golan Heights and slopes of Hermon mountains on the Syrian side exceeds 800 mm (Droubi, 1992).

III-3 Soil Types and Vegetation

Soil and vegetation are closely connected and both of them are affected directly by the climate. Nevertheless, geology plays a big part in the formation of the soils, by providing the parent material. The distribution of the natural vegetation is governed by the amount of rainfall as a dominant factor.

Abu-Ajamieh, et al., (1988), reviewed the studies of several authors who conducted pedological investigations in different parts of Jordan. The soil covers an

extensive part of the study area with three soil groups: (i) grey desert soil (Siorezems) in the North Desert. Parent soil materials are derived from weathering products of basalt and tuff consist of brown silty loam to clayey loam with varying amounts of basalt fragments and calcium carbonate concretions. The associated soil is shallow and contains fragments of basalt and in some cases limestone; (ii) Red Mediterranean soils in the Ajloun area, the parent material consists of limestone. The soils cover more than 60% of the area. The soil colour is dark as it is rich with the organic matter. The soil contains a large amount of montmorillonite clay with a cation exchange capacity of more than 50 meq/100 g of soil; (iii) Yellow Mediterranean soil in the JRV. The soil contains mainly alluvial fans, medium to heavy in texture, and clayey to loamy or clayey. The soil in this area is intensively irrigated.

The vegetation in the Ajloun area is natural trees, mainly oak and pinaceous. In addition, there are agricultural activities including cultivation of the following crops: wheat, barely, lentils and tobacco. These kinds of trees and vegetables belong to the Calvic cycle or C-3 type of plants. The isotopic composition of the plants is of great importance because plants control the abundance and isotopic composition of soil CO₂, which is the dominant source of ¹⁴C in groundwater (See, VI-5.2.3).

III-4 Geology and Groundwater Flow Systems

A brief description of the geology of Jordan will be presented here, in order to give a better understanding of the geology of the study area. This section will combine the hydrogeology and the geology together. The aquifer systems will be described in

detail in order of their stratigraphic sequence. The direction of the flow system, which is based on the previous studies will be described. Emphasis will be given to interpretation of flow system in the north, whose validity this study questions.

Jordan lies between the Precambrian Nubo-Arabian Shield to the south and the Neogene Anatolian-Iranian mobile belt to the north (Bender, 1974). Most of Jordan is underlain by sedimentary rocks which blanket the basement. The basement outcrops only in the south, over an area of about 1400 km². The sedimentary formations range from Lower Palaeozoic to Quaternary. The Palaeozoic consists mainly of sandstones and conglomerates, overlain by partially lagoonal to fully marine, calcareous sandy sediments of Triassic and Jurassic age. The sedimentation follows with Lower Cretaceous sandstone. In most of Jordan, Cretaceous sandstones are covered by Upper Cretaceous and Lower Tertiary carbonate sediments. The Upper Cretaceous sediment is entirely marine and is exposed in the study area. Large scale tectonism during the Oligocene perpetuated the basin and swell structures over the East Plateau with an accumulation of alternating marine and continental sediments.

A complete succession from Lower Cretaceous to Quaternary sediments is outcropping in the study area. The Jordanian litho-stratigraphic nomenclature with the equivalent universal epoch is used and presented in Table III-2.

The geology of the Yarmouk area has been studied by Burdon (1952); Baker & Harza (1955); Quennell, 1959; Wiesemann & Abdullatif (1963), and recently by Abdelhamid, et al., (1991). The latest study produced a preliminary geological map at 1:100,000 scale (Fig.III-3) and Cross section (Fig.III-3A).

Table III-2 The litho-stratigraphic unit of the study area

Geological Time Scale			Quennel, 1951			Masri 1963	German Mission 1966	FAO 1970				
Era	Period	Epoch	Group	Symbol								
CENOZOIC	Quatern.	Holocene	Balqa Group		Balqa Series		Basalt Flows					
		Pleistocene		Ba								
	Tertiary	Oligocene		B5					Chert and Limestone	Shallala		
		Eocene		B4								
		Paleocene		B3			Rijam					
	MESOZOIC	CRETACEOUS		Maast.			B2	Ajloun Group	Ajloun Series	Muaqar	Chalk-Marl	Muaqar
				Campanian			B1			Amman	Phosp. L'st.	Amman
							Santonian				A7	
				Cenomanian			A5/6			Wadi Sir	Echinoidal L'st.	W.Ghudran
							A4					
A3			Shuaib		Shuelb							
A1/2						Hummar	Hummar					
Albian												Kurnub Group
	Aptian	K1	Nodular L'st.	Na'ur								
					Subeihl	Kurnub Sandstone						
			Ard'a									

III-4.1 Aptian-Albian (Kurnub)

The Kurnub Formation outcrops in different locations within the study area. In Jarash area, the thickness is in the range of 300-350 m (Al-Suleiman, A. 1992). It is an unconformably underlain by different portions of Jurassic sequence.

It is characterized by a basal conglomerate, grading up into thick beds of coarse grained sandstone, with lenses of medium-grained quartz arenite and laminated siltstone, mudstone, and shale. It represents a fluvial system interrupted by short periods of marine transgression.

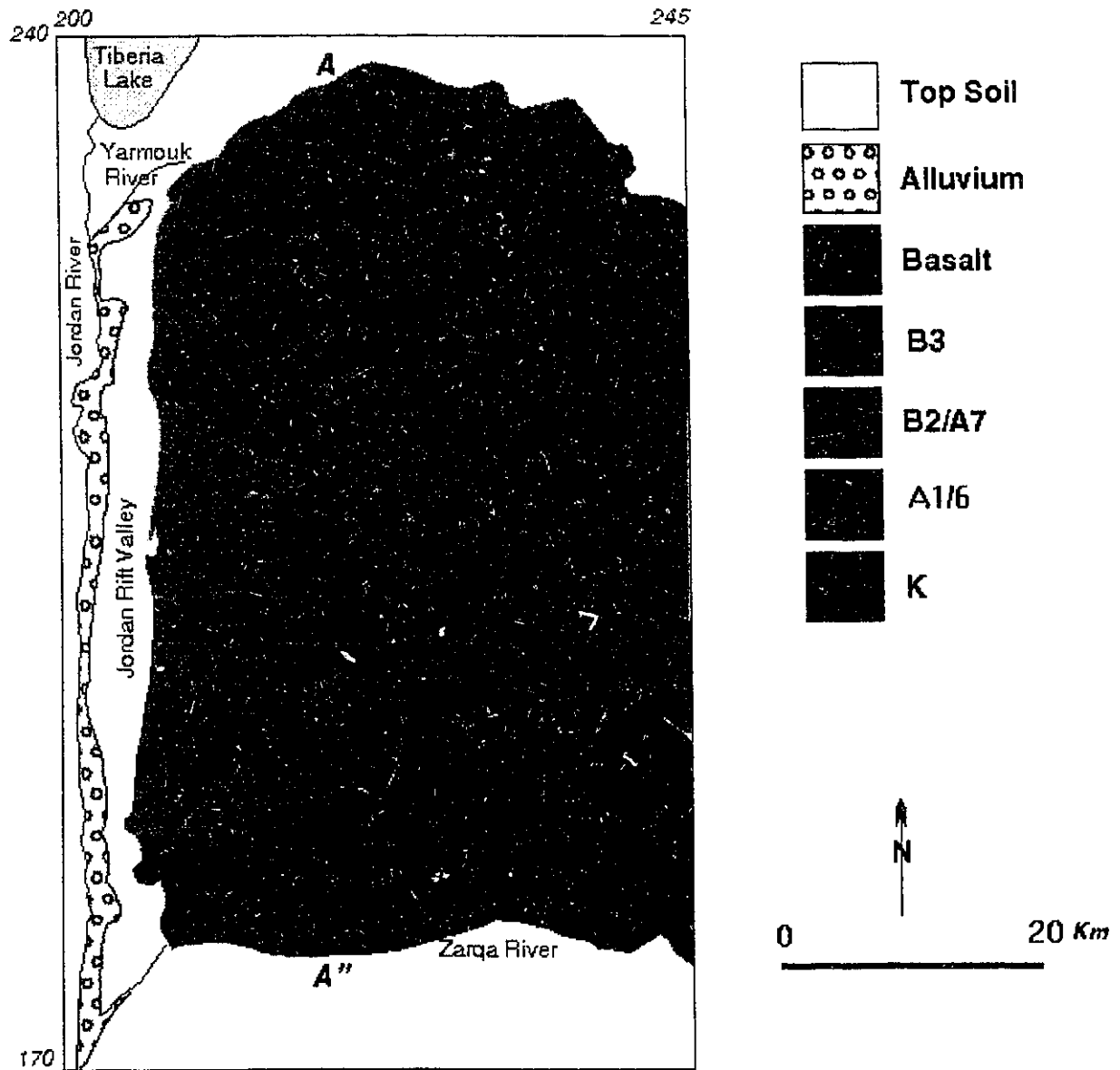


Fig.III-3 Simplified Geological Map of the Northern part of the study area

(after Abdelhamid et al., 1991)

The sandstone also outcropping in east of Jordan within the territory of Iraq in Rutba area. The thickness of the formation is approximately 20 to 40 meters and dipping toward Jordan (Fig.III-4). The Kurnub is found at depth in oil exploratory wells (AJ-1, ER-1 and S-90), with a thickness of 183, 247 and 294 m. Porosity ranges between 3.6 to 26.4 % (Abdel Hadi, 1991).

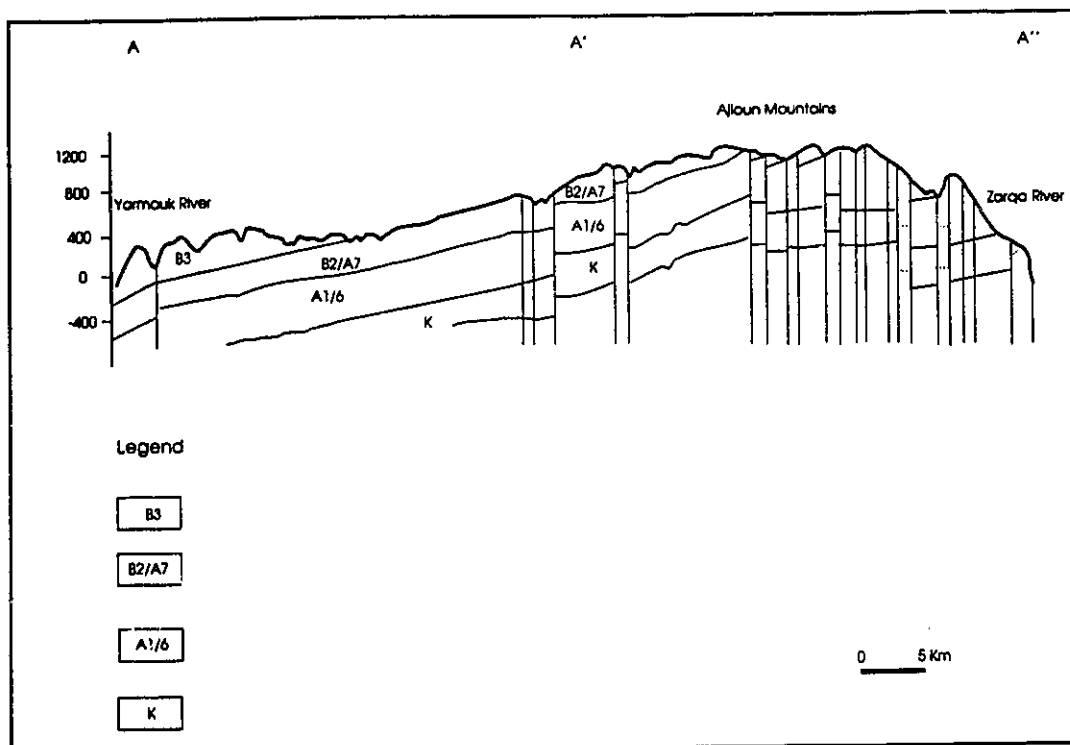


Fig.III-3A Simplified Cross Section Between Zarqa River and Yarmouk River

(after Abdelhamid et al., 1991)

The Kurnub is considered an aquifer, and underlies almost the entire study area. On a large regional scale the flow system and the recharge into the Kurnub in the study area is not known.

In general, modern recharge in Jordan to the Kurnub is limited and restricted mainly to the leakages from the Upper and Middle Cretaceous carbonate aquifer systems. Bender, et al., 1991, suggested that the recharge to the sandstone aquifers (Disi-Kurnub) in Central Jordan, is the downward leakage from the overlying fractured carbonate formation through the A1-6 aquitard. Elsewhere, the Kurnub sediments outcrop on steep slopes or in areas of low rainfall, therefore low recharge rate took place (Parker, 1969).

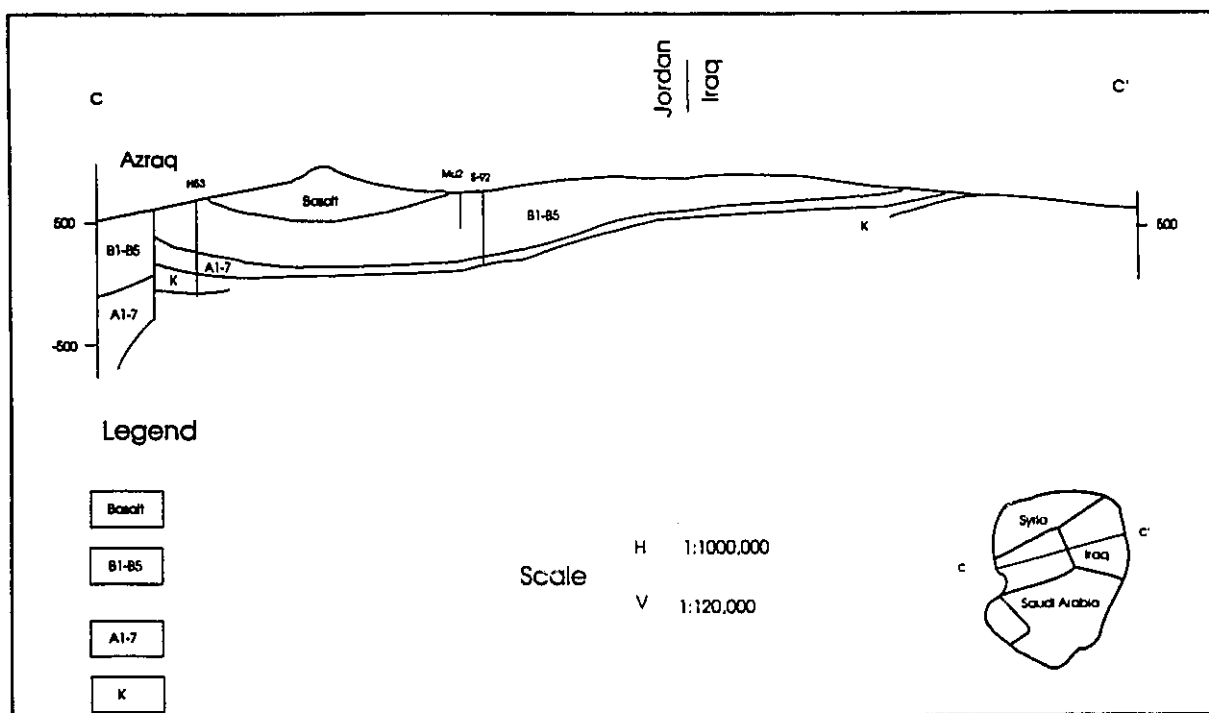


Fig.III-4 Cross Section for Kurnub Between Jordan and Iraq (after Acsad, 1983).

El-Naser, 1991, indicated that the flow system of Kurnub in the study area is from the north, north east and east (Syria) sides, mainly westward to the JRV and partially converging along the Zarqa River. He also concluded that the potentiometric surface of the Kurnub aquifer is higher than that of the B2/A7 aquifer, therefore a

considerable amount of water is lost from the former to the latter, especially in the thermal well fields areas, Ramtha, Mukhebeh, and JRV . His assumption was based on the potentiometric surface of two deep oil exploratory wells in Ramtha area (S-90 and ER-1).

The transmissivity and yield of the Kurnub is quite variable and it range from 60 to 1700 m²/d, and from 8 to 2000 m³/h respectively. The total dissolved solids (TDS) salinity of the Kurnub is also variable. In Baqa south to the study area is less than 600 mg/l, while in the JRV lies between 1400 to more than 5000 mg/l (Joudeh, et. al., 1980). In some area the Kurnub is hydraulically connected with the Triassic-Jurassic (Zarqa Group) forming one aquifer system. The Zarqa Group consists of limestone, dolomites, and about 30 m evaporite, mainly gypsum and anhydride. Wells tapping this aquifer recorded brackish groundwater. In the study area there is one thermal well (S-90) in Ramtha area. Its TDS is 2400 mg/l, and the yield was estimated to be 70 m³/h (WAJ-Files). The big depth, high TDS and low yield makes the Kurnub aquifer in the study area not exploitable. The water in the well is elevated in temperature (56 °C), and contains H₂S.

III-4.2 Cenomanian to Turonian - Ajloun Group

The Kurnub aquifer is overlain in the study area by carbonate sequence range in age from Cenomanian to Eocene (Table III-2). The succession has been subdivided into two groups: Ajloun (A1-7) and Balqa Groups (B1-5).

The Ajloun group includes rocks of the Cenomanian and Turonian epoch. The

Ajloun group consists mainly of marl and marly limestone and is more distinguished in the southern and south eastern part of the study area (Fig.III-3). The Ajloun group increases in thickness northwards. The total thickness of this group in Mukhebeh area represented by the deep JRV1 well is 734 m. Seven lithostratigraphic unit have been defined for this group. This succession include three aquifer system; A1-2, A4 and the B2/A7, the latter is a combination of lower Ajloun and upper Balqa Groups. The strata are gently dipping into northeasterly direction in the eastern part of the study area, while to the west, the dip gradually turned to the north (Fig. III-3A).

1. Naur Formation (A_{1,2}) Two subunits are recognised within the Naur Formation: The A1 consist mainly of marl and having a thickness range between 60 to 120 m, while the A2 consist of marly and marly limestone with 100 to 150 m thickness. Along the southern escarpment, where the aquifer is exposed, the predominant lithology is limestone, but the proportion of sandstone increases to the south-east of the country to become arenaceous.

WAJ-files indicate that the yield of some wells tapping this formation is in the range of 30 to 70 m³/h. Salem, (1984), indicated that the hydraulic conductivity is in the range of 2.0×10^{-8} to 3.1×10^{-5} m/s. This low permeability is related to the weak groundwater circulation pattern. In the Mukhebeh area this aquifer is tapped by the deep JRV1 well.

2. Fuheis Formation (A3). It is cropping largely in the south part of the study area. It consist of yellowish, brown - olive green marl, and thin bedded nodular limestone, it also contain some dark grey shale and black carbonaceous materials. The A3

formation acts as an aquitard separating the Naur aquifer from the overlying Hummar aquifer.

3. Hummar Formation (A₄) This one is composed of grey limestone and dolomitic limestone (micrite and wackstone), with lenses of dolomite. The formation is highly fractured, and highly solution fissured to cavernous. It is exposed in Ajloun mountains with thickness 50 to 70 m (Al-Suleiman, 1992). In the study area the aquifer is under artesian condition. In Mukhebeh area the aquifer is penetrated by two wells the deep JRV1 and Mukhebeh No.4. The yield of the aquifer is variable from place to place, in general it is in between 50 to 250 m³/h.

4. Shueh formation (A5-6), is consists of thin bedded nodular chalky limestone, dolomitic limestone intercalated with marly limestone. The A5-6 is known to be as an aquiclude or aquitard in other parts of Jordan is a good aquifer in the Mukhebeh area (Joudeh, 1983). It is fractured and maintain a high secondary transmissivity and storativity.

5. Wadi Sir Formation (A₇) The Wadi Sir Formation consist of thin bedded limestone with chert bands and nodules. It corresponds to the Massive Limestone and the overlying Sandy Limestone unit of Turonian age. It exposed in Ajloun Mountains, were 80 m outcropping in Wadi Taiybeh. The thickness of the A7 in the thermal wells is about 200 m in Mukhebeh and north of the JRV areas.

III-4.3 Santonian to Eocene - Balqa Group

This group overlies the Ajloun group, and is well exposed in Balqa district of NW Jordan, from were the name is given. The Balqa Group subdivided into five formation,

its age range from Santonian to Upper Eocene. The group is characterized by the abundance of chert within the carbonate sequence of chalk, limestone and marl.

1. Wadi Ghudran formation (B1), This formation forms the lower impermeable unit (aquitard) of Balqa Group. It consist of white to buff chalk with occasional thin chert and concretion. Its thickness is 15-30 m and reach up to 50 m in Yarmouk Basin (Al-Suleiman, 1992).

2. Amman Formation (B₂). The Amman formation outcrops extensively in the Northern Highlands, in west Irbed area and the eastern part of Wadi Al-Arab. This formation consists of fairly thin alternating layer of chert, marl, chalk, limestone, and phosphate. The thickness ranges between 50-80 meters in Irbed area.

3. Muaqqar Formation (B3). This formation is exposed in the northern part of the study area. Green clayey marls, mudstone with intercalated marly limestone. The bitumen content in the marly limestone is widely different laterally as well as vertically (Al-Suleiman, 1992). The thickness of the B3 in the Mukhebeh and JRV areas ranges between 300 and 500 m. This thick formation keep the aquifer under artesian pressure. In some wells the pressure reaches up to 275 PSI (Joudeh, 1983).

4. Rijam Formation (B4). The Rijam is exposed with a total thickness of 200 m, in Wadi Shallala in Yarmouk River and Ramtha area. It consist of limestone, slightly marly and chalky limestone. The B4 is considered a good aquifer and recharged locally by precipitation in Northern Irbed and Ramtha area. The flow system is directed toward the Yarmouk river. The aquifer discharges as contact spring in several locations. The local recharge has been estimated to be 4.55 MCM/y (NJWRIPS, 1989).

The B4 aquifer is found mainly in Ramtha area, under water table condition. The hydraulic properties of the aquifer varies from place to place. The transmissivity is found to be between 5 and 300 m²/day. The yield of the wells is in the range of 20 to 60 m³/h. The salinity of the groundwater varies widely from about 300 to 1500 mg/l.

5. Wadi Shallala Formation (B5). This formation outcrops out in wadi Shallala in the north. This formation which attains a total thickness of 100-150 m, is of Middle to Upper Eocene age. The formation consists mainly of chalks, chalky limestone with little chert.

III-4.4 The B2/A7 Aquifer. The Amman (B2) and Wadi Sir (A7) formations are considered to be one aquifer as they are hydraulically connected. The B2/A7 is the main aquifer in this study, and crop out mainly in the Ajloun Mountains. The thickness is increasing from East toward Westend and it ranges between 150 m in the outcropping area (Nuaimah) and up to more than 500m in Manshieh well in the JRV area. The groundwater in the B2/A7 aquifer is stored under water table condition in Ajloun Mountains and eastern part of the study and under artesian condition in the JRV and Wadi Al-Arab areas. The depth to the water level in the unconfined aquifer vary from 110 to 250 m.

The aquifer has varying transmissivity from 10 to 7500 m²/d (WAJ-Files). The lowest was found in the water table condition and the highest in the artesian section in Mukhebeh area. The yield of the wells differs from area to area. The highest yield in the basin, was recorded in Mukhebeh, JRV and Wadi Al-Arab areas, where the wells

discharge under artesian pressure. Yields found to range from 150 to 6000 m³/h, while in the rest of the area the yield is much less, it is in the range between 25 to 200 m³/h (Appendix 2).

The permeability of the aquifer is of secondary origin and is characterised by fissures, fractures and karstic features. Therefore the potential for the direct recharge of precipitation is high. The recharge to the B2/A7 aquifer was estimated to vary between 20 and 140 MCM/Year (Joudeh, 1983; Salem, 1984; NJWRIPS, 1989; and El-Nasser et al., 1992). The percolating water radiates from Ajloun Highlands toward the north, northwest and west (Fig.I-3).

The indirect recharge is also coming as subsurface flow originating from the northeast part through the basalt aquifer from the Jabel Al Druze in Syria (NJWRIPS, 1989; and El-Nasser 1991).

In some areas a tremendous abstraction from the groundwater for different purposes caused either a reduction or complete drying up of discharge of the springs. Maqla and Balsam springs in Mukhebeh area decreased from approximately 17 MCM to 11 MCM, while in Wadi Al-Arab area the springs is completely ceased (WAJ-Files). The abstracted water in Mukhebeh and Wadi Al-Arab is estimated to be between 50 to 55 MCM/y for the last 10 years (WAJ-Files). The TDS of the aquifer is generally good, it is less than 1000 ppm.

III-4.5 Oligocene to Holocene

1. The Basalt Formation, Between Miocene and Holocene times and due to the tectonic

movement of the Rift Zone, several phases of outpouring of basalt took place in the area near and east of the Jordan Valley and lake Tiberia in Jabel Druze, Hauran and the Golan Heights (Wieseaman and Abdullatif, 1991). The basalt flows occur in North Jordan over more than 11,000 km² as a result of these volcanic activities. They consist mainly of six massive alkali layers separated by interflows of clay, sand, and gravels (Bender, 1974). The flows covers the eastern and Northern part of the study area.

The basalt overlies the B2/A7 aquifer, and they are considered to be hydraulically connected and form one aquifer system. The rate of abstraction from this part of the basin increased from 6.3 MCM in 1978 to 21 MCM in 1987 due to expand in agriculture (NJWRIPS, 1989). This practice caused a drop in water level and deteriorated the quality of water in some locations.

Transmissivity in the Basalt aquifer wells ranges from 130 to 100,000 m²/day. The water is stored under water table conditions, and the aquifer thickness ranges from 5 to 165 m.

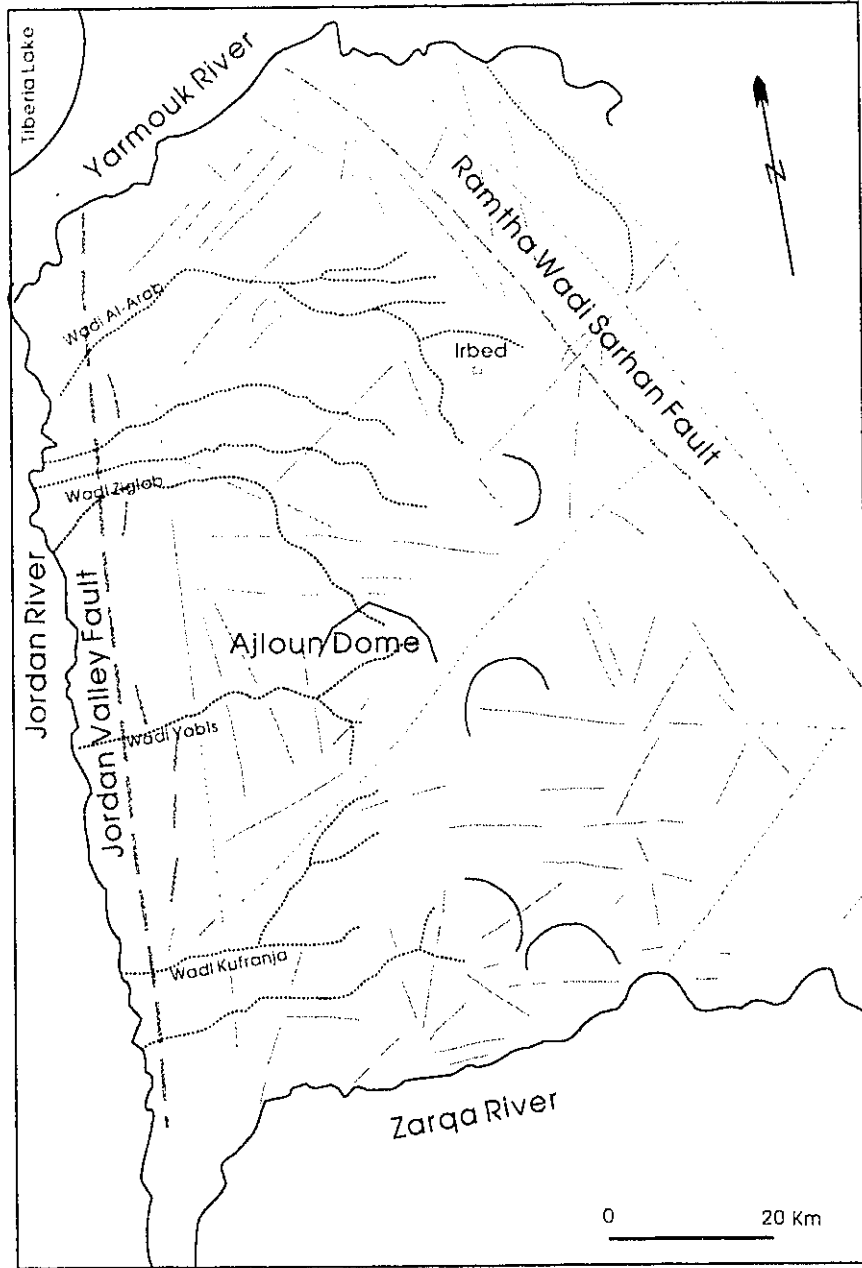
2. Quaternary Alluvium of the Jordan Valley Group. The Jordan Valley group consists of massive and thick bedded conglomerates in hard calcareous and siliceous cement, and has an average thickness of 100 m. The upper member (Lisan Beds) consist of alternating marls, clay, chalk, and evaporite. This has a thickness of about 300m and form about 70 % of the Jordan Valley. The groundwater occurrence and quality depends on the proportion of the alluvium and the absence of the Lisan marl intercalations. The aquifer in Adasyia area is stored under water table conditions. The depth to the water table range from 0.6 to 18 m. The yield of the aquifers is between 64 and 170 m³/h.

III-5 Structural Geology

The structure of the study area has been described by several workers, (Bender, 1974; Quennell, 1983; Mikbel and Attalah, 1983). Formations outcropping in the area are mainly fractured and jointed. Fault related fracture system are usually shear fractures parallel to the fault. Fractures generally, play an important role in groundwater recharge and its circulation. The structural features are highly related to the structure of the JRV. Structurally, the area is divided into three parts (Fig.III-5): The Jordan Rift Valley west of the Jordan Valley fault, Ajloun Dome to the east of this fault and a third region east of the ramtha Wadi Sarhan fault. The major structural features of the area was defined through field work, aerial photographs and Landsat 1: 25000 coloured images to observe lineaments (Abdelhamid, et al., 1991).

III-5.1 Jordan Rift Valley

The major structural elements in the study area is the Jordan Rift Valley (JRV) which has a NNE orientation. The system extends for 105 km from the Tiberia basin in the north to the Dead Sea in the south and its maximum width is about 20 km. This rift system is a complex structure and links the Taurus collision zone in the north with the Red Sea in the south. It is connected with the East African Rift by the Afar depression in south. The total length of this rift is 6000 km. It separates the Arabian plate and the Palestine-Sinai plate (Garfunkel, 1981). This structure is believed to be a major left lateral strike-slip fault with a total proven horizontal displacement slightly exceeding 100 km (Hatcher, et al., 1981).



Legend



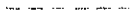

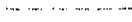
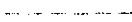
- | | | | |
|---|--------------------|---|-------------------|
|  | Major Fault |  | Circular Features |
|  | Possible Extention |  | Wadi |
|  | Lineament | | |
|  | Minor Fault | | |

Fig.III-5 Major structural Features in the study area (Modified from Abdelhamid, 1991)

Movement along the JRV began in Mid-Miocene and is currently still active, with the rate of movement varying temporally (Garfunkel et al., 1981). El-Isa and Mustafa (1986) proved through the prehistorical earthquake activity along the Rift valley a 0.64 cm/y seismic slip rate along the Araba fault. This rift zone presents a zone of structural weakness which has existed since Cambrian time. Two fault systems have been observed: N-S and W-E (Fig.III-5). There are many changes between these two major tectonic systems. Due to the block rotation, several faults are traceable from the rift zone many kilometres inside the Jordan (Barjous and Mikbel, 1990).

The offset along the faults generally decreases eastward, where they extend into monoclinial flexures. The sinistral strike - slip that distinguished by two major blocks along the rift give rise to very complicated tectonics on the east border of the Dead Sea Rift. While ongoing movement opens several directions of faults, some faults and fractures remain closed (Myslil, 1988).

The interaction of the two systems of faults has acted locally as conduits for young basalt extrusions i.e. Marnat Um Hasan in Zarqa-Ma'in area east to the Dead Sea. The Hammamat Ma'in hot springs (63 °C) are associated with such an intersection.

III-5.2 Ajloun Dome, is an east-west double plunging, highly faulted anticline, covering an area of 78 km², with 416 m of vertical closure (Anderson, 1976). This structure is a dome, in which strata are dipping in all directions (Fig.III-3A). It is bound by the JRV in the west. This dome is characteristically dissected by ESE to E and some NNW faults and ENE to E-W folds. Major faults following this trend are frequently accompanied

with extensive land-sliding and most probably, responsible for the presence of the major E-W wadies (Abdelhamid, et al., 1991).

III-5.3 Ramtha Wadi Sarhan Fault This fault is more than 325 Km long and can be traced from to northern Jordan where it reach the Dead Sea fault zone (Beicip, 1981; Mikbel, 1985; and Futyan and Jawzi, 1991). The Ramtha-Wadi Sarhan fault, a major strike slip fault. Futyan and Jawzi, 1991, tied this faulting trend to the Proterozoic suture observed in Saudi Arabia and named the Najd Fault system, where it reactivated more than once during it's history. It may also represent the rejuvenation of more ancient fractures.

Chapter 4

Precipitation and Surface Water

The isotopic composition, in particular ^{18}O , of the precipitation is of special importance in the appraisal of the origin of water resources. Surface waters include mainly the Yarmouk River and some other springs discharging along its flow path. This section establishes the isotope geochemistry of precipitation as the input function for examining groundwater recharge origin and age. The isotope chemistry of surface water provides insights on groundwater discharge and runoff processes.

IV-1 Precipitation

An isotopic and chemical analysis of precipitation in the study area was undertaken as a basis for investigating the origin and subsurface history of groundwater in the basin. Samples were collected from three rainfall stations (Ras Munif, Irbed and Deir Alla) of differing altitudes (Fig.I-2 and Fig.IV-2). The stations were chosen to monitor the isotopic and chemical signature of the rain, so it could be used as a guideline to evaluate the groundwater recharge processes in the study area. The locations of the rainfall stations are more or less representative of the general climate of the study area. Ras Munif and Irbed are located 1150 and 555 m respectively asl in the Northern Highlands of the Yarmouk Basin and the Deir Alla is situated 224 m bsl in the JRV.

Due to the variation in isotopic composition of precipitation (Dansgaard, 1964; Yurtsever and Gat 1981), the long term weighted average is taken as the input function into a hydrological system. Mixing in the recharge environment attenuates these

variations, which permits use of mean annual values for hydrogeological applications of environmental isotopes. The isotope data from the three rainfall stations were chosen to provide such averages based on monthly composite precipitation samples Appendix 1. In addition, the average monthly rainfall for each station was collected, and the deuterium excess (d) of each month was also calculated.

IV-1.1 Chemical Composition of Precipitation :

Chemical analyses of the precipitation (Table IV-1), show that salinity ranges between 38 and 211 ppm. This range is exceedingly high for precipitation, and may be attributed to the generally arid landscape high altitude dust and proximity to major saline water bodies. The rain water is classified mainly as Ca^{2+} - HCO_3^- type of water. Some parameters shows high concentration e.g. Ca^{2+} , Mg^{2+} and the HCO_3^- . From Table IV-1 we can conclude that the variability of the major cations and anions, in addition to their high load, can be attributed to the dust content of the air with a secondary component of marine aerosol. The regional bedrock in the study area is carbonate. The relatively high concentration of SO_4^{2-} , Mg^{2+} and the correlation of Cl^- with Na^+ , may also indicate a contribution from the aerosol originating either from the Mediterranean Sea (Na^+ - Cl^-) and the Dead Sea (Mg^{2+} - Na^+ - Cl^-). The latter contributes to the high concentration of Mg^{2+} . The concentration of SO_4^{2-} in the rain water is much higher than the groundwater in Nuaimh recharge area (see Table V-1.1).

A high concentration of NO_3^- (up to 30 mg/l) is observed at the Deir Alla station. In this area there is intensive agriculture activity, and dust storms carrying fertilizers may

Table VI-1 General Hydrogeological Information about the Wells

No.	NAME	Elev m	Depth m	Cemented Slotting	Open Hole m	Aquifer	Yield m ³ /h	SWL m	TDS oc/100m	G.G	Toc
Mukhebeh											
8	Balsam Spr.	-50					1969		653		34.5
9	Maqla Spr.	-50					1969		902		41.8
10	JRV1	-70	1230	0-218	218-1230	B2/A7, A4, A1/2	157	11	1056	1.82	42.5
11	Mukhebeh 1	-80	350	0-14	14-350	B2	6000	FLOW	538	2.74	29.6
12	Mukhebeh 2	-110	488	0-284	284-488	B2	800	FLOW	525	2.54	32.4
13	Mukhebeh 3	-80	333	0-173	173-333	B2	2822	FLOW	544	4.20	34.0
14	Mukhebeh 4	-110	892	0-220	220-892	B2/A7, A4	2200	FLOW	538	1.82	36.3
15	Mukhebeh 5	-118	900	0-549	549-896	B2/A7	200	FLOW	582	2.84	45.6
16	Mukhebeh 6	-95	475	0-200	200-475	B2	2000	FLOW	506	3.76	37.9
17	Mukhebeh 7	-115	500	0-150	150-500	B2	2100	FLOW	461	4.40	42.0
JRV											
18	North Shuneh	-178	967	0-268	268-840	B2/A7	900	Flow	672	3.49	53.8
19	Manshieh	-175	1150	0-857	857-1150	B2/A7	200	Flow	486	2.60	50.0
21	Abuziad	-120	1126	0-631	631-1126	B2/A7	90	Flow	1360	2.80	51.6
22	Waqas	-90	1300	0-916	916-1300	B2/A7	60	Flow	435	2.36	50.8
Ramtha											
24	S-90	566	2190	0-1116	1116-2190	B2/A7, K, Z		151	2400	2.54	56.0
23	Mahasi 6	481	702	0-470	470-702	B2/A7	100	282	493	3.13	42.0

G.G: geothermal gradient

be responsible for the high nitrate values and may be also related to the contribution of dust accumulation in the rain samples between the rain events.

IV-1.2 Isotopic Composition of Precipitation:

Understanding the relationship between the variation of $\delta^{18}\text{O}$ and δD content of precipitation during its evolution through primary evaporation, condensation, re-evaporation, and infiltration is essential for studying groundwater origin. Isotopic models of precipitation are generally based on the Rayleigh fractionation mechanism: as rain or snow falls from the cloud, a depletion in ^{18}O and D is observed in the residual condensed air mass and thus in subsequent precipitation.

On a global average, the general relation between $\delta^{18}\text{O}$ and δD for natural waters is found to be linear and can be expressed by the following equation (Craig, 1961).

$$\delta\text{D} = 8\delta^{18}\text{O} + 10 (\text{‰})$$

The deviation from this global meteoric water line (GMWL), called the local meteoric water line (LMWL), can be expressed through the deuterium excess parameter (d). The d-parameter is defined as $d = \delta\text{D} - 8\delta^{18}\text{O}$ (Dansgaard, 1964). The location of the data on the LMWL indicates the origin of the air moisture.

Precipitation throughout the Eastern Mediterranean area, shows a different correlation between the $\delta^{18}\text{O}$ and δD , namely, $d \sim 22 \text{‰}$ (Gat and Carmi, 1970).

The relationship between the $\delta^{18}\text{O}$ and δD of the three rainfall stations precipitation in the study area are shown in (Fig.IV-1).

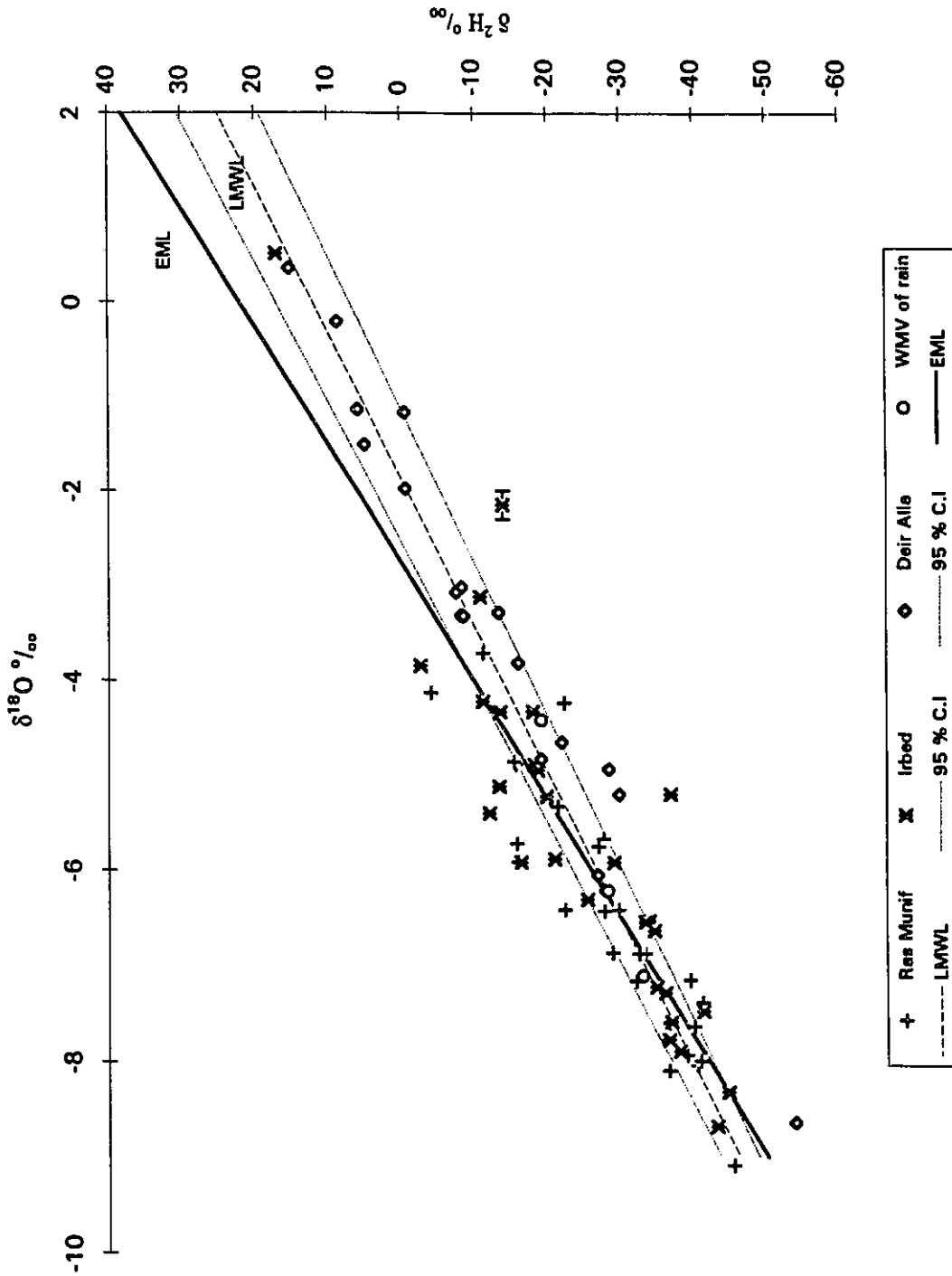


Fig. IV - 1 The oxygen-18 and deuterium diagram of the monthly precipitation of ras Munif, Irbed and Deir Alla. The WMV, LMWL, EML and 95 % confidence interval is also plotted, the error bar of one sample is also shown

It should be mentioned that the values used in the graph represent the monthly precipitation samples for both the $\delta^{18}\text{O}$ and δD at each station from the period of 1987-1991.

The regression line for the three stations of $\delta^{18}\text{O}$ and δD of all the data plotted in (Fig.IV-1) is:

$$\delta\text{D} = (6.46 \pm 0.26) \delta^{18}\text{O} + (12.07 \pm 5.02)$$

with a correlation coefficient; $R^2 = 0.89$ and number of data = 73. The \pm indicates the 95 % confidence interval on the slope and the intercept. This line is labelled LMWL (Local Meteoric Water Line) in Fig.IV-1. The weighted mean values (WMV) for samples having precipitation of more than 10 mm rain have been used for this interpretation (Table VI-2).

We can see from (Fig.IV-1) that the monthly samples and the WMV for the 5 years at all the stations fall very close to LMWL and to the 95% confidence band. Notice, however that the samples of the two rainfall stations Ras Munif and Irbed and their WMV fall on both the EML and LMWL. Deir Alla data show deviation from the EML and scatter widely along the LMWL.

The most divergent values relative to EML in Fig.IV-1, usually enriched in both oxygen-18 and deuterium, are those of months with deficient rainfall (March, April, June and October). Some data show the effect of enrichments, which in some months are extreme. This fact is well shown at Deir Alla Station (March, 1988, February, 1988 and February 1990). Two samples recorded in June of the Ras Munif and Irbed stations showed evaporation effect and deviation from the EML. The amount of precipitation for these cases is of little influence on the WMV for the rainy season.

Table IV-2 Weighted Mean Value of Stable and Radioactive Isotope in Precipitation

Name	Period	WMV For All Samples				WMV For Samples > 10 mm			
		O-18 o/oo	D o/oo	TU T.U	d o/oo	O-18 o/oo	D o/oo	TU T.U	d o/oo
Ras Munif	Oct.87-Apr.88	-7.7	-35.8	8.4	25.4	-7.7	-35.8	8.4	25.4
	Nov.88-Jun.89	-6.6	-29.7	8.2	23.0	-6.6	-29.7	8.2	23.0
	Oct.89-Apr.90	-7.0	-33.3	6.1	22.6	-7.0	-33.3	6.1	22.6
	Oct.90-Apr.91	-7.2	-32.9	5.3	24.7	-7.2	-33.2	5.3	24.7
Avg		-7.1	-32.9	7.0	23.9	-7.1	-33.0	7.0	23.9
Irbed	Oct.87-Apr.88	-7.1	-32.9	8.1	24.0	-7.1	-33.1	8.1	23.9
	Oct.88-Jun.89	-5.5	-22.8	8.5	21.3	-5.5	-23.1	8.5	21.3
	Oct.89-Apr.90	-6.6	-33.1	6.8	19.3	-6.6	-33.2	6.8	19.3
	Oct.90-Apr.91	-5.5	-23.0	5.9	21.0	-5.6	-23.4	5.9	21.1
Avg		-6.2	-28.0	7.3	21.4	-6.2	-28.2	7.3	21.4
Deir Alla	Dec.87-Mar.88	-5.3	-21.7	10.3	20.3	-5.3	-21.7	10.3	20.3
	Oct.88-Feb.89	-2.8	-6.4	9.9	16.3	-2.9	-6.6	9.9	16.4
	Oct.89-Mar.90	-3.5	-13.2	7.0	14.9	-3.6	-13.8	7.0	15.0
	Jan.90-Apr.91	-5.8	-33.1	6.9	13.6	-6.0	-34.1	6.9	13.8
Avg		-4.4	-18.6	8.5	16.3	-4.4	-19.1	8.5	16.4

Based on the confidence intervals for the slope and the intercept, the regression line of $\delta^{18}\text{O}$ and δD (Table IV-3) indicates that the rainfall of the three stations have a slope significantly less than 8. The intercept could not shown to be significantly different than the EML value of 22.

Table IV-3 The least square fit line relationship between $\delta^{18}\text{O}$ - δD

Ras Munif	$\delta\text{D} = (7.17 \pm 0.64)\delta^{18}\text{O} + (17.88 \pm 4.49)$	$R^2 = 0.84$	$N = 26$
Irbed	$\delta\text{D} = (6.47 \pm 0.57)\delta^{18}\text{O} + (12.44 \pm 0.83)$	$R^2 = 0.83$	$N = 28$
Deir Alla	$\delta\text{D} = (7.28 \pm 0.34)\delta^{18}\text{O} + (12.84 \pm 3.30)$	$R^2 = 0.96$	$N = 19$
Ras Munif	$\delta^{18} = (0.22 \pm 0.03)\text{T} - (8.7 \pm 0.49)$	$R^2 = 0.87,$	$N = 8$
Irbed	$\delta^{18} = (0.29 \pm 0.07)\text{T} - (9.6 \pm 0.94)$	$R^2 = 0.76,$	$N = 8$
Deir Alla	$\delta^{18} = (0.25 \pm 0.07)\text{T} - (9.34 \pm 0.83)$	$R^2 = 0.75,$	$N = 7$
Ras Munif	$\delta^{18} = (-0.02 \pm 0.003)\text{P} - (5.06 \pm 0.97)$	$R^2 = 0.53,$	$N = 26$
Irbed	$\delta^{18} = (-0.02 \pm 0.007)\text{P} - (4.6 \pm 1.86)$	$R^2 = 0.17,$	$N = 28$
Deir Alla	$\delta^{18} = (-0.05 \pm 0.008)\text{P} - (0.75 \pm 1.35)$	$R^2 = 0.65,$	$N = 19$

T-Temperature of air, P-Amount of Rain and N-Number of samples

The high d-parameter persists in rain throughout Jordan (Bajjali, 1990a) and is regarded as a characteristic of Eastern Mediterranean precipitation (Gat and Carmi, 1970). The high d-parameter for the stations indicates that in winter, the cold and dry continental air masses come in contact with the warm Mediterranean Sea, resulting in rapid

evaporation and large scale convergence (Gat and Carmi, 1970). The low slope indicates secondary evaporation after condensation.

Precipitation at Deir Alla shows enrichment and significant variability in isotopic composition and consequently in the calculated deuterium excess. An exception is precipitation of March 1991 which is the most isotopically depleted (Fig.IV-1). This could be the result of a storm in this month that effected the JRV only and not the rest of the country.

A statistical evaluation for these three stations is listed in (Table IV-4). We can notice that the average of $\delta^{18}\text{O}$, δD and d is more depleted at Ras Munif, Irbed and Deir Alla respectively, while the range, standard deviation and variance are greater at Deir Alla, Irbed and Ras Munif respectively. These spatial variations can be attributed to several factors:

1 Seasonal Temperature Effect:

The stable isotope composition of precipitation generally shows a wide range of seasonal variation mainly due to temperature effect (Dansgaard, 1964). The isotopic data of the three rainfall stations show more depletion in cold months than warm months.

The least square fit defining the relationship between the $\delta^{18}\text{O}$ and temperature of the three station is listed in (Table IV-3).

Since temperature of condensation at the cloud base is unknown, the mean monthly temperature of each station was used instead. The isotopic composition of a given amount of precipitation can generally not be used as an indication of condensation

Table IV-4 Statistical Treatment of Isotope Data and Rainfall

Name	Parameter	Mean	S.D	Variance	Max	Min	Range	Skewness	N
Ras Munif	Oxygen-18	-6.52	1.37	1.89	-3.70	-9.09	5.39	0.40	25
	Deuterium	-29.01	10.76	115.98	-4.00	-45.29	41.29	0.57	25
	Tritium	7.89	3.07	9.48	16.00	4.40	11.60	1.23	22
	Deuterium Excess	23.19	4.64	21.59	31.33	11.46	19.87	-0.36	25
	Amount of Rain	86.96	59.55	3546.79	195.60	13.90	181.70	0.54	25
Irbed	Oxygen-18	-5.98	1.68	2.83	-2.14	-8.68	6.54	0.45	24
	Deuterium	-26.94	12.03	144.61	-2.60	-44.60	42.00	0.33	24
	Tritium	7.92	3.68	13.56	21.70	3.80	17.90	2.65	22
	Deuterium Excess	20.90	6.59	43.45	31.12	3.22	27.90	-1.30	24
	Amount of Rain	72.16	47.18	2226.70	165.70	15.60	150.10	0.63	24
Deir Alla	Oxygen-18	-4.08	2.10	4.42	0.36	-8.64	9.00	-0.03	17
	Deuterium	-16.00	15.98	255.56	15.22	-53.70	68.92	-0.24	17
	Tritium	9.19	3.16	10.04	15.80	5.00	10.80	0.57	17
	Deuterium Excess	16.40	3.39	11.51	21.76	11.06	10.70	0.18	17
	Amount of Rain	66.10	33.24	1105.00	130.40	21.30	109.10	0.60	17

S.D. Standard Deviation

temperature, because the observed composition of individual rain events is a function of several parameters (Craig and Gordon, 1965).

The relationship of the $\delta^{18}\text{O}$ measurements versus temperature for the three stations is given by the following equation:

$$\delta^{18}\text{O} = (0.25 \pm 0.02) T - (9.03 \pm 0.49) \quad R^2 = 0.87, \quad N=23$$

The variation in the stable isotope composition of monthly precipitation is strongly dependent on the temperature. The seasonal variations are more pronounced in the stations Ras Munif and Irbed (Northern Highlands), than at the Deir Alla (JRV). The relatively large variation in $\delta^{18}\text{O}$ for the Deir Alla station should be mainly due to the amount effect.

2 Altitude Effect:

There is a tendency that at high altitude the $\delta^{18}\text{O}$ value of precipitation is more depleted than at low altitude. This effect is temperature related, because the condensation is caused by the temperature drop with increasing altitudes. This spatial variation in stable isotope composition is of practical significance for identifying the recharge environment of the thermal water of this study.

The WMV of $\delta^{18}\text{O}$ and δD at Ras Munif is more depleted than at the Deir Alla Station. The depletion of the heavy isotope at Ras Munif can be seen in (Table IV-2), where the range of $\delta^{18}\text{O}$ values for Ras Munif is -6.58 to -7.65 ‰ as compared to the Deir Alla station, which is -2.84 to -5.84 ‰.

Figure (IV-2) shows the evolution of the isotope composition along a cross section

from Deir Alla (the lowest altitude station, and the nearest to the Mediterranean sea) in the JRV to Ras Munif and Irbed (Northern Highlands).

This cross section reflects the typical movement of air masses, from different origins (Atlantic Ocean and Continental Polar), passing over the Mediterranean Sea then proceeding eastward inland. From this figure an isotopic depletion is evident during the ascent of air mass from the JRV to the Ajloun Mountain. The altitude effects is demonstrated by the enriched values observed for Deir Alla (lowest elevation),

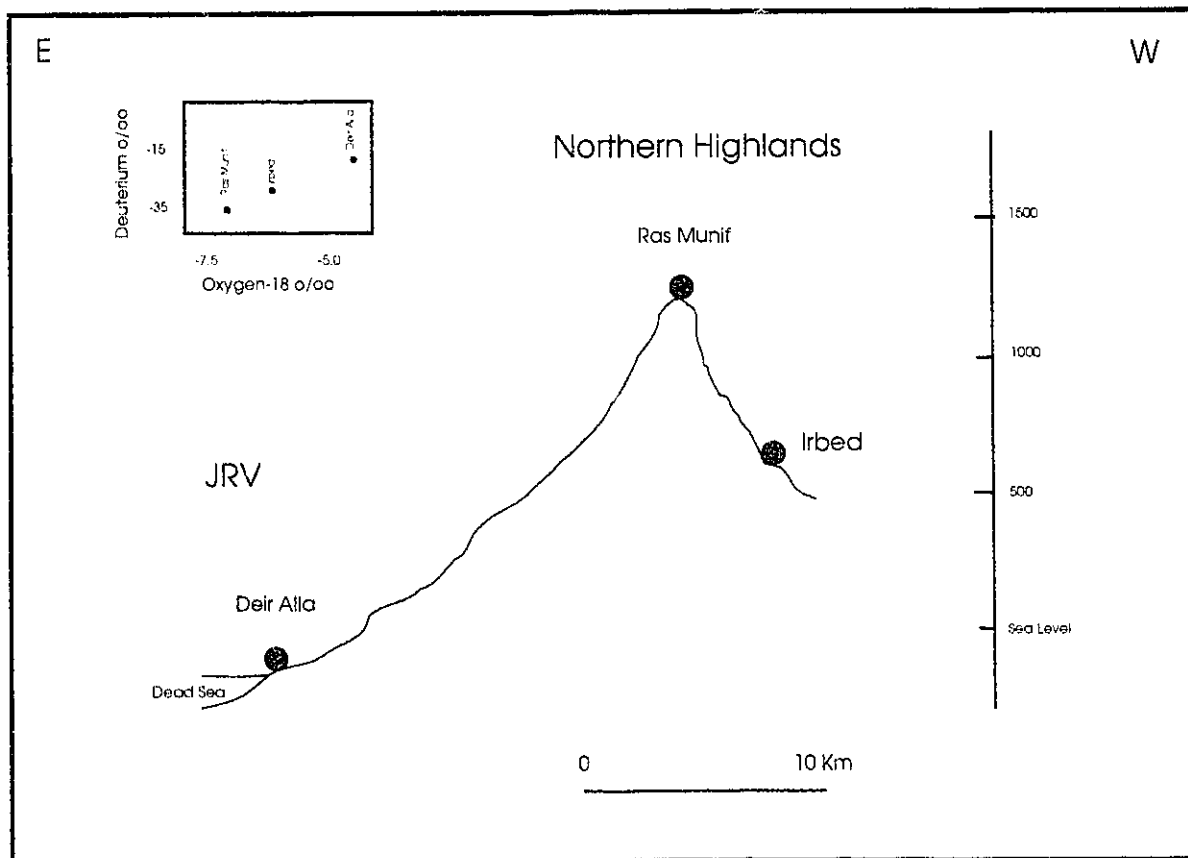


Fig.IV-2 Evolution of WMV of isotope composition of precipitation samples along cross section between JRV and Ajloun Mountains.

intermediate values for Irbed, and the most depleted values at the high elevation station of Ras Munif (Fig.IV-1). The change in ^{18}O content of precipitation with altitude is found to be - 0.2 ‰ per 100 m.

3 Amount Effect:

In the JRV the rain is scarce and the distribution of the rainfall is often random. In addition the average amount of rain is less than the Northern Highlands (Fig.III-2). This causes large variations in the stable isotopic composition. Nevertheless a slight enrichment of the heavy isotopes in months with small amounts of rain can be observed in general in all stations. Some intense rain events are more depleted in their isotopic values Appendix 1. The combined least squares calculation of amount effect and $\delta^{18}\text{O}$ for the 3 rainfall stations is:

$$\delta^{18}\text{O} = (-0.02 \pm 0.004) P - (3.7 \pm 1.82) \quad R^2 = 0.33 \quad N = 73.$$

and for individual stations are listed in Table IV-3. A relatively high correlation (0.65) for Deir Alla in comparison with the other two stations was observed. The correlation suggests that the months with higher amounts of rainfall tend to have more negative values of $\delta^{18}\text{O}$. The month with low amount of rain recorded an enriched isotope value. The average depletion rate observed in $\delta^{18}\text{O}$ for the three stations as a function of precipitation amount is approximately 1.4 ‰ per 100 mm. The large variations observed may be attributed to the evaporation effect, which can be observed from the low deuterium excess for these samples (Appendix 1) and the position of the samples in (Fig.IV-1).

IV-1.3 Tritium concentration in precipitation:

Tritium data are listed in Appendix 1, with the mean seasonal weighted values given in Table IV-2. Large variations in tritium occur during the period from 1987 to 1991, while little variation exists between the three stations. A slight increase in the weighted mean value is observed in the concentration of tritium with a decrease in distance from the Mediterranean. The weighted mean value of tritium concentration at the Deir Alla station is slightly higher than the other two stations in the mountainous region (Table IV-2). This in general found to be reverse process from what found in the adjacent area. Carmi and Gat (1973) found that there are a build up of tritium concentrations with increasing distance from the Mediterranean Sea, which parallels a depletion in stable isotopes (Gat and Dansgaard, 1972). That this not observed in the study area could be due to various topographic features that affect the cloud path, wind directions and interaction between air masses of different origin entering the area.

In general there is a decreasing tritium level in precipitation with time, which reflects the global trend following the ban on the atmospheric testing of hydrogen bombs. The good correlation between the Irbed and Ottawa rainfall stations (Ottawa station has the longest term tritium record in the world) allowed a tentative establishment of a local record for Irbed for the pre 1965 period where no monitoring was done. This correlation shows that the highest level of tritium in Irbed was approximately 600 TU in 1963 (Bajjali, 1990a). The average tritium concentration in the atmosphere from the three rainfall stations for the winter season of 1990/1991 is approximately 6 TU.

IV-2 Surface Water

Surface water represent only a minor reservoir of water resources in Jordan, with the exception of the Yarmouk River. This section includes the Yarmouk River and some sampled springs within the catchment area of the river in the study. The Mukhebeh thermal springs are the largest ones, and they will be discussed in detail in chapter six.

In the territory of Jordan there are two gauge stations at the Yarmouk River; one at the Syrian border (Maqaren, entrance of the river to the country) and the second at the Israeli border (Adasyia, before joining the Jordan River). The elevation difference between Maqaren and Adasyia is around 250 m. The base flow and the flood are measured at both stations to monitor water quantity. The flow of the river has been reduced due to the water development in Jordan and Syria (PRIDE, 1992). The average total flow of the Yarmouk River between the period 1980/1990 is 382.5 MCM/Y at Adasyia and 212.9 at Maqaren, while the base flow for the same period is 286.3 and 200.6 MCM/Y in the two stations respectively (JVA, 1992). The 85.7 MCM difference in the base flow between the two gauge stations is mainly due to the contributions from other sources downstream of Maqaren area.

Between the two stations there are two huge spring fields on both the Jordanian and Israeli sides (Fig.VI-2). Mukhebeh thermal springs on the Jordanian side have an average discharge of 11 MCM/y (after the development of the thermal water, (see section VI-2) and the Hammat Gader on the Israeli side has an average of 22.8 MCM/y (Strainsky, et al., 1979). In addition, there are other low discharge springs along the path of the river.

IV-2.1 Isotopic and chemical characteristic of Yarmouk River

The river was sampled and analyzed periodically for chemistry and isotope data in order to show the origin of the base flow of the Yarmouk River and its relationship to regional groundwater discharge. There are many springs along the path of the river used for irrigation and later the return irrigation drains toward the Yarmouk River. This water greatly influences the isotope and chemistry of the river. The isotope composition of the Yarmouk River waters shows much larger variation over time than do the springs (Table IV-5).

The isotope data of the river from the Maqaren and Adasyia areas, in addition to the average of the Maqla, Balsam, and Khaled springs and Al-Arayes pool in the Mukhebeh area, are plotted in the $\delta^{18}\text{O}$ - δD diagram (Fig.IV-3).

The graph shows that the isotopic composition of the river is clustered in two groups. The first group is more enriched in heavy isotopes and represents base flow during the dry season. The second group is more depleted, and consist of samples collected during the rainy season and winter flooding. It is clear that the water originates as precipitation coming from high altitude upstream of the river on the Syrian side.

The Khaled spring and to some degree Balsam spring are plotted in the first group. This suggest that the base flow of the river can be represented by these springs beside, which are typical of the shallow underground drainage through a system of large springs in the Syrian side. In addition, evaporation losses is an important factor during the dry season. The evaporation is assumed to occur continuously along the stream flow accompanied by changes in its isotope composition.

Table IV-5 Isotope and chemistry of Yarmouk River and some springs

NAME	DATE	0-18 o/oo	D o/oo	T.U	EC	TDS ppm	pH	Ca meq/l	Mg meq/l	Na meq/l	K meq/l	Cl meq/l	SO4 meq/l	HC03 meq/l	NO3 ppm	SiO2 ppm
Al-Arayes Pool	29-Nov-92	-2.8	-14.0	1000	640	8.8	2.2	4.2	3.8	0.1	3.7	2.6	3.8	4.6	21.5	
Balsam Sp. (Avg)		-6.0	-28.6	1.00	1009	644	7.1	5.0	2.6	3.2	0.2	3.1	1.9	5.8	0.5	25.7
Khaled Spr.	12-Oct-92	-5.6	-25.3	1.20	1320	845	7.1	4.2	5.0	4.2	0.1	4.9	2.3	6.1	7.1	
Maqla Sp. (Avg)		-6.4	-31.1	0.64	1401	894	7.2	5.9	2.7	5.3	0.3	5.6	3.3	5.4	3.8	28.7
Yarmouk R (Maq)	24-Nov-88	-5.6	-32.2	1.50	740	474	8.3	1.2	2.3	3.7	0.1	2.5	1.3	5.3	20.3	
Yarmouk R (Maq)	24-Jan-89	-5.9	-27.4	1.30	700	448	8.4	1.3	2.2	3.3	0.2	2.3	1.5	3.0	11.9	
Yarmouk R (Maq)	11-Mar-90	-5.7	-27.3	1.40	700	441	8.2	2.0	3.1	3.5	0.1	2.6	2.2	3.4	22.7	
Yarmouk R (Muk)	20-Jul-89	-5.6	-30.3	1.00	810	518	8.5	2.3	2.5	3.8	0.1	2.7	1.9	3.6	16.2	
Yarmouk R (Muk)	08-Mar-92	-7.2	-37.1	4.20	480	302	8.0	1.9	1.2	1.4	0.1	1.3	0.7	2.4	19.5	12.1
Yarmouk R (Muk)	08-Mar-92	-7.7	-38.3	4.60	520	328	8.0	2.1	1.1	1.5	0.1	1.4	0.8	2.4	20.4	12.2
Yarmouk R (Muk)	12-Oct-92	-5.6	-26.1	0.20	880	563	8.3	2.5	2.5	3.6	0.2	2.9	1.5	4.2	16.8	
Yarmouk R (Muk)	02-Dec-92	-5.4	-26.1	0.00	900	576	8.2	2.5	2.8	3.7	0.2	3.1	1.5	4.2	17.0	20.1

Balsam and Maqla Spring Represent the average of 10 samples from the period of (1987-1992)

Maq = Maqaren

Muk = Mukhebeh

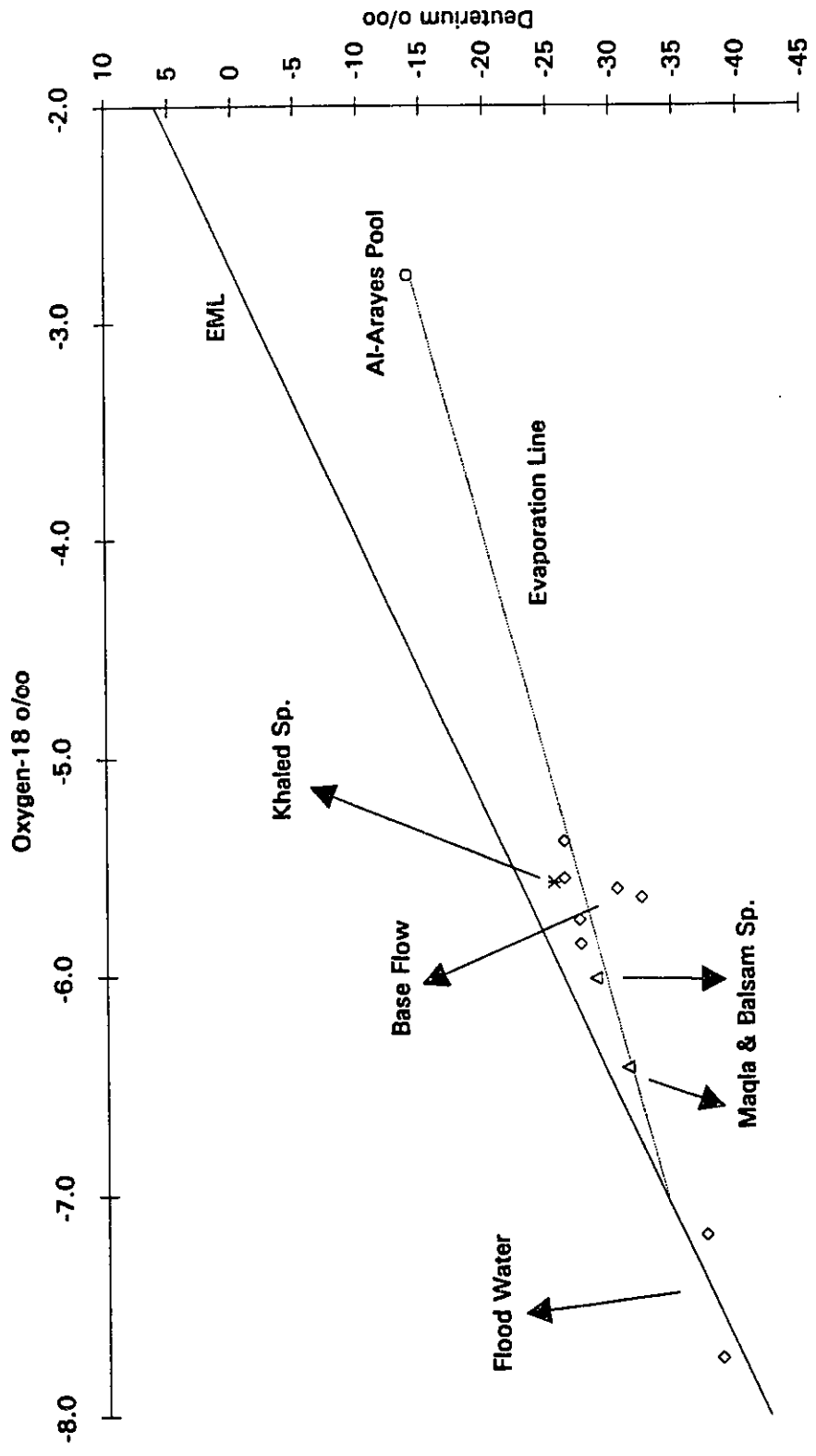


Fig.IV-3 Isotopic composition of Yarmouk River and some springs in Mukhebeh area. The EML and the evaporation line are shown also on the figure.

The graph also shows that the water of Al-Arayes pool is subject to evaporation and plots in the following regression line:

$$\delta D = 4.71 \delta^{18}O - 1.13 \quad (R^2 = 0.84)$$

Tritium measurements of the river water sampled at different times show a variation. The tritiated water is the flood water during the winter season. A stable isotope depletion associated with the high tritium concentration demonstrates this seasonality. The water having a low tritium content originates as groundwater discharge, with subsurface circulation of greater than 35 years.

The relative contribution of these two sources are further demonstrated by the isotopes and chemistry of the Yarmouk River (Fig.IV-4). Large variation in chemistry are associated with isotopic composition. The depleted and low salinity samples are flood water generated by rain, while the enriched samples represent groundwater and irrigation water overflow in addition to the evaporation losses. In addition two types of water were observed $Ca^{2+} - HCO_3^-$ and $Na^+ - HCO_3^-$. The former was observed for the more depleted isotope and the latter for the more enriched isotope. From both graphs we can observe that the Yarmouk samples with low tritium values are located between the spring waters and the Yarmouk River water with high tritium. This means that the base flow of the river is a mixture of groundwater and flood water in winter time, and dominated by groundwater discharge in summer time.

The Yarmouk River waters also have a contribution from the irrigation water overflow indicated by the high NO_3^- concentration of the river waters Table IV-5.

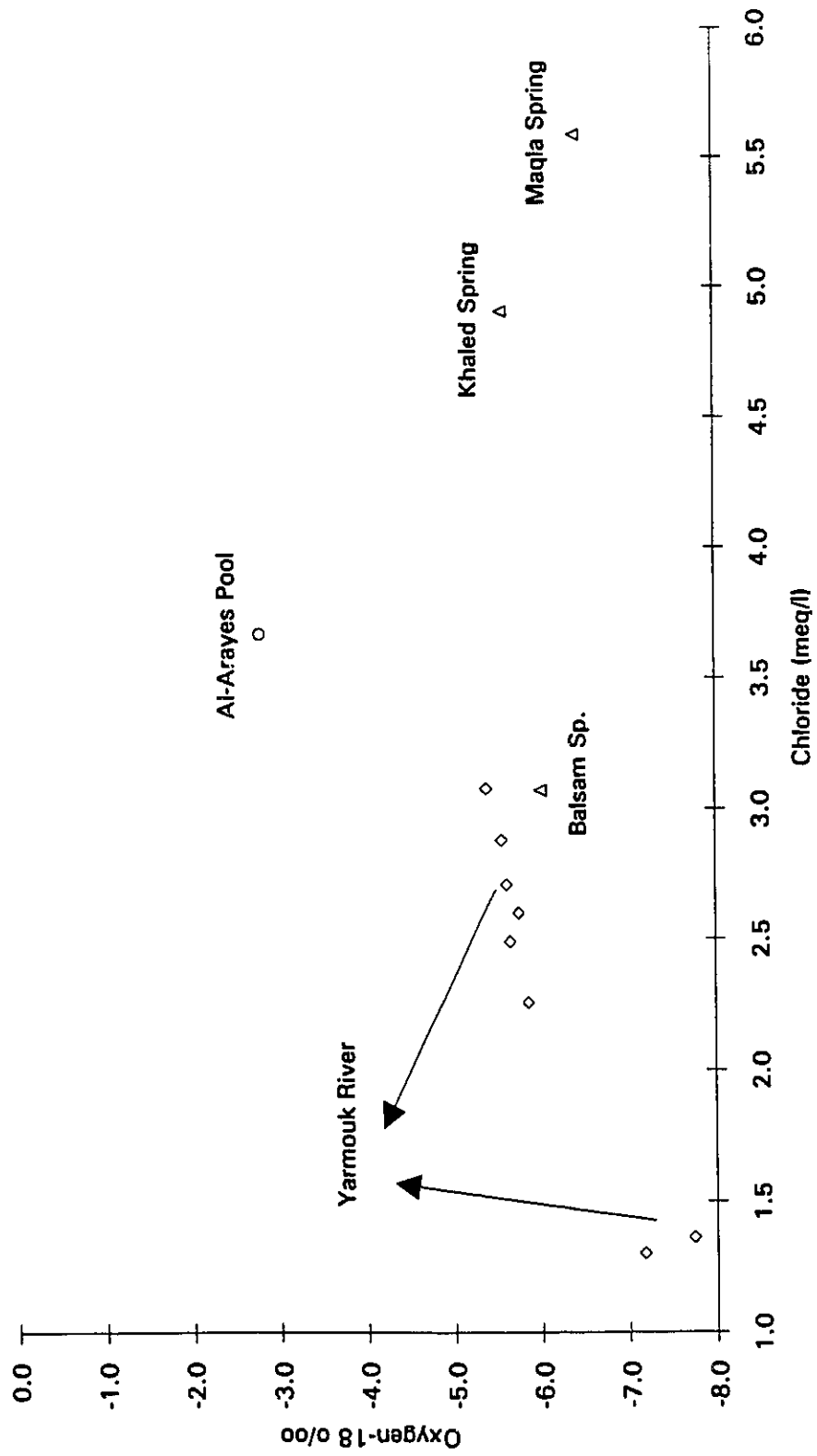


Fig.IV-4 Chloride concentration versus oxygen-18 for the Yarmouk River and some of the Mukhebeh springs.

Chapter 5

Non-Thermal Groundwater

There are several well fields in the study area, where non-thermal groundwater exists. These non-thermal groundwaters are of great importance for this study. The non-thermal groundwater will help us to understand the origin and general circulation pattern for deep thermal groundwaters and their discharge in the JRV, Mukhebeh and Ramtha areas. The chemistry and isotopic composition of the groundwaters are vital to understand the mechanism of recharge and the direction of the subsurface flow. In addition it will assist in determining the relation between the thermal and non-thermal groundwaters. There are 5 non-thermal well fields located in the study area (Fig.I-2), (i) Nuaimah (Ajloun Mountains) (ii) Side Wadies (iii) Adasyia (JRV) (iv) Ramtha and (v) North-East Desert.

The groundwater in these aquifers is under phreatic conditions, with exception Wadi Al-Arab area in the Side Wadies. The aquifer in this well field is confined and its temperature varies between 25 to 30 °C.

There are three distinct, actively-recharged aquifer systems with groundwater of different ages. The first aquifer is the alluvium and found in Adasyia, the second aquifer is the (B4), and is found in the Ramtha area. Both are considered shallow aquifers. The third aquifer is the major aquifer (B2/A7), which outcrops in different places of the study area, mainly in Nuaimah and along the side wadies. Since there are different types of aquifers, the area can be divided to 3 main sectors.

Groundwater can be classified according to location, water table condition, salinity,

temperature and residence time. The following reviews these major characteristics followed by more detailed discussion for each area.

1-The first group is located in Nuaimah and the side wadies. The groundwater is fresh, of meteoric origin and modern in age. The temperature is about 20 °C.

2-The second group consist of fresh meteoric groundwater of non-contemporary recharge is located in Wadi Al-Arab area, Ramtha and North Desert. The aquifer is under water table and artesian conditions. The type of water is considered warm in Wadi Al-Arab and Ramtha areas with temperatures around 30°C.

3-The third group is comprised of brackish meteoric groundwater from contemporary recharge. The area is located in the Adasyia area near the convergence of Yarmouk River with the Jordan River. The salinity of the aquifer is considered brackish and ranges between 1500 and 13,000 ppm.

This study will begin with the Nuaimah area, defined by previous researchers as a recharge area, and then will be followed by the areas listed above. These areas are of great importance in order to establish the recharge areas for the deep thermal groundwaters.

V-1 Nuaimah area

Nuaimah (down hill from the Ajloun Mountains), is situated in the southern part of the study area (Fig.I-2), covers an area of over 100 km². The average annual rainfall is approximately 600 mm. The carbonate bedrock terrain is covered by thin soil up to one meter deep. The texture of the soil is clay and silty loams over permeable subsoil gravel

and karstic limestone (Abu-Ajamieh, et al., 1988). Several karstic caves are exposed in the area of Nuaimah town. Such karstic caves can be seen in the vicinity of the productive wells in the Nuaimah area. The elevation of the study area varies from 1000 m south-west (Qita Yunis) to 620 m north-east in the Khirbat ad Dahma.

There are seven wells drilled in the area (Fig.V-1.1), designated by numbers 1 to 7. The general information about these wells is listed in Appendix 2. The unsaturated zone is 150 to 250 m deep. Five wells (1 to 5) were sampled several times during the period 1987 to 1993 for chemical and environmental isotope (Appendix 3).

The outcropping formation in the area is late Cretaceous (Turonian-Campanian) which consists of limestone and silicious limestone. The Turonian formation is a Carboniferous karstic limestone with a very low matrix porosity. The water movement is almost entirely by means of dissolution features and fractures. All the wells in the area penetrate the Turonian carbonate aquifer (A7).

Several investigators (Parker, 1969, Joudeh, 1983, NJWRIJS, 1989, EL-Naser, 1991) indicated that groundwater flow is north and north-west from the Nuaimah area (Fig.I-3). Their study is based on the water level gradients from limited number of drilled boreholes.

In the area there is only one observation well (Yamoon), well No.6 on the map. This well had been abandoned for several years, and only in 1991 was the well started to be used to monitor the groundwater level in the area. The total depth of the well is 267 m. Monitoring data show that there are fluctuations in the water level (Fig. V-1.2). The sharp fluctuation shown in the graph was due to the rainy season in the winter of 1991.

In this particular winter season, the area received a large amount of rain. This amount of rain in the winter season affects directly the recharge to the B2/A7 aquifer. The water level thus rises by up to 25 m. This value is a good indication of the sensitivity of this karst terrain area to the precipitation. The amount of rain for the period from October 1991 to April 1992 was found to be 1151.4 mm in the Ras Munif rainfall station, while the 7 year average for the same station is 633.5 mm Table III-1. From these available values, we can conclude that the amount of recharge to the aquifer is variable. A temperature of 20.9 - 21.8 °C has been observed in the wells of the recharge area.

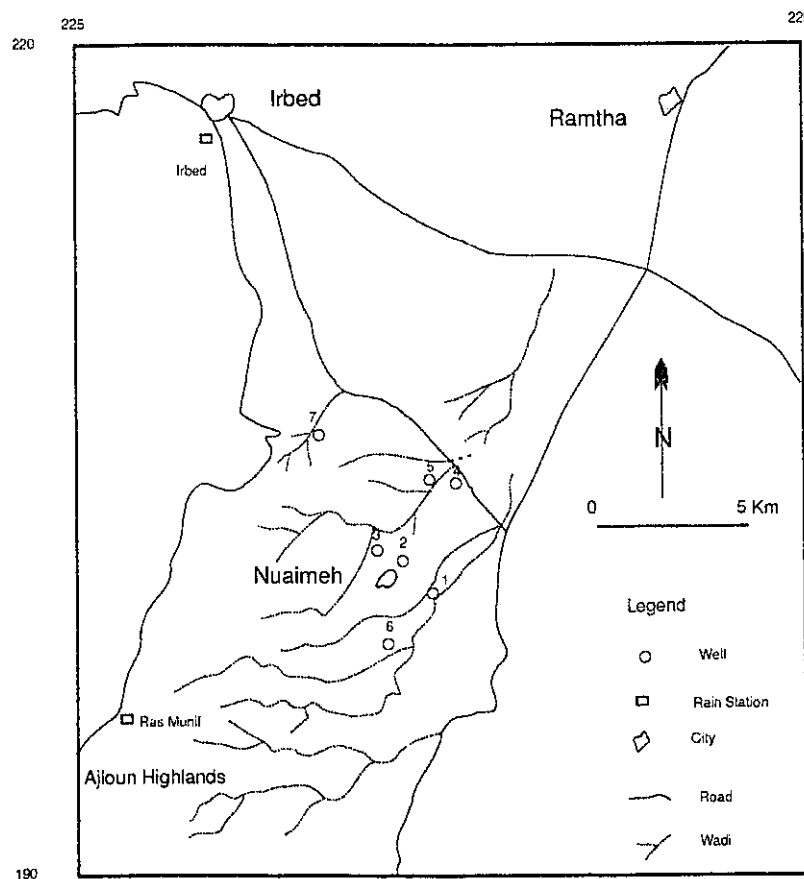


Fig.V-1.1 Location Map of Nuaimah Area

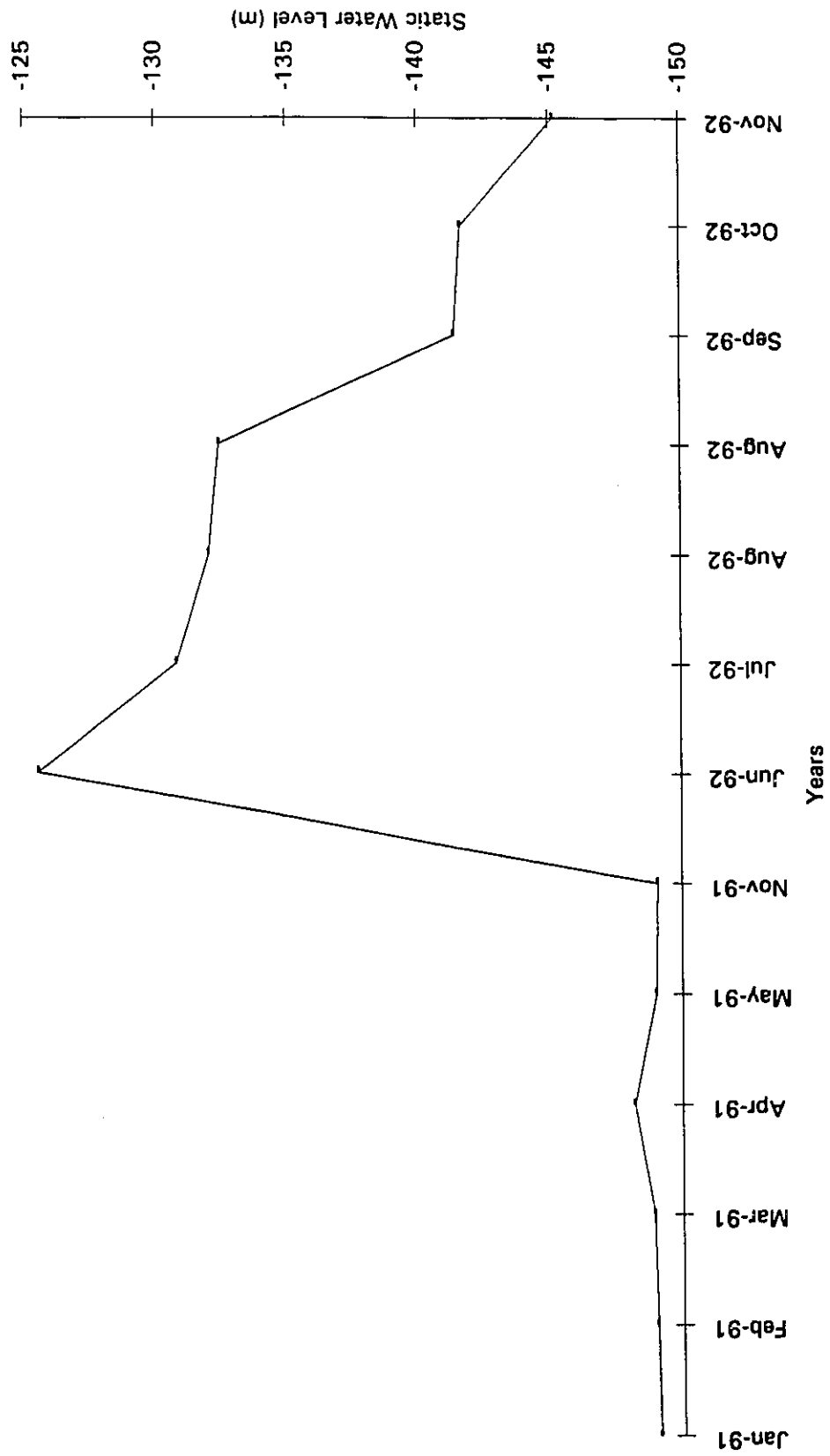


Fig. V-1.2 Water Level Hydrograph for Yamoon Observation Well

V-1.1 Recharge Estimation

Recently several researchers tried to estimate the recharge to the area. El-Naser, et al. 1992 estimated the direct recharge in 1991/1992 to the area from the Yamoon observation well to be 45.6 MCM, while previous studies estimated the mean annual direct recharge to the area to be 21.5 MCM (NJWRIJS, 1989).

In this study an attempt was made to estimate the recharge by a chloride mass balance. This technique relies on the chloride concentration of both the rain and groundwater (Houston, 1987). Except in areas of evaporite deposits, chloride is generally a conservative anion in natural water. Therefore, chloride in rainfall (derived from sea water aerosol) usually passes through the soil zone to the water table without change in concentration. The ratio of chloride concentration in rainfall to that of groundwater is then a measure of recharge, thus:

$$\text{Recharge (mm)} = \frac{\text{rainfall (mm)} \times \text{mg Cl}^{-1} \text{ rainfall}}{\text{mg Cl}^{-1} \text{ groundwater}}$$

The recharge from the above equation can be estimated to be between 19 and 27 MCM. The chloride concentration of the Irbed and Ras Munif rainfall stations (Table IV-1) was used to calculate the recharge. This calculation does not account for contribution from the aquifer material by leaching in the subsurface flow. Yet the concentration of evaporite containing Cl⁻ anion in the limestone is usually negligible.

V-1.2 Hydrochemistry of Groundwater

The chemistry of well samples is considered fresh, TDS values range between 340

and 435 ppm. The composition of the water (by equivalent) is: $\text{Ca}^{2+} > \text{Mg}^{2+} > \text{Na}^+$ and $\text{HCO}_3^- > \text{Cl}^- > \text{SO}_4^{2-}$. The average data of dissolved ions (Table V-1.1) are plotted in a fingerprint diagram (Fig. V-1.3), showing similarity for the ionic composition of water in all five wells. The results indicate that even if the groundwater apparently underwent similar patterns of geochemical evolution, their water quality varied slightly among the five wells. The $\text{Ca}^{2+} - \text{HCO}_3^-$ chemical facies of these groundwaters reflect dissolution of carbonate aquifer. The homogeneity of these two parameters indicates that the lithology is mainly composed of calcite.

Table V-1.1 Average Chemical Composition of the groundwater

No. of well	TDS	pH	Ca^{2+}	Mg^{2+}	Na^+	K^+	Cl^-	SO_4^{2-}	HCO_3^-	NO_3^-
	ppm		meq/l	meq/l	meq/l	meq/l	meq/l	meq/l	meq/l	ppm
1	403	7.7	3.57	2.14	0.8	0.11	1.21	0.18	4.6	33.5
2	402	7.5	3.45	1.98	0.89	0.07	1.16	0.22	4.45	40.8
3	349	7.4	3.15	1.65	0.54	0.04	0.94	0.17	4.27	20.7
4	382	7.4	3.45	1.79	0.78	0.05	0.98	0.11	4.57	25.1
5	397	7.4	3.66	1.8	0.85	0.04	1.1	0.3	4.67	27.4

The water is supersaturated with respect to calcite and dolomite, both in winter and summer (Table V-1.2). The reason for this is the dominance of calcite in the local Upper Ajloun Group. As the water enters the saturated zone, it continues to dissolve more calcite and dolomite until saturation. The water infiltrates through the karstic formation, and at this stage the water attains a stable chemical composition.

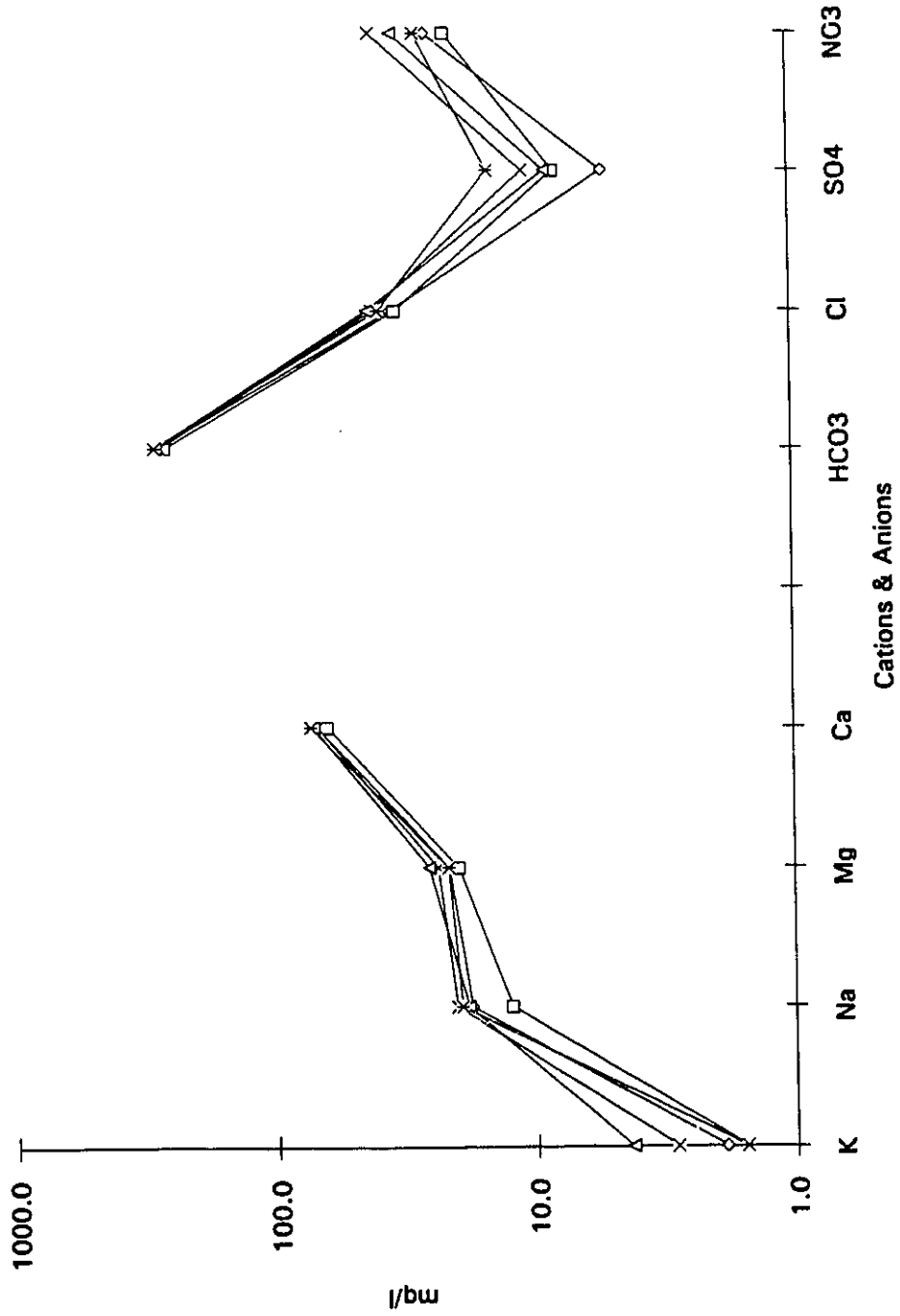


Fig.V-1.3 Fingerprint diagram for Nuaimah area, Composition of the dissolved salts (Table V-1.1)

Table V-1.2 Ionic strength, ratio and saturated indexes

No. of well	Ionic Strength	Log P_{CO_2}	SI _{calcite}	SI _{dolomite}	Na ⁺ /Cl ⁻ molar ratio
1	0.0091	-2.28	0.49	1.85	0.66
2	0.0089	-2.09	0.27	1.38	0.76
3	0.0077	-2.02	0.15	1.09	0.57
4	0.0119	-1.98	0.16	1.12	0.79
5	0.0089	-1.96	0.21	1.21	0.77

The log partial pressure of the CO₂ of the samples is in the range between -1.96 and -2.28. This value is much higher than the log P_{CO_2} of the atmosphere (-3.5), which shows that CO₂ from the soil is incorporated during the infiltration through the unsaturated zone.

Groundwater SO₄²⁻ concentrations vary with well location and depth. They range from 0 to 0.30 meq/l, with one extreme value of 0.86 in well No.3. The deeper wells (Appendix 2, > 300 m) recorded relatively constant SO₄²⁻ concentrations and are elevated compared with those of shallower depth. The low concentration and the wide variability of SO₄²⁻ concentration in well No.3 (Depth 196 m) can only indicate that there are variable sources of SO₄²⁻ other than the soluble sedimentary minerals such as gypsum (CaSO₄·2H₂O) and anhydrite (CaSO₄), that are responsible for the origin of SO₄²⁻ in groundwater. Some SO₄²⁻ may be introduced into the groundwater from rainfall. The rainfall at the Ras Munif and Irbed stations was enriched in sulphate Table IV-1. In

addition the seasonal fertilizing with ammonium sulphate may also affect the concentration of SO_4^{2-} in groundwater.

The pH of the groundwater ranges between 7.19 and 8.03; therefore, essentially all the dissolved carbonate and all the alkalinity is in the form of HCO_3^- . Chloride is the most important anion after HCO_3^- , and the Na^+/Cl^- show a range from 0.57 to 0.79 Table V-1.2. Three sources of Cl^- likely dominate: 1-Salt derived from rainwater and air borne salts. 2- The dissolution and/or leaching from marine carbonate rock including its impurities. 3- Anthropogenic sources, since chloride is a very common pollutant from organic and inorganic sources. In the Nuaimah area it can occur particularly from human and animal wastes. All these possibilities exist since the Na^+/Cl^- is highly variable.

The composition of the water demonstrated a slight variation in the TDS (Department of Water Resources Develop., 1987). However, significant variations were recorded for the NO_3^- concentration. The concentration of nitrate in all the wells was found to be higher than the average nitrate level of the natural abundance of groundwater which is less than 5 ppm. The elevated NO_3^- level can be attributed to anthropogenic sources, which clearly classifies the Nuaimah region as a recharge area. Atmospheric precipitation is an important source. The concentrations of NO_3^- in rainfall at the Ras Munif and Irbed stations are in the range of 1.2 to 5 ppm.

Other NO_3^- sources may include sewage effluent through seepage from septic tanks, agricultural activity and the use of manure and nitrogen fertilizers, and storm-water runoff in wadis transfer of soil nitrate to the groundwater. Well 1 is located in the middle of an animal farm (poultry). Both natural (manure) and chemical fertilizers are used for

the cultivated crops in the area. As yet, none of the well samples shows a nitrate concentration exceeding the permissible limits for drinking purposes (45 mg/l) over a period of 20 years.

V-1.3 Isotopic Composition of Groundwater

The stable isotope data of the five wells in conjunction with the WMV of rain of the three rainfall stations (Ras Munif, Irbed and Deir Alla) are plotted on the $\delta^{18}\text{O}$ - δD diagram in (Fig.V-1.4). The groundwater samples reveal a wide variation in stable isotope contents. The variation in the stable isotopic composition of the groundwater extend over a range of 2 ‰ and 4.5 ‰ in $\delta^{18}\text{O}$ and δD respectively. In addition, the samples are clustered widely between the EML and GML.

The variation indicates that the groundwater is a mixture of two sources: 1-direct recharge, the karstic limestone aquifer respond directly to the precipitation. The direct recharge to the area is very well demonstrated by the low TDS and high concentration of tritium in the groundwater. The precipitation data given in (Fig. IV-1) also show this wide variation in isotopic composition and the groundwater composition falls between the WMV of Irbed and Ras Munif precipitation.

From the graph we can see that the recharge altitude for the groundwater in Nuaimah area is located in the highlands between Ras Munif and Irbed. This suggest that the precipitation that fell in the South-West of the Nuaimah area presents the main recharge altitude for the groundwater, which is between 850 and 950 m elevation. The topography of the 30 km² area where the wells are located have a variation in altitude of

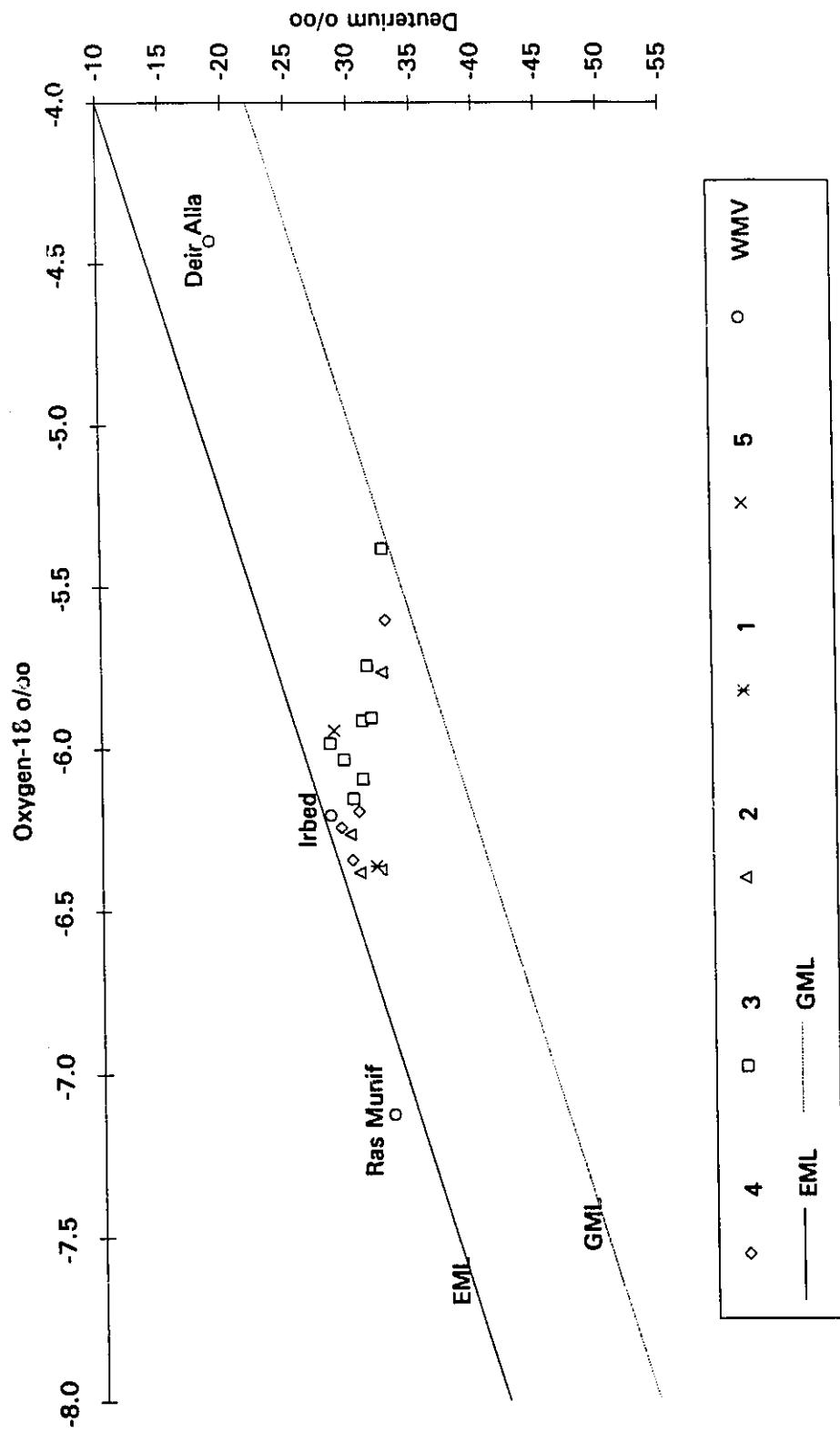


Fig. V-1.4 Isotope data of the five wells in Nuaimah area and the WMV of the precipitation

approximately 400 m. This generates isotopic heterogeneities in precipitation and shallow groundwaters.

2-The second source is the irrigation return flow, the irrigated water takes a longer time to infiltrate and become enriched owing to evaporation. This phenomena is very well seen from the deviation of some samples from the EML, The larger deviation is seen in summer. In summer, there is no rain and the groundwater becomes the main source for irrigation and part of the water goes back into the aquifer as an evaporated return flow.

V-1.4 Radioactive isotope of Groundwater

1-Tritium:

Tritium can be used to elucidate the residence time of recently recharged groundwater (Erikson, 1967). The groundwater in Nuaimah wells have variable tritium concentrations (Fig.V-1.5). The tritium concentration in all five wells shows a significant contribution from bomb-tritium, which means recent contributions to the aquifer system. The concentrations of tritium in some wells are close to those found in precipitation of Ras Munif for the same period. Thus the transit time through the unsaturated zone is relatively short. Seasonal variations are also observed.

The water sources show at times an irregular pattern indicating that tritium introduction may come about by an irregular event, such as flooding (cf., No.2). Well No.2 is located within Wadi Al Assara passing through Nuaimah town. The high rate of infiltration from the bottom of the wadi during winter time is the most probable evidence for the high concentration of tritium in this well. In addition, the rapid response of the

water level in the Yamoon observation well, rising up about 25 m in winter 1991 due to the intense rain is another indication of the good correlation between the amount of rain and the recharge events. The replenishment area is in the formation outcrops in the Ajloun Mountains and in the area of the wells.

Replenishment to the phreatic aquifer is believed to occur from local rain, flood flows and excess irrigation waters. Carmi and Gat (1973), observed that the flood events were immediately (during the same or the following day) reflected in the tritium data of wells.

2-Carbon-14:

The ^{14}C were sampled from few non-thermal wells from different parts of the study area to establish input function for thermal waters. Due to the complexity of carbon geochemistry in the groundwater, the ^{14}C systematics of non-thermal and thermal water are discussed together in one section (VI-5.2). This will enable us to characterize the various processes affecting the initial ^{14}C content in groundwater which must be corrected for. The ^{14}C activity in Nuaimah wells was found between 59.6 and 63.1 pmc in wells No.3 and 1 respectively. These groundwaters are tritiated and hence, modern, these low ^{14}C activities reflect closed system carbonate dissolution. They can therefore be considered as initial ^{14}C activities (A_0) for radiocarbon age calculations carried out for older groundwater discussed in chapter six.

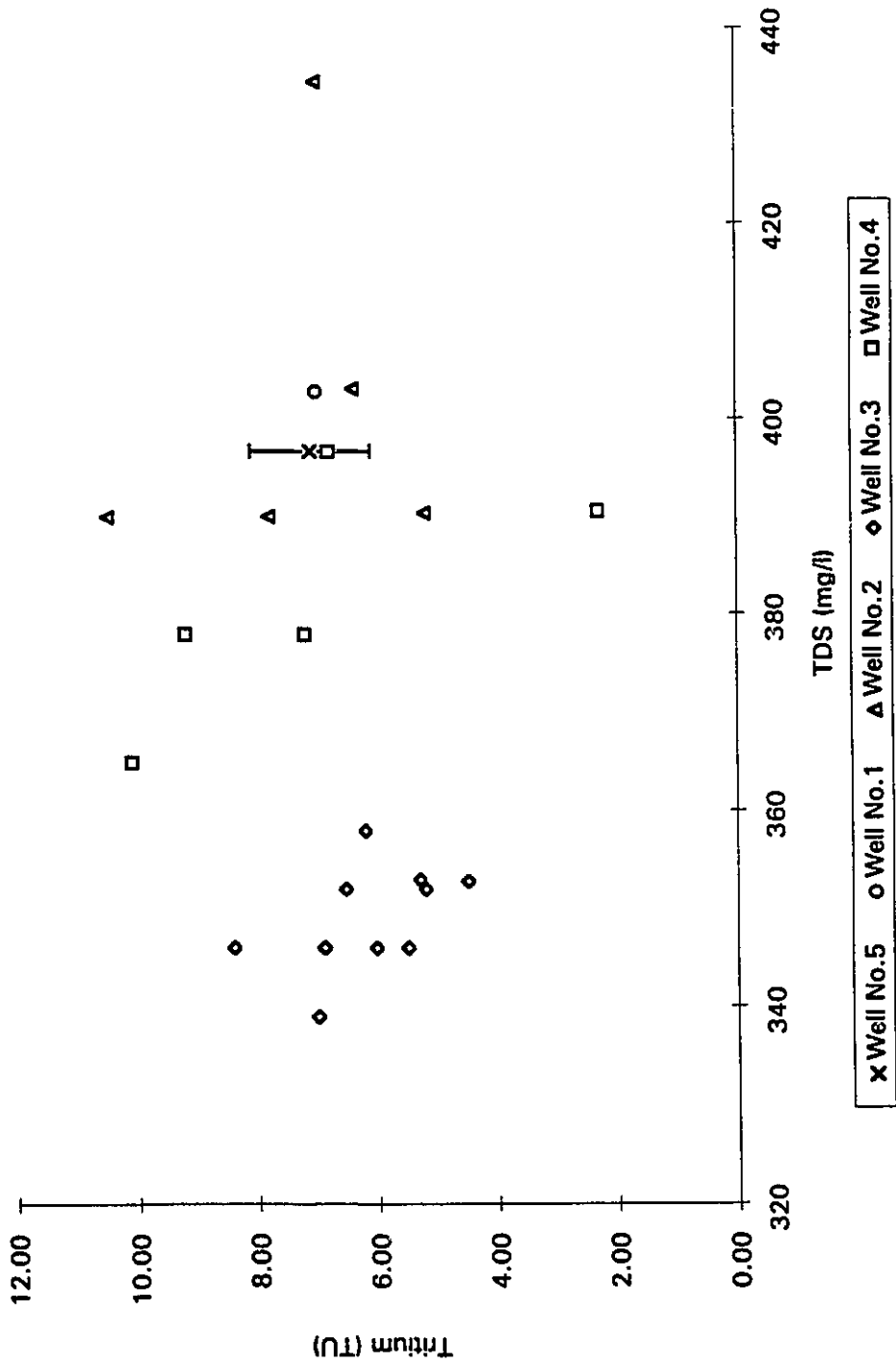


FIG.V-1.5 TDS versus the Tritium in the Groundwater of Nuaimah area. The error bar of the tritium is shown in Wadi Al-Arab well No.5

V-2 Side Wadies Area

This area is of significance as it is located downhill of the recharge area of the Ajloun Mountains. The importance of this area is due to its local recharge as it lies at an elevation (200 to 600 m asl) below that of the Nuaimah area. The area is hilly and located to the east of the JRV and to the west of the Ajloun Mountains (Fig.V-2.1). Several wadies run from east to west, where they drain toward the JRV.

The catchment area of these wadies starts from Ajloun Dome and ends up in the JRV. The topography is very steep, ranging from approximately 1200 m asl in the Ajloun Mountains to 200 m bsl in the Rift Valley. The difference in elevations creates a significant runoff in winter time: the combined average annual runoff from Wadi Al-Arab, Wadi Ziglab, Wadi Jurum and Wadi Yabis) was estimated to be 53 to 61 MCM (Baker and Harza, 1955; GTZ, 1977).

Two dams were constructed in Wadi Al-Arab and Wadi Ziglab. They collect flood water in upstream areas of the Jordan Valley. Then their water flows by gravity to the JRV to be used for different purposes, mainly for irrigation. The capacity of the two dams is 20 and 4.3 MCM respectively.

In the side wadies there are several springs discharging from different aquifer systems (NJWRIJS, 1989). The total discharge of the springs in the whole side wadies was estimated to be 82 MCM/Y, while the total number of springs is 210 (Department of Water Resources Development, 1987).

In the beginning of the 1980's a number of wells were drilled in the Wadi Al Arab area. The purpose of drilling is to meet the increasing demand for water supply to the

Irbed area. The increasing abstraction from the Wadi Al-Arab well field affected the discharge of the springs and gradually these springs disappeared (Al-Momani and El-Mousa, 1987). The base flow of Wadi Al-Arab decreased from 30.14 MCM in 1982 to 3.12 MCM in 1987 and to zero in the following years (WAJ-Files). In addition, a number of private wells are used as a main source for irrigation purposes.

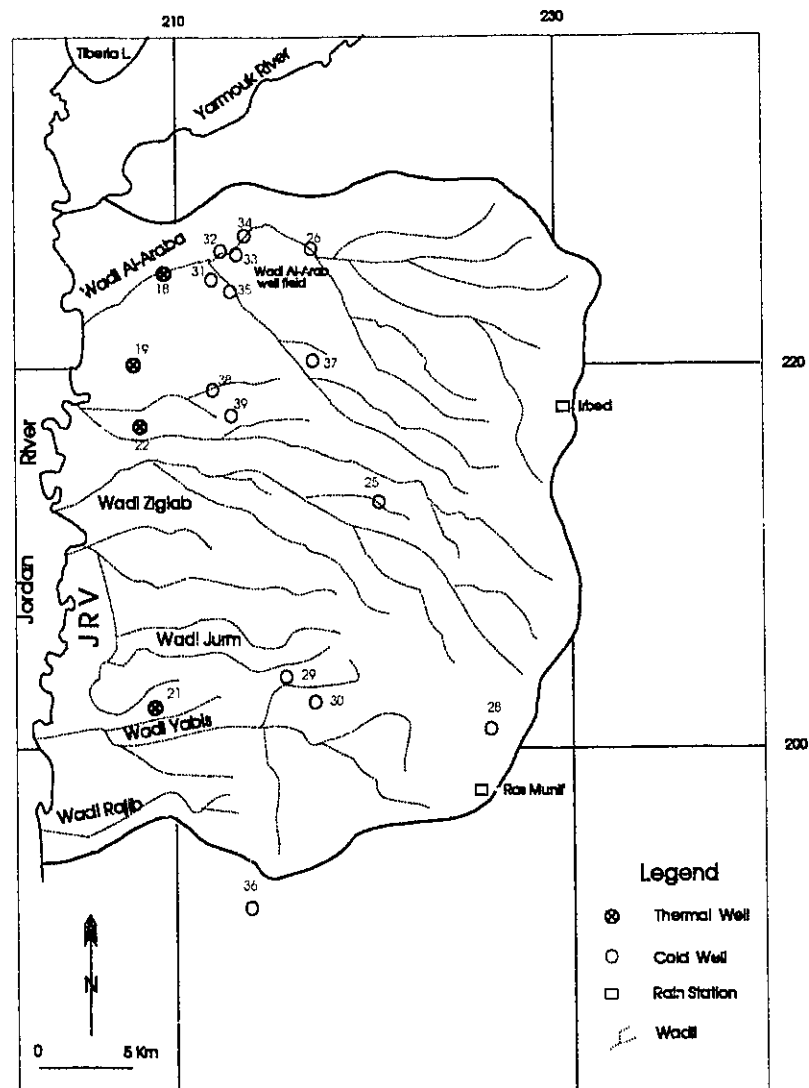


Fig. V-2.1 Location Map of the Side wadies well fields

The recharge to the side wadies is from the Ajloun Highland region and Yarmouk Basin. (Parker, 1969, Joudeh, 1983, NJWRIJS, 1989). The Ajloun Dome is considered to be a water divide for both the Yarmouk Basin and Side Wadies (NJWRIJS, 1989). The groundwater moves under (i) water table conditions, and then shifts to (ii) confined conditions. The former is close to the recharge area while the latter is located in Wadi Al-Arab.

V-2.1 Phreatic aquifer

There are several wells tapping the B2/A7 in different parts of the side wadies (Fig.V-2.1). The depth of these wells is between 260 to 600 m, and they are located above sea level. Government wells are used for domestic water supply in the villages within the area and private wells are used for irrigation. The yield, water level and other information about the wells can be found in Appendix 2.

In the area there is one observation well, Kufr Assad, constructed in 1982 to monitor the level and quality of groundwater. The hydrograph (V-2.2) indicates there was a general decline in the water table and that a clear recharge took place in the area during the rainy season. The rainy period in winter 1991/1992 is very clearly demonstrated in the graph. In this year the area received a large amount of rain in comparison with previous years.

V-2.1.1 Hydrochemistry of the groundwater

Very low variations in salt content were observed in water samples. The TDS

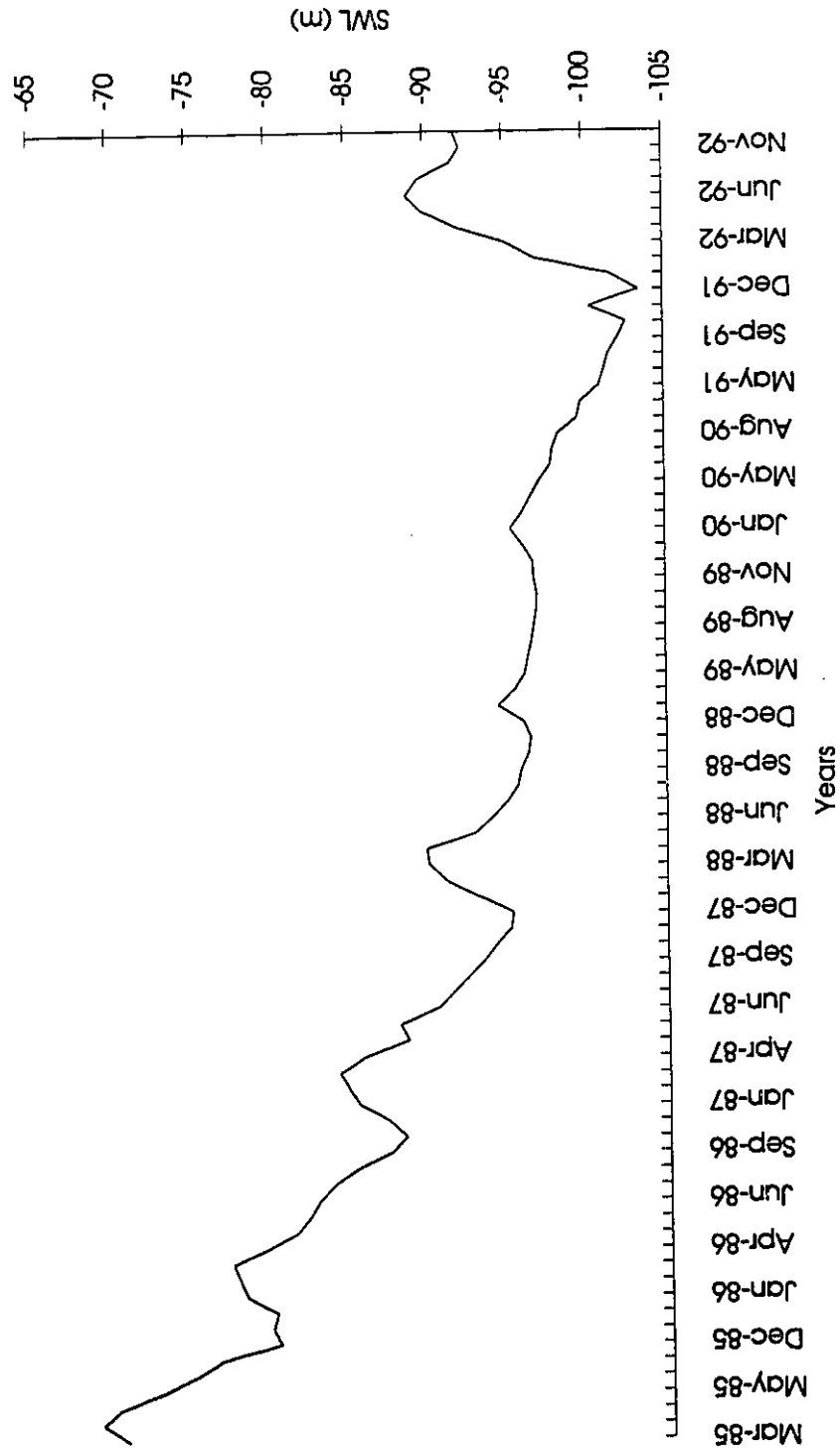


Fig. V-2.2 Water Level Fluctuation In Kufr Assad Well

varied between 275 to 880 ppm Appendix 3. The chemical composition of some water samples was collected several times, the average is listed in (Table V-2.1).

Table V-2.1 Average Chemical Composition of the groundwater

Well NO.	TDS	pH	Ca ²⁺	Mg ²⁺	Na ⁺	K ⁺	Cl ⁻	SO ₄ ²⁻	HCO ₃ ⁻	NO ₃ ⁻
	ppm		mg/l	mg/l	mg/l	mg/l	mg/l	mg/l	mg/l	mg/l
30	557	6.9	120.7	29.26	22.48	2.64	39.70	43.30	430.7	17.26
29	533	7.3	123.0	24.30	19.32	2.83	37.31	34.56	432.4	8.82
27	275	7.7	58.2	13.37	9.20	4.30	12.76	4.80	226.9	26.80
36	470	7.3	92.2	26.59	14.15	2.28	39.59	17.84	358.4	22.28
28	356	7.5	70.0	18.95	12.94	3.03	26.45	19.87	271.2	26.98
26	534	7.2	111.7	22.62	33.67	2.89	59.34	78.14	313.7	34.83

The chemical composition of groundwater is controlled by rock-water interaction. The groundwater in these side wadies wells was found to be of Ca²⁺ - HCO₃⁻ type. Ion composition of all groundwater shows the pattern Ca²⁺ > Mg²⁺ > Na⁺ and HCO₃⁻ > Cl⁻ > SO₄²⁻. The ionic distribution for Kufr Assad is an exception: the groundwater is Ca²⁺ > Na⁺ > Mg²⁺ and HCO₃⁻ > SO₄²⁻ > Cl⁻. The well location is in one of the main wadies in the Wadi Al-Arab area, where the waste water used to be disposed in the wadi from the Irbed treatment plant before 1987 (Rashdan and Al-Momani, 1990). The waste water used to discharge in the wadi, and after 1987 the water connected with a pipe to discharge downstream of the Wadi Al-Arab Dam. The chemistry of the groundwater well deteriorated significantly due to infiltration from the waste water base flow to the aquifer. The relatively high concentration of Ca²⁺, Na⁺, SO₄²⁻, Cl⁻ and NO₃⁻ (Table, V-2.1 and Fig.

V-2.3) in the Kufr Assad well (No.26) is a strong indication that a source of sewage pollution affected the area of the well. This is also obvious from the high level of nitrate which increases 4 to 5 times the concentration of natural abundance of nitrate in groundwater. The sources of this nitrate is organic (sewage) and inorganic (fertilizer). In some wells where results of water analyses were available from the same well for several years, salinity has increased within 7 years by 45 to 130 mg/l (Appendix 3). The highest salinity in the area is recorded for the Kufr Assad well, it is as high as 883 mg/l of TDS. The groundwater is calculated to be supersaturated with respect to calcite and dolomite (Table V-2.2). The log of P_{CO_2} is higher than that of the atmosphere, which indicates that the unsaturated zone is rich in organic material. That can affect the rapid dissolution of carbonate material and attain the saturation level of calcite in a very short period.

Table V-2.2 Ionic Strength and Saturation Indexes

Well No.	Ionic Strength	SI _{Calcite}	SI _{Dolomite}	Log P_{CO_2}
30	0.013	0.12	0.91	-1.42
29	0.013	0.47	1.50	-1.77
27	0.006	0.41	1.46	-2.52
36	0.011	0.28	1.31	-1.82
28	0.008	0.32	1.37	-2.22
26	0.020	0.25	0.94	-1.47

V-2.1.2 Isotopic composition of the groundwater

The stable isotope data for the side wadies for all samples from the study area that have an appreciable amount of tritium are plotted on a $\delta^{18}O$ - δD diagram (Fig.V-2.4).

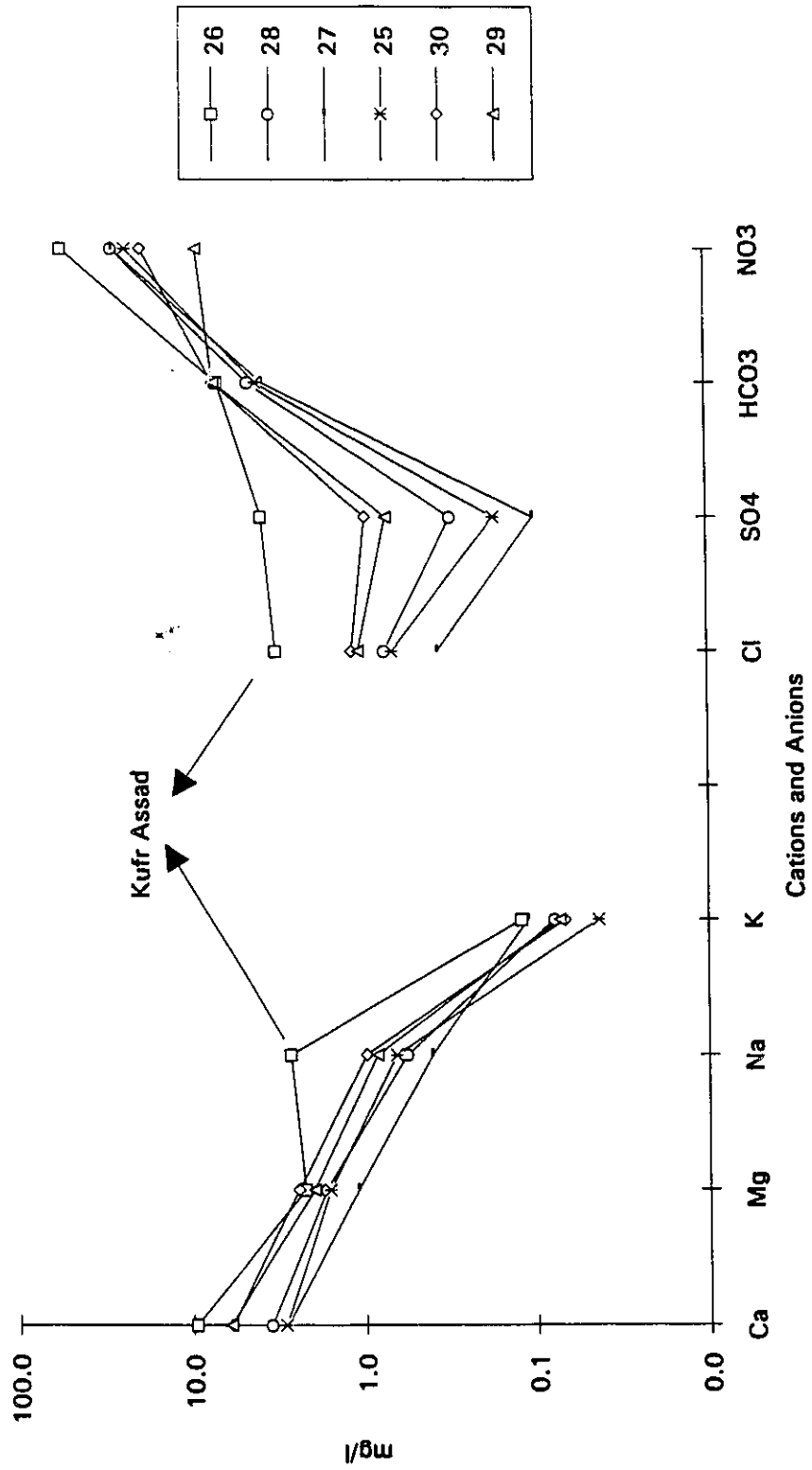


Fig. V-2.3 Composition of the six wells in the Side Wadi area. Sample 26 is enriched in Cl, Na and NO3

The groundwater samples are scattered widely around the EML. They show a similar pattern to the stable isotope composition of groundwater in the Nuaimah area.

The data in general plotted close to the Nuaimah wells and some samples show a slight enrichment from the groundwater of Nuaimah groundwater. This suggest that the recharge elevation are similar for both areas. Some groundwater was sampled more than twice and these samples showed a variation in stable isotope content. These variations are identical to the variation of the stable isotope content of the precipitation that recharge the aquifer in the area, which demonstrates modern, direct recharge to the aquifer.

Two samples from the observation Kufr Assad well (No. 26) deviated from the EML, which suggests that enriched surface waters occur in the area. The enriched values come from contaminated water subject to evaporation before infiltration into the aquifer. This water is the wastewater from Irbed Treatment Plant.

Based on the location of the groundwater and rain samples in the diagram we can say that there are two factors that affect the difference in their isotopic composition. The first is a direct recharge from precipitation and runoff. The second is that the water is subject to evaporation before infiltration.

V-2.1.3 Radioactive isotopes in the groundwater

The tritium content in these groundwaters vary between 3.5 to 9.9 TU. These values are close to the current level in the precipitation, indicating a residence time between 2 to 5 years. Deir Yusef well (No. 27) demonstrated the highest tritium level (9.9) and the lowest salt content (275 ppm):

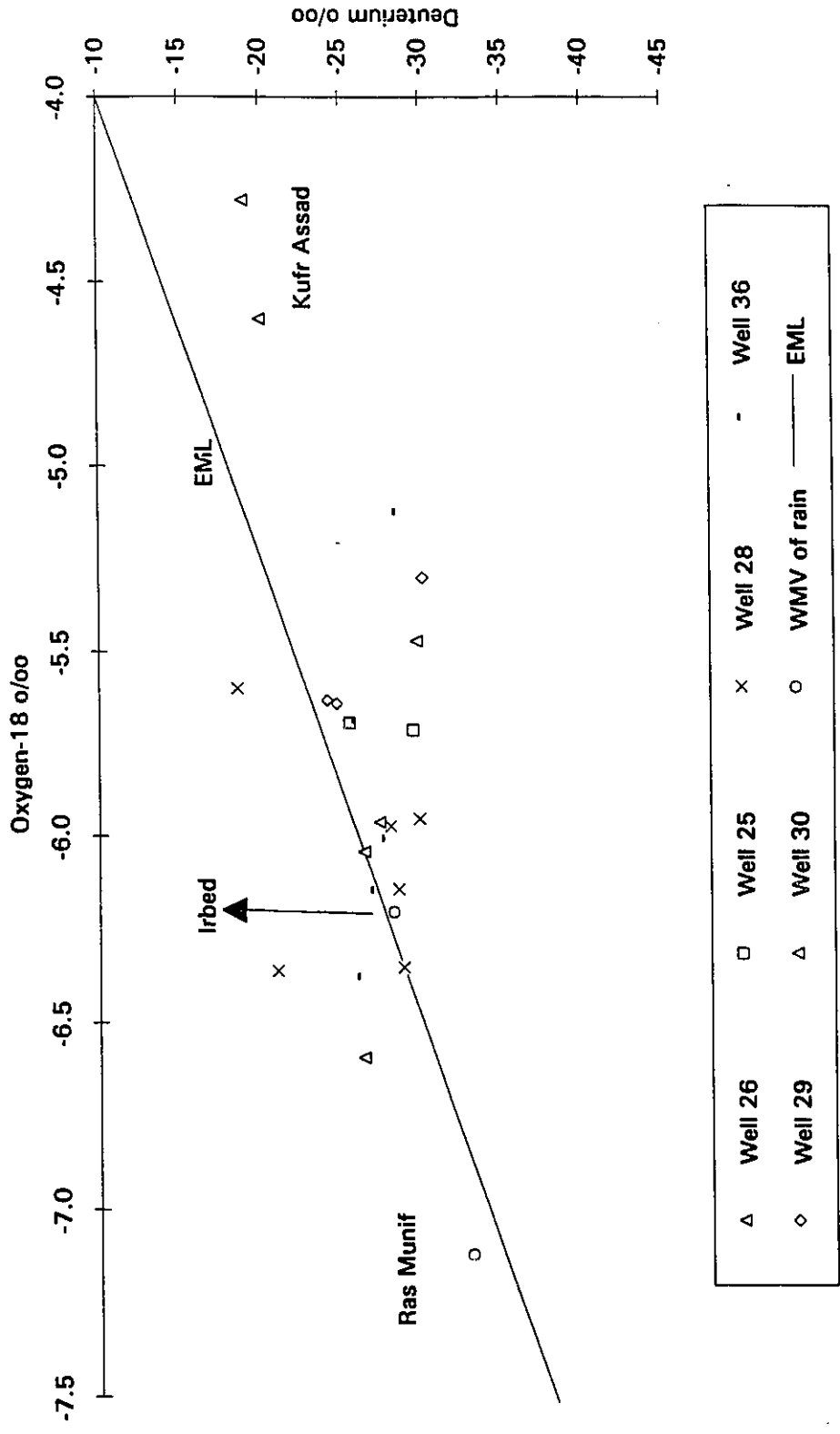


Fig. V-2.4 Isotopic composition of the Side Wadi Water. Some samples especially No. 26 seem to show evaporation effects.

this is an indication of a fast transit time in the unsaturated zone.

The high tritium content of the groundwater can simply be interpreted as rapid infiltration recharge.

The ^{14}C activity was measured only in the Jdeita well (No. 36) and was found to be 73.4 pmc. The tritium content of this well is 6.9 TU and the $\delta^{13}\text{C}$ is -13.3 ‰. As in Nuaimh area the carbonate karstic rocks outcropping in the area are dissolved by the infiltrating water, leading to lower the ^{14}C activity of groundwater by substitution of dead carbon from the limestone aquifer.

V-2.2 Confined Aquifer: (Wadi Al-Arab Well Field)

Wadi Al-Arab well field lies in the northern part of the side wadi and about 20 km NW from the city of Irbed (Fig.V-2.1).

In this area there are five wells drilled by the Jordan Valley Authority (JVA) in the early 1980's, in order to evaluate the groundwater potential in this area (Joudeh, 1983). The depth of the wells ranges from 195 to 703 m, where the elevation of the top casing is around the sea level. The highest discharge ($\sim 1500 \text{ m}^3/\text{h}$) is recorded for wells located around -20 m bsl. In the middle of the well field, on a local hill top, there is a low discharge spring. In addition there are number of private wells in the area, three of them are included in this study. The hydrogeological information about all the wells can be found in Appendix 2. The governmental wells are used for domestic supply in the Irbed area, while the private wells are used for irrigation. The former designated as WA1-5, while the latter No. 37 to 39 (Fig. I-1, Table V-2.3).

The potentiometric surface of the Wadi Al-Arab wells is higher than the land surface, therefore the wells are flowing under artesian condition. Increased pumpage for water supply has lowered the potentiometric surface by 84, 57, and 42 meters in wells No. 1, 4 and 3 respectively (WAJ-Files). The average abstraction from the well field for the years 1990/1992 is 16.5 MCM annually. As mentioned earlier many springs in the Cretaceous rocks have ceased to flow because pumpage has resulted in the decline of water levels until only a few springs are left. The outcrop of Cretaceous aquifer in this area is small and limited to a narrow strip within the Wadi Al-Arab wadi. The infiltration rate to the Wadi Al-Arab area is calculated to be 28 % of the precipitation (El-Naser, et

al., 1992). The recharge source of the Cretaceous aquifer has been commonly attributed to groundwater percolating from the outcrop B2/A7 in the Ajloun Mountains and the side wadies (Parker, 1969; Joudeh, 1983; and NJWRIJS, 1989).

V-2.2.1 Hydrochemistry of groundwater

The chemical analysis of all the wells indicates that the groundwater is fresh, as the TDS does not exceed 650 mg/l. Table V-2.3 represents the average composition of the wells from different period as the water shows a remarkable compositional stability. The other private wells with more or less the same depth have demonstrated different salinity.

The chloride values in mg/l of the wells are plotted against the TDS (Fig.V-2.5), in order to distinguish the elements that participate in the salinity variation. It was seen from the graph that there is a strong correlation between the TDS and Cl⁻. Two groups were observed. The first group includes the Wadi Al-Arab wells No.1 to 4 as well as the spring. The correlation in this group is high ($R^2 = 0.73$), where the salinity increases with an increase in the Cl⁻ and the depth. The second group is the private wells and the Wadi Al-Arab well No.5. The correlation is much higher ($R^2 = 0.94$) for this group.

Wadi Al-Arab well No.5 (WA5) has the lowest concentration of bicarbonate and highest concentration of nitrate and chloride among the other Wadi Al-Arab wells (WA1 to WA4). In addition the well shows a wide range of chloride concentration. This indicate that the water well is subject to contamination. The well is the shallowest in term of penetrating the B2/A7 aquifer and is located 50 m asl. In addition, the site of the well is

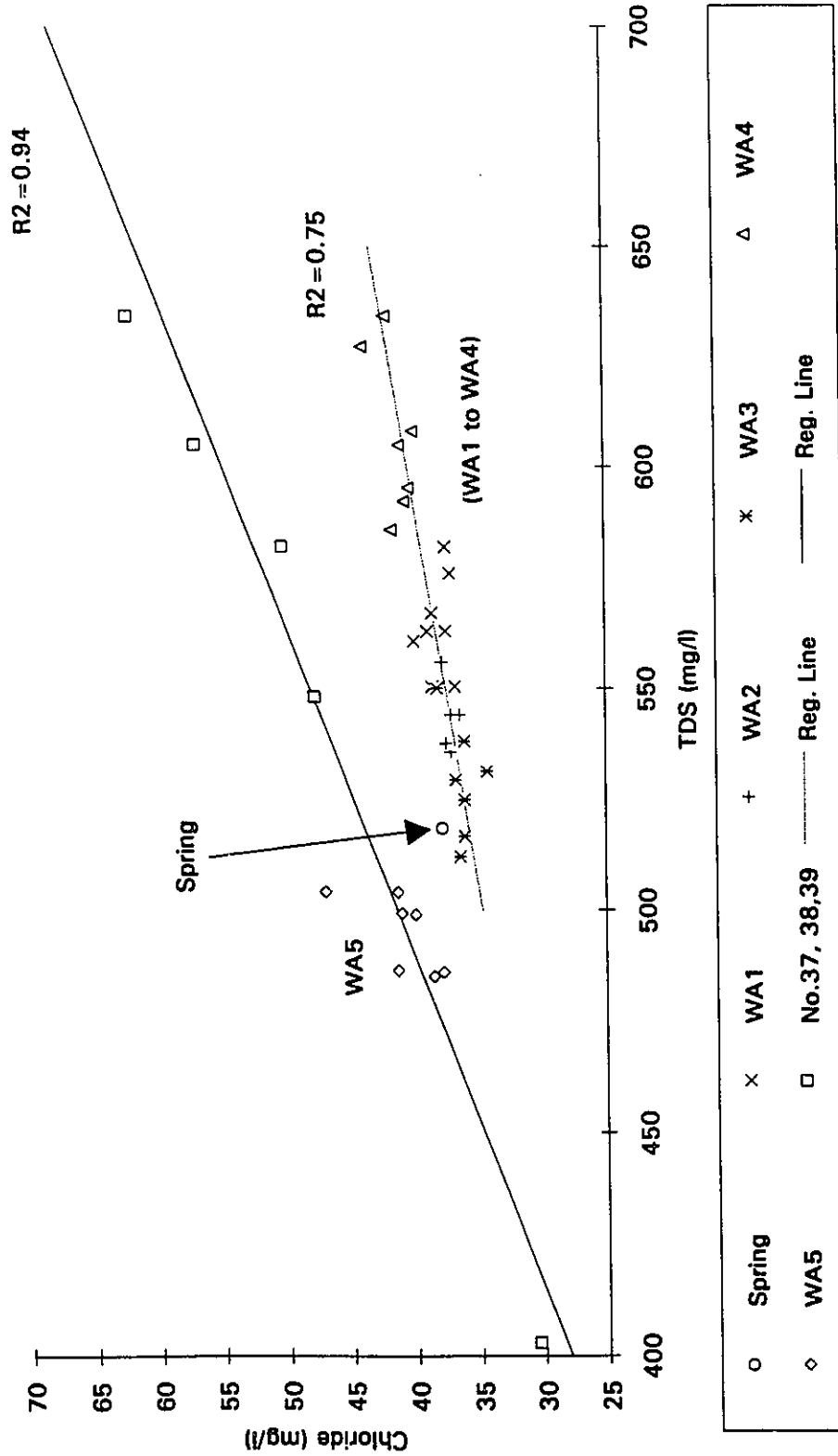


Fig. V-2.5 Relation of TDS to Chloride, Wadi Al-Arab wells No 1 to 5, Wadi Al-Arab spring and three private wells,

in Wadi Zuhar, one of the main wadies of Wadi Al-Arab (Fig. V-2.1).

Table V-2.3 Chemical Average Of Wadi Al-Arab wells

No. of well	TDS	T °C	pH	Ca ²⁺	Mg ²⁺	Na ⁺	K ⁺	Cl ⁻	SO ₄ ²⁻	HCO ₃ ⁻	NO ₃ ⁻
	ppm			mg/l	mg/l	mg/l	mg/l	mg/l	mg/l	mg/l	mg/l
Spring	518		7.14	104	34.0	22.1	2.7	37.9	50.8	411	2.61
WA1	564	30.6	7.11	109	38.7	22.4	2.0	38.2	71.5	434	0.88
WA2	544	26.9	7.04	109	35.7	22.3	2.9	37.1	66.3	428	0.84
WA3	529	27.3	7.10	108	33.3	20.2	2.3	36.3	60.3	414	1.0
WA4	607	28.7	7.05	115	40.6	34.6	4.0	41.4	116	436	0.66
WA5	495	25.1	7.19	96	32.8	18.5	2.7	41.1	27.8	394	12.9
38	634	24.3	7.04	111	39.6	41.3	3.9	62.3	73.9	435	4.51
39	593		6.99	123	30.3	36.1	4.5	53.7	80.4	426	1.33
37	403		7.61	71.5	26.2	18.4	3.9	30.4	1.92	319	27.0

The upper lithology of the well consists of 27 m gravel, the casing is from 0 to 21 m grouted pipe, while from 0 to 227.5 m it is slotted, and from 227.5 to 375 m it is an open hole. This means that approximately 147 m of the water bearing formation is uncased. The Al-Hazaimeh well also shows a high NO₃ concentration and very low SO₄ content. This could mean that the well is affected directly by a source of contamination.

From Fig.V-2.5, we can observe that the water of the spring discharges groundwater similar to well No.3 (WA3).

The type of water in all the wells is classified as calcium bicarbonate. The cation meq/l ratio for all the wells is Ca²⁺ > Mg²⁺ > Na⁺, but the anion ratio is HCO₃⁻ > SO₄²⁻

> Cl⁻ for the Wadi Al- Arab wells (1 to 4), and HCO₃⁻ > Cl⁻ > SO₄²⁻, for No.5 well.

The SO₄²⁻ concentration in Wadi Al-Arab 4 (116) is the highest in comparison with the other wells. This could be due to dissolution of sulphate minerals at depth. The Ca²⁺/Mg²⁺ ratio, is in the range of 1.71 to 2.47. This indicates the circulation of groundwater in limestone or chalk aquifer.

Table V-2.4 Chemical Ratios, Ionic Strength, Log_{PCO2} and Saturation Indexes

No. of well	Na ⁺ /Cl ⁻	Ca ²⁺ /Mg ²⁺	Ionic Strength	SI _{calcite}	SI _{dolomite}	Log _{PCO2}
Spring	0.89	1.86	0.013	0.253	1.35	-1.55
31	0.91	1.71	0.013	0.292	1.51	-1.45
32	0.93	1.85	0.013	0.193	1.24	-1.42
33	0.86	1.96	0.013	0.235	1.30	-1.49
34	1.29	1.72	0.015	0.224	1.35	-1.41
35	0.70	1.78	0.012	0.256	1.37	-1.62
38	1.02	1.71	0.015	0.173	1.21	-1.44
39	1.04	2.47	0.015	0.193	1.45	-1.47
37	0.93	1.65	0.009	0.463	1.79	-1.16

The water in all the wells is oversaturated with respect to calcite and dolomite which suggests that this is caused by dissolution of calcium carbonate. This also could be caused by dissolution of gypsum. The SO₄²⁻ concentration in the wells is 2 to 3 fold higher than the SO₄²⁻ content of the phreatic aquifer of the side wadies (see table V-2.1).

V-2.2.2 Isotopic composition of the groundwater

Most of the sites, the locations of which are shown in (Fig.V-2.1), have been sampled repeatedly during the years 1987-1993. The isotopic composition of groundwater in the confined aquifer in Wadi Al-Arab is controlled by the isotopic composition of rainfall and show evaporation effects. In the $\delta^{18}\text{O}$ - δD diagram, the groundwater and the WMV of Irbed, Ras Munif and Deir Alla precipitation is plotted in (Fig.V-2.6).

However, the isotopic composition of all groundwater is enriched compared to the WMV of Irbed precipitation. It is seen from the graph that some samples are fall on the EML, while others deviate from that line due to the effect of evaporation. The deviated samples can be represented by the following evaporation line:

$$\delta\text{D} = 4.8\delta^{18}\text{O} + 2.15 \text{‰}$$

Regional groundwater that flows from the higher Ajloun Mountains (Nuaimah) and Side wadies to the Wadi Al-Arab area and the western part of the study area cannot account for the isotopic enrichment of groundwater relative to precipitation and recharge water in the side wadies. A possible explanation could be the percolation of partly evaporated water from a recharge area, which is lower than the altitude of the recharge of the tritiated Nuaimah and side wadies in an area between Deir Alla and Ras Munif (Fig. IV-2). The stable isotope content of the groundwater in the Wadi Al-Arab well field is due to a different altitude and would show a more enriched isotope than the one in the Irbed area.

The graph also shows a variation in stable isotopes for the same well sampled at different times. This could indicate that the input to the aquifer is transient.

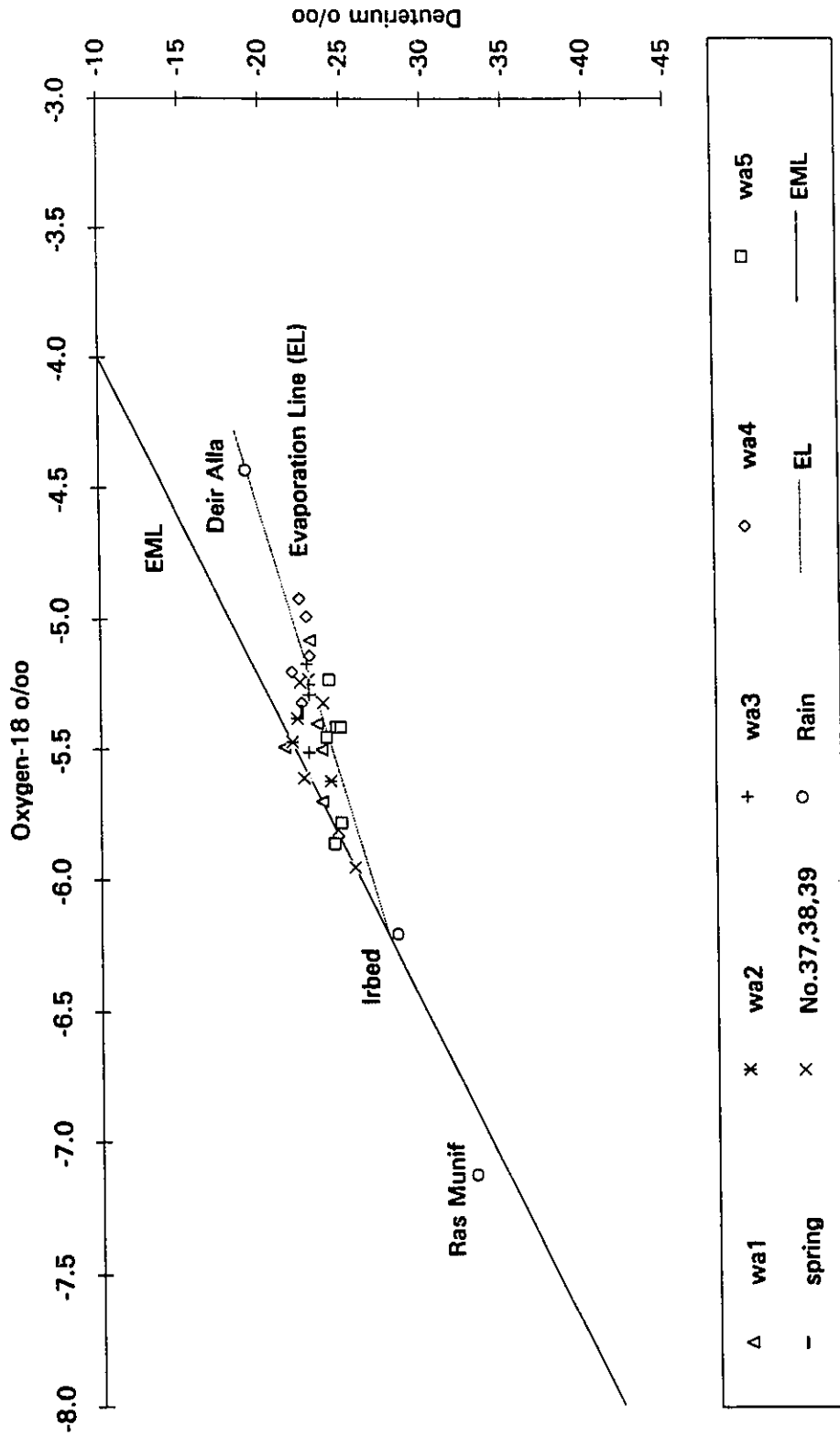


Fig V-2.6 Isotopic composition of Wadi Al-Arab well field. Dashed line represent the evaporation line (EL).

The maximum thickness of the B2/A7 aquifer is 520 m in well No.4. The Wadi Al-Arab water treatment plant is located in the midst of the well field and discharges waste water to the small wadies of the area.

One hypothesis for the enrichment of the stable isotopes is that the intensive pumping from the wells causes a drop in the water levels as an extended cone of depression, which promotes contaminant infiltration to the aquifer. Waste water running along the wadi undergoes slight evaporation before infiltrating the aquifer. This explains the variation of the $\delta^{18}\text{O}$ and δD values of the groundwater and is very well seen in wells No. 1,2,3 and 4. Well No.5 the variation is quite wide.

The B3 formation overlying the B2/A7 aquifer is not completely impermeable, it is highly fractured. It is important to recall that through this formation several springs discharged in the past, and only they ceased after the heavy pumping from Wadi Al-Arab well field started. Further studies are required to characterize the hydraulic nature of the aquifer.

V-2.2.3 Radioactive isotopes of groundwater

1-Tritium: The groundwater of the Wadi Al-Arab well field, in general, is tritium free. Some wells sampled several times recorded a tritium values from 0.0 to 2.4 TU (Appendix 3). The highest tritium activity was observed in well WA3 (2.4 TU). This well is bsl and has the shallowest depth (257) among the wells of the Wadi Al-Arab well field. In addition, the dynamic water level (DWL) of the well fluctuated in 1992 between 32 and 42 m. This could mean that there is a contribution from local precipitation to the

groundwater. The wells are cased to a certain depth and then either left as an open hole or slotted casing to permit the water to come into the well from the water bearing formation. The infiltration could be through the fracture of the overlying B3 formation.

2 - Carbon-14: The Wadi Al-Arab wells reveal a wide spectrum of ^{14}C from 10.97 (WA1) to 35.3 (WA5) pmc. All of the samples must be corrected for sulphate reduction (see VI-5.3.2), which artificially ages the groundwater. The well field is rich in sulphide, this is indicated by the H_2S odour from the water which is a characteristic of SO_4^{2-} reduction. In addition the calculated total hardness of the groundwater is very high and ranges between 375 to 400 mg/l. This with the alkalinity and higher P_{CO_2} in this well field (Table V-2.4) than in the recharge area indicates that additional CO_2 is introduced to the aquifer. This CO_2 can be the result of oxidation of the organic material in the aquifer, leading to further dilution of the ^{14}C , therefore generate older ages. This is discussed more extensively on chapter six.

V-3 Adasyia Area

There are several wells in the JRV, close to the convergence of the Yarmouk and Jordan rivers. Five wells and one spring in Adasyia are subject to the study (Fig.V-3.1), and are located, some 1 to 2 km from the Yarmouk River and in a distance of 5 km NW of the North Shuneh and 2 km SW of Mukhebeh 5 thermal water wells.

The average depth of the wells is around 80 meters, and they are located approximately 200 m bsl. The water level in the wells ranges between 1.35 and 23.72 m. General information about the wells included in the study can be found in Appendix 2. The lithology consists of top soil (2-3 m), Basaltic Gravel (20-25 m) Lisan Marl (5 to 7 m) and Basalt (30 to 50 m).

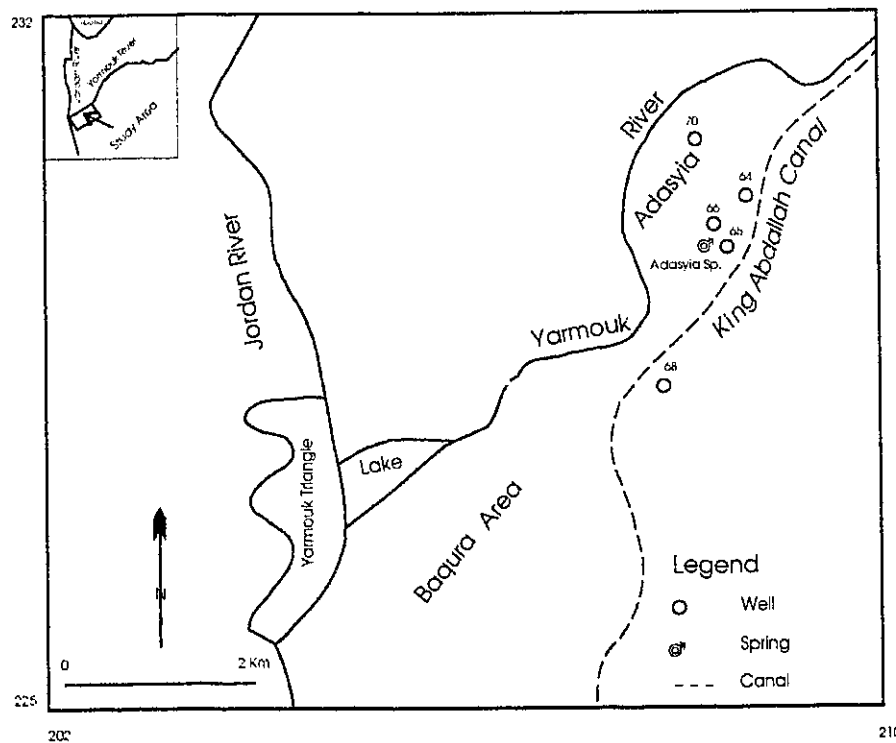


Fig.V-3.1 Location Map of the wells in Adasyia area

The Lisan Marl formation consists mainly of alternating grey calcareous clay and evaporite beds, mainly with halite and sylvite.

The recharge to the area is considered to come from higher mountains further to the east (Hirzallah, 1973, Al Hawi, 1990).

The area is highly cultivated, with the source of irrigation water being mainly the Yarmouk River. The river water is taken into the KAC and later distributed to the farmers by a small open canal system. Some of the farmers take the water directly from the river. The irrigation method is direct spreading over the land. The quality of the Yarmouk River as we saw earlier (see IV-2.1), is very fresh and does not exceed 500 ppm. When samples were taken only one well was pumping and the others were abandoned. The samples were taken by bailer from within the casing.

Studying the isotope and chemistry of these non-thermal wells will elucidate the relation with thermal wells, as both are located in the same area in the JRV, which considered as a discharge area.

V-3.1 Hydrochemistry of the groundwater

The salinity of the groundwater is considered brackish, where it is higher than 1000 ppm Table V-3.1. The most saline well is the deepest well, No.70 (TDS=8000 mg/l and TD 350 m). A fingerprint diagram of the data of Table V-3.1 was plotted in (Fig.V-3.2). From the diagram we can notice that the groundwater in general is enriched in Na⁺ and Cl⁻. Well No.70 has the maximum concentration of Na⁺ and Cl⁻.

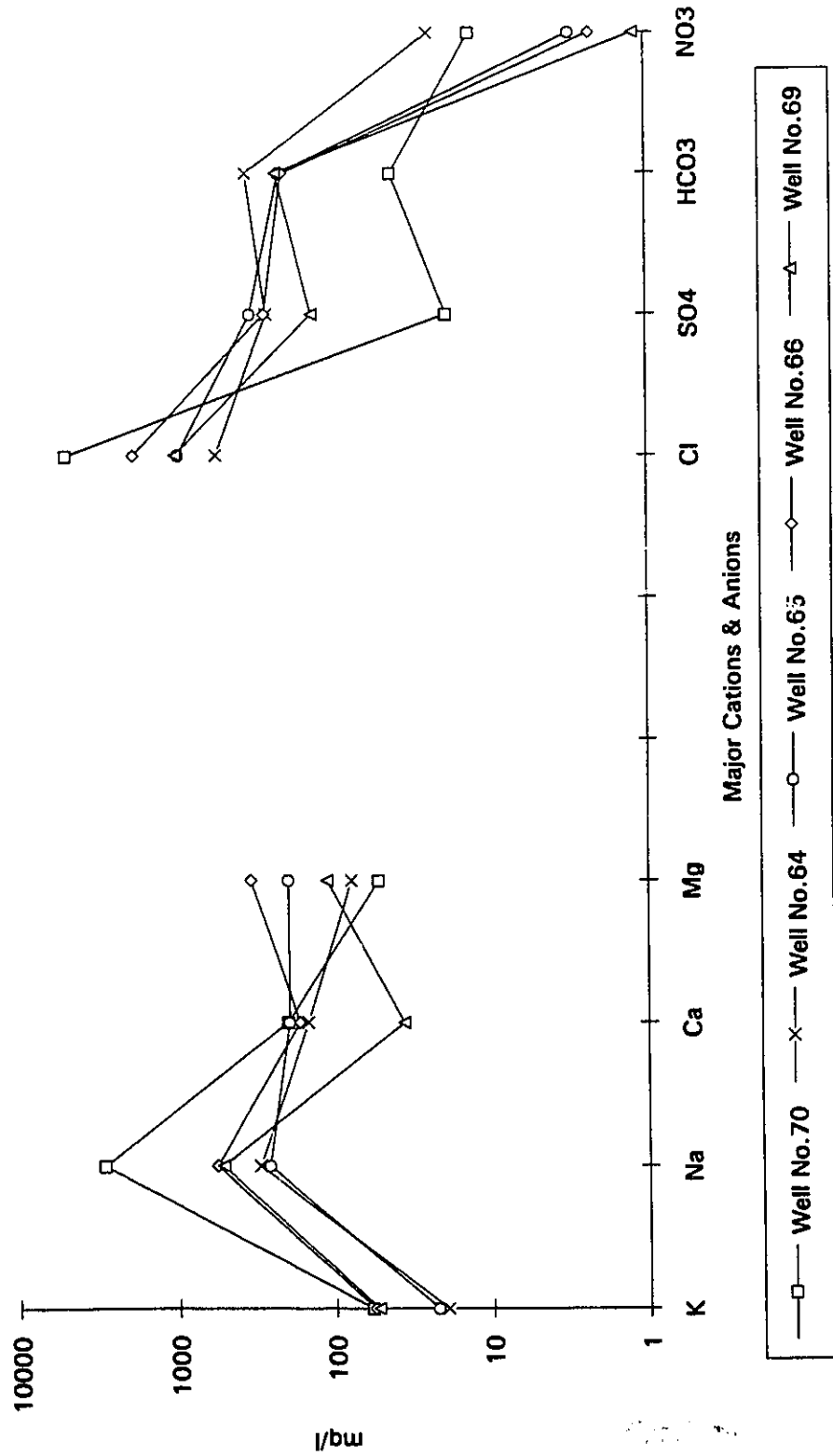


Fig. V-3.2 Fingerpruit diagram for Adasyia groundwater, composition of the dissolved salts (table (V-3.1))

Table V-3.1 Average Chemical Composition of the groundwater

Well No.	TDS	pH	Ca ²⁺	Mg ²⁺	Na ⁺	K ⁺	Cl ⁻	SO ₄ ²⁻	HCO ₃ ⁻	NO ₃ ⁻
	mg/l		mg/l	mg/l	mg/l	mg/l	mg/l	mg/l	mg/l	mg/l
70	8832	8.3	200	52	2944	59	4987	19	42	13
64	1667	7.3	148	78	302	20	555	261	352	24
65	2349	7.2	197	197	264	22	974	332	217	3
66	3842	7.7	169	342	569	57	1880	272	209	2
69	2304	7.9	36	112	520	54	1016	135	228	1
spring	1363	7.2	123	74	215	13	359	205	405	54

The different sources will be characterized by different cation to anion ratios.

The groundwater does not show a similar relationship between the Na⁺/Cl⁻ and Ca²⁺/Mg²⁺ ratio and salt content Table V-3.2. In well No.70, the value of Ca²⁺/Mg²⁺ (3.82) is calculated to be the maximum. The well also recorded relatively low Na⁺/Cl⁻ ratio and low SO₄²⁻, HCO₃⁻ and very high Na⁺ and Cl⁻ concentration in comparison with the other wells. Thus suggests that the evaporite, mainly halite dissolution, is the main process responsible for its chemical load. Such an evaporite is abundant in the JRV and around the Lake Tiberia (Strainsky, et al., 1979). Some 2 Km to the west of the Dead Sea, a halite layer 6.5 m thick at a depth of 24-30.5 m in the gravel and a very thin layers of aragonite and gypsum at 33 m depth was found in the deep (DSIF) drillhole (Yechieli, et al., 1993). The low Na⁺/Cl⁻ ratios of the groundwater (0.27 to 0.61) could be explained by the cation exchange, where Na⁺ is adsorbed by clay minerals within the Lisan marl. Wells No. 65 and 66 recorded the lower values of Na⁺/Cl⁻ ratio 0.27 and 0.30 and their waters are

classified as Mg^{2+} - Cl^- type of water like the Dead Sea. In addition both wells demonstrate the highest SO_4^{2-} and Mg^{2+} concentration. This suggests that cation exchange behaviour of Ca^{2+} and Mg^{2+} also plays a major role in modifying the groundwater. Therefore all water in all the wells is classified as Na^+ - Cl^- type of water, while wells (No. 65 and 66) have a Mg^{2+} - Cl^- type of water.

Table V-3.2 Chemical Ratios, Ionic Strength and saturation Indexes

Well No.	Na^+/Cl^-	Ca^{2+}/Mg^{2+}	Ionic Strength	LOG_{PCO_2}	$SI_{Calcite}$	$SI_{Dolomite}$	SI_{Gypsum}
	mg/l	mg/l					
70	0.59	3.82	0.149	-1.85	0.35	1.49	-2.6
64	0.54	1.89	0.033	-1.82	0.35	1.75	-1.2
65	0.27	1.00	0.049	-1.99	0.15	1.64	-1.10
66	0.3	0.49	0.07	-2.53	0.47	2.61	-1.40
69	0.51	0.32	0.04	-2.62	0.14	2.12	-2.11
Spring	0.61	1.67	0.02	-1.64	0.25	1.62	-1.32

The concentration of NO_3^- in groundwater is much higher than in natural water. The highest concentration was recorded in the Adasyia spring. The spring demonstrate wide variation of NO_3^- content where the recorded value range between 21 and 102 ppm Appendix 3. This is clear evidence that the return flow is responsible for the contamination.

V-3.2 Isotopic Composition of the Groundwater

Stable isotope data of $\delta^{18}O$ and δD obtained on groundwater from the Adasyia

area lie in the range of -3.43 to -4.81 ‰ and -15.9 and -24.77 ‰ respectively. The groundwater, the Yarmouk River water and the WMV of the rain in Irbed and Deir Alla are plotted in the $\delta^{18}\text{O}$ - δD diagram (Fig.V-3.3).

The main features observed in the groundwater and the spring water are (i) the isotopic enrichment and wide variation of the same source sampled at different times (No. 64, 65 and 66). For example, well No.65 shows that the most enriched sample are the one tritiated. (ii) The occurrence of the groundwater and the spring deviate from the EML and are located on an evaporation line of

$$\delta\text{D} = 5.57 \delta^{18}\text{O} - 3.28 \text{‰} \quad \text{with} \quad R^2 = 0.91.$$

The recharge area of the groundwater is difficult to assess based on the comparison of their isotopic composition with that of rain in Irbed and Deir Alla.

The most enriched samples do not agree completely with the WMV of rain in Deir Alla. In addition the stable isotope of the groundwater show an ^{18}O enrichment of about 2-3 ‰ from Irbed precipitation. However, the most depleted samples does not show significant shift from the Yarmouk River. The δD and the $\delta^{18}\text{O}$ pattern of the groundwater seem to indicate that the isotopic composition of the recharge source has been modified prior or during infiltration.

The groundwater is characterized by deuterium excess less than that of precipitation (21 ‰) in Irbed Table IV-2. The calculated deuterium excess for the groundwater and the spring ranges between 9 and 16. A decrease in deuterium excess is an expression of the secondary evaporation process (Gat, 1981). Commonly, evaporation from a fresh water surface results in an evaporation line with a low slope.

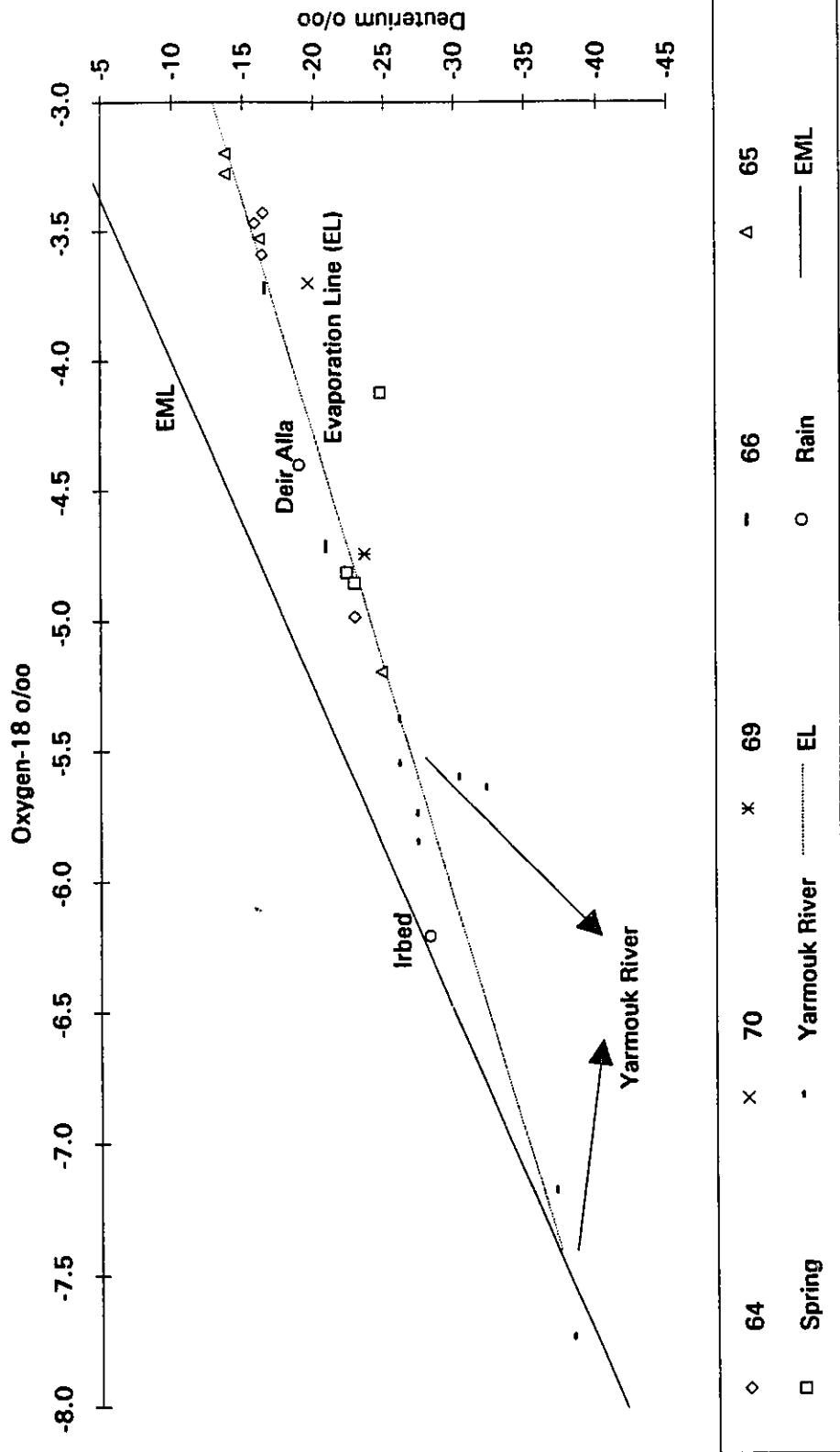


Fig. V-3.3 Isotopic composition of the groundwater in Adasyia area, samples with the Yarmouk River show evaporation effects.

From above we can suggest that the regional flow to the groundwater come from east from altitude close to 500 m asl. The enrichment observed is due to the contribution of Yarmouk River and return flow.

V-3.3 Tritium in the groundwater

The high content of tritium in the groundwater is evidence that there is modern local recharge in the area. The concentration of the tritium ranges from 2.6 to 10.7 TU. The exception is well No.68, where the water is not tritiated suggesting a predominance of pre-bomb recharge to this groundwater. Well No.68 is located to the east of KAC (Fig.V-3.1), while the rest of the wells are located between the Yarmouk River and KAC. The water level in this well is approximately 18 m below the surface, which is much deeper than the water level of the other wells in the Adasyia area (Appendix 2).

The tritium content of some wells is close to the value of the rain in the Deir Alla station in the JRV. The tritium analysis of rainwater in Deir Alla in the period 1987-1991 yielded values ranging from 5 to 15.8 TU. Wells No.64, 65, 66 and the Adasyia spring have high tritium concentrations in winter: from 5.3 to 10.7 TU. That can be interpreted as being due to the recharge that occurs within the same year. These wells penetrate conglomerate with basalt beds that outcrop in the study area.

The Adasyia spring demonstrates a wide range of tritium content. The tritium fluctuates between 1.8 to 8.3 TU for the year 1988. The lowest tritium is recorded in the summer (August 1988, 1.8 TU), while the content of tritium in winter (February 1988) is 8.3 TU. This means that the aquifer in the rainy season receives an appreciable amount

of recharge, where the residence time of the infiltrated water is very fast through the unsaturated zone.

The river water contributes to the aquifer recharge as Yarmouk River water is the main source of irrigation. The Yarmouk River is rarely sampled and the recorded samples represent different periods. The tritium content of the river in March 1992 is approximately 4.4 TU Table IV-5. The value of Adasyia groundwater is between 2.6 and 10.7 TU.

Well No.68 is free of tritium could emphasis that the King Abdallah Canal represents a barrier preventing any contribution from the Yarmouk River water.

V-4 Ramtha Area

As discussed above previous studies (see I-2), suggest that flow in the major aquifer B2/A7 in Ramtha area comes from three directions; the Ajloun Highlands, Syrian side via North-East Desert and the Amman Zarqa Basin as subsurface flow. In the Ramtha area there are three aquifer systems related to the Cretaceous and Tertiary. The shallow aquifer belongs to the (B4), the intermediate aquifer (B2/A7), and the deep aquifer (K). The non-thermal water of the first and second aquifer will be discussed here, while the hot Mahasi 6 and S-90 wells of the second and third aquifer will be addressed in detail in chapter 6.

The (B4) aquifer exists in a very limited area in the North Irbed and Ramtha areas and has no further extension. The recharge into the aquifer occurs locally from the precipitation in the Northern Irbed and Southern Ramtha areas. The flow system is from the Irbed area toward the Yarmouk river, following the general pattern of the surface drainage (NJRWIPS, 1989). The aquifer water is stored under water table conditions. For the study, 5 wells, two springs and wadi runoff from Wadi Shieh were sampled (Fig.V-4.1). The depth of the wells tapping this aquifer is in the range between 70 to 300 m. The shallowest wells (depth less than 85 m), are located close to Wadi Shieh. The wells have fluctuations in water table of about 10 m (NJRWIPS, 1989)

In 1986 the Ramtha Waste-Water Treatment Plant (RWTP) was established in the Ramtha area to treat 2335 m³/day of waste water. The location of the RWTP is 1.6 km radius from the shallow Mahasi wells. The plant was found to act as a non-controlled artificial recharge into the groundwater because of a construction defect in the base of the

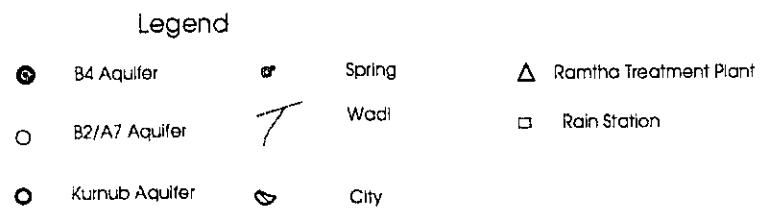
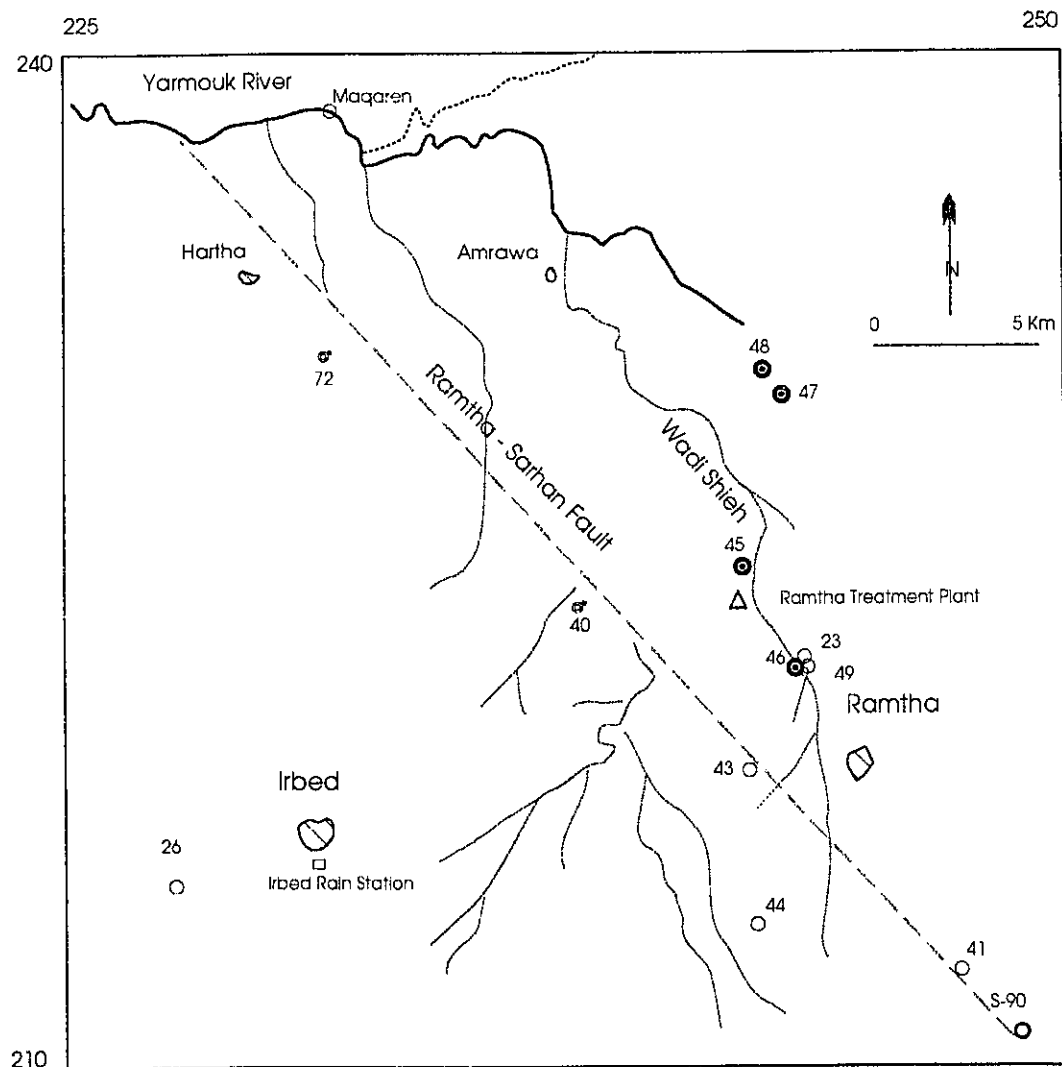


Fig. V-4.1 Location map of the well field in Ramtha area

plant. The estimated seepage in 1988 from the plant to the groundwater was 90,000 m³ (Saqqar, et al. 1989).

The second aquifer (B2/A7), is the main aquifer, where the water is stored under artesian conditions. The study is represented by 5 wells, where the depths range between 390 and 702 m. The deepest well (No.23) is a thermal source.

The temperature of the groundwater is classified as cold (< 20 °C) in the shallow aquifer (B4), and warm in the B2/A7 (> 20°C). The H₂S gas is apparent in some of the B2/A7 wells.

The Ramtha-Sarhan fault crosses Ramtha area, where most of the wells tapping the B2/A7 aquifer are situated.

The general hydrogeological information of the wells in this area are shown in Appendix 2.

V-4.1 Hydrochemistry of groundwater

The TDS in the well of the shallow aquifer is in the range of 525 to 1500 ppm Table V-4.1. The highest recorded TDS is the well near the RWTP (No.49, and No.45). The springs (No.72 and 40) issuing from the B4 have the lowest salinity (300 to 372 ppm). The B2/A7 aquifer recorded TDS between 479 and 888 ppm. The groundwater is classified as Ca²⁺ - HCO₃⁻ in the B2/A7 aquifer and Na⁺ - Cl⁻ in the B4 aquifer.

The Cl⁻ versus Na⁺ in mg/l of the sample presented in (Fig.V-4.2). The data plot more or less in a straight line with a slope of 0.54 and intercept of 11.78 with 0.97 correlation coefficient.

Table V-4.1 Average Chemical Composition of the groundwater

Well No.	TDS	pH	Ca ²⁺	Mg ²⁺	Na ⁺	K ⁺	Cl ⁻	SO ₄ ²⁻	HCO ₃ ⁻	NO ₃ ⁻
	ppm		ppm	ppm	ppm	ppm	ppm	ppm	ppm	ppm
40	372	7.5	65.3	9.72	39.1	1.17	55.6	12.5	215	24.2
41	813	7.0	113.5	47.1	89.7	3.91	113.7	133	432	2.3
42	700	7.0	101.5	42.1	71.3	1.37	102	104	404	1.0
43	717	7.5	82.6	36.4	86.5	3.52	164	55.5	324	1.5
44	733	6.9	106	43.9	83.9	2.93	115	112	431	0.94
45	879	7.4	79.08	27.6	164	4.69	250	70.5	244	56
46	695	7.9	63.8	20.7	118	12.5	201	45.3	167	67
47	567	7.6	63.3	28.6	75.9	3.52	134	42.7	223	27.3
48	756	7.5	75.7	34.0	122	3.91	211	79.7	214	46
49	1502	7.4	129	55.2	232	30.5	409	98.9	254	264
72	301	7.5	69.9	7.4	13.8	1.56	24.1	5.7	213	27.6
Wadi Shieh	1404	7.2	147	54.0	221	30.1	399	64.3	313	271

Departures from the regression line show that sources of the ions other than halite (NaCl) are involved. The ionic ratios in mg/l are listed in Table V-4.2. In some of the high salinity wells of the B4 aquifer, the ratio of Na⁺/Cl⁻ becomes close to one.

The B4 aquifer shows much more variation in all the ions, but the Ca²⁺ and HCO₃⁻ are exceptional. This is very well observed in the wide range of K⁺, Na⁺, Cl⁻ and SO₄²⁻. This could be due to a source of contamination mainly from a sewage source and partly from agricultural activities.

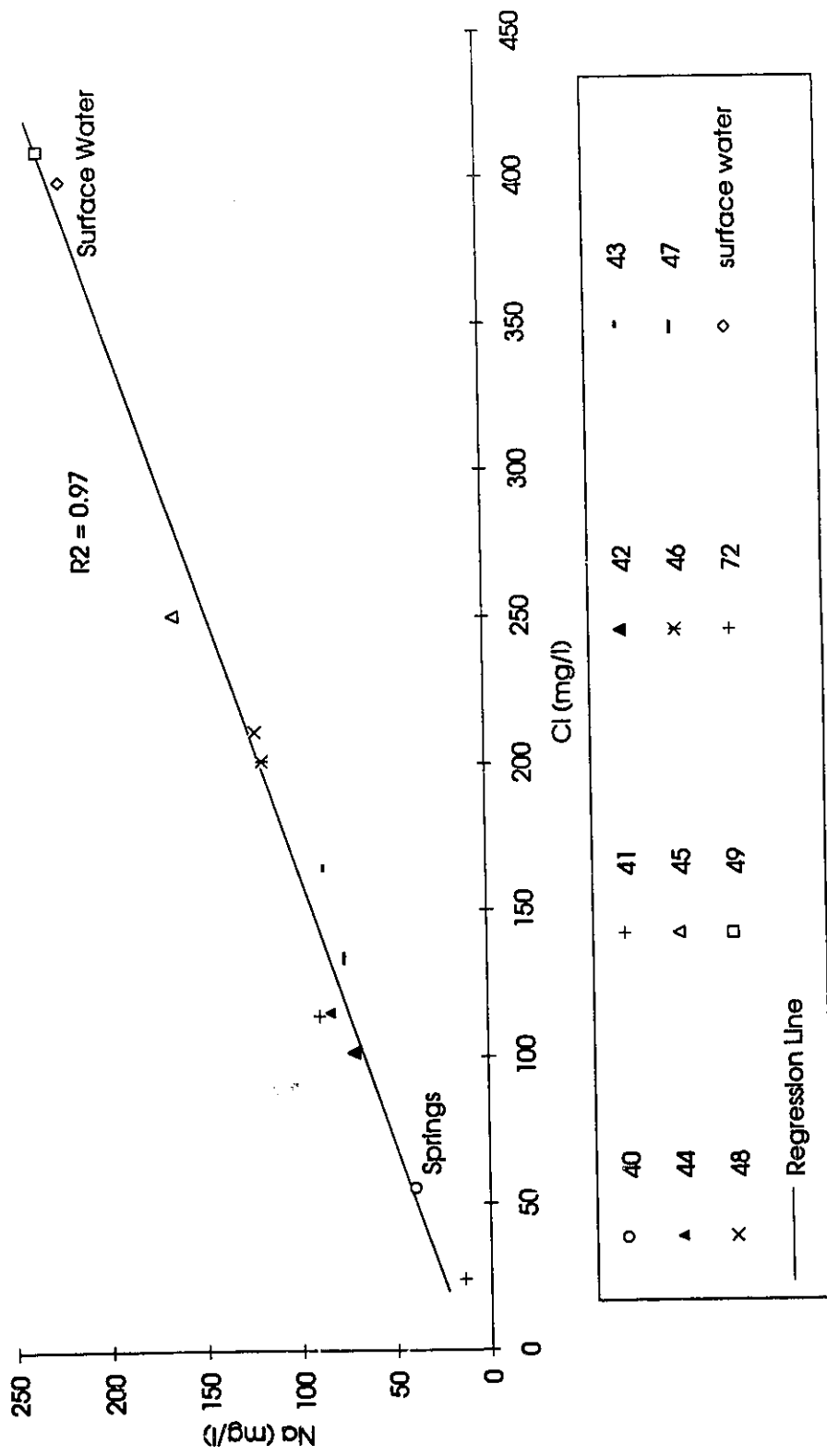


Fig. V-4.2 Relationship of chloride to sodium, groundwaters from the B4 and the B2/A7 aquifers in Ramtha area

Table V-4.2 Ionic Ratio

Well No.	Mg ²⁺ /Ca ²⁺ (mg/l)	Na ⁺ /Cl ⁻ (mg/l)
	Range	Range
40	0.25	1.08
41	0.53 - 0.80	1.13
42	0.65 - 0.72	1.05 - 1.1
43	0.62 - 0.82	0.79 - 0.82
44	0.61 - 0.75	1.11 - 1.14
45	0.54 - 0.66	0.98 - 1.03
46	0.45 - 0.87	0.82 - 1.03
47	0.75	0.88
48	0.74	0.89
49	0.71	0.87
72	0.17	0.88

Well No. 43 of the B2/A7 also shows a variation in the Na⁺/Cl⁻, and plots between the B4 and B2/A7 aquifers. In addition it demonstrates higher Cl⁻ concentration in comparison with the other B2/A7 aquifer. This suggests that the water of well No.43 is a mixture between the two aquifers, the B4 and the B2/A7. The well is located close to Ramtha-Sarhan fault (Fig.V-4.1). This was tested by calculating the mixture resulting from 80 % of well No.23 (B2/A7) with 20 % of the well No.49 (B4). The output results (Table V-4.3) shows that the calculated Cl⁻ concentration coincide with the measured Cl⁻

concentration of well No.43.

Table V-4.3 Mixed ratio Between the B2/A7 and B4 in Ramtha Area

Parameter	Well No.49	Well No.23	Mixed Water	Well No.43
Mixing ratio	20 %	80 %		
T °C	18	41.7	34.8	35
Ca ²⁺ (ppm)	128	53.69	68	87
Mg ²⁺ (ppm)	55.2	30.84	35.7	35.7
Na ⁺ (ppm)	231	55.6	90	86
K ⁺ (ppm)	30.46	2.72	8.28	3.11
Cl ⁻ (ppm)	408	102	163	160
SO ₄ ²⁻ (ppm)	98.8	24	38	59.4
HCO ₃ ⁻ (ppm)	254.14	251	251	313

The Mg²⁺/Ca²⁺ ratio of the B4 aquifer varies between 0.45 and 0.74, which indicates that the circulation took place through limestone or chalk aquifer (Hsu, 1963). The B2/A7 aquifer also shows a wide variation: between 0.6 to 0.82. Ratios in the range 0.7 - 0.9 are commonly associated with dolomitic aquifers (Hsu, 1963).

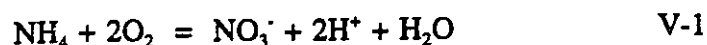
The ionic strength, partial pressure, saturation index were calculated for all the groundwater (Table V-4.4). The calculated P_{CO_2} values for all the groundwater indicates that they are higher than the P_{CO_2} of the earth's atmosphere ($10^{-3.5}$). This indicates that the groundwater in the upper aquifer (B4) became charged with CO_2 during infiltration through soil zone. The majority of the groundwater is supersaturated with respect to calcite and dolomite and undersaturated with respect to gypsum.

Nitrate is the most common contaminant identified in the upper aquifer of the Ramtha area. It is present in high concentrations and is found to be a very distinguishable parameter within the two aquifer groups. The B2/A7 aquifer recorded a very low NO_3^- concentration (less than 5 ppm). The B4 aquifer shows a wide range of NO_3^- , between 10 and 270 mg/l. Ain Mahasi and Mahasi 1 recorded the highest concentration of nitrate (270 ppm). The high NO_3^- concentration is due to sewage contamination. Ain Mahasi seepage occurs from the bottom of the wadi in winter time due to the rain. Its water is formed from different sources, mainly waste water running along the wadi coming from near by houses and workshops. In addition part of the water is the natural discharge of groundwater aquifer through seepage caused by the rising of the water table. The Mahasi 4 well has two NO_3^- measurements: the first is 10.7 ppm and the second is 124 ppm. The first sample contains NH_4 with a concentration of 10 mg/l. This indicates that the origin of NO_3^- in groundwater is organic and the process of ammonification is slow due to the high concentration of the organic matter. This high source can come only from sewage, not from fertilizer.

Table V-4.4 Ionic Strength, P_{CO_2} and Saturation Indices

No.of well	Ionic Strength	Log P_{CO_2}	SI _{Calcite}	SI _{Dolomite}	SI _{Gypsum}
40	0.008	-2.22	0.135	0.714	-2.49
41	0.019	-1.13	0.073	1.190	-1.31
42	0.016	-1.06	-0.04	0.976	-1.49
43	0.014	-1.62	0.167	1.369	-1.83
44	0.019	-1.22	0.012	1.050	-1.37
45	0.020	-1.72	-0.11	0.558	-1.76
46	0.017	-2.52	0.415	1.548	-1.74
47	0.012	-2.30	0.214	1.37	-2.06
48	0.015	-2.30	0.119	1.162	-1.76
49	0.027	-2.10	0.259	1.428	-1.58
72	0.007	-2.22	0.124	0.545	-2.77
S.W	0.028	-1.89	0.243	1.33	-1.72

The second sample indicates that nitrification took place, which means the conversion of NH_4 to NO_3 according to the following equation (Freeze and Cherry, 1979):



In this reaction, the dissolved oxygen is consumed and the pH decreases from 8.07 to 7.7.

V-4.2 Isotope Composition of Groundwater

In Fig.V-4.3 the δD versus $\delta^{18}\text{O}$ of all groundwater, springs and the WMV of rainfall stations of the Ras Munif and Irbed have been plotted. The wide variation shown by the hydrogen and oxygen stable isotopes in the water can be used to distinguish the different type of water existing in the Ramtha area.

From the $\delta^{18}\text{O}$ - δD diagram, we can distinguish clearly the groundwater of the two aquifer types. The $\delta^{18}\text{O}$ of the B2/A7 aquifer is more depleted than the $\delta^{18}\text{O}$ of the B4 aquifer. This is due to different recharge altitude. The B2/A7 is recharged from an elevation close to or higher than the Ras Munif rainfall station, while the recharge elevation of the B4 aquifer is close to the Irbed rainfall station. The deviation of the groundwaters in both aquifers from the EML seems to indicate that the isotopic composition of the rain has been evaporated prior to, or during, infiltration in the recharge area. These appear to be seasonal variations where winter rainfall and recharge is the most depleted and least evaporated.

Well No. 45 was sampled at different times, and shows a wide variation in the stable isotope. The well location is near Wadi Shieh, downstream of RWTP. Contamination of the well from the plant is very clear from the high NO_3^- in the well water Appendix 3. The water of the Qualbeh spring can be considered representative of the water which may recharge the shallow aquifer.

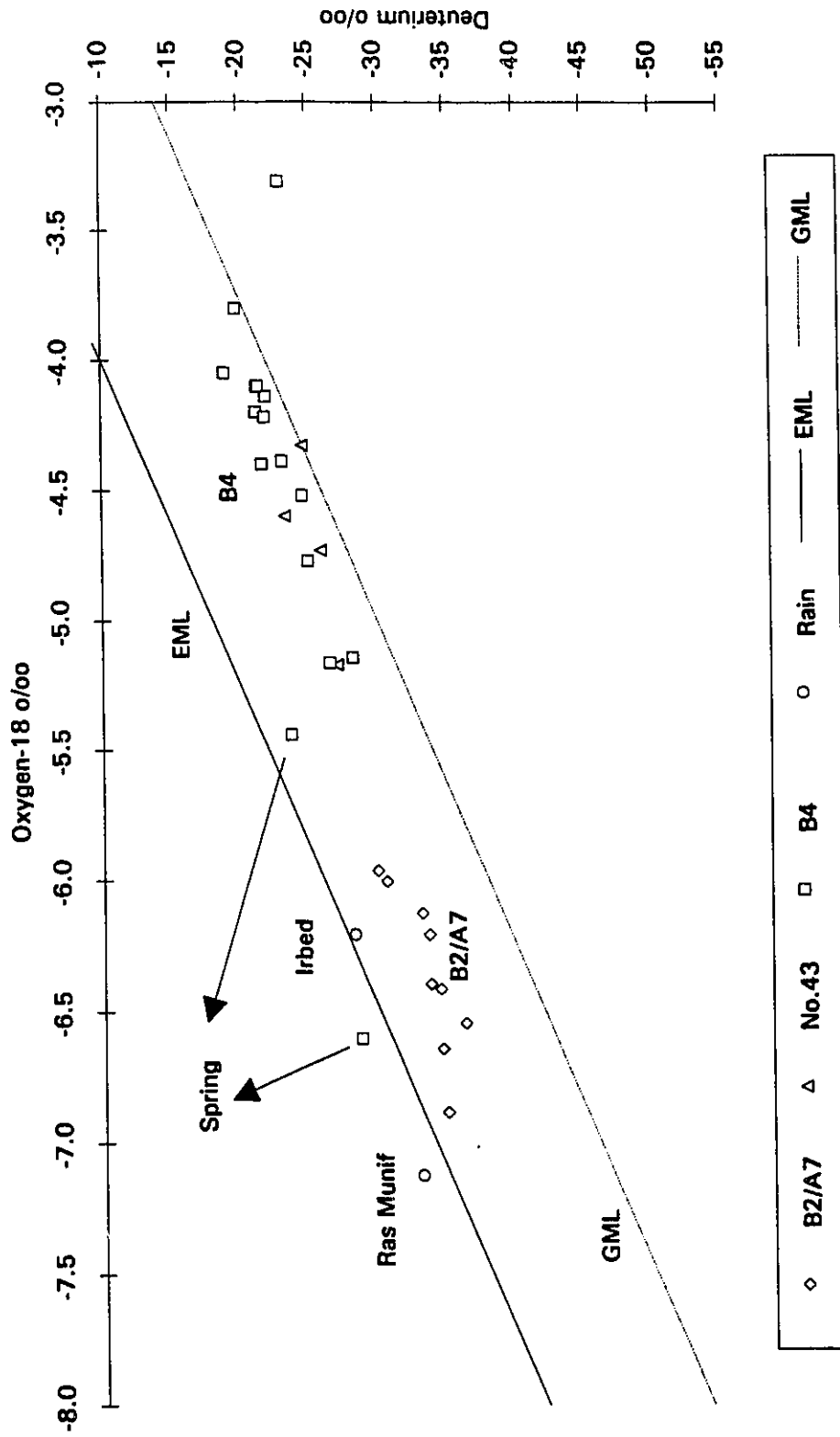


Fig. V-4.3 Oxygen-18-Deuterium Diagram showing the groundwaters of the B4 and B2/A7 aquifers in Ramtha area. The B4 aquifer demonstrate evaporation effects.

The well No.43, which taps the B2/A7 aquifer, recorded a heavier stable isotope content than the other wells tapping the same aquifer. Four samples were taken during different periods: the $\delta^{18}\text{O}$ value recorded of the end of autumn was (-4.33 ‰) in the summer (May and July) it was -4.73 and -4.6 ‰ respectively; and in mid winter it was -5.17 ‰. The values indicate that in winter the groundwater becomes more depleted. The salinity versus $\delta^{18}\text{O}$ has been plotted, and two different type of waters are evident (Fig.V-4.4). The first group is the B2/A7 groundwater, and the second is the B4 aquifer. Well No.43 is plotted in between the B4 and the other wells of the B2/A7 aquifer. The enrichment and variations of the isotope and chemical parameters of this well attributed to the contribution of the B4 water to the B2/A7 aquifer.

The B4 aquifer shows a wide variation in both $\delta^{18}\text{O}$ and TDS. The springs of the B4 (No.72 and 40) show variability in stable isotope and tritium but stability in salinity, which could be explained by the variation in the input function, which comes mainly from rain. The low salinity of the spring water indicates limited contact time between the circulating water and the rock matrix.

V-4.3 Radioactive Isotope of Groundwater

1 Tritium

The shallow aquifer reveals a relatively high tritium level. In winter time some of the sources recorded a value of tritium concentration similar to the value of rain in the Irbed area such as the Mahasi well 4 and the Qualbeh spring. The Qualbeh spring showed a variation in tritium and stable isotope within two days of sampling (5.4 and 9.3 TU).

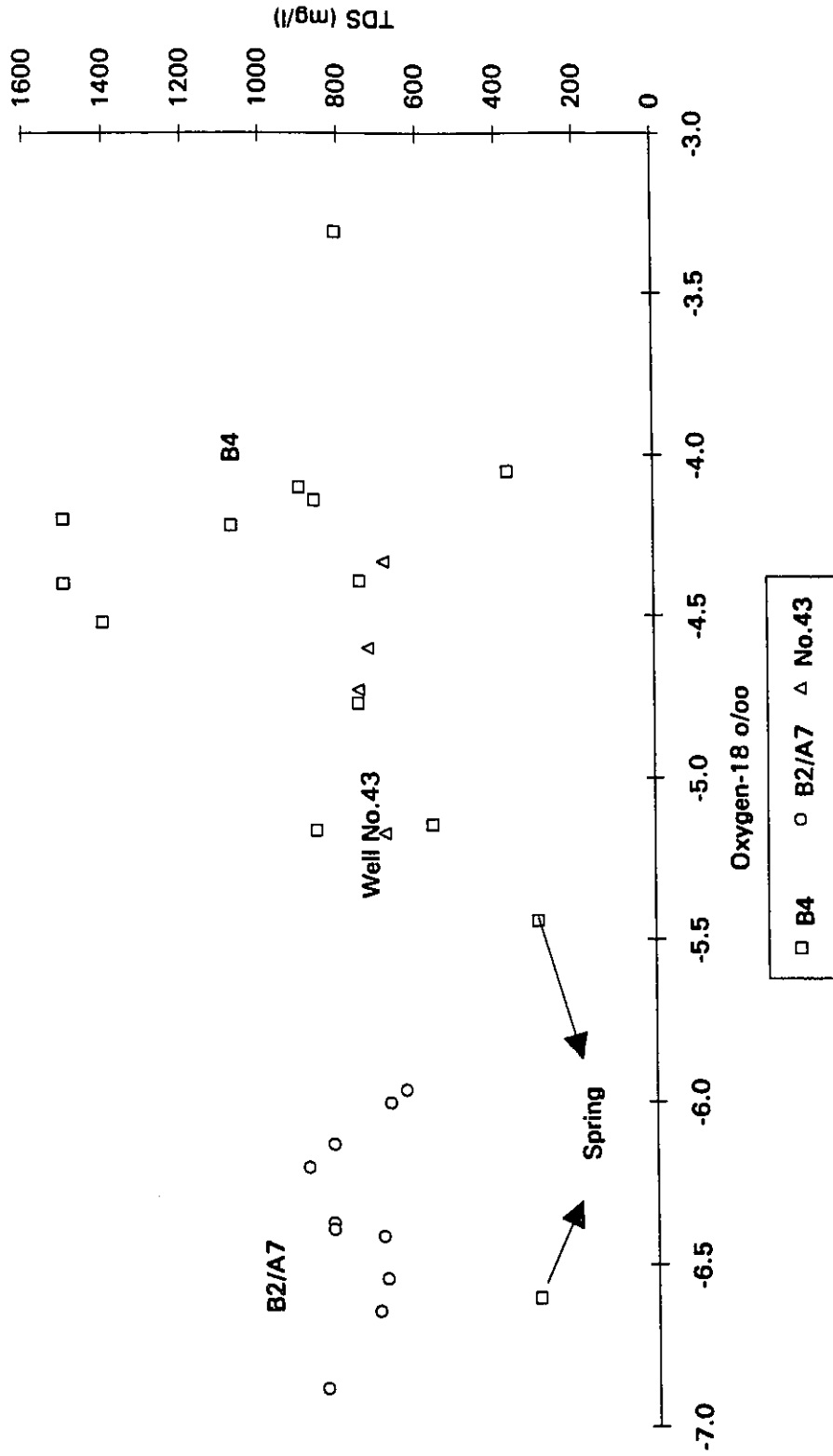


Fig. V-4.4 Plot of oxygen-18 against the TDS, showing two groups, The B4 and the B2/A7 aquifers in Ramtha area. Well No.43 (mixed water) plots between these two groups.

A high tritium level is also recorded in the Mahasi Wadi, which runs only in winter and becomes dry in summer.

The shallow Mahasi wells are located along the Wadi Shieh. They show a variation in both the stable and tritium isotopes. The variation is related mainly to the seepage from the (RWTP) and not only to rain water infiltration.

In general, the B2/A7 aquifer shows no tritium or very low tritium levels (less than 1 T.U). Well No.43 demonstrated variable amount of tritium (0 to 0.9), stable isotope and chemistry Appendix 3. This could be leakage from the contaminated B4 aquifer as mentioned above.

2-Carbon-14

Three carbon-14 samples are available from the B2/A7 aquifer only. The samples reveal low pmc of less than 10. However, H₂S has been generated in this groundwater by sulphur reducing bacteria which has disturbed the carbon system.

V-5 North-East Desert

As discussed in previous studies presented above part of the flow system in the study area is considered to come from Syria via North-East Desert. The flow system is believed to be from north and north-east toward the south and south-west (Barber, 1975, GTZ, 1977, Rimawi, 1985, NJRWIPS, 1989). None of the wells in this area (Fig.V-5.1) is thermal, but as the subsurface flow proceeds to the Ramtha area, some wells of the B2/A7 aquifer encounter hot water.

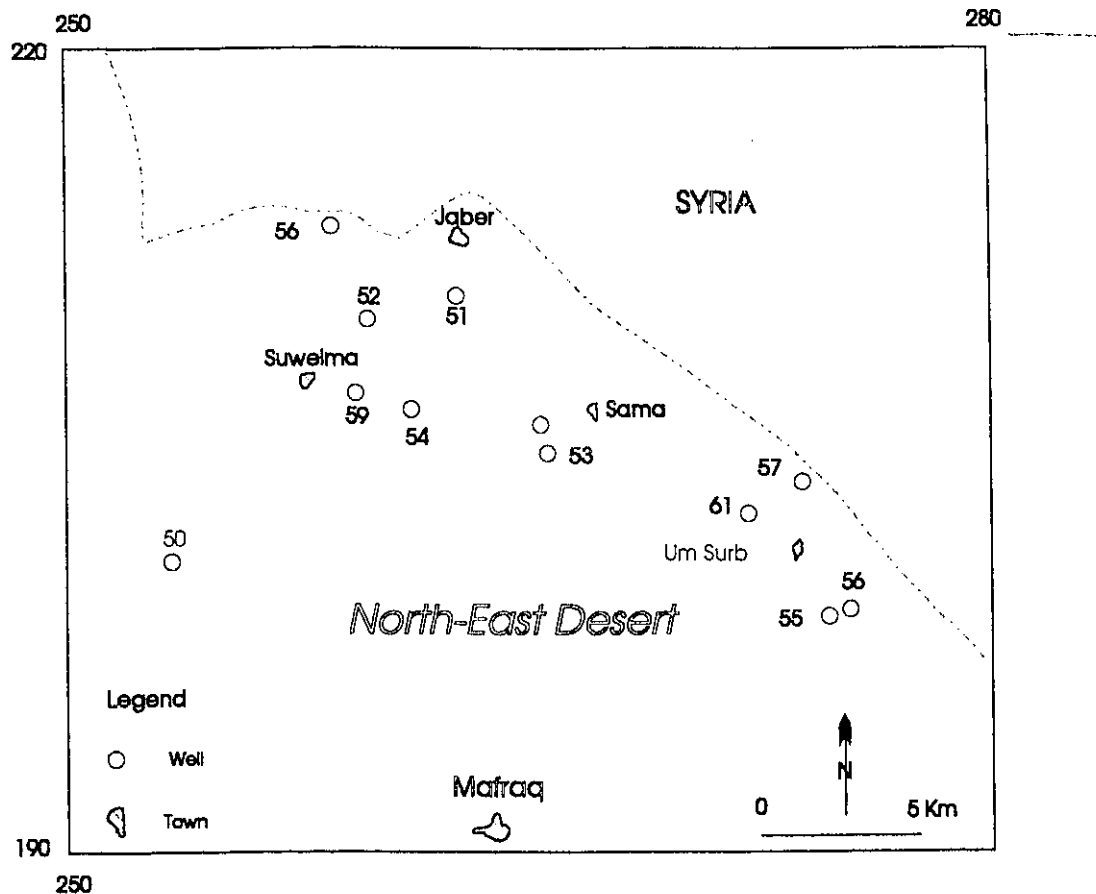


Fig.V-5.1 Location map of the well field in North-East Desert

To verify the proposed flow system in the whole study area and find out the relation between the cold and thermal waters along the flow path, it is of great importance to study the geochemical evolution of groundwater in the North-East Desert. Basalt is outcropping in the area where the thickness of the basalt is not consistent and reaches a maximum thickness in Um-Al Gotan, some 3 km east of Um Surb where it can be up to 500 m. Thickness reaches only several meters in the villages of Sama and Jaber within the study area and it is unsaturated. The B2/A7 aquifer underlies the basalt formation. The water is stored under water table conditions. There are several structures in the area (Hijazin, 1980), which influence the permeability of the water. The transmissibility is variable: between $4.5 \times 10^{-2} \text{ m}^2/\text{s}$ and $1.87 \times 10^{-3} \text{ m}^2/\text{s}$ (Wishah, 1979).

There are six basalt flows in the North-East Desert intercalated with gravel and clay beds. The maximum thickness of the latter is approximately 10 meters.

The elevation of the area is between 950 m asl on the boundary between Jordan and Syria and drops to 650 m asl southward in Sama area. There are several wadies in the area. They begin in Jabal Al-Druze in Syria and end in the Jordanian territory. In the winter time, a base flow formed in these wadies due to the intense rain in the Jabal Al-Druze Mountains. The long term average rainfall is less than 170 mm/y, rain occurs in the form of storms which are irregular in intensity and duration. In the area, there are 3 small dams; their capacity is less than 2 MCM, and they are used for cattle feeding.

The abstraction from the NE Desert well field is estimated to be 52 MCM in 1984. In the area there are several wells (Fig.V-5.1). General information about these well can be found in Appendix 2. The chemistry and isotope composition of all the wells can

be found in Appendix 3. The water level is monitored in several wells, and observation of wells in the area indicates that there has been a general drop in the water level due to heavy pumping. A general drop and fluctuation in groundwater level was observed in the Baej well (Figure V-5.2). Decreasing mean water level accompanied by increasing yearly escalation is the result of intensified groundwater abstraction.

It is worthwhile to mention here that the area is lacking a sanitary sewage system. The available facilities consist of subsurface septic tanks, which may bring about contamination to the groundwater. The septic tanks have no cement vessel to prevent the sewage to infiltrate down to the water table. In addition, the farmers use poultry manure as natural fertilizers, containing high amount nitrogen and artificial fertilizer (pailed Urea), which has a high concentration of nitrogen (46 %).

V-5.1 Hydrochemistry of Groundwater

The salinity of the groundwater of the area ranges from 420 to 660 mg/l Table V-5.1. The chemistry was sampled more than once for some wells, and the TDS showed a slight variation in time for the same well Appendix 3. The chemistry of the groundwater reflects the water rock interaction which mainly consists of basalt and/or carbonate material. The variation in TDS of some wells like No.53, 61, and 55 indicates evaporation and irrigation return flow contribution. This is very well seen from the high NO_3^- concentration in wells No. 61, 55 and 50 (Appendix 3). Table V-5.2 indicates that the $\text{Na}^+ - \text{Cl}^-$ type is the most abundant type of groundwater due to salt deposits above the surface during the evaporation of irrigation water and to sewage contamination.

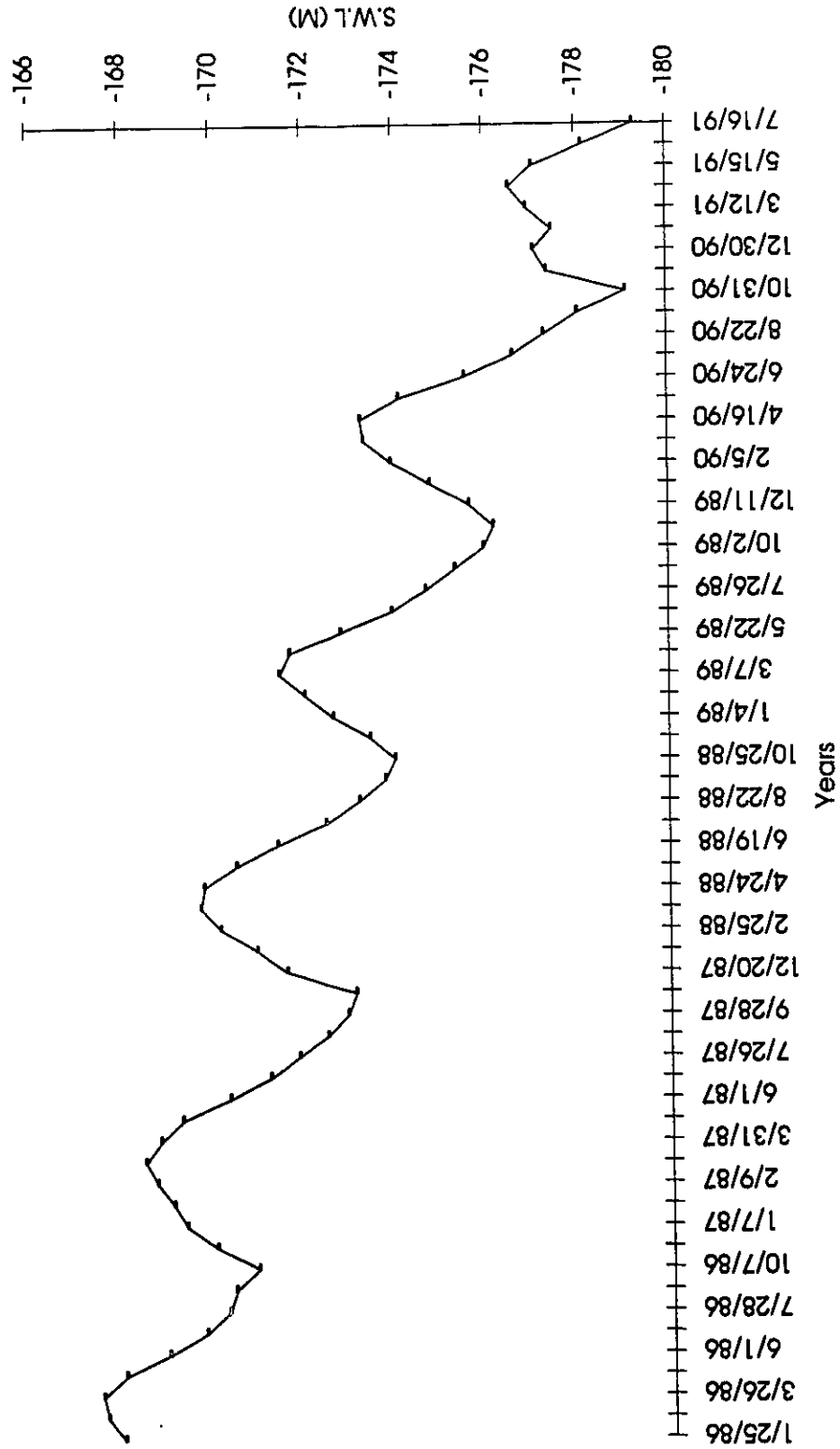


Fig. V-5.2 Water level fluctuation in Baej well in the North-East Desert

Table V-5.1 Average Chemical Composition of the Groundwater

Well No.	TDS	pH	Ca ⁺²	Mg ⁺²	Na ⁺	K ⁺	Cl ⁻	SO ₄ ²⁻	HCO ₃ ⁻	NO ₃ ⁻
	ppm		ppm	ppm	ppm	ppm	ppm	ppm	ppm	ppm
50	653	7.2	70	40	71	1.5	160	43.2	249	28.4
51	610	7.3	57	31	71	4.5	131	37.5	305	1.1
52	533	7.2	67	26	65	4.0	101	32.1	297	0.28
53	516	7.9	24	22	103	7.7	128	54.7	170	13.8
54	483	7.6	31	22	88	6.4	104	51	198	10.1
55	563	7.9	25	28	105	6.4	145	68	146	19.7
56	454	7.9	20	22	90	5.1	99	48	176	12.9
57	605	8.1	64	19	87	6.3	116	48	302	0.0
58	429	7.6	47	26	48	2.7	72	36	244	0.3
59	499	7.8	37	24	86	6.0	103	57	224	1.8
60	564	7.9	29	23	117	7.4	152	59	183	10.6
61	611	7.8	24.6	33.6	112	6.06	176	63.6	156	20.3

In this area the potential evaporation exceed annual precipitation by a considerable amount (NJRWIPS, 1982). The Cl⁻ versus Na⁺ graph (Fig.V-5.3), where the NO₃⁻ concentration is the label for some wells, shows that the low nitrate groundwater plot close to the regression line, and the high NO₃⁻ deviates to the right or to the left. The samples to the right can be explained by the adsorption of sodium by the clay minerals during the infiltration of the return flow. Those to the left show that the Na⁺ exceeds the Cl⁻ concentration and this can come from (organic) sewage seepage.

Table V-5.2 shows that there are three groups of water. The first group Ca²⁺ - HCO₃⁻ represent the carbonate water rock interaction.

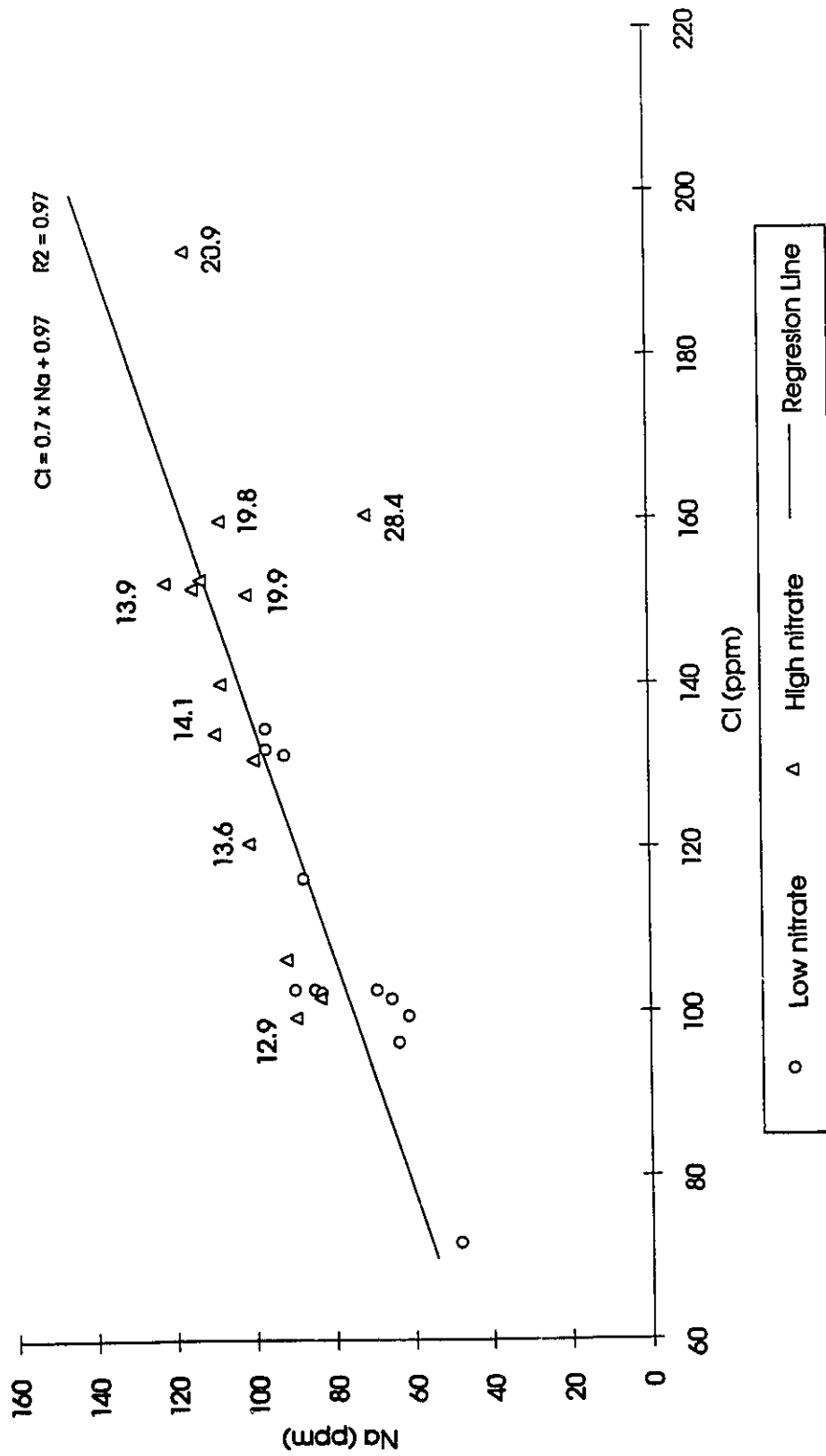


Fig.V-5.3 Relationship of chloride to sodium for North-East Desert groundwater, including the regression line. Some samples are labeled by the concentration of nitrate.

This type of water is well represented in the Swelmeh area (No.52 well). The second type is the $\text{Na}^+ - \text{Cl}^-$ type of water. This type of water found mostly in the eastern part of the North-East Desert. The third group is the $(\text{Na}^+ - \text{HCO}_3^-)$ type of water. The latter is characterized for groundwater flowing through the basalt formation. Such a groundwater was observed for the base flow of the Yarmouk River in dry season, which is mainly coming from the springs discharge from the basalt aquifer (see section IV-2.1).

The water characterized with $\text{Ca}^{2+} - \text{HCO}_3^-$ circulates mainly through the carbonate formations, while the $\text{Na}^+ - \text{HCO}_3^-$ within the basalt. The wide variation of the Na^+/Cl^- and $\text{Ca}^{2+}/\text{Mg}^{2+}$ can be attributed mainly to contamination rather than the dissolution of the halite and to cation exchange.

Table V-5.2 Ionic ratios

No of Well	Type of Water	$\text{Ca}^{2+}/\text{Mg}^{2+}$	Na^+/Cl^-
		ppm	ppm
50	$\text{Na}^+ - \text{Cl}^-$	1.75	0.44
51	$\text{Na}^+ - \text{HCO}_3^-$	1.8	0.54
52	$\text{Ca}^{2+} - \text{HCO}_3^-$	2.37	0.64
53	$\text{Na}^+ - \text{Cl}^-$	1.09	0.80
54	$\text{Na}^+ - \text{Cl}^-$	1.4	0.84
55	$\text{Na}^+ - \text{Cl}^-$	0.89	0.72
56	$\text{Na}^+ - \text{Cl}^-$	0.9	0.91
57	$\text{Na}^+ - \text{HCO}_3^-$	3.36	0.75
58	$\text{Ca}^{2+} - \text{HCO}_3^-$	1.80	0.66
59	$\text{Na}^+ - \text{HCO}_3^-$	1.54	0.83
60	$\text{Na}^+ - \text{Cl}^-$	1.26	0.76
61	$\text{Na}^+ - \text{Cl}^-$	0.73	0.63

V-5.2 Isotopic Composition of Groundwater:

The WMV of the Ras Munif and Irbed rainfall stations are shown in the $\delta^{18}\text{O}$ - δD diagram (Fig.V-5.4). The groundwater samples show strong variations in $\delta^{18}\text{O}$ and δD ranging from -5.2 to -6.5 ‰ and -26.8 to -35.7 ‰ respectively (Appendix 3).

A wide range of stable isotope contents was observed in the same well sampled in different periods of time (No. 52 and 59).

Evaporation plays a significant role as evidenced by some samples which show a deviation from the EML. From Fig.V-5.4 we can notice the following: Firstly some well samples plot along an evaporation line originating on the EML.

$$\delta\text{D} = 1.45\delta^{18}\text{O} - 22.8 \text{‰}$$

This origin on the EML is much more depleted than the isotopic composition of the Ras Munif station. This means that a recharge with elevation higher than Ajloun Mountains is responsible for such a recharge. This recharge most probably comes from the high elevation of Jabal AL-Druze Mountains in Syria north to the study area. Secondly, a wide variation is observed in the water of some samples. It is possible that the variation of the isotope in the wells could be due to the stratification of the groundwater:

The basalt aquifer is divided by six clay layers, so every layer represents a separate path to the groundwater from the recharge area back from Jabal Al-Druze or from the return flow above the study area to the point where the water is captured by a drilling well.

The heavy pumping in summer can also create a mixing condition of the different layers supporting the groundwater. Geyh, et al. 1985, suggested that the recharge area in Jabal Al-Druze consists of wide outcropping basalt, covered by impermeable so...

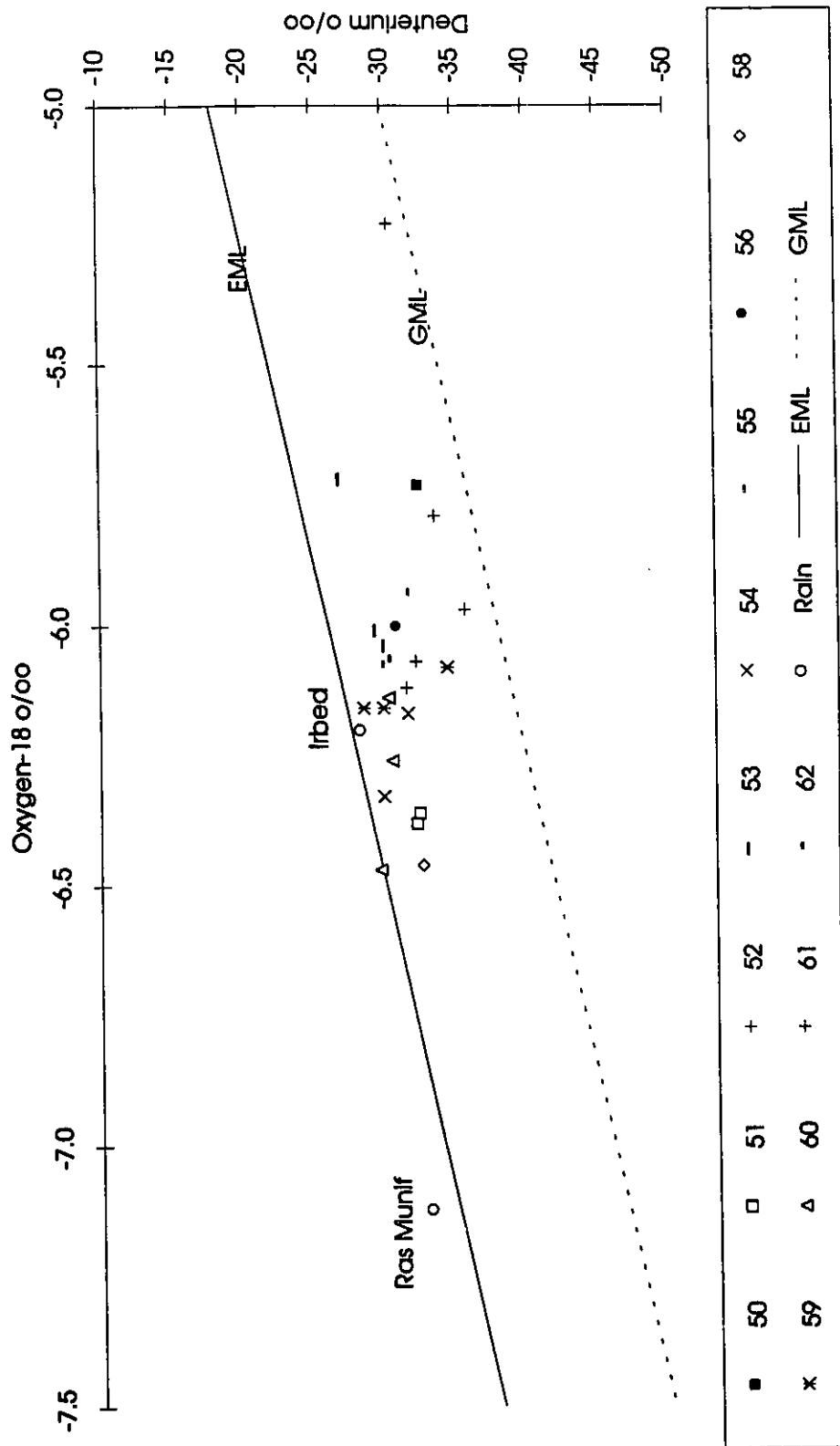


Fig.V-5.4 Plot of oxygen-18 and deuterium, including the EML and the GML. The majority of samples show evaporation effects.

This soil can postpone the infiltration of precipitation water in a small depression of lakes that has undergone evaporation before infiltrate to the groundwater. In addition, the area is under an extensive irrigation especially in summer when, the source of water for irrigation is groundwater. The return flow from irrigation is subject to evaporation before infiltration back to the aquifer.

V-5.3 Radioactive Isotopes of Groundwater

1 Tritium: The majority of the wells show untritiated water (Appendix 3), but some wells recorded a low concentration of tritium. This indicates that the majority of groundwater was recharged before 1952. The low concentration of tritium indicates that there is a minor contribution from local rainfall and return flow. The non-perennial wadies in winter time became perennial after an intense rain or flood which can come from Jabal Al-Druze mountains, and the chance of infiltration is possible through fractures. For that reason we can observe that some wells recorded variable concentrations of tritium at different times. Wells such as No. 60 show a range of tritium of between 0.6 and 1.1 T.U, and No.53 of between 0.0 and 2.9 T.U. This indicates that recharge occurs rapidly along fractures or along basalt channels underneath the wadies.

2 Carbon-14: There is only one ^{14}C sample from the study area and it is from the well No.51, which penetrate the B2/A7 aquifer. The ^{14}C value is 3.28 pmc and the ^{13}C is -9.10 ‰. The low ^{14}C and ^{13}C indicates that both of these parameters were modified by reaction with the aquifer materials. The silicate mineral in general will react with the water, but

the ^{14}C and ^{13}C will be maintained. The chemistry of the well indicates that some of the water passes through the carbonate. The stable isotope of the wells indicate that the groundwater is of meteoric origin and recharged in our predominant climate. Further studies are needed from the recharge area in Syria as well as from other well field in the North-East Desert in Jordan, in order to explain the low ^{14}C of the groundwater.

V-6 Summary of non-thermal groundwater

- 1) Tritiated groundwater identified in the regional B2/A7 aquifer only in Nuaimh area on the Ajloun Mountains and side wadies.
- 2) Shallow tritiated groundwater are also found in overlying aquifer, including the B4 Ramtha area) and alluvium aquifer (Adasyia area).
- 3) The stable isotopic composition of the tritiated groundwater indicates local recharge corresponding to the elevation of the local terrain.
- 4) The stable isotopic content of the B2/A7 groundwaters for Nuaimh fall between the weighted mean value of Ras Munif and Irbed precipitation, in the region of outcrop of this aquifer. As will be shown below, this group ($\delta^{18}\text{O} = -5.5$ to -6.5 ‰ -25 to -35 ‰) can be identified to the recharge water for a group of thermal groundwater discharging in the rift zone of the JRV and Mukhebeh.

Chapter Six

Thermal Water

VI.1 Geothermal Setting in Northern Jordan

The current interest in geothermal energy and water resources has stimulated research related to the origin and distribution of geothermal groundwaters. Geothermal fields are areas where the temperature of the groundwater is well above average annual temperature and where the groundwater can be exploited for various purposes. Sources of hot and warm water with temperatures of only a few degrees Celsius above the mean annual air temperature (20 °C) is common in different parts of Jordan. Thermal water in the study area is found mainly in the northern JRV, at Mukhebeh and in the Ramtha area (Fig.I-2). At all sites, the hot water discharges naturally as springs or drilled boreholes, producing a high volume yield and excellent quality. None of the wells produces steam: The highest temperature recorded so far at two wells is 56 °C, while others are in the range of 30 to 54 °C.

In all cases, the discharge issues from a carbonate aquifer except for S-90 whose water issues from a deep sandstone aquifer. This chapter will examine the origin, recharge areas, the residence time and source of heat of the thermal waters.

VI-1.1 Location and Development of Thermal Waters

Over 16 thermal sources with surface temperatures ranging from 30 to 56 °C are scattered throughout the study area. The hot springs occupy a large area of the JRV and have a rather high flow rate. The hot springs are associated with zones of large tectonic

faults and especially with the junctions of intersecting faults (Bender, 1974, Truesdell, 1979; Abu-Ajamieh; 1980; Myslil, 1988). The system of the fracture zones in the sedimentary rocks is the main channel for the hot flow to ascend as springs. The density of such fissures, the depth to which they penetrate, the thickness of the covering layers of sedimentary rocks, as well as other factors predetermine the different conditions of distribution and formation of the composition and resources of the hot springs.

At the beginning of the 1980's, along the main eastern fault of the JRV, several wells were drilled to evaluate the groundwater potential of the area to meet the increased demand for water supply. The thermal water in the study area is found in three areas (Mukhebeh, north JRV, and Ramtha).

(1) Mukhebeh Area

In the Mukhebeh area of Northern Jordan, two fresh water thermal springs, Maqla and Balsam, issue into the Yarmouk Valley some 500 m from the Yarmouk River at approximately 50 m bsl (Fig.VI-1). The discharge temperatures of the springs are 31 and 43 °C for Balsam and Maqla respectively. The two springs emerge along a structural feature in the very thick (300 m) impervious bituminous B3 marl.

The two springs are less than 50 meters apart from each other. The spring waters have been used since ancient times for curative purposes. The Mukhebeh springs constitute the base flow of the Yarmouk River joining with other springs upstream and downstream along the River.

Between 1981/1984, eight wells of different depths were drilled in the Mukhebeh

area, near the thermal springs, in order to investigate the groundwater potential in this area. These wells penetrated different aquifer layers Table VI-1. The shallower wells, up to 500 m, tapped the upper part of the carbonate aquifer B2/A7 (No. 1, 2, 3, 6 and 7). Mukhebeh No.4, with a depth of up to 892 m, tapped, in addition to the B2/A7, the lower aquifer A4, while the deepest well, JRV1 (depth of 1230 m), tapped the three carbonate aquifer systems A1-2, A4 and B2/A7.

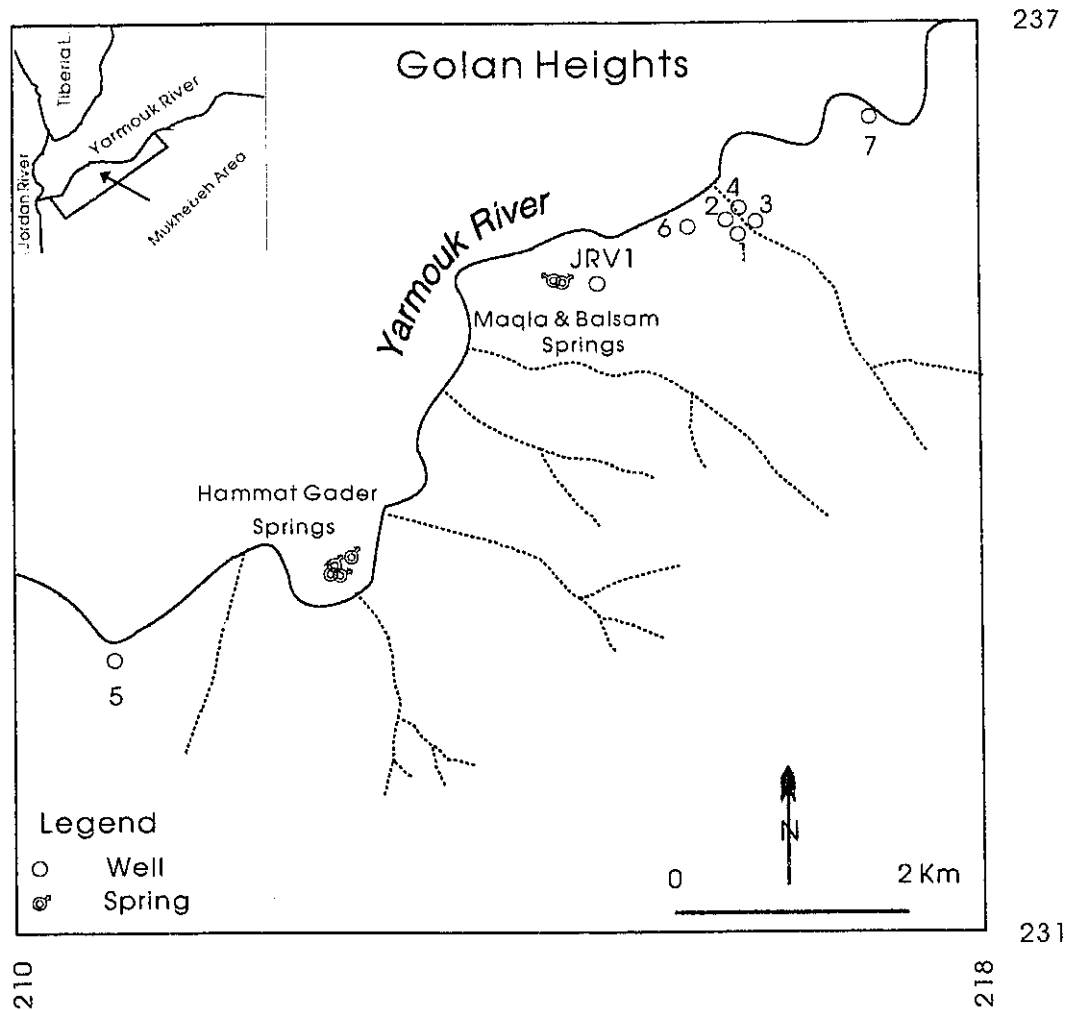


Fig.VI-1 Location map of Mukhebeh area

None of the wells tapped the deeper Lower Cretaceous sandstone aquifer (Kurnub). Mukhebeh wells 1 to 7 struck an artesian aquifer bringing water to the surface at a flow rate of from 200 to 6000 m³/h and with a discharge temperature range of between 29.6 and 45.6 °C. Mukhebeh well No.1 is the shallowest well, completed as an open hole. The other wells are blind cased to different depths with slotted casing to the bottom (WAJ-Files). The hydrostatic pressure of some wells is as high as 172.5 pounds per square inch (PSI). This pressure was recorded in Mukhebeh 7 in 1983, and dropped to 136 PSI in 1988. In Mukhebeh 5, the PSI was 43 in 1983 and fell to 23 PSI in 1988. No pump is required to extract the water from the Mukhebeh wells, with the exception of the deep JRV1 well.

The discharge of the two springs (Maqla and Balsam) decreased from about 17.2 MCM/y (long term average) to about 11 MCM/y over a period of 10 years (WAJ-Files). This decrease is due to the heavy abstraction from the Mukhebeh well field which increased from about 8 MCM in 1983 to about 30 MCM in 1991. The water is used for irrigation throughout the year. During summer, some is pumped to Amman for domestic purposes.

The deep JRV1 well is under non-flowing artesian pressure. The water level in the well has been monitored from 1982 to 1992 (Fig.VI-2). The graph indicates that there are fluctuations and general declines in the water level. These data represent the static water level, and the sharp fluctuation in October 1991 is the result of intensified groundwater abstraction.

Table VI-1 General Hydrogeological Information about the Wells

No.	NAME	Elev m	Depth m	Casing Slotting m	Open Hole m	Aquifer	Yield m ³ /h	SWL m	TDS	G.G oC/100m	Toc
Mukhebeh											
8	Balsam Spr.	-50					1969		653		34.5
9	Maqla Spr.	-50					1969		902		41.8
10	JRV1	-70	1230	0-218	218-1230	B2/A7, A4, A1/2	157	11	1056	1.82	42.5
11	Mukhebeh 1	-80	350	0-14	14-350	B2	6000	FLOW	538	2.74	29.6
12	Mukhebeh 2	-110	488	0-284	284-488	B2	800	FLOW	525	2.54	32.4
13	Mukhebeh 3	-80	333	0-173	173-333	B2	2822	FLOW	544	4.20	34.0
14	Mukhebeh 4	-110	892	0-220	220-892	B2/A7, A4	2200	FLOW	538	1.82	36.3
15	Mukhebeh 5	-118	900	0-549	549-896	B2/A7	200	FLOW	582	2.84	45.6
16	Mukhebeh 6	-95	475	0-200	200-475	B2	2000	FLOW	506	3.76	37.9
17	Mukhebeh 7	-115	500	0-150	150-500	B2	2100	FLOW	461	4.40	42.0
JRV											
18	North Shuneh	-178	967	0-268	268-840	B2/A7	900	Flow	672	3.49	53.8
19	Manshieh	-175	1150	0-857	857-1150	B2/A7	200	Flow	486	2.60	50.0
21	Abuziad	-120	1126	0-631	631-1126	B2/A7	90	Flow	1360	2.80	51.6
22	Wagas	-90	1300	0-916	916-1300	B2/A7	60	Flow	435	2.36	50.8
Ramtha											
24	S-90	566	2190	0-1116	1116-2190	B2/A7, K, Z		151	2400	2.54	56.0
23	Mahasi 6	481	702	0-470	470-702	B2/A7	100	282	493	3.13	42.0

G.G: geothermal gradient

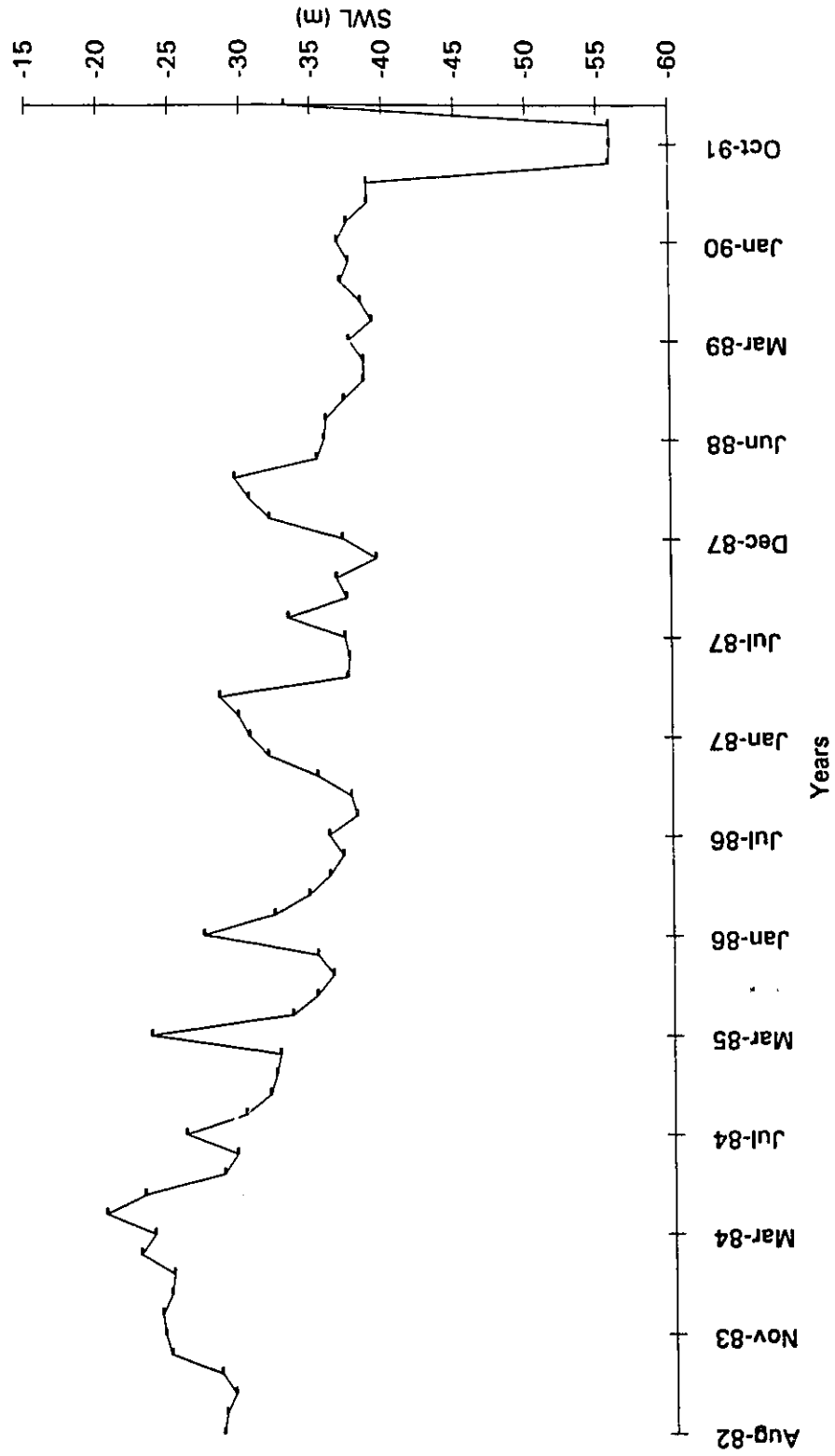


Fig. VI-2 Water level fluctuation in JRV1 well in Mukhebeh area.

(2) Jordan Rift Valley (JRV)

The JRV, which extends between Lake Tiberias and the Red Sea, is rich in thermal waters issuing as springs. Many of these hot springs, especially Zarqa Ma'in and Zara which are located close to the Dead Sea shore, have been described in detail by Bender, (1974), Truesdell, (1979), Abu-Ajamieh, (1980), Salameh and Rimawi, (1984) Rimawi and Salameh, (1988), and Bajjali, 1988). The study area comprises the junction of the JRV and Yarmouk River fault zone wadies extending from the convergence of the Yarmouk River and the Jordan River to 20 km south. In this area 4 drilled wells penetrate the B2/A7 aquifer, where the groundwater was found under artesian conditions (Fig.V-2.1). Well depths range between 967 and 1300 m Table VI-1. The wells are partially cased with either an open hole or slotted casing screen. The Abuziad well is an open hole after 631 m, Manshieh after 857, Waqas after 916, while Hot Shuneh is slotted after a depth of 268 m. The measured pressure for the Hot Shuneh well is stable at about 100 PSI for the period 1987 to 1990. The discharging temperature varies between 52 and 56 °C.

(3) Ramtha area

Ramtha is located in the north-east of the Ajloun Mountains in the eastern Yarmouk basin (Fig.V-4.1). Elevations are approximately 500 m asl. The groundwater of the B2/A7 aquifer has temperature elevated above similar depth wells elsewhere in Jordan. The area is characterized by complicated faulting systems and it is located close to the flood basalts of NE of Jordan.

The thermal water is encountered in two aquifer systems; the deep and hot Kurnub

sandstone aquifer (56 °C) and the intermediate carbonate (B2/A7) aquifer (42 °C). In the sandstone aquifer there is only one deep well, drilled during the investigation for oil in this area, while there are several wells tapping the B2/A7 aquifer Table VI-1.

The deep (S-90) well was drilled in 1970 to a depth of 2191 m in the search for petroleum. The well penetrated four aquifer systems: The (K-Z), A1-2, A4 and the B2/A7 aquifers. The upper carbonate aquifers (B2/A7, A4 and the A1/2) are cased. The Kurnub groundwater in this well is brackish (2400 mg/l) with a temperature of 56 °C. The B2/A7 aquifer is developed by the Mahasi 6 well, with a depth of 702 m and a temperature of 42 °C. All wells in both aquifers are under artesian conditions and discharge groundwater with H₂S.

VI-1.2 Groundwater Temperature and geothermal gradients

The highest groundwater temperature in the study area is encountered in the wells in the JRV area, some 1 to 3 km from the main Jordan Rift fault zone. This area is known to host the hottest springs in Jordan, with temperature in the range of 30 to 56 °C.

Present day groundwater temperatures of the wells in Mukhebeh area are not as high as the JRV wells, and range between 29.6 and 46 °C. In the past (1981-1982), when the wells were drilled, temperatures slightly higher than at present were recorded (Table VI-2). This suggests that the aquifer has been affected by withdrawal, presently estimated to be an average of 30 MCM/y. In addition, the pressure in the Mukhebeh wells has dropped since exploitation began. This fact supports the conclusion that the thermal reserve is directly influenced by the total withdrawal extracted by boreholes which

intercept the fluid supplying the springs.

Observation also reveals a slight variation in the temperature of these thermal waters. Generally, the most noticeable variations were observed for the Mukhebeh springs which have recorded temperature variations of approximately 4 °C. Of particular note, the Mukhebeh wells No. 6 and 7 recorded a temperature variation of less than 2 °C. It is important to mention that the recorded temperatures are those taken of water discharging from the orifice of the well and not temperatures taken from bottom-hole water taken at depth. The measurement error is in the range of 1 °C. The slight variation of some sources (the springs and Mukhebeh 1) could be attributed to the slight mixing with cold water prior to its emerging at the surface (See section VI-5.1). During the drilling process in the Mukhebeh area, a slight discharge of cold groundwater appeared at shallow depth, before it encountered the main aquifer from which the large volume of hot groundwater was discharged (WAJ-Files).

The temperature of the hot sources in the three areas is plotted against the total depth (Fig.VI-3). The regression line for these data is:

$$\text{Depth (m)} = 44 T(^{\circ}\text{C}) - 986 \quad (R^2 = 0.80)$$

We can see from the graph (Fig.VI-3) a trend toward increased temperature at greater depth. However, a clear contradiction is observed in the JRV wells and in some borehole in the Mukhebeh well field.

In the JRV well field, the data show that the North Shuneh well, which has the shallowest depth (967 m) has the highest temperature (54 °C), and the Waqas well which has the greatest depth (1300 m) has a temperature of only 51 °C.

Table VI-2 Temperature fluctuation of some thermal wells.

Name	T°C During Drilling	Temperature range
Maqla Sp.	-	39.0-43.0
Balsam Sp.	-	33.0-34.4
JRV1	42.5	41.5-42.5
Mukhebeh 1	32.0	29.6-32.0
Mukhebeh 2	35.0	32.4-35.0
Mukhebeh 3	-	32.4-34.0
Mukhebeh 4	-	36.3
Mukhebeh 5	45.0	45.0-45.6
Mukhebeh 6	38.0	37.9-38.0
Mukhebeh 7	42.0	40.1-42.1
N. Shuneh	56.0	52.5-56.0
Manshieh	-	49.8-50.0
Waqas	51.0	51.0-52.5

The relation between total depth (TD) and temperature in the Mukhebeh groundwaters provides an even poorer correlation:

$$\text{Depth (m)} = 37 T (\text{°C}) - 726 \quad (R^2 = 0.68)$$

Specific wells which contribute to this poor correlation include:

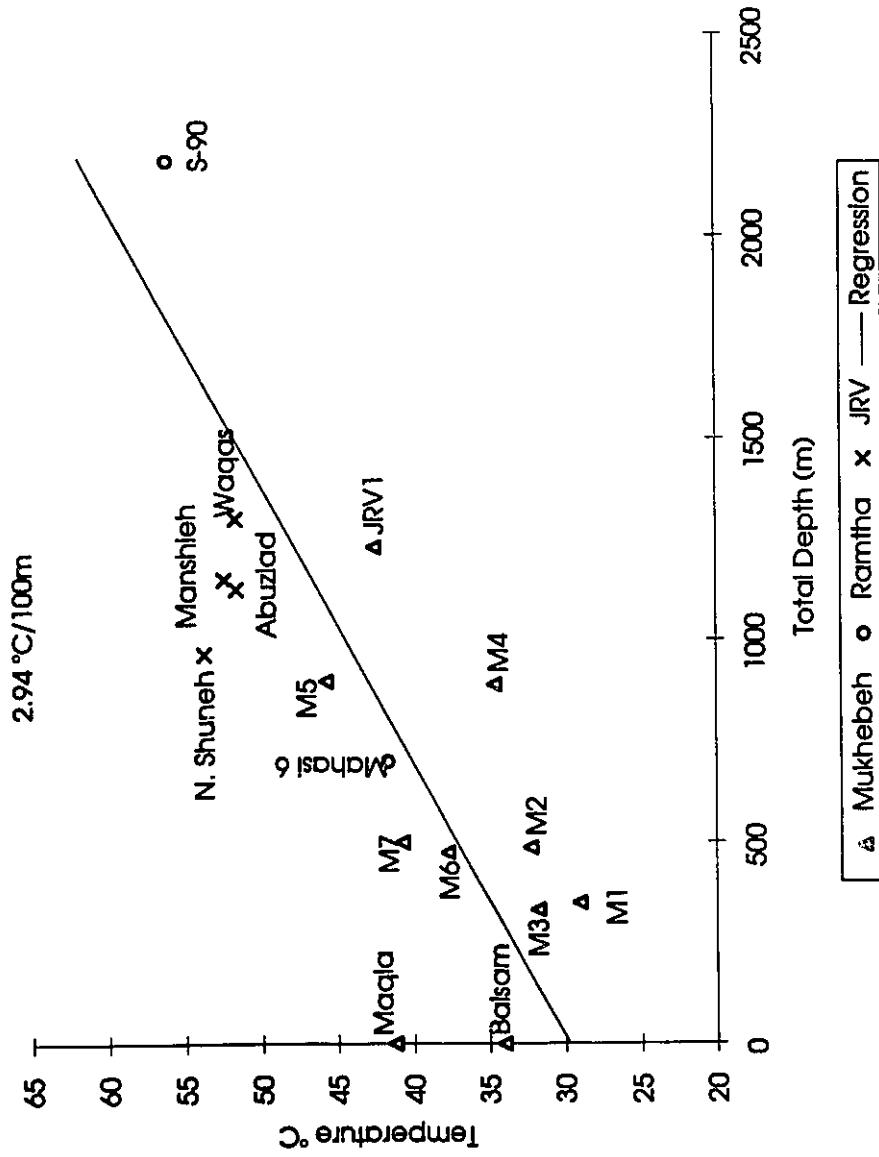


Fig. VI-3 Depth versus the temperature in the Mukhebeh (designated as M1-7), JRV and Ramitha area, the line show the geothermal gradient of 2.94 °C/100m.

(i) Mukhebeh wells No. 2 and 7 have a 8 to 10 °C temperature difference is recorded at equal depths (488 and 500 m TD respectively). Both have relatively similar TDS (544 and 461 ppm respectively). The same is observed for Mukhebeh 4 and 5, the former have 36.3 °C, 899 TD, 538 TDS, while the latter 45 °C, 900 m TD, 582 TDS. (ii) The high temperature recorded for the shallow depth Mukhebeh well No. 7 (500 m total depth and 41.5 °C), as respond to Mukhebeh No. 4 (892 m total depth and 36.3 °C) or JRV1 (1230 m, 42 °C) despite the 730 m depth difference.

The gradient calculated from the regression in Fig VI-3 is 2.94 °C/100 m, which corresponds to estimates reported by earlier investigators (Williams, et al., 1990). Figure VI-4 is a geothermal gradient map for Jordan and shows a gradient of 3 °C/100 m for the JRV region. The geothermal gradient for areas adjacent to the JRV (Israel) is 2.43 °C/100m and was estimated from bottom hole temperatures measured in oil drilling at depths between 0.5 and 3 Km (Strainsky, et al., 1979). The geothermal gradient of the thermal wells was calculated because the temperature at the bottom of the wells is unknown. (The gradient was calculated using the temperature of the well discharge, considering it as representative of the temperature at the well bottom, and the mean annual air temperature). This gave a geothermal gradient varying between 1.82 (JRV1) and 4.4 (Mukhebeh 7) Table VI-1. The latter has the highest geothermal gradient among Mukhebeh wells.

A high geothermal gradient of 4.5 °C/100 m was recorded for En Sa'id well (Israel), located 3.5 km north to Mukhebeh well field. The temperature of the remainder of the wells lie well within the average geothermal gradient (~ 2.5 °C/100 m) for this

region. The great variation in geothermal gradients between many of these wells may be due to either (i) rapid ascent of deep heated groundwaters due to tectonic fracturing to a shallower aquifer zone, or (ii) heterogeneity in subsurface heating related to magmatic intrusion beneath the Yarmouk River near Mukhebeh well No.7.

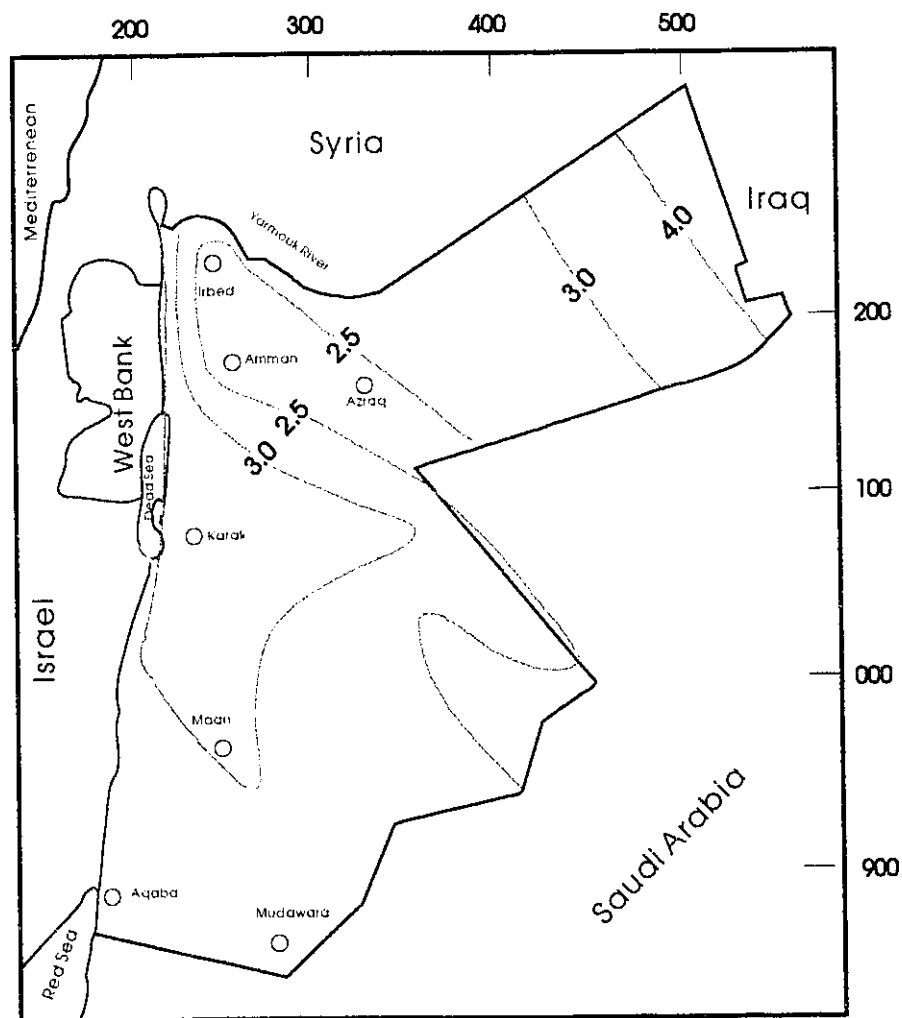


Fig. VI-4 Geothermal Gradient Map of Jordan ($^{\circ}\text{C}/100\text{m}$) (after Williams et al., 1990)

Some Mukhebeh wells are also characterized by variations in salinity and temperature. The highest salinities were observed in the JRV1 well (1000 ppm TDS, 1238 m total depth, and 42.5 °C), in the Mukhebeh No. 7 (460 ppm TDS, 500 m total depth, and 42 °C) and the Mukhebeh 5 (565 ppm TDS, 900 m total depth, 45 °C). The first two wells are located 2.45 km apart. Like depth, the correlation between salinity and temperature is not good.

In the JRV well field, the possibility of deep circulation is enhanced by tectonic faulting which can act as conduit for groundwater flow. The high temperature could come from a zone at a greater depth through a deep seated fault. A fast groundwater circulation through this zone reduces the contact time between the circulating water and the host rock. Bodverson, (1961), and Mazor, et al., (1969) indicated that the thermal water could appear in areas with normal geothermal gradient but with special hydrological mechanisms that enable the water to penetrate deeply enough to gain enthalpy, and then ascend quickly so that heat losses are low. The heating process in this part of the JRV area seems to have a similar pattern. The circulation took place under normal geothermal gradient recorded in the JRV area (~ 3 °C/100m).

In the Ramtha area the S-90 (2190 m) and Mahasi 6 (702 m) wells recorded temperature of 56 and 42 °C from the wells' orifice respectively. The bottom hole temperature in the S-90 well provides a gradient of 2.54 °C/100m (Galanis et al., 1986). The temperature recorded at 701 m depth was 43 °C. This is almost identical to the recorded temperature (42 °C) from orifice of the Mahasi 6 well. From these observations we can conclude that the groundwater temperature in this area is heated at depth by a

normal geothermal gradient of (~ 2.54 °C/100m).

VI-1.3 Tectonic Environment

The area of the JRV between the Red Sea and Lake Tiberia is a fragment of the African-Syrian transform fault. This area forms the boundary between the Arabian plate and the Palestine-Sinai plate (Garfunkel, 1981). The Arabian plate is moving north in an oblique fashion in response to the Red Sea opening in the south. Transverse faults offsetting the Red Sea spreading ridge include the JRV system. Garfunkel et al., (1981), using historical earthquake data, calculated a slip rate along the JRV ranging from 0.13 to 0.35 cm/y during the last 1000 to 1500 years, and from 0.7 to 1 cm/y during the last 5 Ma.

Numerous earthquakes have occurred in the JRV area. The 1927 earthquake in the Jericho area, 15 km north-west of the Dead Sea, was recorded in Europe, North America and the former USSR. The land mass on the west moved south during the earthquake by perhaps as much as 50 cm (Amos Nur, 1991).

Magma extrusion to the surface or subsurface intrusion occurred along this corridor since Tertiary time. For example, to the NE of the Dead Sea, a small pluton has emerged at the surface through a crossing of two fault systems. The hottest spring (63°C) recorded in Jordan is associated with this pluton (Abu-Ajamieh, 1980).

Hatcher et al., (1981) indicated that in the area of Yarmouk Valley exists a magnetic anomaly. A gravity survey in the Yarmouk Basin conducted by Qura'an (1991), concluded that there are 3 subsurface intrusions, at a depth of 3 to 4 km.

The extensive basaltic tuff cover the area indicates there has been a long period of volcanic activity (Bender, 1974). A radioactive ^{14}C dating of bone associated with the basalt in the Yarmouk Valley indicated an age of 4075 ± 160 years (Muati, 1970).

Additional examples of present volcanism activity exist along the East African Rift where there are several active volcanoes (Gass, 1970). Hot water and steam, associated with this rift, were recorded in Kenya and Ethiopia by Endeshaw (1988) and Kamondo, (1988).

VI-2 Hydrochemistry of the thermal water

The chemical data is important to understanding the geochemical evolution of the flow system of the thermal waters. Understanding the water - rock interaction of the groundwater will help to: (i) evaluate the origin of the water and the dissolved constituents; (ii) trace the recharge area and verify the validity of the flow direction proposed by previous studies and; (iii) characterize the redox state of the aquifer to be used as a basis for consideration on the evolution of groundwater chemistry and radiocarbon dating; (iv) estimate the subsurface temperature of the reservoir rocks by different chemical geothermometers.

The thermal waters are sampled during the period 1987 to 1992 Appendix 3. The average composition of all the samples is represented in Table VI-3. The data show a remarkable compositional stability for this period. The groundwater is considered fresh (less than 1000 mg/l), with the exception of the S-90 and Abuziad wells in the Ramtha and JRV areas. The salinity of these two sources is 2400 and 1300 mg/l respectively. In order to relate the chemical characteristics of the groundwater to the lithologic pattern, the dominant cation and anion, expressed in meq/l, are used for classification.

The thermal water can be categorized into four groups Table VI-3: (1) calcium bicarbonate (Ca^{2+} - HCO_3^-); (2) calcium, sodium chloride (Ca^{2+} , Na^+ - Cl^-); (3) sodium chloride Na^+ - Cl^- ; and (4) calcium sulphate Ca^{2+} - SO_4^{2-} .

In the Mukhebeh, area the (Ca^{2+} , Na^+ - Cl^-) and (Ca^{2+} - HCO_3^-) types of water are found. The former is identical for the deep JRV1 well and Maqla spring, while the latter for Mukhebeh wells No. 1 to 7 and the Balsam spring.

Table VI-3 Average Chemical Parameters and Type of Water

NAME	TDS ppm	pH	T OC	Kh mV	Ca meq/l	Mg meq/l	Na meq/l	K meq/l	Cl meq/l	SO4 meq/l	HS meq/l	HCO3 meq/l	NO3 ppm	LA ppm	F ppm	SiO2 ppm	T.Water
JRV1	989	7.19	42.5	93	6.42	3.62	5.93	0.37	5.83	4.90	0.7	5.46	2.15	0.66	1.1	21.25	Ca, Na-Cl
Magla Spring	891	7.16	41.8	-59	5.83	2.79	5.28	0.34	5.61	3.30		5.35	3.79	0.58	1.3	28.23	Ca, Na-Cl
Balsam Spring	644	7.05	34.5	240	4.92	2.60	3.17	0.18	3.17	1.89		5.77	0.46	0.35		25.70	Ca-HCO3
Mukhebeh 1	531	7.24	29.6	163	4.63	2.61	1.76	0.10	1.67	1.18		6.21	0.60	0.26	0.5	15.10	Ca-HCO3
Mukhebeh 2	522	7.22	32.4	118	4.40	2.60	1.80	0.09	1.65	1.09		6.02	0.77	0.25	0.6	15.20	Ca-HCO3
Mukhebeh 3	539	7.25	34.0	103	4.63	2.62	1.79	0.09	1.75	1.14		6.18	0.56	0.24	0.6	15.00	Ca-HCO3
Mukhebeh 4	482	7.72	36.3	73	3.71	2.50	1.87	0.10	1.76	0.97		5.15	1.04	0.25		14.60	Ca-HCO3
Mukhebeh 5	565	7.04	45.6	-58	4.22	3.64	1.85	0.10	1.72	1.06	1.9	6.97	2.72	0.27	0.6	18.35	Ca-HCO3
Mukhebeh 6	491	7.22	37.9	-44	3.83	2.24	1.98	0.13	1.81	0.77	0.8	5.42	3.36	0.24	0.7	20.15	Ca-HCO3
Mukhebeh 7	472	7.36	40.1	-32	3.60	2.17	1.93	0.11	1.59	0.77		5.30	3.24	0.24	0.8	13.70	Ca-HCO3
Manshieh	495	7.11	49.8	-61	3.89	3.27	1.32	0.02	1.33	0.99	1.3	6.01	0.37	0.22	0.5	17.40	Ca-HCO3
Maggas	433	7.28	50.8	-98	3.34	2.92	1.15	0.07	1.07	0.59		5.69	1.01	0.21	0.7	17.55	Ca-HCO3
North Shuneh	653	7.02	53.8	-101	3.99	3.60	3.12	0.14	2.79	1.56	1.2	6.43	2.03	0.29	0.7	19.73	Ca-HCO3
Abuziad	1373	7.01	51.6	-96	7.88	4.90	9.53	0.71	9.48	4.62		8.69	1.88	0.92	0.7	18.50	Na-Cl
Mahasi 6	494	7.52	41.7	55	2.68	2.56	2.58	0.07	2.81	0.70	0.6	4.25	1.10	0.24		16.50	Ca-HCO3
S-90	2438	6.30			26.32	3.65	13.15	3.83	4.70	28.85		12.79	2.06				Ca-SO4
H.G. (A)	1488				7.58	3.28	10.65	0.55	14.27	3.68		5.41					
H.G. (B)	1077				5.24	3.66	6.08	0.34	8.46	2.52		5.63					
H.G. (C)	975				6.18	3.08	5.21	0.27	6.14	2.08		5.91					
H.G. (D)	710				4.44	2.69	2.39	0.1	2.45	1.2		6.24					

H.G.: Hammat Gader is taken from Mazor et al., 1973

The salinity is approximately 1000 mg/l for the Ca^{2+} , Na^+ - Cl^- type of water and about 500 mg/l for the Ca^{2+} - HCO_3^- type of water. The exception is the Balsam spring with salinity of 650 mg/l.

In the JRV area the type of water is Ca^{2+} - HCO_3^- with the exception of the Abuziad deep well. Its water is of the Na^+ - Cl^- type.

In the Ramtha area the Ca^{2+} - SO_4^{2-} and Ca^{2+} - HCO_3^- types are found. The first type is found in the sandstone aquifer (S-90) and the latter in the B2/A7 aquifer (Mahasi 6).

VI-2.1 Geochemistry of Mukhebeh area groundwater:

The JRV1 well and Maqla spring have the highest TDS and the lowest HCO_3^- in comparison with the rest of the Mukhebeh groundwaters. The major cations and anions (Na^+ , K^+ , Ca^{2+} , Mg^{2+} , Cl^- , and SO_4^{2-}) increase with increasing TDS, but the HCO_3^- concentration decreases.

The Mukhebeh well field data of Table VI-3 is presented in the fingerprint diagram of Fig.(VI-5). In the figure, each water source is represented by one line. From the graph we can divide the water into three groups: (i) Mukhebeh wells (1 to 7) are very similar on the fingerprint diagram. They show that their ionic ratios are preserved. (ii) the JRV1 well and Maqla spring they preserved the relative abundance of the ions similar to wells No. 1 to 7. However, they show higher values in Na^+ , Ca^{2+} , Cl^- , SO_4^{2-} , while the Mg^{2+} , and HCO_3^- are more or less constant. (iii) The Balsam spring is located between the (Ca^{2+} , Na^+ - Cl^-) type of water and the Ca^{2+} - HCO_3^- type. This suggests that the water of Balsam spring is a mixing between two end members, Maqla spring and Mukhebeh 1.

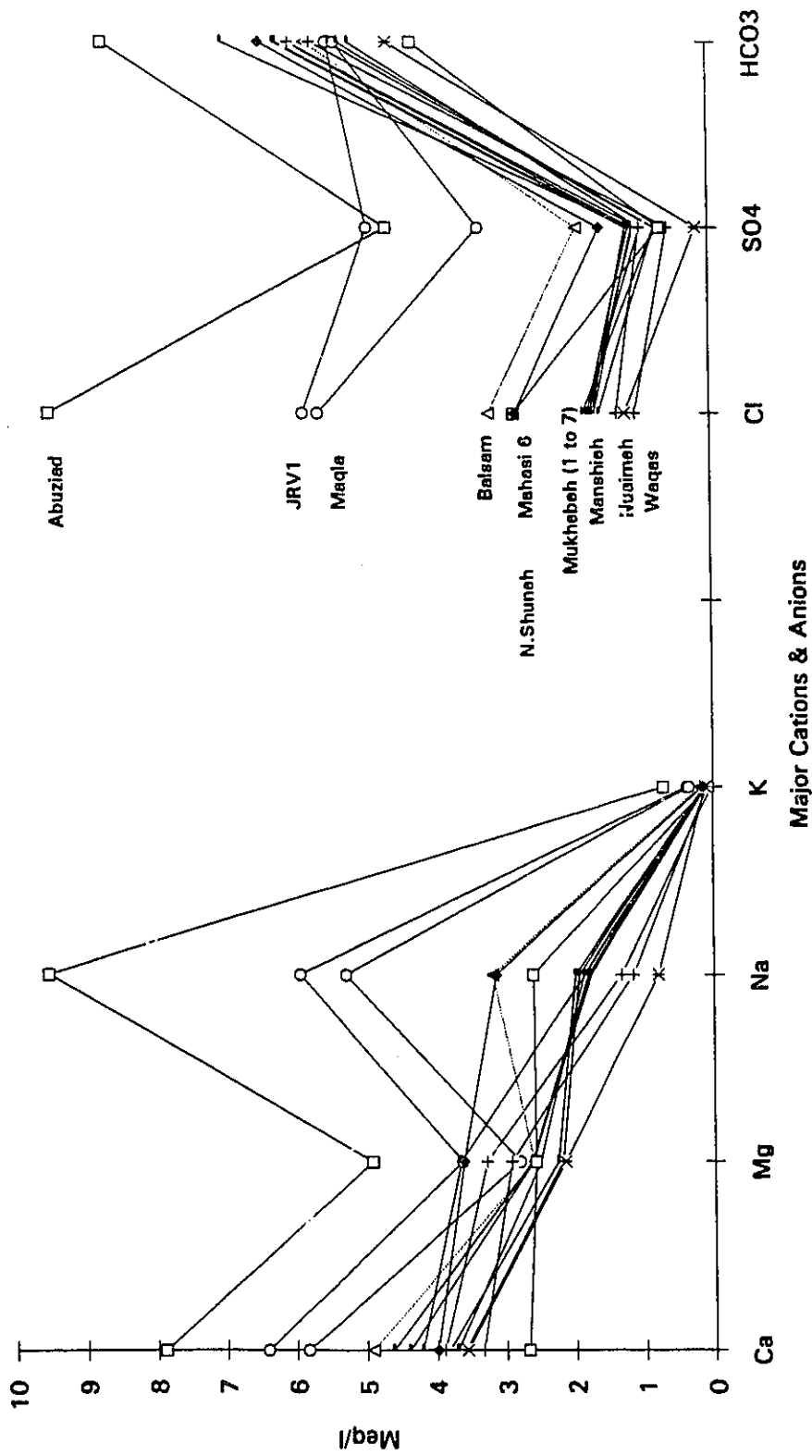


Fig.VI-5 Composition diagram of Mukhebeh and JRV well fields and one sample from Ramtha area (Mahaat 6) and Nuaimah area. Balsam spring designated as dashed line

VI-2.1.1 Mukhebeh wells (1 to 7)

The Ca^{2+} - HCO_3^- type of water in all the Mukhebeh resources is supersaturated with respect to calcite and dolomite Table VI-4. Mukhebeh 5 is in equilibrium with respect to calcite and supersaturated with respect to dolomite. The Mg^{2+} concentration in Mukhebeh 5 (3.64 meq/l) and the $\text{Mg}^{2+}/\text{Ca}^{2+}$ ratio (0.86) are the highest among the other sources (Table VI-4). The other wells are recorded ratio between 0.56 to 0.67. Hsu, (1963) indicated that ratios in range 0.5 - 0.7 are typical for groundwater flowing through limestone aquifers. Ratios in the range 0.7 - 0.9 are commonly associated with dolomitic aquifers. This suggest that at Mukhebeh 5 there are dolomitic layers at depth. This well also recorded the highest temperature (45 °C), greatest depth (900 m) and the lowest discharge rate (200 m³/h) among the Mukhebeh wells (No. 1 to 7).

Mukhebeh wells No. 6 and 7 recorded low SO_4^{2-} concentration, low Eh values and low $\text{SO}_4^{2-}/\text{Cl}^-$ compared to the rest of the Mukhebeh wells Table VI-3 and VI-4. The Eh is -44 and -32 mV, the SO_4^{2-} is 0.77 meq/l and the $\text{SO}_4^{2-}/\text{Cl}^-$ is 0.43 and 0.49 for Mukhebeh wells No. 6 and 7 respectively. A major reason for this could be the reduction of SO_4^{2-} (see VI-2.1.3).

VI-2.1.2 JRV1 well and Maqla spring. The relatively high TDS, Ca^{2+} and SO_4^{2-} and low HCO_3^- concentrations in the JRV1 well and Maqla spring cannot be accounted for only by the dissolution of carbonate material. The dissolution of carbonate material within the flow system will cause an increase in both the Ca^{2+} and the HCO_3^- .

Table IV-4 Statistical Treatment of Isotope Data and Rainfall

Name	Parameter	Mean	S.D	Variance	Max	Min	Range	Skewness	N
Ras Munif	Oxygen-18	-6.52	1.37	1.89	-3.70	-9.09	5.39	0.40	25
	Deuterium	-29.01	10.76	115.98	-4.00	-45.29	41.29	0.57	25
	Tritium	7.89	3.07	9.48	16.00	4.40	11.60	1.23	22
	Deuterium Excess	23.19	4.64	21.59	31.33	11.46	19.87	-0.36	25
	Amount of Rain	86.96	59.55	3546.79	195.60	13.90	181.70	0.54	25
Irbed	Oxygen-18	-5.98	1.68	2.83	-2.14	-8.68	6.54	0.45	24
	Deuterium	-26.94	12.03	144.61	-2.60	-44.60	42.00	0.33	24
	Tritium	7.92	3.68	13.56	21.70	3.80	17.90	2.65	22
	Deuterium Excess	20.90	6.59	43.45	31.12	3.22	27.90	-1.30	24
	Amount of Rain	72.16	47.18	2226.70	165.70	15.60	150.10	0.63	24
Deir Alla	Oxygen-18	-4.08	2.10	4.42	0.36	-8.64	9.00	-0.03	17
	Deuterium	-16.00	15.98	255.56	15.22	-53.70	68.92	-0.24	17
	Tritium	9.19	3.16	10.04	15.80	5.00	10.80	0.57	17
	Deuterium Excess	16.40	3.39	11.51	21.76	11.06	10.70	0.18	17
	Amount of Rain	66.10	33.24	1105.00	130.40	21.30	109.10	0.60	17

S.D. Standard Deviation

Other processes are responsible for this phenomenon such as the dissolution of evaporite associated with rocks at depth. [gypsum ($\text{CaSO}_4 \cdot 2\text{H}_2\text{O}$), anhydrite (CaSO_4), halite (NaCl), and sylvite (KCl)]. Such evaporites are found in the aquifer at depth. Strainsky, et al., (1979) indicated that sea water ingress into the Rift Valley during the Neogene period could result in the evolution to precipitation of halite and in the evolution of brine water. Chemical diagenesis of the brine by reaction with aquifers and dilution by meteoric water, are all likely processes. In addition, the common occurrence of gypsum in the Cenomanian Formation was noticed in the various drill boreholes in the JRV (Mazor and Rosenthal, 1967).

The JRV1 well penetrates three aquifer systems, B2/A7, A4 and the A1-2 (Cenomanian to Campanian). The exploratory drilling results from the JRV1 well also indicated that these aquifers are hydraulically interconnected to form one aquifer system (Joudeh, 1983). The A1-2 aquifer consists of soft to medium marl and marly limestone. This aquifer is well known in different parts of Jordan as poorly productive and often contains slightly brackish water (1000 to 2000 mg/l) (Charalambous, 1991). The casing in the JRV1 well is a slotted casing from a depth of 218 m to the end of the borehole Table VI-1. Water discharged during pumping represents a mixture of water of different qualities from different aquifers zones.

The correlation between the major cations and anions (Table VI-5), maintain a high correlation between Ca^{2+} - Cl^- (0.91), Ca^{2+} - SO_4^{2-} (0.94), Na^+ - Cl^- (0.99), Na^+ - SO_4^{2-} (0.97), and K^+ - Cl^- (0.99), while the correlation between the Ca^{2+} - HCO_3^- (-0.06), Mg^{2+} - HCO_3^- (0.48) is very weak. This is further evidence that the chemistry of the water is

affected directly by the dissolution of evaporite minerals, not from the simple dissolution of carbonate materials. This is very well demonstrated by the high $\text{Ca}^{2+}/\text{HCO}_3^-$ ratio (1.09 - 1.17) in comparison with the Mukhebeh wells 1 to 7 (0.68 - 0.75) Table VI-4.

Table VI-5 Matrix correlation coefficient between the ions of groundwater

	TDS	Ca^{2+}	Mg^{2+}	Na^+	K^+	Cl^-	SO_4^{2-}	HCO_3^-
TDS	1.0							
Ca^{2+}	0.96	1.0						
Mg^{2+}	0.61	0.59	1.0					
Na^+	0.98	0.90	0.49	1.0				
K^+	0.97	0.89	0.45	0.99	1.0			
Cl^-	0.98	0.91	0.48	1.0	0.99	1.0		
SO_4^{2-}	0.98	0.94	0.60	0.97	0.96	0.96	1.0	
HCO_3^-	-0.21	-0.06	0.48	-0.37	-0.40	-0.36	-0.26	1.0

Nevertheless the JRV1 well and Maqla spring are deficient in sulphate (Table VI-3), especially the latter, probably because of the occurrence of sulphate reduction. The two groundwaters contain H_2S . The sulphate reduction and effects of geochemical evolution in these waters will be discussed later. The TDS and SO_4^{2-} concentrations in the JRV1 well are slightly higher than in the Maqla spring. The Eh field measurement of Maqla

spring water is -59 mV while the JRV1 well is 93 mV. This is quite observed by the low ratio of $\text{SO}_4^{2-}/\text{Cl}^-$ in Maqla spring (0.59) in comparison with the JRV1 (0.84).

The difference in TDS and SO_4^{2-} between the JRV1 well and Maqla spring is about 60 mg/l. Considering that the difference in TDS is mainly due to the depletion of SO_4^{2-} in the Maqla spring, one can assume that the two sources have the same origin. Based on the similarity of the chemical characteristic of the JRV1 well and the Maqla spring, we can estimate that the depth from which the Maqla water ascends is about 1200 m (See Fig. VI-3).

VI-2.1.3 Redox Conditions

The redox potential (Eh) measure the tendency of the water to oxidize or to reduce dissolved constituents. To get a better picture about the reduction and oxidation processes in the groundwater along its flow path from the recharge area to the thermal well fields, the Eh was measured in several wells Table VI-6. The water from the recharge area represented by Nuaimah 1 and Hammad Farhan yielded higher values than those from the thermal well fields. The Eh result measurements of the thermal water show disturbingly large variations, where a range between 240 to -101 mV was obtained. The JRV wells demonstrate the lower Eh values in comparison with the rest of the thermal well fields. It has generally proved to be very difficult to obtain a meaningful quantitative interpretation for the Eh (Appelo and Postama, 1993). Nevertheless, generally lower values are observed in the thermal waters. These low values are attributed to sulphate reduction supported by oxidation of organic (kerogen) from the B2/A7 aquifer.

Table VI-6 Eh, pH, HS⁻, and SO₄²⁻

Name	Eh	pH	T	SO ₄ ²⁻ (*)	HS ⁻
	mV		°C	mmol/l	mmol/l
Nuaimeh 1	314	7.33	21.8	0.04	
Hammad F.	234	7.34	20.9	0.08	
Abuziad	-96	6.29	51.6	2.90	
Manshieh	-61	6.66	49.8	0.55	1.3
Waqas	-98	6.98	50.8	0.26	
N.Shuneh	-101	6.75	53.8	0.68	1.20
JRV1	93	6.99	42.5	2.65	0.72
Maqla	-59	7.00	41.8	1.77	
Balsam	240	6.99	34.5	0.90	
Mukhebeh 1	163	7.21	29.6	0.53	
Mukhebeh 2	118	7.29	32.4	0.46	
Mukhebeh 3	103	7.16	34.0	0.30	
Mukhebeh 4	73	7.4	36.3	0.44	
Mukhebeh 5	-58	6.75	45.6	0.47	1.90
Mukhebeh 6	-44	7.18	37.9	0.32	0.80
Mukhebeh 7	-32	7.20	40.1	0.21	
Mahasi 6	55	7.25	41.7	0.35	0.60

(*) Data for single sample used for ¹⁴C measurement

Sulphide is found in the thermal groundwater at concentrations between 0.60 to 1.9 mmol/l Table VI-6. The dissolved sulphide was preserved in the field by precipitation as CdS with cadmium acetate during the sulphur isotope sampling. In the laboratory the CdS was converted to silver sulphide by addition of silver nitrate (see section II-4).

The powder was then analyzed by X-ray fluorescence (XRF) to determine HS⁻ content semi quantitatively (PSA).

VI-2.1.4 Balsam and Hammat Gader - mixed system

Maqla and Balsam springs are situated close to each other, some 50 m apart, while Mukhebeh 1 is located about 2 km to the east (Fig.VI-1). Based on initial temperatures a mixing ratio of 65 % of Mukhebeh 1 water and 35 % Maqla spring water is evident for the Balsam spring. The geochemical mass balance for this mixture was tested with the geochemical model (SOLMINEQ88) according to the formulation:

$$\sum m_i(\text{mixture}) = \sum X1 m_{i,1} + \sum X2 m_{i,2}$$

Where m_i is the analytical molality of the species of the i^{th} element and X1 and X2 are the proportion of water (by weight) in which solution 1 and 2 are mixed.

The output result (Table VI-7) shows that the mixing solution is chemically similar to the Balsam spring. The output for Cl^- coincides with the measured Cl^- of the Balsam. Even the less conservative elements show an excellent correlation.

Chemically the Mukhebeh springs (Maqla and Balsam) are found to be similar to the Hammat Gader springs Table VI-3. Hammat Gader springs located on the Yarmouk River, some 2 km to the south-west from the thermal springs Maqla and Balsam in Mukhebeh area (Fig.VI-1). Mazor et al., (1973) proposed a mixing model for the discharging water of the Hammat Gader springs.

A hot saline end member mix to various degrees with a cold fresh end member, with water of both reservoirs having a meteoric origin. Strainsky, et al., (1979), suggested that the discharging water of the Hammat Gader spring is a mix of fresh meteoric water with brine waters that have been brought together in the subsurface area.

Table VI-7 Calculation the mixing water between Maqla spring and Mukhebeh 1 to produce Balsam spring water.

<i>Parameter</i>	<i>Maqla Sp. Measured</i>	<i>Mukhebeh1 Measured</i>	<i>Mixed Water Calculated</i>	<i>Balsam Sp. Measured</i>
Mix. Ratio	35 %	65 %		
T °C	41.80	29.60	33.87	34.00
Ca ²⁺ (ppm)	122.95	92.14	102.21	98.50
Mg ²⁺ (ppm)	32.78	30.36	31.21	31.59
Na ⁺ (ppm)	120.66	39.54	67.00	72.00
K ⁺ (ppm)	16.36	3.51	8.01	7.04
Cl ⁻ (ppm)	211.48	59.17	112.49	112.00
SO ₄ ²⁻ (ppm)	169.32	50.85	92.00	90.72
HCO ₃ ⁻ (ppm)	310.88	384.12	358.00	352.00

The proposals of the above mentioned study required two aquifer systems: saline aquifer and fresh aquifer. However, if the groundwater was mixed with brine water, the $\delta^{18}\text{O}$ would show a higher value. This is not confirmed by the isotopic data of the Ca²⁺,Na⁺-Cl⁻ in Mukhebeh and Hammat Gader springs in Mukhebeh area (see text VI-3.1.1.1).

VI-2.2 Geochemistry of JRV area groundwater

The JRV groundwaters demonstrate different chemical behaviour from each other.

The deepest wells, Waqas and Manshieh reveal low TDS, (less than 500 mg/l), North Shuneh well 650 mg/l, while the shallower well Abuziad recorded TDS 11400 mg/l. The chemistry of the Ca^{2+} - HCO_3^- water of the deep wells, Manshieh and Waqas, is similar to the carbonate aquifer in the recharge area of the Ajloun Highlands. The chemistry of these two wells is plotted on fingerprint diagram (Fig.VI-5), and the relative abundance of the ions is shown to be similar to the Ca^{2+} - HCO_3^- type of water in the Nuaimah area. The fresh water of JRV wells is chemically similar to the carbonate groundwater from Nuaimah. The chemical analyses from this area was discussed earlier in section (V-1.2) and plotted on (Fig.VI-5). The chemistry of Nuaimah area plots within the Manshieh and Waqas wells. The low concentration of Na^+ and Cl^- of Nuaimah water in comparison with the JRV well field is due to dissolution of halite from the matrix of the aquifer during the circulation of thermal water in the JRV area. This suggests that the tectonic activity in the JRV creates very high transmissivity in this zone and can facilitate the recharge water to circulate deep through an extensive fracture system in the carbonate formation. The contact time between the infiltrated water and the carbonate rocks is minimum. The infiltrated water moves downward rapidly, gets heated and ascends quickly to the surface, preserving its high temperature. The Na^+ - Cl^- type of water in the Abuziad well indicates that the contact time between the groundwater and aquifer matrix is longer. A wide variation is observed in the Na^+/K^+ ratio 15.7 to 66 Table VI-4. The high value is recorded for Manshieh well and could attributed to adsorption of potassium to clay minerals.

VI-2.3 Geochemistry of Ramtha area groundwater

The chemistry of the Ramtha area represented by S-90 well, completed in a deep sandstone aquifer. The aquifer water contains high concentrations of Ca^{2+} and SO_4^{2-} . These high values are attributed to dissolution of sulphate minerals, either gypsum or anhydrite. The Na^+ in excess (13.15 meq/l) of Cl^- (4.7 meq/l) can be attributed to sodium ion exchange with calcium or magnesium.

The chemistry of the B2/A7 aquifer water is represented by the Mahasi well No.6 is typical of a carbonate aquifer. The aquifer water of the well shows the same trend as the chemistry of groundwater in the Mukhebeh and JRV areas with elevated Cl^- concentration. sulphate reduction also occur, and contributes to the low Eh (55 mV) and $\text{SO}_4^{2-}/\text{Cl}^-$ (0.25) ratio. Both the deep sandstone and the B2/A7 aquifers, are supersaturated with respect to calcite and dolomite.

VI-2.4 General Discussion

Figure VI-6 plots the Na^+ concentration against the Cl^- concentration, in meq/l, for all the thermal samples. The data plotted in a regression line of approximately 1:1, with the exception of the S-90 well. The slope of the line is 0.96 and the R^2 is 0.99, which means the dissolution of halite is the main source of Na^+ and Cl^- in the groundwater.

As stated earlier, the previous studies indicated that a subsurface flow comes from the North-East Desert Via Ramtha, discharging in the Mukhebeh area. The observed Cl^- concentration in Mahasi well No.6 in the Ramtha area, as shown in (Fig.VI-5 & 6), is higher than the concentration in the Mukhebeh and JRV areas. However, Cl^- is

conservative and is not depleted along following the flow path, but significant gains of Cl⁻ often occur along the flow paths. The chloride can come from sources such as dissolution of evaporite minerals (halite or sylvite) within the aquifer or its aquitard or diffusion from the aquitard solution. Therefore it is hard to accept that the flow of groundwater in the Mukhebeh area is coming from Ramtha area.

From a geochemical point of view, the anion-evolution of the thermal waters in the whole study area indicates that the groundwater originates from precipitation falling over the carbonate terrain in the recharge area. The recharge origin will be determined in the next section (VI-3).

The HCO₃⁻ content of the groundwater in the Mukhebeh, JRV, and Ramtha areas is derived from soil zone and from dissolution of aquifer matrix, which consist mainly of carbonate materials.

The P_{CO2} of the groundwater in these three areas is in the range of 0.01 to 0.3 Table VI-4. It is worthwhile to mention here that the observed P_{CO2} value of the thermal water is higher than the values recorded in Nuaimah area in Ajloun Highlands. This suggest other sources of CO₂ encountered in these thermal systems (see section VI-5.3.2).

The fluoride concentration was found to increase with higher salinity Table VI-3. The range of F⁻ is between 0.56 and 1.31 ppm in the Mukhebeh area, while the concentration of F⁻ in the recharge area and side wadies is in the range of 0.28 to 0.33 ppm. Nordstrom and Jenne (1977) showed that the concentration of both Ca²⁺ and F⁻ is controlled by the solubility of calcite and fluoride. The JRV1 well and Maqla spring reveal higher concentrations of F⁻ than the Mukhebeh well field (1 to 7). All thermal

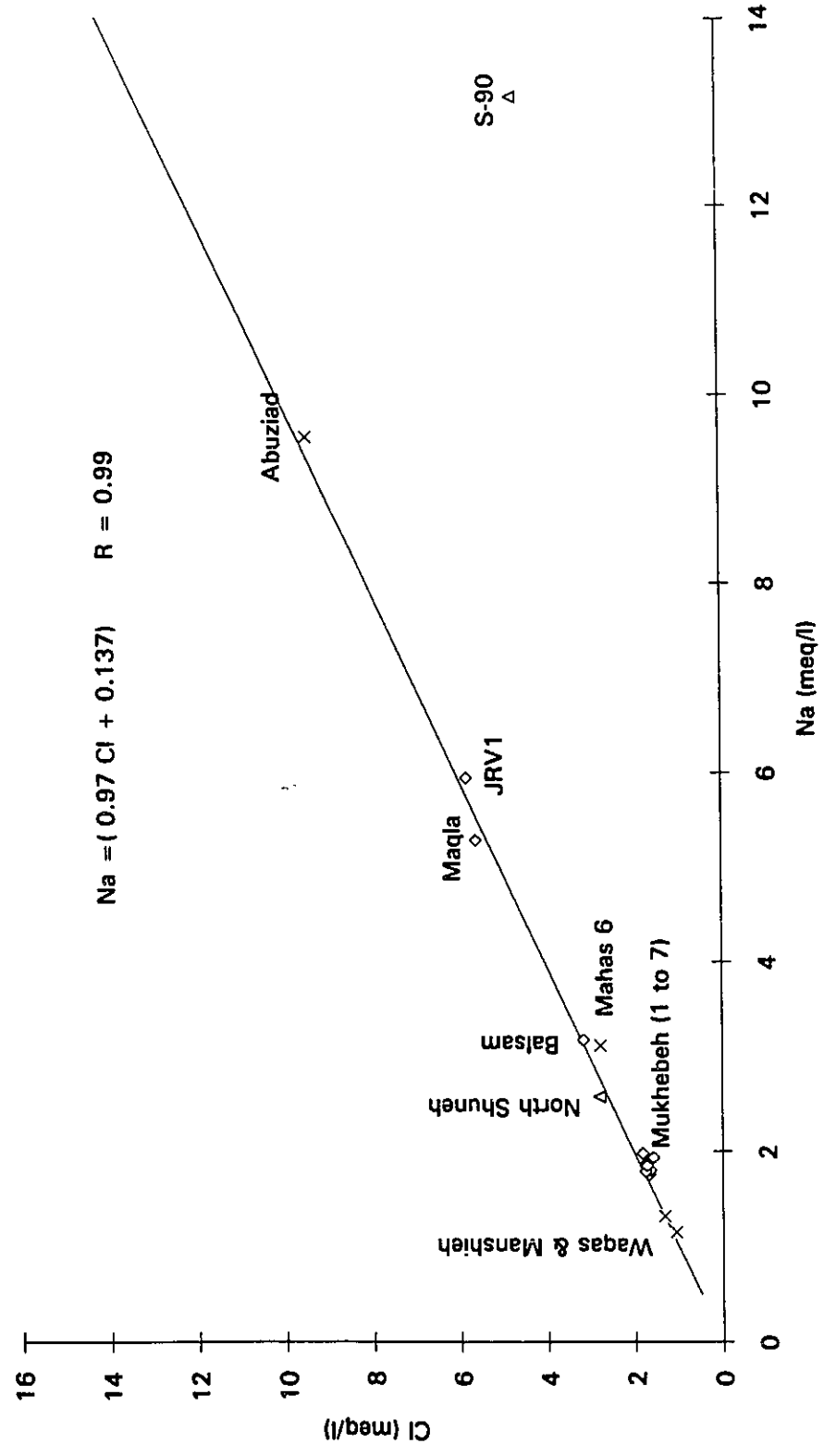


Fig. VI-6 Relationship of chloride to sodium from the thermal water in the three well fields. Mahasi 6 in ramtha area plotted in the regression line between JRV1 and the rest of Mukhebeh wells (NO.1 to7)

water is undersaturated with respect to fluorite Table VI-4. The increase of F⁻ in the thermal water compared to the non-thermal waters could be explained by the effect of temperature.

VI-2.5 Temperature Calculation by different Geothermometers

Chemical geothermometers, based on the concentration of silica, sodium, potassium, calcium, magnesium and lithium have been used successfully to estimate the subsurface temperature of the reservoir rocks. (Truesdell and Hulston, 1980; Fournier, 1977; Kharaka and Mariner, 1989). At present, the most widely used are silica (Fournier and Rowe, 1966), Na-K-Ca (Fournier and Truesdell, 1973; Kharaka and Mariner, 1989), and Li-Mg (Kharaka and Mariner, 1989). The application of these empirically derived geothermometers assumes that these dissolved ions are controlled by equilibrium exchange reaction with the aquifer mineral at aquifer temperatures. The contents of these chemicals in thermal waters have been shown to be temperature and rock type dependent. Mixing of waters from aquifers with different temperatures could alter the concentration of constituents used in geothermometers and require the application of specified mixing models (Fournier, 1981).

The silica geothermometer depends on the type of silica mineral (quartz, cristobalite, chalcedony etc.) in equilibrium with the water. Deep drill-holes tapping high - temperature water are found supersaturated with respect to quartz. Fournier and Rowe (1966) used this discovery to accurately determine the temperature of the reservoir. Nevertheless a weak correlation was found between the temperature and silica content of

the thermal water in the study area. The JRV1 well and the Maqla spring ($T = 42\text{ }^{\circ}\text{C}$) in the Mukhebeh area recorded high silica concentrations ($> 25\text{ ppm}$), while the Mukhebeh 7 ($T = 42\text{ }^{\circ}\text{C}$) recorded low silica content (19.5). In addition, the thermal water in the JRV area demonstrate higher surface temperature and less silica content than the JRV1 well and Maqla spring in Mukhebeh area. In Mukhebeh area the high correlation was found between the TDS and silica content Table VI-3.

Some of the Mukhebeh sources show a slight variation in silica content when observed at different times Appendix 3. These variation may be attributed to several factors: Possible polymerization and / or precipitation of silica after sample collection due to improper preservation. Dilution of hot water with cold water before the thermal water reaches the surface may also occur. The silica contents of the Mukhebeh springs (Maqla and Balsam) vary regularly with their temperature, which suggests that mixing with a cooler lower silica water has occurred.

Both quartz and chalcedony found to be supersaturated in most thermal waters in Mukhebeh area. Mukhebeh wells 2 and 5 are undersaturated with respect to chalcedony. Thus assuming quartz to be the source of silica, and that precipitation kinetics have precluded an equilibrium with a silica polymorph, this geothermometer provides temperature estimates in the range of 50 to 70 $^{\circ}\text{C}$ for the Mukhebeh wells and around 60 $^{\circ}\text{C}$ for the JRV type water Table VI-8.

In the JRV and Ramtha areas the water found supersaturated with respect to quartz and undersaturated with respect to chalcedony, with exception North Shuneh well.

Table VI-8 Chemical and Isotopic Geothermometers

Name	T°C Measured	SiO, ppm	Quartz °C	Chalced °C	Li-Mg °C	Na-K-Ca °C	t _{Mg} °C	SO ₄ -H ₂ O °C
JRV1	42.5	26.1	74	42	66	118	47	66
Maqla Sp	41.8	27.4	76	44	67	119	54	-
Balsam Sp	34.0	17.5	59	26	56	94	54	-
Mukhebeh1	29.6	14.6	52	20	51	80	57	-
Mukhebeh2	32.4	11.7	45	12	50	72	59	-
Mukhebeh3	34.0	16.9	57	25	53	71	60	-
Mukhebeh4	36.3	15.3	54	21	50	80	49	-
Mukhebeh5	45.6	17.4	58	26	49	78	40	115
Mukhebeh6	37.9	18.5	61	29	51	97	49	134
Mukhebeh7	42.0	19.5	63	30	51	86	52	-
N. Shuneh	53.8	21.0	65	33	49	78	39	-
Manshieh	49.8	19.0	62	29	45	-2	95	98
Waqas	50.8	18.1	60	28	46	79	40	97
Abuziad	51.6	20.0	63	32	72	148	40	-
Mahasi 6	41.7	16.0	55	23	49	43	54	72
S-90	56.0	-	-	-	-	359	234	

Quartz no Steam Loss t°C = [1309/(5.19-Log(SiO₂))-273.15

Fournier, 1981

Chalcedony t°C = [1032/(4.69-Log(SiO₂))-273.15

Fournier, 1981

Na-K-Ca t°C = 1647/[(Log(Na/K)+β[Log(√Ca/Na)+2.06]+2.47]

Fournier, 1981

(β = 0.33)

Mg-Li t°C = [2200/((Log √Mg/Li)+5.47) - 273.15

Kharaka et al., 1985

δ¹⁸O(SO₄-H₂O) 1000L_nα = 2.88(10⁶T²)-4.1

Fournier, 1981

α = (1000 + δ¹⁸O(HSO₄))/(1000 + δ¹⁸O(H₂O)) and T = °K

The supersaturation with respect to quartz, suggest that the groundwater received their silica contents from equilibrium with quartz at about 50 to 80 °C Table VI-8. Chalcedony and other form of silica cannot control silica in the thermal waters because they are mainly undersaturated with respect to these minerals at their orifice temperature. In addition, the equilibrium temperatures for the chalcedony yield lower temperature than those measured at the surface .

The Li-Mg geothermometer: It is generally recognised that the concentration of Mg decrease with increasing temperatures (White, 1965), on the other hand, the Li increase with increasing temperature (Kharaka et al., 1985). suggesting that the Li-Mg ratio may be a sensitive indicator of temperature. Both cations have almost identical crystalline ionic radii and substitute each other in different minerals e.g clay minerals. The Li-Mg, geothermometer shows reliability and produces output results close to the SiO₂ geothermometer.

The uncorrected Na-K-Ca geothermometer produced relatively high temperatures (> 100 °C) especially for S-90, JRV1 and Maqla. The low temperature recorded for Mianshieh well most probably due to the low concentration of potassium. The Na-K-Ca geothermometer with a Mg correction give more reliable temperature results for thermal waters, especially for the JRV well field. The results of the Na-K-Ca with Mg correction is in agreement with the Li-Mg model for the Mukhebeh well (No.1 to 7) and Balsam spring. The Mg-corrected Na-K-Ca geothermometer is based a variable R given by: $R = [(C_{Mg}) / (C_{Mg} + 0.61C_{Ca} + 0.31C_K)] * 100$, where concentrations are expressed in mg/l (Kharaka and Mariner, 1989). For R values from 5 to 50 the correction is given by Δt_{Mg}

$$= 10.66 - 4.741R + 325.87(\log R)^2 - 1.032 \times 10^5 (\log R)^2/T - 1.968 \times 10^7 (\log R)^2/T^2 + 1.605 \times 10^7 (\log R)^3/T^2.$$

where Δt_{Mg} is the temperature correction in °C that should be subtracted from the Na-K-Ca geothermometer. The Mg-corrected Na-K-Ca temperature (t_{Mg}) is given by

$$t_{Mg} = t_{Na-K-Ca} - \Delta t_{Mg}$$

Mukhebeh (No.5 and 6) produced temperature 115 and 134 °C by the sulphur isotope geothermometer. This geothermometer must be used in caution in sedimentary areas because dissolution of anhydride may contribute sulphate out of equilibrium (Truesdell, 1979). The results from the calculation by various geothermometers and the absence of $\delta^{18}O$ shift suggests that the temperature of the groundwater at depth not higher than 100 °C.

VI-3 Origin of the recharge of the Thermal Waters

The thermal water as stated previously, is found at different elevations in the rifted regions, surrounded the mountains of Jordan and Syria. The environmental isotope in this case offers a good potential to evaluate the recharge origin and the subsurface history of the hot water.

VI-3.1 Stable Isotope of Thermal Waters

The stable isotope data for all thermal sources (Appendix 3) in the Mukhebeh, JRV, and Ramtha areas for all samples (wells and springs) in conjunction with groundwater in Nuaimah area (Ajloun Highlands), the WMV of Ras Munif and Irbed precipitation, some Syrian precipitation (Kattan, 1991) and Hammat Gader springs (Mazor et al., 1973) are plotted on a $\delta^{18}\text{O}$ - $\delta^2\text{D}$ diagram (Fig.VI-7). These data show that the groundwater in the Mukhebeh and JRV area are largely associated with the (EML), signifying recharge under the climatic region which dominates today in North Jordan. By contrast, the two groundwaters sampled for the S-90 in Ramtha area are more depleted and associated with the GML, signifying recharge under more humid conditions in the past.

VI-3.1.1 Mukhebeh and JRV groundwater

A close look to isotopic data of Mukhebeh and JRV well fields, we observe that there is at least a 1 ‰ and 7 ‰ range in both $\delta^{18}\text{O}$ and δD . The average and standard deviation of the isotopic composition of the Mukhebeh and JRV well field are calculated Table VI-9. These sample can be divided into two distinct groups:

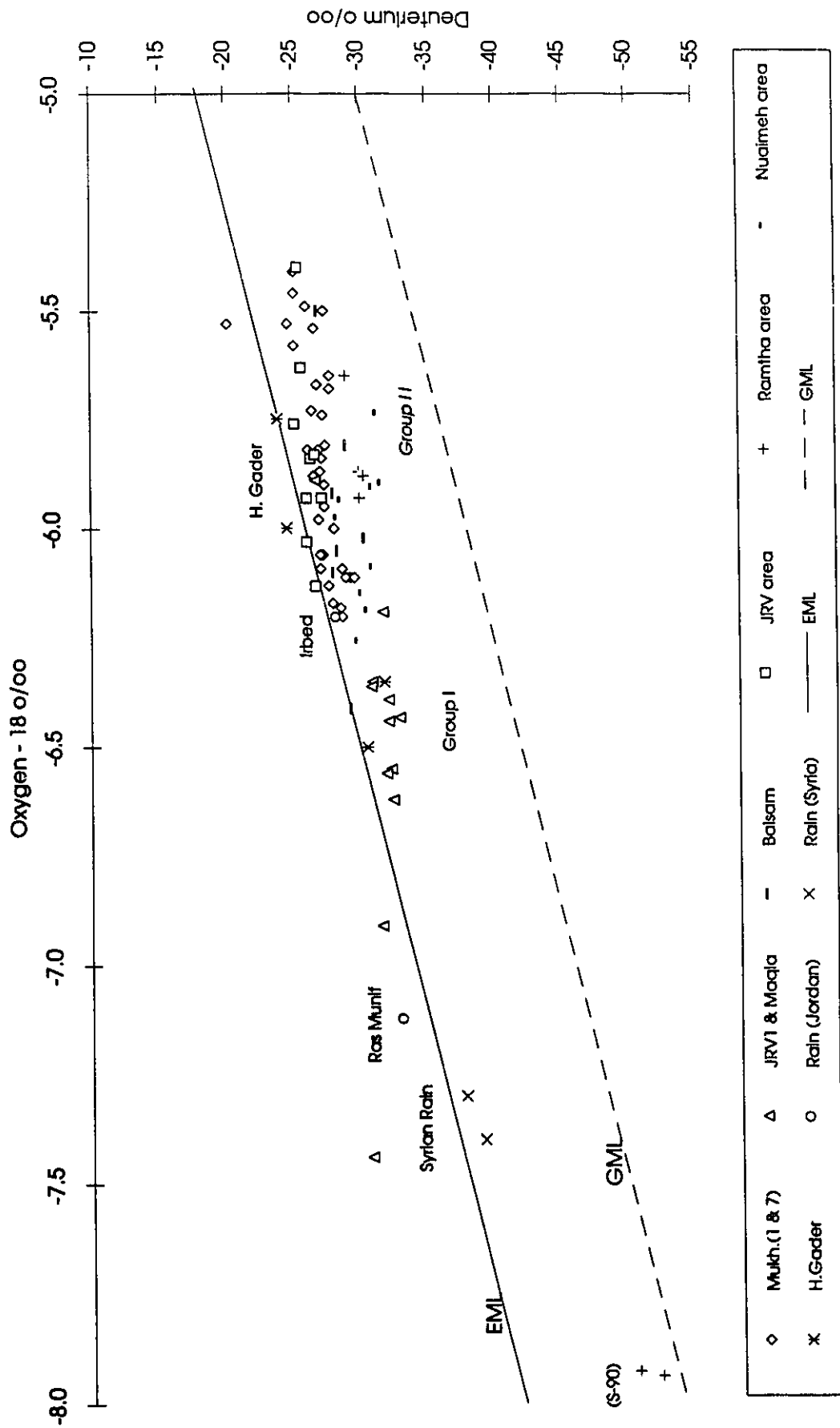


Fig. VI-7 Plot of oxygen-18 versus deuterium for the thermal groundwater from the Mukhebeh, JRV and Ramitha area. The WMV of precipitation from Jordan and Syria and the Hammat Gader springs (Israel) also included. The EMI and GML are included.

- (i) The first group contains the deep well JRV1 and Maqla spring. This group is plotted somewhat apart from the field representing the thermal well fields in Mukhebeh, JRV and Ramtha and are much more depleted in stable isotope content.
- (ii) The second group contains the thermal waters from the B2/A7 aquifer in all three areas. The isotopic composition of the thermal water with the groundwater in Nuaimeh area is more enriched than the first group and scatter much more widely on the EML.

VI-3.1.1.1 Recharge elevations and Regions

The average and standard deviation for data of group 1 and group 2 and the EML are plotted in the δ -diagram (Fig.VI-8). This presentation shows that these two groups have a statistical difference. The diagram shows that the JRV1 and Maqla springs are clustered in one group at the more depleted end of the EML. The Mukhebeh No.1 to 5 wells and JRV wells plot in the second group. The Balsam, Mukhebeh (No.6 and 7) plot in between them. These are clearly a mixture between group 1 and group 2 waters (see section VI-2.1.4). The graph also shows that Maqla, Balsam spring and JRV1 and Mukhebeh well No.1 demonstrate a higher standard deviation. These springs indicate a slight mixing with shallow tritiated groundwater (see VI-5.1).

An altitude effect may be apparent in the difference in isotopic composition between the first and second group (Fig.VI-7 and 8). The position of the isotopic composition of the first group on the EML indicate that the input function for the water should come from a recharge area which has a higher altitude than that of the second group.

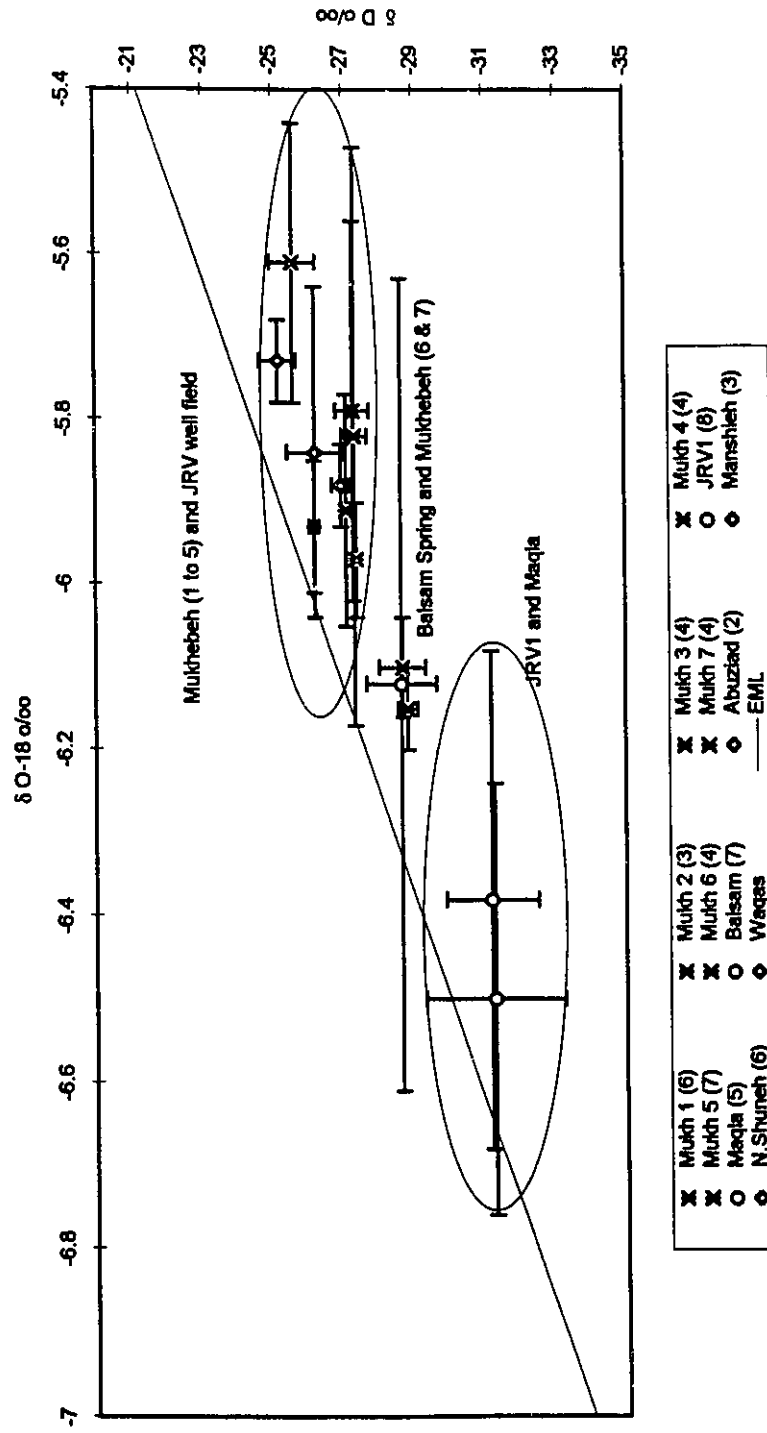


Fig. VI-8 Plot of oxygen-18 against deuterium for groundwater from Mukhebeh and JRV well fields. The standard deviation from Table VI-9 is shown, The graph includes the EML

The isotopic composition of the WMV of the precipitation from Ras Munif (1150 m) demonstrate more depletion than the groundwater of the first and second group. Irbed (555) precipitation demonstrates values which are more enriched than both groups, and plots close to the second group and the Nuaimah groundwater in the Ajloun recharge area.

The isotopic composition of the groundwater of the second group and the Nuaimah area indicate that the general recharge area will be lower than that of the Ras Munif elevation and similar or higher than that of the Irbed area (see V-1.1). However, precipitation at Ras Munif does not mean that the recharge for first group comes from this location. The reason is simply that if the recharge to the groundwater in the first group comes from Ras Munif, the stable isotope composition of groups (one and two) in Mukhebeh area, besides the groundwater in Nuaimah area, should be similar. We observed in the Mukhebeh area two different isotopic compositions, one is depleted (group one), and the second is more enriched (group two). This simply suggests that the Mukhebeh area is a discharge area for two different flows coming from different altitudes.

Previous studies attribute recharge of all Mukhebeh area thermal waters (groups 1 and 2) to rain in the Ajloun area (Parker, 1969, Joudeh, 1983, NJRWIPS, 1989, El-Naser, 1991). Hammat Gader springs (see text VI-2.1.4) are also considered to come from the Ajloun Mountains (Mazor, et al., 1973 and Strainsky et al., 1979).

The isotopic composition of the Hammat Gader springs are plotted with those of Jordanian groundwater Fig. (VI-7). The hottest springs (52 and 42 °C) plot in the first group, while the warm ones (37 and 29 °C) plot in the second group. Mazor et al., 1973 observed the difference in isotopic composition of these springs. The isotopic composition

of the saline springs is significantly lighter than that of less saline and plot with group 1 water from Mukhebeh.

Table VI-9 The average and standard deviation of Mukhebeh and JRV well Field

Name	$\delta^{18}\text{O} \text{‰}$	STD	$\delta\text{D} \text{‰}$	STD	N
Mukhebeh 1	-5.82	0.35	-27.3	0.35	6
Mukhebeh 2	-5.97	0.07	-27.4	0.05	3
Mukhebeh 3	-5.91	0.14	-27.1	0.12	4
Mukhebeh 4	-5.79	0.23	-27.3	0.46	4
Mukhebeh 5	-5.61	0.17	-25.6	0.65	7
Mukhebeh 6	-6.10	0.06	-28.7	0.66	4
Mukhebeh 7	-6.15	0.05	-28.8	0.28	4
JRV1	-6.50	0.26	-31.3	1.98	8
Maqla spring	-6.38	0.30	-31.2	1.30	5
Balsam spring	-6.12	0.49	-28.6	1.00	7
Abuziad	-5.88	0.05	-26.9	0.25	2
Manshieh	-5.73	0.05	-25.2	0.53	3
N.Shuneh	-5.84	0.20	-26.2	0.77	6
Waqas	-5.93	0.08	-26.2	0.14	3

STD - Standard Deviation, N- Number of samples

Arad and Bein (1986), reported $\delta^{18}\text{O}$ values of -6.2 and -6.1 ‰ for En Makle Spring and En Balsam vents of the Hammat Gader springs (names exactly as published). The corresponding average values for Jordanian Maqla and Balsam Springs are -6.4 and -6.1 ‰ respectively. In addition one thermal well (Mezar 2, 65 °C) from east of Tiberia lake also has a close value to that of the first group ($\delta^{18}\text{O} = -6.9 \text{‰}$). Furthermore the weighted mean value of Syrian precipitation (Kattan, 1991) representing the rainy period

of December, 1989 to April, 1990 is depleted with respect to the average for precipitation in the Nuaimah region, as represented by the shallow groundwater.

Mukhebeh No.5 has an isotopic composition similar to the JRV well field. The location of the well is closer to the JRV well field than Mukhebeh well field. In addition the ionic ratio of the well is similar to the JRV well field (see section VI-2.1.1 and Table VI-4).

A simplified cross section extending some 120 km from Zarqa anticline in the south of the study area to the Mount Hermon anticlinal block in the north is presented in (Fig.VI-9). The Mukhebeh springs and the other 8 wells discharge at the synclinal axis between these two structures. From the cross section we can see that the Upper Cretaceous carbonate aquifer (B2/A7), the Lower Cretaceous (Kurnub sandstone) and Jurassic aquifer are outcropping on the Syrian side.

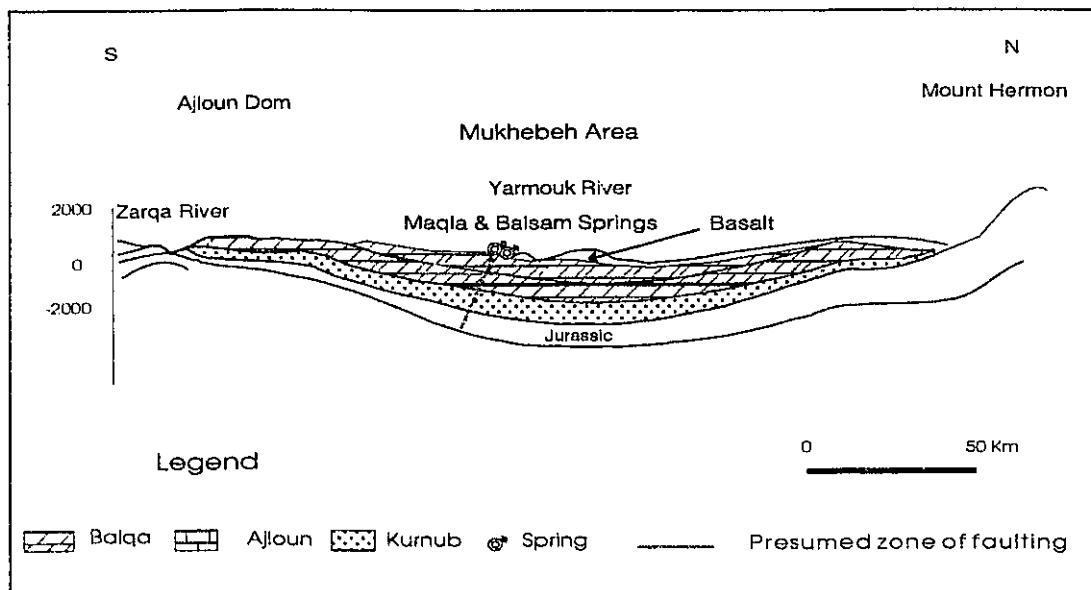


Fig.VI-9 Cross Section Between Zarqa River and Mount Hermon (After Arad et al., 1986)

Arad and Bein (1986), considered, on the basis of low $\delta^{18}\text{O}$ values, Mount Hermon and northern Golan Heights a potential recharge for Mukhebeh area.

From the above observation we can conclude that the Mukhebeh area is a discharge area for two flow systems coming from two areas with different recharge elevations. The Jordanian side which is represented by the Ajloun Mountains and the Syrian side which is represented by the Hermon Mountains and Golan Heights. Water discharging in the Mukhebeh and JRV well fields most probably comes from the Ajloun Mountains, while the JRV1 well and Maqla spring come from the Syrian side (Golan Heights). The Balsam spring and Mukhebeh (No. 6 and 7) represent a mixing of the flow coming from both sides (see VI-2.1.4).

VI-3.1.2 Palaeowater for the Ramtha area

The third group is represented by the deep S-90 well which taps the sandstone aquifer in Ramtha area. The S-90 well plots on the GML rather than the EML which now dominates the local precipitation in Jordan. The stable isotope content of the (S-90) is the most depleted; the isotopic composition of this groundwater is different from the rest of the groundwater in the study area. Water of this well is depleted in deuterium by $\sim -20\text{‰}$ in comparison to present precipitation in the study area.

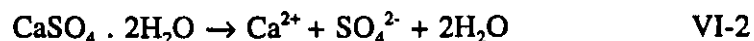
Similar groundwater is found in some thermal groundwaters in the Hammad area (Bajjali, 1990b), and in the Southern Desert (Lloyd, 1980). Most of these water are characterized by deuterium excess values between 4 to 10 ‰ which is substantially lower than presently observed in precipitation and recharge groundwater.

Several authors (Sonntag et al., 1979; Moser et al., 1983; Rozanski, 1985) indicated such low excess values reflect the old nature of the groundwater (paleowater). The term old is used for groundwater that has been recharged during the Pleistocene under an atmospheric regime dominated by latitudinally compressed climatic zones at a time when ice sheets existed in northern Europe and Asia.

VI-4 Origin of salinity and sulphate reduction

Sulphur is present in nearly all natural environments, mostly as sulphide and sulphate in marine sediments. As a result of chemical and biochemical interaction between waters and the material along the flow path, the water acquires varying degrees of salinity.

The SO_4^{2-} in groundwater can have several sources: (i) The dissolution of sulphate-bearing minerals in the aquifer material, the most common being gypsum and anhydrite. Concentration in excess of about 30 mg/l SO_4^{2-} suggest contact with gypsum bearing rocks (Mandel and Shiftan, 1981). These minerals dissolve readily when in contact with water. i.e dissolution reaction of gypsum is



(ii) Oxidation of sulphide minerals e.g pyrite.

(iii) atmospheric precipitation. A range between 5 to 30 mg/l of sulphate was recorded in the precipitation in north Jordan Table IV-1.

The SO_4^{2-} in groundwater is thermodynamically unstable with respect to various reduced sulphur species in the presence of organic carbon compounds and with the presence of the sulphate reducing bacteria (Holser et al., 1988). The result of sulphate reduction is production of H_2S and low redox potential.

Sulphur is bound in various oxidation states, from sulphide to elemental sulphur, to sulphate. ^{34}S has been used, in conjunction with other isotopes, for the delineation of aquifer systems and flow paths (Krouse, 1980). In addition it is used to determine the origin of SO_4^{2-} in groundwater and provide information on the condition over the deeper

part of the system.

The $\delta^{34}\text{S}$ distribution ranges in natural materials are shown in Table VI-10 (Mondel and Shiftan, 1981).

Table VI-10 $\delta^{34}\text{S}$ ‰ variations in sulphate from different materials

Natural Materials	$\delta^{34}\text{S}$ ‰
Seawater	+18.9 to +20.7
Marine evaporites	+8 to +32
Precipitation	-1.5 to +19.4
Biogenic sulphur	-35 to +4
H ₂ S derived from gypsum	-10 to -60

The above listed figures show that sulphur compounds vary widely. The highest values are associated with marine evaporite, while negative values are typical of a diagenetic environment where reduced sulphur compounds are found. Krouse, (1980) stated that the variation of the $\delta^{34}\text{S}$ values in different sources ranges between -40 to +40 ‰. The $\delta^{34}\text{S}$ in the oxidized sulphur species is more enriched than the reduced species. Several factors can affect the $\delta^{34}\text{S}$ of SO_4^{2-} in groundwater (Holser and Kaplan, 1966; Claypool et al., 1980). Primary factors include the source of SO_4^{2-} , whereas secondary factors include subsequent modification by geochemical processes. When significant quantities of sulphate are present in groundwater, the dissolution of marine evaporite is

necessarily implicated. Oxidation of pyrite is also a significant source of sulphate.

It is well documented (Holser and Kaplan, 1966), that the $\delta^{34}\text{S}$ of evaporite has not been constant with time, and ranges between $\delta^{34}\text{S} = +10$ and $+30$ ‰. The $\delta^{34}\text{S}$ value in dissolved sulphate in modern seawater is found to be very constant throughout the oceans ($+20$ ‰), while the $\delta^{18}\text{O}$ of the oceanic SO_4^{2-} is $+9.6$ ‰. Upper Cretaceous values range between approximately $+16$ to 22 ‰ for $\delta^{34}\text{S}$ and $+13$ to 16 ‰ for $\delta^{18}\text{O}$ (Claypool, et al., 1980).

The sulphate reduction reactions identified in the thermal waters (section VI-2.1.2) can significantly modify the stable isotopes. The bacterial reduction of SO_4^{2-} removes preferentially the lighter isotopes of oxygen and sulphur from the SO_4^{2-} reservoir and causes isotopic enrichment for both ^{18}O and $\delta^{34}\text{S}$ in the residual SO_4^{2-} (Krouse, 1980). Fritz et al., (1989) show that for ^{18}O a steady state value representing isotopic equilibrium with water is eventually attained, while for ^{34}S , a Rayleigh enrichment is followed.

In order to get information about the origin of sulphur compounds in the groundwater, and the geochemical processes affecting them the chemistry and isotopic content of sulphur species from 7 wells in the study area were obtained. The results of the analyses including the concentration of SO_4^{2-} , HS^- and Cl^- are shown in Table VI-11. The samples demonstrate a wide variation of $\delta^{34}\text{S}$ in the range from $+3.4$ to $+25.8$ ‰. The variation of dissolved SO_4^{2-} concentration with $\delta^{34}\text{S}$ is shown in (Fig.VI-10A). This figure shows high values for $\delta^{34}\text{S}$ in the samples (JRV1 and Abuziad wells) having a high concentration of SO_4^{2-} and Cl^- . These values are close to the range for Upper Cretaceous evaporite gypsum or anhydrite. On the other hand, there appears to be no correlation

between SO_4^{2-} concentration and the $\delta^{34}\text{S}$ value for the rest of the samples.

Table VI-11 $\delta^{34}\text{SO}_4$, $\delta^{18}\text{O}$ of SO_4^{2-} , H_2^{18}O , HS^- , Eh, SO_4^{2-} , and Cl^-

Name	$\delta^{34}\text{S}$	Eh	$\delta^{18}\text{O}_4$	HS^-	SO_4^{2-}	Cl^-	$\delta\text{H}_2^{18}\text{O}$
	‰ CDT	mV	‰ SMOW	mmol/l	mmol/l	mmol/l	‰ SMOW
JRV1	25.8	93	14.59	0.72	2.65	5.74	-6.44
Mukhebeh 5	13.9	-58	9.43	1.54	0.47	1.66	-5.60
Mukhebeh 6	9.6	-44	7.12	1.60	0.32	1.77	-6.10
N. Shuneh	11.0	-101	10.99	1.20	0.68	2.55	-5.76
Manshieh	3.4	-61	11.15	0.80	0.55	1.33	-5.73
Abuziad	21.9	-96	14.33	0.41	2.90	9.63	-5.88
Mahasi 6	16.7	55	15.25	0.74	0.35	2.79	-5.82

Fig. (VI-10B) shows the ^{18}O content of the dissolved SO_4^{2-} relative to that of the water. The figure demonstrates a much wider variation in the ^{18}O content of the SO_4^{2-} than that of water, which suggests (i) variations in the source of SO_4^{2-} and (ii) the oxygen isotope equilibrium between the water and the SO_4^{2-} does not occur for if it did there would be a much closer relationship between the ^{18}O content of the SO_4^{2-} and the water (Fontes and Zuppi, 1976). The data on Fig.VI-11 cluster close to a regression line with a slope of 1.55 and -1.89 intercept ($R^2 = 0.7$).

The low $\delta^{34}\text{S}$ in Manshieh, N.Shuneh and Mukhebeh (No.5 and 6) may be attributed to oxidation of organic material or incorporation of volcanogenic SO_2 . The Bitumen of the B3 formation within the study area is rich in organic sulphur, which can

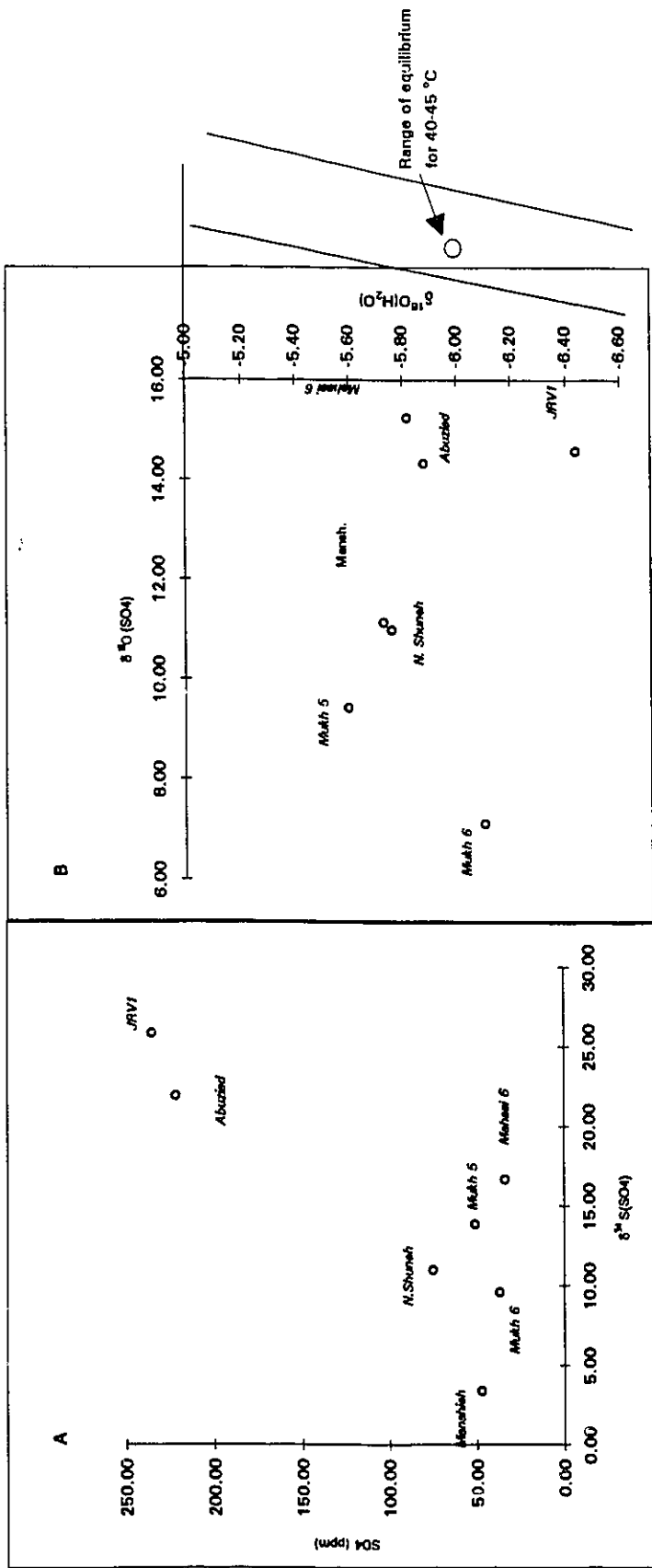


Fig. VI-10 plot of δ³⁴S(SO₄) vs SO₄ and δ¹⁸O of H₂O for the thermal water in the study area

reach up to 12 % by weight. Samples from Maqaren (Yarmouk valley) show enrichment in S, where the level ranges between 9.4 and 73 mg/g. A $\delta^{34}\text{S}$ value between -5 and 0 ‰ was recorded for gypsum and shallow hyperalkaline water from Maqaren area (Clark et al., 1992). Contribution of such sulphur during oxidation of organic carbon may have influenced the isotopic content of sulphate in these waters with low sulphate content.

The most saline samples (JRV1 and Abuziad) have sulphate with the highest values for ^{18}O (excepting Mahasi 6), and fall within the range of Upper Cretaceous evaporite gypsum. This supports the ^{34}S data indicating such gypsum to be the source of sulphate (Fig.VI-11).

In conclusions we can say that the large variations in isotopic composition in these waters suggest that sulphur originates from evaporites and organic sulphur. The variation may be related to input from different geological due to the different paths and circulation and to isotopic fractionation during the biological activity.

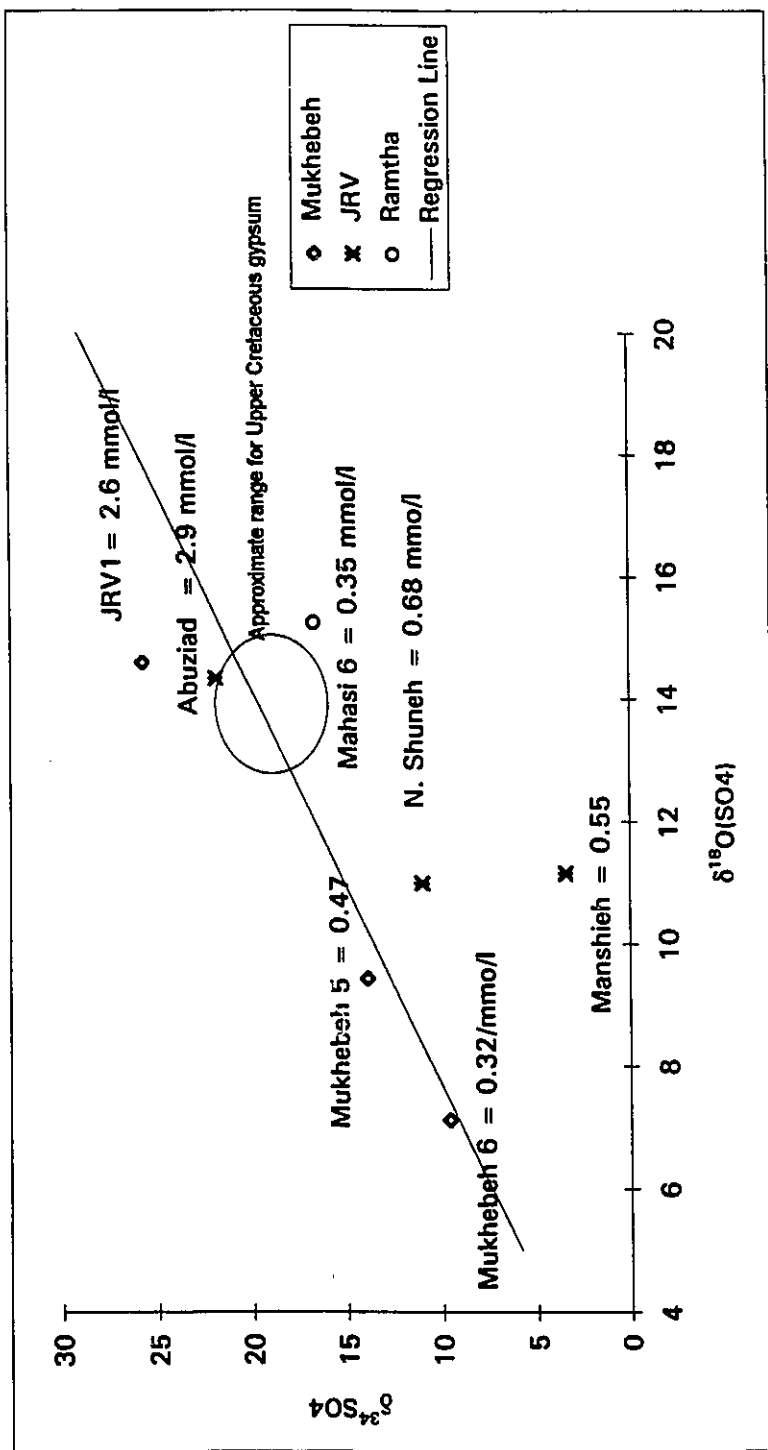


Fig.VI-11 $\delta^{34}\text{S}(\text{SO}_4)$ vs $\delta^{18}\text{O}$ for dissolved sulphate sampled from the thermal waters of the three well fields, Mukhebeh, JRV and Ramtha. The regression line of $\delta^{34}\text{S}(\text{SO}_4) = 1.55 * \delta^{18}\text{O}(\text{SO}_4) - 1.89$ is shown. Approximate Range for Upper Cretaceous Marine Sulphate is from Claypool, et al., 1980.

VI-5 Mean Residence Time of Groundwater

In this section the ^{14}C concentration data of all thermal and non-thermal water in the whole study area will be discussed. Combining all the ^{14}C data together will give better understanding to the behaviour of ^{14}C in the TDIC along the flow path, from the recharge area to the sampling point. As an introduction to this examination of groundwater ages, tritium is used to identify modern waters and as evidence of groundwater mixing.

VI-5.1 Tritium

In general, thermal waters in Mukhebeh, JRV, and Ramtha thermal fields have very low tritium concentrations. The majority of the sources in these three areas were found to have a tritium level less than the analytical error of 1 TU. The highest tritium concentration was recorded in the Mukhebeh area (Table VI-12 and Appendix 3). Mukhebeh well No. 1 was found to have a fluctuation of tritium between 0.3 and 2.1 TU. The well, as mentioned previously, was completed as an open hole below 14 m with 350 m total depth. The springs (Maqla and Balsam) have also recorded detectable tritium with levels ranging between 0 and 1.6 TU. Balsam spring always has tritium higher than 1 TU, with the exception of one sample from January 1987 Appendix 3. The TU in the deep JRV1 well is always less than one, with the exception one sample recorded in summer 1989 (1.5 TU). Mukhebeh wells (2 to 7) show tritium levels: less than one TU. The exception is the Mukhebeh well (4), where one sample had 1.1 TU. This value is the highest recorded in the well field.

It is worthwhile to recall that the majority of the wells in the Mukhebeh area have an open hole section extending approximately from 220 m to the bottom of the well. The side wadies well field, (total depth of 226 to 411 m) some 10 to 15 km south to the Mukhebeh area, see (section, V-2.1.3), recorded a high tritium level range between 0.4 and 9.9 TU. This indicates that an infiltrated water from rainfall can circulate to those depths within a period of decades only. However the recharge contribution from precipitation to the thermal water is most likely very small in comparison to the discharge from the deep B2/A7 of the aquifer. This is documented by the Mukhebeh springs (Maqla and Balsam), which issue from depth to the surface through the local fault system.

Thermal wells in the JRV and Ramtha areas also recorded tritium less than 1 TU, only one sample (1.2 TU) observed in North Shuneh well in the summer period. The North Shuneh well as mentioned previously has a slotted casing from 268 m. The water with little, but measurable, tritium (between 0.5 and 3 TU) seems to be a mixture of pre-1952 and post-1952 water. This indicates that the area is receiving small contribution from a shallow rechargeable groundwater.

It is also notable that those groundwater in which measurable tritium has been observed, were sampled during summer. Although shallow groundwater recharge occurs mainly during the wetter winter months, this may reflect basin dynamics and a long effect for the circulation of seasonal recharge.

VI-5.2 Carbon-14

The carbon-14 is an alternative label of recent recharge, due to its negligible decay

over a time scale of some tens of years.

Table VI-12 TOC, Tritium, ^{13}C and ^{14}C

Name	TOC	Tritium	Carbon-13	Carbon-14
	ppm	TU	‰	pmc
Nuaimch 1	-	6.6	-10.9	59.6 ± 0.7
Hammad Farhan	-	9.2	-11.3	63.1 ± 0.7
Jdcita	-	6.9	-13.3	73.4 ± 1.7
JRV1	3.3	0.0-1.5	-9.3 to -8.4	5.36 ± 0.5 22.9 ± 0.6
Maqla	37.8-54.8	0.0-1.6	-9.6 to -6.6	16.58 ± 0.9
Mukhebeh 1	0.64	0.3-2.1	-12.8 to -11.6	16.86 ± 0.6
Mukhebeh 2	0.80	0.0-1.1	-11.6 to -10.2	18.0 ± 0.9
Mukhebeh 4	1.48	0.0-1.1	-11.5 to -9.2	17.3 ± 0.9
Mukhebeh 5	0.7-1.2	0.0-0.9	-12.8 to -11.9	3.6 ± 0.5
Mukhebeh 6	2.9-65.8	0.0-0.8	-12.0 to -11.5	16.56 ± 0.9
Mukhebeh 7	0.7	0.0-0.7	-12.5 to -9.1	16.06 ± 0.6
N.Shunch	1.6	0.0-1.2	-10.2	8.0 ± 1.0
Manahieh	1.9-5.6	0.0-0.4	-9.4	4.72 ± 0.7
Abuziad	0.7-1.2	-	-3.2	-
Mahasi 6	2.7		-10.3 -8.9	3.04 ± 0.5 21.7 ± 1.2
S-90	-		-	3.75 ± 0.7

Further, anthropogenic contributions from thermonuclear bomb tests raised atmospheric $^{14}\text{CO}_2$ activities, providing an enhanced indication of modern recharge.

The geochemistry of radiocarbon in groundwater is affected by a variety of present and past infiltration processes which control the isotopic composition of the TDIC in the flow system. This research study focuses on the TDIC, as it is commonly the most significant reservoir of ^{14}C in groundwater. However dissolved organic carbon (DOC) also plays a major role in groundwater dating both as a possible reservoir for dating as well as by its impact on DIC through redox reactions (Chapel and Knobel, 1985; Wassenaar, et al., 1991; Aravena, 1993).

In this study effects on TDIC and $^{14}\text{C}_{\text{DIC}}$ are examined through their role in sulphate reduction. In some areas the overburden sediments (B3) of the main B2/A7 aquifer consist mainly of bituminous marly limestone (oil shale), chalks and chalky limestone of Maestrichtian age. In the Maqaren area within the study area the content of the organic matter in the B3 formation was found to be 20.8 wt % as an average of the total rock (Abed and Amireh, 1983).

The soil carbon and organic-rich sediment present in the aquifer material are the main two sources for DOC in the aquifer. The analyses of the total organic carbon (TOC) of the thermal water in the JRV and Mukhebeh areas vary between 0.64 to 54.8 mg/l Tab¹ VI-12. However, since this DOC originates in old, organic-rich rocks, ^{14}C -dating is not possible.

Radiocarbon ages of groundwater based only on the TDIC analyses of the ^{14}C , $\delta^{13}\text{C}$ and chemistry of water are difficult to determine. The $\delta^{13}\text{C}$ values of the

groundwater in different parts of the study area range from -13.6 to -3.3 ‰, while the radiocarbon data for TDIC range from 1.77 to 73 pmc, with an analytical error between 0.5 to 1.7 pmc (Table VI-12). Further, repeat sampling in some wells yield different ^{14}C and ^{13}C values.

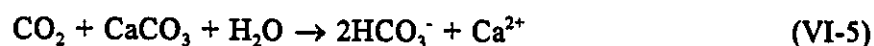
VI-5.2.1 Radiocarbon dating-controls on the input function (A_0)

The ^{14}C activity of CO_2 in the atmosphere and soils in the past is generally taken to be 100 pmc, despite indications that it was several percent more enriched (e.g. Bard, et al., 1990). Interpretation of such CO_2 provides the initial ^{14}C activity (A_0) of groundwater recharge, which corrected for subsequent geochemical modification is the basis for $^{14}\text{C}_{\text{DIC}}$ dating. More recently, atmospheric ^{14}C activity (A_0) reached a maximum level of about 180 pmc following the nuclear testing in the early 60's. The atmospheric ^{14}C activity was measured four times (1987 to 1989) above the WAJ laboratories in the Amman area, and the average value found to be 115 pmc (Jawawdeh and Amro, 1989).

The following section examines and attempts to quantify the dilution and exchange processes responsible for this exchange in ^{14}C during recharge. Such calculations are based on a knowledge of the geochemistry and vegetation of the recharge area. This is true for environments such as Jordan where recharge takes place in vegetated as well as desert environments. The objectives of this examination is to determine the dilution factors used later in section (VI-5.3).

VI-5.2.2 Radiocarbon activities in recharge waters

Radiocarbon enters the groundwater system via the uptake of soil CO₂ during the infiltration of precipitation and runoff to the groundwater in the recharge area. The ¹⁴C in groundwater originates essentially as soil CO₂ from decay of vegetation and root respiration, and has a ¹⁴C activity close to that of contemporary atmospheric CO₂. The infiltrated water is typically in contact with a CO₂ reservoir in the unsaturated zone. Carbonate dissolution is modulated by the partial pressure of CO_{2(g)}. Under open system conditions, dissociated H₂CO₃ will be replenished by dissolving more CO₂ from the soil atmosphere reservoir (Eq. VI-3). Subsequent DIC increases are due largely to carbonate dissolution. The amount of DIC resulting from calcite dissolution is controlled by temperature and P_{CO₂} (Eq. VI-5).



The dissolution of carbonate by water-carbonate rock interactions lowers the ¹⁴C activity of groundwater by substitution of "dead " carbon from the aquifer rocks. As the water infiltrates down to the water table, it becomes isolated from the influence of the soil CO₂ reservoir. Any H₂CO₃ dissociation will not be replenished as in the case of the open system. The pH and the alkalinity will increase as a result of carbonate dissolution.

Carbonate dissolution under closed system conditions depends on the quantity of dissolved CO₂, which the water received from the soil zone. If this CO₂ is consumed to dissolve carbonate, 50% of the carbon in the groundwater HCO₃⁻ originate from modern

CO₂ and then other 50 % from dead carbon from the matrix.

The above mentioned processes require the use of a model to estimate the initial activity of the total dissolve carbon (Vogel, 1970, Tamers, 1975, Mook, 1976, Fontes and Garnier, 1979). A dilution factor is thus defined as a parameter (q) which reduces the initial activity of a sample for non-decay ¹⁴C. This parameter is then used to modify the initial ¹⁴C activity in the decay equation:

$$A = A_0 q e^{-\lambda t} \quad (\text{VI-6})$$

Subsequent geochemical modification can impact additional dilution on ¹⁴C. This can be approximated by additional dilution factors (q₁, q₂, q₃) in the decay equation. These dilution factors are determined on the basis of the relevant geochemical and isotopic processes (see below).

For carbonate dissolution (q₁), the application of correction models relies to varying degrees on a knowledge of the following parameters:

I-Geochemical Parameter: The P_{CO₂} in the soil gas, the pH of infiltrated water and the chemistry of groundwater. The initial P_{CO₂} and pH is of great importance to model the chemistry of the groundwater flow from open to close systems. Both parameters affect directly the (q) factor, and consequently the A₀ and the δ¹³C of the TDIC. The calculated P_{CO₂} from the recharge groundwater in addition to the field pH was used as an initial parameters to account for final condition and compute A₀ for the various models.

II-Isotopic parameters: The δ¹³C and ¹⁴C of soil CO₂, δ¹³C and ¹⁴C of groundwater and the δ¹³C of carbonate rock in the aquifer are also used as input values for these models. Some effort was made to adapt published data to replace data not measured in this study.

The purpose is to use these parameters as an important variable in the groundwater dating.

The most important parameters are:

(i) Soil CO₂. The $\delta^{13}\text{C}$ content of the soil water is controlled by the soil CO₂. The equilibrium isotope fractionation between soil CO₂ and various dissolved carbon species causes the TDIC to be isotopically enriched by up to 10 ‰ in comparison to $\delta^{13}\text{C}$ of soil CO₂ which in temperate climates is approximately -25 ‰ (Dorr, et al. 1987). In lower pH soil waters, this enrichment factor is only a few ‰ or less. The stable isotopic composition of ^{13}C of soil CO₂ was taken from published literature from the Karmel mountains (Israel) in the vicinity area where the geological environment is similar (Kroitoru et al., 1989). To leave a minimum of freedom to the models, a value of -22 ‰ for soil CO₂ was chosen.

(ii) Carbonate Minerals. The knowledge of the isotopic composition of carbonate minerals which dissolve in the groundwater is of great importance for age calculation. The value of $\delta^{13}\text{C}$ marine carbonate varies generally between -2 ‰ and +2 ‰ and is set at 0 ‰ in the ^{14}C models calculation (Appendix A). Clark, (1987), recorded $\delta^{13}\text{C}$ value between -5.8 to +6.3 ‰ from carbonate Cretaceous aquifer rock in Oman.

The calculation of q_1 is then determined from the carbon mass balance (Pearson and Hanshaw, 1970) using the measured $\delta^{13}\text{C}_{\text{recharge}}$ of the recharge water (-11.8 ‰) and assumption of 0 ‰ for aquifer calcite and -22 ‰ for soil CO₂ in the recharge area. The value of $\delta^{13}\text{C}_{\text{recharge}}$ (-11.8 ‰) is an average of three samples measured in the tritiated water in Nuaimah and side wadies areas.

$$q_1 = \frac{\delta^{13}\text{C}_{\text{recharge}} - \delta^{13}\text{C}_{\text{Carb}}}{\delta^{13}\text{C}_{\text{IN}} - \delta^{13}\text{C}_{\text{Carb}}} \quad \text{VI-7}$$

$$\delta^{13}\text{C}_{\text{IN}} = \delta^{13}\text{C}_{\text{Soil}} + \epsilon \quad (\text{see section II-5 and equation II-12})$$

The modeled value of $\delta^{13}\text{C}_{\text{IN}}$ is -22 ‰ and the obtained q_1 is 0.54.

As is clear from the above discussion, there are problems in accurately assessing the various contributions to DIC during recharge and calculating a carbonate dilution factor q .

Here, a second approach is used to verify the q_1 ; that of examining the ^{14}C activities and ^{13}C contents of TDIC in groundwater for the regional recharge area in the Ajloun highlands and Side Wadies.

The ^{14}C activity in the groundwater of the recharge areas Nuaimah and Side Wadies was found to be between 59.6, 63.1, and 73.4 pmc in the Nuaimah 1, Hamad Farhan and Jdeita wells respectively. The ^{14}C values of groundwater in recharge areas have been observed elsewhere to vary from 50 to 150 pmc (Vogel, 1970; Fontes, 1983; Kroitoru et al., 1989). The tritium content was found for the same period to be 6.6, 9.2 and 6.9 T.U, in these three wells respectively.

The decrease in ^{14}C activity through geochemical reaction in these recharge waters can be used to determine the dilution factor q , according to:

$$q = \frac{A_r}{A_{at}} \quad \text{VI-8}$$

Where A_r (65 pmc) and A_{at} (115 pmc) are average values of ^{14}C measured in the recharge area and the atmosphere. A value of 0.56 is obtained. The average of q_1 from the two

approaches is 0.55 (Table VI-13).

The ^{14}C value of the three measured samples had dropped from 115 pmc (atmospheric) to 65 pmc in groundwater (average of the three samples) due to carbonate dissolution in the recharge area. The associated shift in $\delta^{13}\text{C} =$ from $\sim -22\text{‰}$ to the measured value of -11.8‰ in the groundwaters can be used to represent the initial condition for thermal waters sampled down gradient in the aquifer prior to further geochemical modification.

VI-5.3 Radiocarbon ages of thermal groundwaters

VI-5.3.1 ^{14}C activity and $\delta^{13}\text{C}$ in the thermal waters

All the thermal waters and non-thermal waters as stated above showed a low ^{14}C value which, on initial inspection, suggest radioactive decay and consequently a significant ^{14}C age. However, a closer examination shows that several geochemical processes are also responsible for this attenuation. The JRV1 well in the Mukhebeh area, and Mahasi 6 well in the Ramtha area revealed a wide spectrum of ^{14}C . A value of (5.36 and 23) and from (3.04 to 21.7) pmc were recorded in the JRV1 and Mahasi 6 wells respectively. These two different values recorded for the same wells were sampled at different times. These two wells are artesian and operated by pump. The ^{14}C values of these two wells are most likely affected by hydraulic disturbance of the groundwater system during the pumping. Pumping can invoke the water to come from various depths, where a vertical age structure may exist (Vogel, 1970). Groundwater stratification within the aquifer matrix can produce different ^{14}C values in the discharge water, depending on

the relative contributions. The ^{14}C age distribution with depth appears as a function of the thickness of the water-bearing formation of the groundwater. The JRV1 well, as stated previously, is tapping 3 aquifer systems open to each other by slotted casing. In addition the water well recorded a slight variation in stable isotope between -5.9 to -6.6 ‰ (Appendix 3). The high pmc value in the Mahasi 6 well in the Ramtha area could be due to contamination from the young B4 upper aquifer (see section V-4.1). The alternative explanation may be that the samples were not collected properly in 1989 and were contaminated.

The low ^{14}C value in Mukhebeh well 5 indicates that it is much older and/or more chemically evolved than the other Mukhebeh samples. This well is located further away, some 5 km south west to the Mukhebeh well field and close to the North Shuneh well in the JRV area. The isotopic composition of the water well is slightly enriched in comparison with the rest of the Mukhebeh area well field and shows chemical and isotopic behaviour similar to the JRV wells (Table VI-10), suggesting that it is not related to the Mukhebeh group samples.

In the JRV area very low ^{14}C values were observed for all the thermal wells (4.7 to 8.0) pmc.

In Ramtha area, the deep S-90 well tapping the sandstone aquifer recorded a low ^{14}C content (3.75) pmc. The ^{14}C value in this well is higher or equal to the ^{14}C content of the upper aquifer (B2/A7) either in the same area or elsewhere in the study area. The ^{14}C value of the S-90 well is ambiguous. In the isotope section (VI-3.1.2), the groundwater of the S-90 well is considered palaeowater. Furthermore the $\delta^{18}\text{O}$, δD and

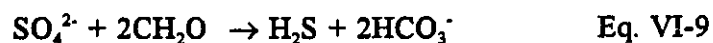
the chemistry of the groundwater provided further support for the lack of communication between the sandstone (K) aquifers represented by the S-90 well and the upper B2/A7 aquifer in Ramtha area. Although the ^{14}C is similar to that of the B2/A7 aquifer and suggests the water has the same residence time, this is not consistent with the $\delta^{18}\text{O}$ and δD which indicate the water is older. For that reason the low ^{14}C can not be attributed to the mixing between the two aquifers. The lack of $\delta^{13}\text{C}$ measurements for DIC in the S-90 well makes the correction of the ^{14}C content of the groundwater impossible.

The $\delta^{13}\text{C}$ values of the thermal waters is found in the range of -3.3 to -12.5 ‰ Table VI-12. The most enriched value recorded in the JRV area was (-3.3 ‰) in the Abuziad well. In the Mukhebeh area the JRV1 well (-8.4 ‰) and Maqla spring (-6.7 ‰) respectively, had the most enriched $\delta^{13}\text{C}$ values.

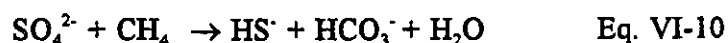
Appendix (A) lists the uncorrected and corrected age by various models for the thermal and non-thermal waters. The difference in age between the different models is several thousand of years. Ages calculated by Tamers and Pearson models showed a good agreement. Nevertheless the various models lead to rather old years (10,000 to 30,000 years). Waters recharged at that time normally exhibit depleted stable isotope contents relative to present precipitation (see section VI-3.1.2). However, these samples have stable isotope values similar to modern values. This leads us to believe that there is a limitation in using these models in the reducing environment observed for the thermal waters in north Jordan. Here, sulphate reduction and oxidation of DOC are considered responsible for an additional dilution of ^{14}C content in these groundwaters.

Sulphur reducing bacteria (*Desulfovibrio desulfuricans*) require organic carbon as

an energy source, although they are selective in choosing the more readily degradable fractions of the total pool of organic carbon (Holser et al., 1988). Intermediate products such as sulphite and thio-sulphite are important steps in the process, and the final product is generally distributed between H_2S and HS^- , depending on the pH. The first dissociation constant for H_2S is 10^{-7} at 25 °C. The overall reaction can be presented schematically as



where the CH_2O is representative of any (degradable) fixed-C organic compound, and the H_2S is representative of any sulphide. Where sulphate reduction proceeds with the oxidation of hydrocarbons (kerogen to methane) the following general reaction can be considered



Sulphur-reducing bacteria vigorously pursue sulphide manufacture in a wide variety of anaerobic situation ($\text{Eh} < +100$ mV; Holser et al., 1988). The Eh range of the thermal water varies between +93 to -100 mV Table VI-6.

Equation (VI-10) indicates that the reduction of one mole SO_4^{2-} will produce one mole of bicarbonate (HCO_3^-). The organic carbon in sedimentary rocks at depth is ^{14}C free. This process could introduce, for each mole of HS^- produced, 1 mole of dead bicarbonate into the groundwater. This process will decrease the ^{14}C activity in the groundwater and therefore affect the groundwater dating.

CH_4 (eq VI-10) best represents the hydrocarbon in the aquifer rather than CH_2O (eq VI-9), as the former is one of the volatile breakdown products of kerogen maturation (Robert, 1980). The Upper Cretaceous formation is rich in organic material, mainly

kerogen type I (alginite) and II (exinite) (Al-Arouri, 1992). Kerogen is a complex molecule, not easily represented by a simple chemical formula, therefore it has been characterized by means of element ratios (i.e. exinite the atomic H/C ~ 1 and the atomic O/C ~ 0.05) (Whelan et al., 1993).

VI-5.3.2 Subsequent ^{14}C age correction in thermal waters - q_2 and q_3

A simple mass balance was adapted to calculate the secondary dilution (q_2) in the thermal waters as well as the output result of the $\delta^{13}\text{C}$ of the thermal water following sulphate reduction. The mass balance is based on equation (VI-10): where one mole of reduced sulphate can produce one mole of HCO_3^- and 1 mole of HS^- .

A q_2 factor based on carbon mass balance similar to the q_1 is adapted as follow:

$$q_2 = \frac{\delta^{13}\text{C}_{\text{calculated}} - \delta^{13}\text{C}_{\text{organic}}}{\delta^{13}\text{C}_{\text{recharge}} - \delta^{13}\text{C}_{\text{organic}}} \quad \text{VI-11}$$

The average of both the $\delta^{13}\text{C}$ (-11.8) and alkalinity (4.26 mmol/l) from the recharge area in Ajloun Mountains are taken to be the initial values for the calculation of q_2 . In addition the estimated concentration of the HS^- of the thermal well and the $\delta^{13}\text{C}$ (-25 ‰) of the organic matter are also used.

The $\delta^{13}\text{C}_{\text{DIC}}$ in the thermal waters is depleted by an amount equivalent to the sulphide produced i.e.

$$\frac{\delta^{13}\text{C}_{(\text{Recharge})} * \text{HCO}_3^- + \delta^{13}\text{C}_{(\text{Organic})} * \text{HS}^-}{\text{HCO}_3^- + \text{HS}^-} = \delta^{13}\text{C}_{(\text{Calculated})} \quad \text{VI-12}$$

The output values of the $\delta^{13}\text{C}_{(\text{Calculated})}$ range from -13.3 to -15.6 ‰ (Table VI-13),

which are values more depleted than the measured $\delta^{13}\text{C}$ of the thermal groundwaters. This implies that a third source of carbonate is incorporated into these waters prior to discharge, which responsible for this enrichment of the $\delta^{13}\text{C}$ of the thermal water.

Such enrichment can be achieved through mantle CO_2 gas migrating from depth related to the active tectonic environment of the rift valley. The CO_2 gas was measured in some natural springs along the JRV area. Clark, 1991 recorded gas discharging in some springs 15 to 50 km south to the study area in the JRV with 47.5 to 97.4 volume percent CO_2 .

The $\delta^{13}\text{C}$ value of the mantle CO_2 is found to range between -5.8 ‰ and -7.1 ‰ (Exley et al., 1986), and that will enrich the $\delta^{13}\text{C}$ of the thermal water. The following mass balance is based on the following input values: $\delta^{13}\text{C}_{(\text{CO}_2)}$, $\delta^{13}\text{C}_{(\text{calculated})}$, $\delta^{13}\text{C}_{(\text{observed})}$ and $\text{HCO}_3^-_{(\text{observed})}$. The amount of mantle CO_2 in mmol ($\text{CO}_{2(m)}$) can be calculated as follow:

$$\text{CO}_{2(m)}\delta^{13}\text{C}_{(\text{CO}_2)} + (\text{HCO}_3^-_{(\text{observed})} - \text{CO}_{2(m)})\delta^{13}\text{C}_{(\text{calculated})} = \text{HCO}_3^-_{(\text{observed})}\delta^{13}\text{C}_{(\text{observed})} \quad \text{VI-12}$$

$$\text{CO}_{2(m)} = \frac{[\text{HCO}_3^-_{(\text{observed})}\delta^{13}\text{C}_{(\text{observed})}] - [(\text{HCO}_3^-_{(\text{observed})}\delta^{13}\text{C}_{(\text{calculated})}]}{\delta^{13}\text{C}_{(\text{CO}_2)} + \delta^{13}\text{C}_{(\text{calculated})}}$$

The result of this calculation shows that the concentration of CO_2 ranges between 1.38 to 4.35 mmol/l if the $\delta^{13}\text{C}_{(\text{CO}_2)}$ is chosen to be -7 ‰ Table VI-13.

In a similar manner to q_1 and q_2 the following carbon mass balance is used:

$$q_3 = \frac{\delta^{13}\text{C}_{\text{measured}} - \delta^{13}\text{C}_{\text{CO}_2}}{\delta^{13}\text{C}_{\text{calculated}} - \delta^{13}\text{C}_{\text{CO}_2}} \quad \text{VI-14}$$

The product of the three dilution factors:

q_1 - carbonate dissolution during infiltration

q_2 - sulphate reduction

q_3 - incorporation of mantle CO_2

are then used in the decay equation to calculate the residence time of the thermal groundwaters:

$$\ln(q_1 * q_2 * q_3 * 100 / {}^{14}\text{C}_{\text{meas.}}) * 8266.7 = \text{Age}$$

For example the residence time of the groundwater in Mukhebeh 6 from the recharge area to the site of the well will give an age:

$$\ln(0.55 * 0.85 * 0.74 * 100 / 16.56) * 8266.7 = 6,100 \text{ years}$$

The 100 pmc is the A_0 for the atmosphere and 16.56 is the measured ${}^{14}\text{C}$ activity in the sample. Correction for all thermal groundwaters for which sulphide data are available are given in Table VI-13.

Table VI-13 ${}^{14}\text{C}$ correction by carbonate dissolution, sulphide and mantle CO_2

Name	${}^{14}\text{C}$	$\delta^{13}\text{C}$	HS^-	q_1	q_2	q_3	${}^{13}\text{C}_{\text{(cal)}}$	CO_2	Age
	pmc	‰	mmol/l				‰	mmol/l	years
Mukhebeh 5	3.6 ± 0.5	-11.96	1.90	0.55	0.71	0.57	-15.6	3.01	15,000
Mukhebeh 6	16.56 ± 0.9	-12.01	0.80	0.55	0.85	0.74	-13.7	1.38	6,100
Mahasi 6	3.04 ± 1.2	-10.3	0.60	0.55	0.88	0.52	-13.3	2.18	17,500
N.Shunch	8.0 ± 1.0	-10.2	0.20	0.55	0.79	0.42	-14.5	3.13	6,900
Manshieh	4.7 ± 0.7	-9.46	1.30	0.55	0.78	0.32	-14.7	4.03	8,800
JRV1	5.36 ± 0.5	-8.4	0.72	0.55	0.86	0.21	-13.6	4.35	5,300

It is worthwhile to mention that with the uncertainty of the available chemical and

isotope data it is not possible to exclude (i) carbon isotope exchange with calcite and dolomite and (ii) incongruent dissolution of dolomite in accounting for some heavier $\delta^{13}\text{C}$ content in some groundwater (Plummer, et al., 1990). The Mukhebeh and JRV well field are supersaturated with respect to calcite, dolomite and undersaturated with respect to gypsum and have different $\text{Mg}^{+2}/\text{Ca}^{+2}$ molal ratio (Table VI-4). Appelo and Postama, (1993). The alkalinity of the thermal water was found to be between 5 and 8 meq/l. This values are greater than the alkalinity of the groundwater observed in the recharge area (4 to 4.6 meq/l).

The results of calculation and ^{14}C correction can be found in Table VI-13. The "age" of the thermal water based on these correction models are less than 15,000 years. As an example, Mukhebeh 6 the measured ^{14}C content is 16.5 pmc is equivalent to age of 14,800 years if no correction is made. Correcting for various model described in section II-5 results in an age of about 7,800 to 11,600 years. When the data corrected according to Table VI-13, the water is estimated to be 6,100 years old. Fig.VI-12 demonstrates the difference between sulphate reduction, carbonate dissolution and uncorrected ages. This is evidence that a clear understanding of the carbonate sources to the groundwater in an aquifer system, are necessary in ^{14}C dating.

Uncertainty also remains in the sulphate reduction approach, as the $\delta^{13}\text{C}$ of the following parameters were assumed: carbonate, soil CO_2 , and organic matter in the rock matrix. In addition, the HS^- values which were estimated semi-quantitatively, are essential parameters for the calculation of q_2 and q_3 , that is essential for estimating the age of groundwater. For example, if we take the Mukhebeh 6 well and calculated the residence

time by assuming 10 % more or less HS^- than the value listed in Table VI-13, the result in age will be about 5,800 (0.88 mmol/l HS^-) and 6,400 (0.72 mmol/l HS^-) years respectively.

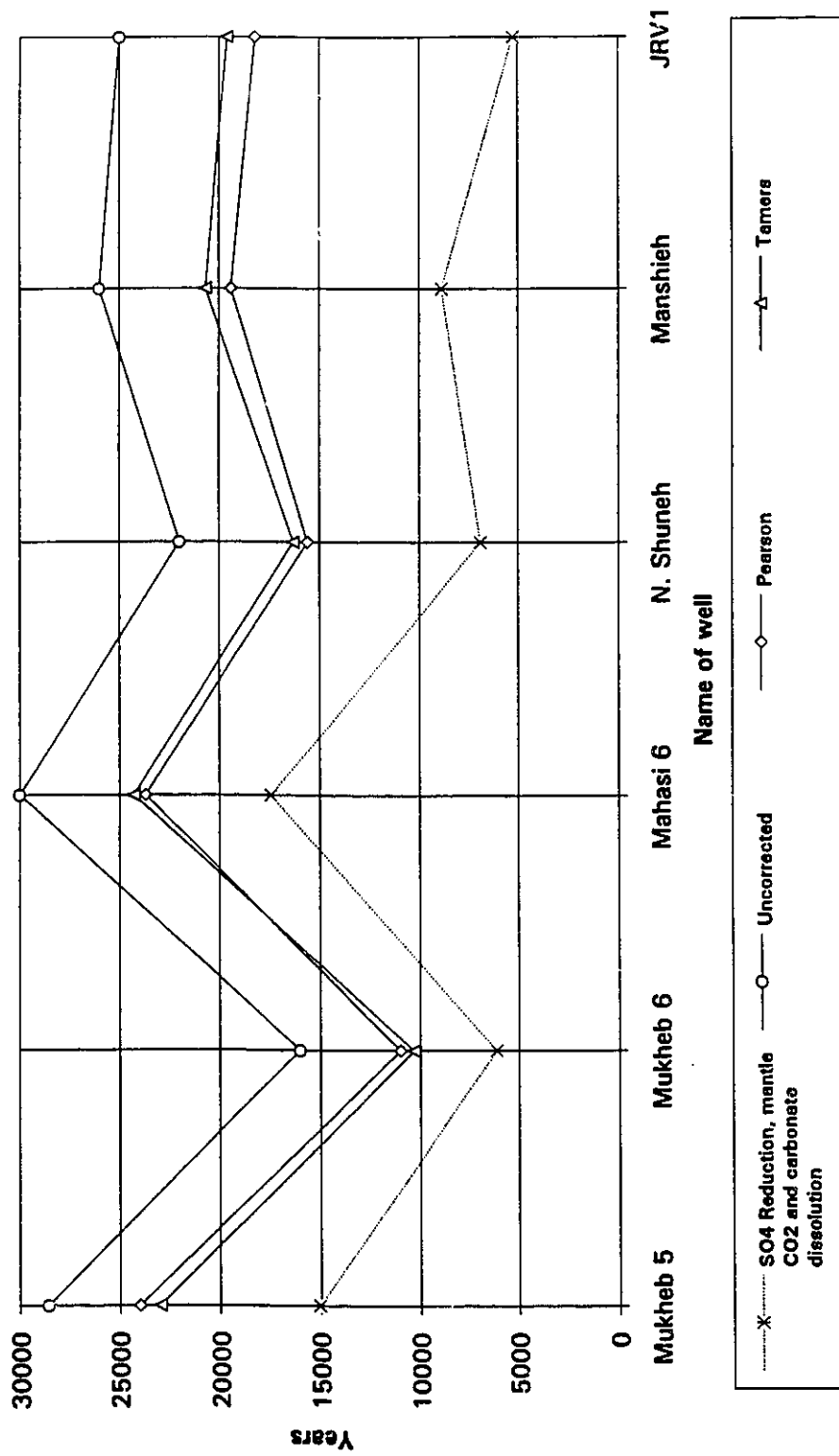


Fig. VI-12 comparison between the "age" of groundwater by using uncorrected, sulphate reduction and carbonate dissolution models (Tamers Pearson)

VI-6 Chloride-36 (³⁶Cl)

The long lived radioisotope of chloride, ³⁶Cl, has been used in an increasing number of saturated and unsaturated zone problems. As a conservative anion, ³⁶Cl is generally considered to be an excellent tracer for the movement of water itself. More importantly ³⁶Cl is a useful tool for determining solute origin and can be used to constrain groundwater residence times.

In comparison with ¹⁴C, ³⁶Cl dating methods have some advantages. (a) The ³⁶Cl has a longer half life (3.01×10^5 years). (b) chloride is generally conservative in groundwater due to its highly solubility in water and that it is not subject to exchange or adsorption during flow.

Sources of ³⁶Cl in groundwater can originate from variety of sources and can provide useful hydrogeological information on recharge and flow:

1. Atmospheric origin: meteoric ³⁶Cl is potentially derived from cosmic-ray spallation of ⁴⁰Ar and by neutron activation of ³⁶Ar. Bentley, et al., (1986), observed that ³⁶Cl varies with latitude. The heaviest fallout is in the mid latitude of both hemisphere.
2. Epigenic (near surface), ³⁶Cl is produced as a result of K and Ca and activation of ³⁵Cl by cosmogenic neutrons (Yokoyama et al., 1977). This ³⁶Cl is released by weathering and thus enters the groundwater and surface system.
3. ³⁶Cl produced in the deep subsurface (hypogenic zone): ³⁵Cl can be activated by the thermal neutron flux originating from radioactive decay of U and Th series elements (Bentley, et al., 1986).

In addition to the natural sources of ³⁶Cl discussed above, ³⁶Cl was also produced

by man made nuclear tests during the period from 1952 to 1964 (Elmore et al., 1982). During this period the level of ^{36}Cl fallout increased several order of magnitude above natural levels.

Groundwater dating based on ^{36}Cl dynamics depends upon an understanding of the Cl^- geochemical evolution of the groundwater in the study area including:

(i) The initial activity in precipitation: This value is not known but can be calculated from a knowledge of fallout rates (Andrews and Fontes, 1992). A value of $14 \text{ atoms m}^{-2} \cdot \text{s}^{-1}$ was adapted by Clark and Fritz, (1994) for the Maqaren area within the study area. Given an average of 600 mm in the recharge area in the Nuaimah area, this would provide a concentration in rainfall of about $7 \times 10^5 \text{ atoms/l}$.

(ii) The rate of epigenic production and evaporative concentration. ^{36}Cl will accumulate in the recharge environment due to evaporation and surface production by cosmic radiation. The ^{36}Cl production at the ground surface could be similar to or greater than atmospheric fallout and may reach levels up to an order of magnitude higher (G. Milton, personal communication).

(iii) The production of ^{36}Cl due to subsurface neutron flux on ^{35}Cl may be significant in some thermal well fields. In the JRV area a value of 16.5 pC/l of ^{226}Ra was measured in the North Shuneh well (Jawawdeh and Amro, 1992). Mazor, et al., (1973) recorded a range between 40 to 420 pC/l for the Hammat Gader spring. As presented in (Table VI-14) the concentration of Cl^- of the sampled wells (30 to 200 ppm) is greater than the concentration of Cl^- in the recharge area (30 to 40 ppm), with the exception of the Waqas well. This subsurface source of Cl^- would then accompanied by hypogenic ^{36}Cl .

Eight samples from the precipitation at Ras Munif and Rabba stations and from three thermal well fields, Mukhebeh, JRV and Ramtha were sampled for ^{36}Cl activity measurements carried out by AECL in Chalk River, Canada. These data are given in Table VI-14, analytical results are presented both as chlorine isotope ratios and as absolute amounts.

Table VI-14 Chlorine concentrations and isotope ratios in selected thermal waters

Source	Depth	^3H	Cl	$^{36}\text{Cl}/^{35}\text{Cl}$	$^{36}\text{Cl}/\text{l}$
	m	TU	mg/l	10^{-15}	10^5
Rain (calculated)		3.8-16	3.5		7
Ras Munif Rain		6.2	7.8	51.7 ± 6.0	37
Rabba Rain		7.0	13.8	109.9 ± 6.0	104
Maqla Spring	0	0.0-1.6	199.0	37 ± 7.0	1243
Mukhebeh 6	475	0.0-0.8	64.3	72 ± 9.0	781
Waqas	1300	0.0-0.5	37.3	32 ± 8.0	204
N.Shuneh	967	0.0-1.2	98.9	20 ± 6.0	334
Mahasi 6	702	0.0-0.6	99.6	40 ± 7.0	673

From Table VI-14, groundwater ^{36}Cl contents are 3 to 15 times higher than the calculated atmospheric fallout level of 7×10^5 atom/l. Measured values in rainfall (Table VI-14) are also several times higher than the calculated value for this geomagnetic latitude. Thus, there are clearly sources of ^{36}Cl for the thermal water in addition to atmospheric production. Given that the tritium contents in these waters are near or below detection,

^{36}Cl from thermonuclear tests can be ruled out. The principal sources, which may be considered are epigenic production with evaporative concentration and subsurface activation of aquifer Cl. As the $^{36}\text{Cl}/^{35}\text{Cl}$ ratios in the thermal waters more or less similar, the high ^{36}Cl contents can be attributed to leaching of activated Cl in the subsurface, rather than to subsurface activation of dissolved Cl⁻ incorporated by the thermal waters during recharge. This argues against long subsurface residence times.

Chapter Seven

Summary, Conclusions and Recommendations

This study attempts to define the recharge area, the geochemical evolution, and the heat source of thermal groundwaters in north Jordan and of shallow non-thermal waters in potential recharge areas. Conclusions presented here are based on the isotopic and chemical compositions of precipitation, surface waters, and groundwater.

I-Precipitation and Yarmouk River water:

- 1) Isotope values for precipitation show a large spread from -33 to -19 ‰ for δD and from -7.1 to -4.4 ‰ for $\delta^{18}O$. The local meteoric water line obtained by linear regression is:

$$\delta D = 6.46 \delta^{18}O + 12.07 \quad (R^2 = 0.94)$$

The Mediterranean Sea plays a large role in modifying the isotopic composition of air masses entering the area from different regions. The isotopic composition of rain water demonstrates an altitude effect, which has been used as a tracer to monitor the source of recharge to the thermal and non-thermal waters. The tritium concentration of the rain in the three stations (average 6 TU) doesn't have an appreciable fluctuation. The tritium average for the three stations is used as a representative value for the modern input function into the groundwater in aquifers B4 and the B2/A7. The high concentrations of SO_4^{2-} , Na^+ , and Cl^- in the precipitation are attributed to aerosol originating either from the Mediterranean or the Dead sea.

- 2) The base flow of the Yarmouk River is generated by rain upstream a higher elevation,

mainly in Syria, and from underground drainage and return flow from irrigation along the river. The river shows an evaporation isotopic enrichment in samples taken in dry season along its course.

II- Regional non-thermal groundwater.

- 1) Phreatic B2/A7 aquifers in the Nuaimah and Side Wadies areas are identified as actively recharged systems. These karstic limestone aquifers respond directly to precipitation events. This is demonstrated by the wide variation of stable isotope and tritium content of the groundwater.
- 2) The origin of ions in groundwater is attributed to dissolution of carbonate rock.
- 3) The recharge elevation in both areas is believed to be between 850 to 950 m asl.
- 4) The recharge in Nuaimah area estimated by Cl⁻ mass balance to be between 18 to 27 MCM/y.
- 5) The isotopic composition of the groundwater in Wadi Al-Arab well field indicates evaporation before infiltration. The altitude of recharge is around 500 - 600 m asl.
- 6) Brackish water in the Adasyia area originates mainly from evaporite dissolution within the Lisan marl. The enriched isotopic composition and the high NO₃⁻ concentration of groundwater indicate the contribution of Yarmouk River and return flow from irrigation.
- 7) The shallow B4 aquifer in Ramtha area has high concentrations of TDS, variation in the chemical ions (mainly the NO₃⁻), and enrichment in stable isotopes. This is attributed to a source of contamination mainly from organic origin (sewage). The

recharge elevation based on the isotopic composition is found to be around 500 - 600 m asl.

- 8) The deeper B2/A7 aquifer in the Ramtha area demonstrated a Ca^{2+} - HCO_3^- type of water. The B4 aquifer was found to contribute around 20 % leakage to Muhamad Haji well tapping the B2/A7 aquifer.
- 9) The groundwater chemistry in the North-East Desert reflects the water interactions with basalt and carbonate rocks. The recharge elevation estimated by the isotopic composition to be higher than the Ras Munif altitude, the recharge most probably Jabal Al-Druze in Syria in the north.

III-Thermal water:

- 1) Three principal thermal waters well fields exist in north Jordan: Mukhebeh ($T = 30\text{ }^\circ\text{C}$ to $45\text{ }^\circ\text{C}$), The north Jordan Rift Valley ($T = 51\text{ }^\circ\text{C}$ to $56\text{ }^\circ\text{C}$), and Ramtha ($T = 42\text{ }^\circ\text{C}$ to $56\text{ }^\circ\text{C}$). Only the Mukhebeh site includes naturally occurring springs.
- 2) A slight decrease in temperature was observed in the Mukhebeh area suggesting that the aquifer has been affected by minor mixing during withdrawal. Temperature fluctuations of the spring and the open hole (Mukhebeh 1) waters are attributed to slight mixing with cold water prior to its emerging to the surface. This observation was also confirmed by tritium which is low to less than detection TU in these thermal waters.
- 3) The geothermal gradient in the three well field varies between 1.8 and $4.4\text{ }^\circ\text{C}/100\text{m}$. The highest is found in the Mukhebeh area and attributed to (i) rapid ascent of deep

groundwaters due to tectonic fracturing to a shallower aquifer zone, and (ii) heterogeneity in subsurface heating related to magmatic intrusion beneath the Yarmouk River.

In the Ramtha and JRV areas the water temperature is dictated by the regional geothermal gradient.

- 4) Chemically the groundwater can be classified into four types of water (1) calcium bicarbonate (Ca^{2+} - HCO_3^-); (2) calcium, sodium chloride (Ca^{2+} , Na^+ - Cl^-); (3) Sodium chloride Na^+ - Cl^- ; and (4) calcium sulphate Ca^{2+} - SO_4^{2-} . In the Mukhebeh area, type 1 was found for Mukhebeh 1 to 7, and type 2 for JRV1 and Maqla. The major processes which are responsible for these geochemical facies are carbonate dissolution to calcite saturation in the regional B2/A7 flow system and by subsequent evaporite dissolution with sulphate reduction. Balsam spring is a mixing ratio of 65 % of the Mukhebeh 1 type water and 35 % of Maqla spring type water.

The Ca^{2+} - SO_4^{2-} type of water in the sandstone aquifer in Ramtha area is attributed to dissolution of sulphate minerals. The 1:1 Na^+ - Cl^- relation indicates that halite dissolution in the aquifer is mainly responsible for its chemistry.

- 5) Modification to regional flow models proposed by previous studies are:

- (i) The flow system of the B2/A7 aquifer in Mukhebeh area come from east via Ramtha was rejected, based on the geochemical evolution of groundwater in both areas.
- (ii) The deep sandstone aquifer cannot contribute groundwater to the B2/A7 aquifer due to their differing isotopic and chemical compositions. The water is old (palaeowater), recharged in the Pleistocene and it is characterized as Ca^{2+} - SO_4^- type of water, which

is completely different than the B2/A7 aquifer water (see points 2 and 8).

- 6) The temperature of the reservoir estimated by several chemical geothermometers produced temperature estimates of less than 100 °C, with a range between 50 to 75 °C.
- 7) The isotopic composition of the thermal water indicates that the recharge took place under one of two climatic conditions. All JRV and Mukhebeh thermal waters were recharged under the climatic region which dominates today in north Jordan. The S-90 well tapping the sandstone aquifer in Ramtha area has a depleted isotopic signature and is considered to be Pleistocene in age.
- 8) Two isotopically distinct groundwater types are found in the Mukhebeh and JRV well fields. This indicates that the areas are a discharge zone for two flow systems coming from areas with different recharge elevations. JRV and Mukhebeh thermal waters come from Ajloun mountains, while the JRV1 and Maqla waters originate most probably in the higher elevation regions of Mount Hermon in Syria.
- 9) The $^{34}\text{S}/^{18}\text{O}$ isotopic composition of sulphate in the JRV1 and some JRV waters indicates that the SO_4^{2-} originates from dissolution of Upper Cretaceous sulphate minerals. Other thermal waters have sulphate which are depleted in stable isotope, suggesting an origin in the high S-kerogen and / or volcanogenic (mantle) SO_2 .
- 10) The carbonate and ^{14}C chemistry of the thermal waters and the groundwaters in the recharge areas was examined in order to constrain groundwater ages. The geochemistry of radiocarbon in groundwater is affected by carbonate dissolution, sulphate reduction and incorporation of mantle CO_2 in the rift zone. The ^{14}C value

decreases from 115 in the atmosphere to 65 pmc in the recharge area due to carbonate dissolution outcropping in the recharge area, giving a dilution factor of 0.56.

Secondary dilution of ^{14}C in thermal groundwaters is due to sulphate reduction. This was corrected by mass balance calculation using dissolved HS^- analyses.

A final correction factor for incorporation of mantle CO_2 is based on $\delta^{13}\text{C}$ and DIC mass balance calculation. The combined ^{14}C correction model produces a range of groundwater "ages" of about 5,300 to 17,500 years, This is 15 to 60 % lower than age estimated by the classical models, which produce ages estimates of 10,000 to 30,000 years B.P. Further, these revised age estimates are consistent with recharge under climatic conditions similar to those prevailing today, as demonstrated by their stable isotope contents.

- 11) The six ^{36}Cl six analyses for thermal waters support the ^{14}C interpretation that the subsurface mean residence times are relatively short.

Recommendation:

1. For future work more chemical and isotopic data should be sampled from the Syrian side in order to better establish the flow system between the two countries, Jordan and Syria. This will shed more light on the geochemical evolution of the groundwater from the recharge area to the discharge zone of the thermal water.
2. Environmental isotopic samples for the gases should be collected at the thermal sites in order to verify the contribution of the mantle CO_2 in the thermal water, especially in the JRV area and their effect on the $\delta^{13}\text{C}$ and ^{14}C of the TDIC of the groundwater.

References

- Abdel Hadi, M., 1991. Reservoir Geology of Yarmouk Basin. Natural Resources Authority (NRA), Amman-Jordan. pp. 34
- Abdelhamid, G., Mohamed, B., and Barjous, M., 1991. The Geology of northwest Jordan. Internal Report. NRA, Amman-Jordan. pp.26
- Abed, A., and Amierh, B., 1983. Petrography and Geochemistry of some Jordanian Oil Shales from North Jordan. J. of Petroleum Geology, 5,3, pp. 261-274.
- Abu-Ajamieh, M.M., 1980. The geothermal resources of Zerqa Ma'in and Zara. NRA-Jordan. Amman-Jordan. pp. 82
- Abu-Ajamieh, M.M., Bender, F.K., and Eicher, R.N., 1988. Natural Resources in Jordan. Inventory-Evaluation-Development Program. Natural Resources Authority (NRA), Amman-Jordan. pp.224
- ACSAD, 1983. Hammad Basin Project, Atlas-Map, Damascus, Syria.
- Al-Aroui, Kh., 1992. Organic Geochemistry & Petroleum Source Rock Evaluation of Phosphorite-Oil Shale Succession in Jordan. M.Sc. thesis, University of Jordan.
- Al-Hawi, M.S., 1990. Hydrogeology and Groundwater Flow system in the Area Between Wadi Yabis and Yarmouk River / Jordan Valley Area. M.Sc. Thesis, University of Jordan, Amman-Jordan. pp. 96
- Allen, R.A., Smith, D.B., Otlet, R. L., and Rawson, D.S., 1966. Nuclear Instrument Method, 45: 61.
- Al-Momani, M., and El Mousa, N., 1987. Water Resources and Exploitation in the Northern Rift Side Wadies of Jordan. Report presented at the 4th international

- advanced course on water resources management, Colombella, Perugia. pp.26
- Al-Suleiman, A.L., 1992. Stratigraphy Review of North Jordan, North Jordan Study Group, NRA, Amman-Jordan. pp.36
- Anderson. D., 1976. Klesh Plotter Photomapping. Geological Report of H.K. of Jordan Ajloun Dome. NRA, Amman-Jordan.
- Amos Nur, 1991. And the walls came tumbling down. New Scientist, July, pp. 45-49.
- Andrews, J.A., and Fontes, J-Ch., 1992. The importance of in situ production of certain radionuclides in hydrology and geochemistry (^{36}Cl and ^{14}C). Proceedings, International Symposium on the Use of Isotope Techniques in Water Resource Development. Int. Atomic Energy Agency, March 11-15, 1991, Vienna.
- Appelo, C.A.J., and Postama, D., 1993. Geochemistry of Groundwater and Pollution. A.A. Balkema Rotterdam.
- Arad, A., and Bein, A., 1986. Saline-versus freshwater contribution to the thermal waters of the northern Jordan Rift Valley, Israel. J. of Hydrology 83, 49-66.
- Aravena, R., 1993. Carbon Isotope Geochemistry of a Confined Methanogenic Groundwater System: The Alliston Aquifer Complex. Ph.D. Thesis, University of Waterloo, Ont., Canada. pp. 168
- Bajjali, W., 1988. Environmental Isotope Study of Some Springs in Jordan. Internal Report, WAJ, Amman-Jordan. pp.5
- Bajjali, W., 1990a. Isotopic and Hydrochemical Characteristics of Precipitation in Jordan, M.Sc. Thesis, Jordan University. Amman-Jordan. pp.99
- Bajjali, W., 1990b. Hydrochemical and Isotopic of some thermal water in Jordan.

- Internal Report. Natural Resources Authority , Amman-Jordan. pp.8
- Baker & Harza Engineering Company, 1955. Yarmouk-Jordan Valley Project, Master Plan Report, Amman-Jordan.
- Barber, W., 1975. An outline for water planning in East-Jordan. Report to Natural Resources Authority. Amman-Jordan. pp.11
- Bard, E., Hamelin, B., Fairbanks, R.G., and Zindler, A., 1990. calibration of the ^{14}C timescale over the past 30,000 years using mass spectrometric U-Th ages from Barbados corals, *Nature*, 345, 405.
- Barjous, M., and Mikbel, Sh., 1990. Tectonic evolution of the Gulf of Aqaba-Dead Sea transform fault system. *Tectonophysics*, 180: pp. 49-59.
- Barker, J., Fritz, P., and Brown, R.M., 1987. ^{14}C measurements in aquifers with methane isotopes in groundwater hydrology: Neuherberg, (Germany) IAEA, Symp. SM-228.
- Beicip, 1981. Structural Study of Jordan, Internal Report, NRA, Amman-Jordan.
- Bein, A., and Feinstein, Sh., 1988. Late Cenozoic thermal Gradients in Dead Sea Transform System Basins. *Journal of Petroleum Geology*, 11 (2) pp. 185-192.
- Bender, F., 1974. *Geology of Jordan*. Gebruder Borntraeger. Berlin. Stuttgart. pp.196.
- Bender, H., Hobler, M., and Rashdan, J., 1991. New Aspect of the groundwater system of Jordan. *Geology of Jordan*, Goethe-Institute, Bundesanstalt fur Geowissenschaften und Rohstoffe, Hannover, Amman-Jordan. pp.3
- Bentley, H.W., Philips, F.M., Davis, S.N., Habermehl, M.A., Airey, P.I., Calf, G. E., Elmore, D., Gove, H.E., Torgersen, T., 1986. Chlorine 36 Dating of Very Old

- Groundwater 1. The Great Artesian Basin, Australia. Water Res., Vol 22, No. 13, pp. 1991-2001.
- Belbeisi, M., 1992. Jordan's water resources and the expected domestic demand by the years 2000 and 2010, detailed according to area. Proceeding of the Symposium 27th and 28th October 1991. Organized by Fredrich Ebert Stiftung, Higher Council for Science and Technology, Amman and Water research and Study Centre. Amman-Jordan. pp. 7-29
- Bodverson, G., 1961. Physical characteristic of Natural Heat Resources in Iceland. U.N. Conference on New resources of Energy, Rome.
- Burdon, P.J., 1952. Report to the Hashemite Kingdom of Jordan on the Geological Features of the Yarmouk Valley Scheme. FAO Report No.61, Rome, pp.1-41. Carmi, I., and Gat, J.R., 1973. Tritium in Precipitation and freshwater sources in Israel. Isr. J. Earth Sci., 22: 71-92.
- Chapelle, F.H., and Knobel, L.L., 1985. Stable carbon isotopes of HCO₃ in Aquia aquifer, Maryland: Evidence for an isotopically heavy source of CO₂. Groundwater 23: 592-599.
- Charalambous, A. N., 1990. Sectorial Report on Groundwater Resources Availability and Use Jordan. UNDP, JOR/87/003.
- Charalambous, A., N., 1991. Water Resources Policies Planning and Management -Jordan Brackish Groundwater Resources. UNDP, USA.
- Clark, I.D., 1987. Groundwater Resources in the Sultanate of Oman: Origin, Circulation Times, Recharge Processes and Palaeoclimatology. Ph.D.Thesis,

University of Paris. pp.264

- Clark, I.D., Fritz, P., Quinn, O.P., Rippon, P., Nash, H., and Bin Galib al Said, 1987. Modern and fossil groundwater in arid environment, A look at the hydrogeology of Southern Oman. Proc., Int. Atomic Energy Agency, Symp. 299, Use of Stable Isotopes in Water Resources Development, Vienna, p. 167-187.
- Clark, I.D., 1991. Gas samples from some springs in Jordan , unpublished data.
- Clark, I. D., and Fritz, P., 1993. Environmental Isotopes in Hydrogeology, Course notes for Geo 5143, Environmental Isotopes and Groundwater Geochemistry. University of Ottawa. pp. 163
- Clark, I.D., Khoury, H.N., Salameh, E., Fritz, P., Seidlitz, H.K., and Milodowski, T.E., 1992. Origin of the Maqaren, Jordan hyperalkaline groundwaters: Isotopic and geochemical evidence for in situ combustion, calcination and recarbonation of bituminous marls. In : Kharaka, Y.K., and Maest, A., (eds.): Proc. of the 7th International Symposium on Water-Rock Interaction-WRI-7/Park City/Utah/USA/13-18 July 1992. pp. 1485-1489.
- Clark, I.D., Fritz, P., 1994. Isotope Hydrogeology of the Maqaren Hyperalkaline Groundwaters, Maqaren Natural Analogue Study Phase II Program, Nagra, Uk., Nirex and S.K.B. pp.15
- Claypool, G.E., Holser, W.T., Kaplan, I.R., Sakai, H., and Zak, I., 1980. The Age Curve of Sulphur and Oxygen Isotopes in Marine Sulphate and Their Mutual Interpretation. Chemical geology, 28, pp. 199-260.
- Craig, H., 1961. Isotopic variations in meteoric waters. Science, 133, 1702-1703.

- Craig, H. and Gordon, L., 1965. Deuterium and oxygen-18 variations in the ocean and marine atmosphere. In: Tongiorgi E., (Ed.), *Stable Isotopes in Oceanographic Studies and Paleotemperatures*. Lab. Div. Geologia Nucleare, Pisa, pp. 9-130.
- Dansgaard, W., 1964. Stable isotope in precipitation. *Tellus*, 216: 436-468.
- Department of Water Resources Development, 1987. *Groundwater Quality Data in Jordan, prior to October 1985*. Technical Paper No.53. WAJ, Amman pp.515.
- Department of Water Resources Development, 1987. *Springs Flow*. Technical Paper No.53. WAJ, Amman- Jordan.
- Dincer, T., Al-Mugrin, A., and Zimmerman, U., 1974. Study of the infiltration and recharge through the sand dunes in arid zones with special reference to the stable isotopes and thermonuclear tritium. *J. Hydrology*. 23, 79-109.
- Dorr, H., Sonntag, C., Regenber, W., 1987. Field study on the initial ^{14}C content as a limiting factor in ^{14}C groundwater dating. *Isotope Techniques in Water Resources Development*. IAEA, Vienna.
- Drever, J.I., 1982. *The geochemistry of Natural Waters*. Prentice-Hall, Englewood Cliffs. N.J. pp.388
- Droubi, A., 1992. *Geochemical and Isotopic Study of the Yarmouk Basin-Syria*. Isotope Workshop supported by IAEA, Ankara-Turkey. pp.39
- El-Issa, Z., and Mustafa, H., 1986. Earthquake deformation in the Lisan deposits and seismotectonic implications. *Geophys. J. R. Astron. Soc.*, 86: 413-424.
- El-Naser, H., 1991. *The groundwater Resources of the Deep Aquifer Systems in NW-Jordan: Hydrogeological and Hydrochemical Quasi 3-Dimensional Modelling*.

- Ph.D. Thesis, University of Wurzburg, p. 144.
- El-Naser, H., Ayed, R., and Al-Momani, M., 1992. Effect of 1991/1992 rainfall on the groundwater Recharge of Yarmouk and Wadi Al Arab Basins. Internal report, WAJ, Amman-Jordan. pp. 28
- Elmore, D., Tubbs, L.E., Newman, D., Ma, X.Z., Finkel, R., Nishiizumi, K., Beer, J., Oeschger, H., and Andr, M., 1982. The 36 bomb pulse measured in a shallow ice core from Dye, Greenland, *Nature*, 300, 735-737.
- Endeshaw, A., 1988. Current Status (1987) of Geothermal Exploration in Ethiopia. *Geothermics*, Vol.17 No.2/3, pp. 477-488.
- Eriksson, E., 1967. Isotope in hydrometeorology, Proc. IAEA Conf. on Isotopes in Hydrology Vienna, pp. 21-33.
- Faure, G., 1977. Principles of Isotope Geology. Smith-Wyllie Intermediate Geology Series. Wiley, New York, N.Y., pp. 464.
- Fontes, J-Ch., and Zubi, C.M., 1976. Isotopes and water chemistry in sulphide-bearing springs of central Italy. In: International of Environmental Isotope and Hydrochemical Data in Groundwater Hydrology. IAEA, Vienna, pp. 143-158.
- Fontes, J-Ch., and Garnier, J.M., 1979. Determination of the initial ^{14}C activity of the total dissolved carbon. A Review of the Existing Models and a New Approach. *Water Resour. Res* 15:399-413
- Fontes, J-Ch., 1983. Dating of Groundwater. In guidebook on Nuclear techniques in hydrology 1983", Technical report series No. 91, IAEA, Vienna, 285-317.
- Fontes, J-Ch., 1985. Some considerations on groundwater dating using

- environmental isotopes. In: *Hydrogeology in the Service of Man*. Mem IAH, Cambridge, pp. 118-154.
- Fournier, R.O., and Rowe, J.J. 1966., Estimation of underground temperatures from the silica content of water from hot springs and wet-steam wells. *Am. Jour. Sci.*, v. 264, p.685-687.
- Fournier, R. O., 1973. Silica in thermal waters: Laboratory and field investigations, *Proceeding of International Symposium on Hydrogeochemistry and Biogeochemistry, Japan 1970, Volume 1, hydrogeochemistry: Washington, D.C.*, 122-139.
- Fournier, R.O., and Truesdell, A.H., 1973. An empirical Na-K-Ca geothermometer for natural waters, *Geochim.Cosmochim. Acta*, 37, 1255-1275.
- Fournier, R.O., 1977. Chemical geothermometers and mixing models for geothermal system, *Geothermics*, 5.
- Fournier, R.O., 1981. Application of water chemistry to geothermal exploration and reservoir engineering. In: Rybach, L., and Muffler, L.J.P. (eds.): *Geothermal Systems: Principles and Case Histories*. New York, Wiley, pp.109-143.
- Freeze, R.A., and Cherry, J.A., 1979. *Groundwater*. Prentice-Hall, Inc. Englewood Cliffs, New Jersey 07632.
- Fritz, P., Gale, J.E., and Reardon, E.J., 1979a. Comment on Carbon-14 Dating of Groundwaters in Crystalline Environments. *Geoscience Canada*. Volume 6, No.1.
- Fritz, P., Silva, C., Suzuki, O., and Salati, E., 1979b. Isotope Hydrology in Northern Chile: *Proc. International Sympos. On Isotope Techn: in Groundwater*

- Hydrology, Neuherberg (Germany) IAEA, Symp. SM-228.
- Fritz, P., and Mozeto, A.A., 1980. Consideration on radiocarbon Dating of groundwater. In Proceeding of a Symposium " Interamerican Symposium on Isotopes Hydrology" Instituto de Asuntos Nucleares, C.O. Rodriquez and C. Bricena de Monoy eds, CIEN, OEA, Colcincias, Bogota, 221-244.
- Fritz, P., and Fontes, J-Ch., 1980. Handbook of Environmental Isotope Geochemistry. Elsevier Scientific Publishing Company.
- Fritz, P., Basharmal, G.M., Drimmie, R.J., Ibsen, J., and Qureshi, R.M., 1989. Oxygen isotope exchange between sulphate and water during bacterial reduction of sulphate. *Chemical Geology*, 79, pp. 99-105.
- Futyán and Jawzi Associates, 1991. The Hydrocarbon Potential of the Arabian Peninsula, NRA, Amman-Jordan.
- Galanis, P.S., Sass, J.H., Munroe, R.J., and Abu-Ajamieh, M., 1986. Heat flow at Zerqa Ma'in and Zara and a geothermal reconnaissance of Jordan. US geological Survey. Menlo Park. pp.110.
- Garfunkel, Z., Zak, I., and Freund, R., 1981. Active faulting in the Dead Sea Rift. In: Freund R., and Garfunkel Z., (Eds.), The Dead Sea Rift. *Tectonophysics*, 80: 1-26.
- Garfunkel, Z., 1981. Internal Structure of the Dead Sea leaky transform (rift) in relation to plate kinematics. In: Freund R., and Garfunkel Z., (Eds.), The Dead Sea Rift. *Tectonophysics*, 80: 81-108.
- Gass, I.G., 1970. The evolution of volcanism in the junction area of the Red Sea, Gulf of Aden and Ethiopian rifts, *Phil. Trans. Soc. Lond.* 267A.

- Gat, J.R., and Carmi, L., 1970. Evolution of the isotopic composition of atmospheric waters in the Mediterranean Sea area. *J. Geophys. Res.*, 75: 3039-3048.
- Gat, J.R., 1971. Comments on the stable isotope method in regional groundwater investigations. *Water Resources Res.*, 7: 980.
- Gat, J.R., and Dansgaard, W., 1972. Stable Isotope Survey of the Fresh Water Occurrences in Israel and The Northern Jordan Rift Valley. *Journal of Hydrology*. 16 pp. 177-212.
- Gat, J.R., 1981. Groundwater. In *stable Isotope Hydrology*. IAEA, Vienna. Tech. Rep. Ser., 210: 223-240.
- Gat, R.J., 1983. Paleoclimates and paleowaters: A collection of Environmental Isotope Studies. International Atomic Energy Agency (IAEA), Vienna.
- Geyh, M.A., 1972. Basic studies in hydrology and ^{14}C and ^3H measurements: Proc. 4th internat. Geolog. Conf., Montreal Sect. 11, pp. 227-234.
- Geyh, M.A., Khoury, J., Rajab, R., Wagner, W., 1985. Environmental Isotope Study in the Hammad region. pp.9
- GTZ: Agrar and Hydrotechnik & GTZ, 1977. National Water Master Plan of Jordan, 8 volume., Essen, Hannover.
- Hatcher R.D., Zeitz I., Regan R.D., and Abu-Ajamieh M., 1981. Sinistral Strike-slip motion on the Dead Sea Rift: Confirmation from new magnetic data. *Geology J.* Vol. 9. No.10.
- Hem, J.D., 1985. Study and Interpretation of the Chemical Characteristics of Natural Water. U.S. Geological Survey, supply paper 2254. Third Edition. pp.263.

- Hijazeen, S., (1980). Etude Hydrodynamique Sur Modele Analogique Electrique de L'aquifere de Sama Sudud (Nord de la Jordanie). Unpublished Ph.D. Thesis. Institute Polytechnique De Lorraine.
- Hirzallah, B., 1973. Groundwater resources of the Jordan valley. Natural Resources Authority (NRA), Amman-Jordan, pp.145
- Holser, W. T., and Kaplan, I.R., 1966. Isotope geochemistry of sedimentary sulfates. Chem. Geol., 1: 93-135 In: Kirkland and Evans R., (Eds.), Marine evaporites: Origin, Diagenesis, and Geochemistry, Dowden, Hutchinson and Ross, Stroudsburg, Pa., 1973, pp. 374-398.
- Holser, W.T., Schidlowski, M., Mackenzie, F.T., and Maynard, J.B., 1988. Geochemical Cycles of Carbon and Sulphur. In: Gregor, C.B., Garrels, R.M., Mackenzie, F.T., and Maynard, J.B., (eds.). Chemical Cycles in the evolution of the earth. John Wiley and Sons, New York.
- Houston, J., 1987. Groundwater Recharge Assessment. Water res. Research. 3, 99-102.
- Hsu, K.J., 1963. Solubility of dolomite and composition of Florida groundwater. J. of Hydrology 1: pp 288-310.
- Ingerson, E., and Pearson, F.Jr., 1964. Estimation of age and rate of motion of groundwater by the ^{14}C method. Recent research in the field of the hydrosphere, atmosphere and nuclear geochemistry, Maruzen, Tokyo, pp. 263-283.
- Jawawdeh J., and Amro H., 1989. Carbon-14 in the atmosphere. Unpublished data. Water Authority of Jordan.
- Jawawdeh J., and Amro H., 1992. ^{226}Ra and ^{222}Rn measurements, Unpublished data,

Water Authority of Jordan.

- Joudeh, O., 1983. Evaluation of the Groundwater Resources in the Deep Aquifer. Internal report, Water Authority of Jordan. Amman-Jordan, pp. 37.
- Joudeh, O., Naim, A., Hashem, I., 1980. Groundwater Resources Along Sweima Area. Internal Report, Jordan Valley Authority, Amman-Jordan, pp.20
- Kally, E., 1991. Water in Peace: Israel Opinion. Institute For Palestinian Studies. Translated to Arabic by Randa Heider, Beirut-Lebanon, p.168.
- Kamondo, W.C., 1988. Possible Uses of Geothermal Fluids in Kenya. Geothermics, Vol.17 No.2/3, pp. 489-501.
- Kattan, Z., 1991. Environmental Isotope Study of the Major Karst Springs in Damascus Limestone Aquifer System: Case of the Figh and Barada Springs. Ankara, IAEA workshop. pp.36
- Kharaka, Y., Hull, R.W., and Carothers, W.W., 1985. Water-rock interaction in sedimentary basin. In: Relation of Organic Matter and Mineral Diagenesis. Society of Economic Paleontologist and Mineralogists Short Course 17. Center for Energy Studies, University of Southwest Louisiana, pp. 79-176.
- Kharaka, Y., and Mariner R.H., 1989. Chemical Geothermometers and Their Application to Formation Waters from Sedimentary Basins. In: Naeser N.D., and McCulloh T.H., (eds.): Thermal history of Sedimentary Basins, Methods and Case Histories. Springer-Verlag, New York.
- Kroitoru, I., Carmi, I., Mazor, E., 1989. Groundwater ^{14}C activity as affected by Initial water-Rock Interaction in the Judean Mountain, Israel. Chemical Geology,

Vol. 79. pp. 259-274.

- Krouse, H.R., 1980. "Sulphur isotopes in our environment", Chapter 11 In: Fritz, P., and Fontes, J-Ch., (eds.). Handbook of Environmental Isotope Geochemistry. Vol. I: 22-44; Amesterdam, Elsevier.
- Langmuir, D., 1971. The geochemistry of some carbonate groundwaters in central Pennsylvania. *Geochim. Cosmochim. Acta*, 35: 1023-1045.
- Levin, M., Gat, J.R., Issar, I., 1979. Precipitation, flood and groundwaters of the Negav highlands: an isotopic study of desert hydrology. Proceeding of an advisory group meeting on arid zone hydrology: Investigation with Isotope Techniques", Vienna 6-9 Nov. 81976, Panel Proceedings series, IAEA, Vienna, 3-22.
- Lloyd, J.W., 1969. The Hydrogeology of the Southern Desert of Jordan, FAO Rep. AGL: SF/Jor9, Tech. Rep. 1 207 pp.
- Lloyd, J.W., 1980. Aspects of environmental isotope chemistry in groundwaters in eastern Jordan. *Arid Zone Hydrology: Investigations with Isotope Techniques*. Proceedings AG-158, International Atomic Energy Agency, Vienna.
- Mandel, S., and Shifan, Z.L., 1981. *Groundwater Resources Investigation and Development*. Academic Press, INC. Ney York, 10003.
- Marinelli, G., 1977. *The Possibility of Developing Geothermal Resources in Jordan*. University of Pisa.
- Matsuhisa, Y., Goldsmith, J.R., Clayton, R.N., Oxygen isotopic fractionation in the system quartz-albite-anorthite-water, *Geochim. Cosmchim. Acta* 43, 1131.
- Mazor, E., and Rosenthal, E., 1967. Notes on the Sulphur in Mineral Waters and

- Rocks of the Lake Tiberias-Dead Sea Rift Valley, Israel. *Israel Journal of Earth-Sciences*, Vol. 16, pp. 198-205.
- Mazor, E., Rosenthal, E., and Ekstein, J., 1969. Geochemical tracing of mineral water sources in the south western Dead Sea Basin, Israel. *Journal of Hydrology*, 7, pp. 246-275.
- Mazor, E., and Kaufman, A., and Carmi, I., 1973. Hammat Gader (Israel): Geochemistry of a mixed thermal spring complex. *J. of Hydrology* 18, 289-303.
- Mazor, E., Levitte, D., Truesdell, A.H., Healy, J., and Nissenbaum, A., 1980. Mixing model and ionic geothermometers applied to warm (up to 60° C) springs: Jordan Rift Valley, Israel. *J. of Hydrology.*, 45: 1-19.
- Mazor, E., 1991. *Applied Chemical and Isotopic Groundwater Hydrology*. Open University Press, By Burns & Smith Ltd, Derby.
- McKenzie, J.A., 1972. A mathematical model for the isotopic balance of sulphur in the ocean. *Geol. Soc. Am., Abstr. Programs*, 4: 197 (abstract).
- Mendenhall, W., and Sincich, T., 1992. *Statistic for engineering and the sciences*. Dellen Pub. Co. Canda 3rd ed.
- McNitt, S.J., 1976. *Geothermal resources in Jordan. Interpretation of the data submitted to the government of Jordan. UNDP report*.
- Meteorological Department, 1988. *Jordan Climatological Data Handbook* Meteorological Department of Jordan, First Edition. Amman-Jordan.
- Michelson, H., 1985. *Geothermal anomaly on the southern Golan Heights and in Northern Transjordan. Tel Aviv, Annual Meeting*.

- Mikbel, Sh., and Attalah, M., 1983. Tectonics of Jordan, contributions to the structures of North Jordan, In: Abed A.M., (ed.). Geology of Jordan, pp. 446-459.
- Mikbel, Sh., 1985. Geological applications of remote sensing in Jordan. 1st national symposium on remote sensing in Iraq, Proceeding, Vol.3.
- Ministry of Water and Irrigation and UN Development Programme, 1992. Water Resources Policies, Planning and Management Project. Groundwater Resources. Jor/87/003, Amman-Jordan.
- Mook, W.G., 1972. "On the reconstruction of the initial ^{14}C content of groundwater from the chemical and isotopic composition", Proc. 8th Int. Conf. on Radiocarbon Dating. Vol.1, Wellington, N.Z.
- Mook, W.G., 1976. The dissolution-Exchange model for dating groundwater with ^{14}C , In: Interpretation of Environmental Isotope and Hydrochemical Data in Groundwater Hydrology, pp. 213-225. IAEA, Vienna.
- Morse, J.W., and Mackenzie, F.T., 1990. Geochemistry of Sedimentary carbonates. Elsevier, New york, NY. pp. 707.
- Moser, H., Stichler, W., and Trimborn, P., 1983. Stable Isotope studies on palaeowater. Palaeoclimates and Palaeowaters: A collection of Environmental Isotope Studies, IAEA, Vienna.
- Muati, M., 1970. Geology of Syria and Lebanon. Syria, Damascus. (In arabic)
- Munnich, K.O., 1957. Messung des ^{14}C -Gehaltes von hartem Grundwasser. Naturwissenschaften 34:32-33
- Munnich, K.O., 1968. Isotopen-Datierung von Grundwasser. Naturwissenschaften

55:158-163

- Myslil, V., 1988. Evaluation of Geothermal Potential of Jordan, report submitted to NRA, Amman-Jordan. pp. 27.
- Naff, T. and Matson, R., (ed.), 1984. Water in the Middle East: Conflict or Cooperation. Westview Press, Boulder, Colorado, U.S.A.
- Nier, A. O., 1950. A determination of the relative abundance of the isotopes of carbon, nitrogen, oxygen, argon and potassium, Phys. rev. 45, 299.
- NJWRIPS, 1989. Yarmouk Basin, Water resources Study. Water Authority of Jordan (WAJ). Amman-Jordan, pp.222.
- Nordstrom, D.H., and Jenne, E.A., 1977. Fluorite solubility equilibria in selected geothermal waters. Geochim. Cosmochim. Acta, 41: 175-188.
- Oeschger, H., Houtermans, J., Loosli, H., and Wahlem, M., 1969. The constancy of radiation from isotope studies in meteorites and on the earth. In: Olsson I.U., (ed.). Radiocarbon variations and Absolute Chronology. pp. 47-486, Wiley Interscience, New York.
- Parker, D.H., 1969. Investigation of the sandstone aquifer of East Jordan. The hydrogeology of the Mesozoic-Cenozoic of the western highland and plateau of East Jordan. United Nations AGL/SF/JOR9, Tech. Rep. 2, pp.278.
- Pearson, F.Jr., 1965. Use of C-13/C-12 ratios to correct radiocarbon ages of material initially diluted by limestone, in Radiocarbon and Tritium Dating. Proceeding of Sixth International Conference on Radiocarbon, pp. 357-366.
- Pearson, F.Jr., Rightmire, C.T., 1980. Sulphur and oxygen isotopes in aqueous

- sulfur compounds. In: Fritz, P., and Fontes, J-Ch (eds.) Handbook of Environmental Isotope Geochemistry. Vol. I: 227-2258; Amesterdam, Elsevier.
- Pearson, F.Jr., Bedinger M.S., and Jones, B.F., 1972. Carbon-14 ages of water from the Arkansas Hot Springs, in Proceeding of Eighth International Conference on Radiocarbon Dating, Vol. 1 pp. 330-341, Royal Society of New Zealand, Wellington.
- Pearson, F.Jr., and Hanshaw, B.B., 1970. Sources of dissolved carbonate species in groundwater and their effects on carbon-14 dating, in Isotope Hydrology. pp.271-285. IAEA, Vienna.
- Phoenix Corporation, 1980. A comprehensive Airborne Magnetic/Radiation Survey of the Hashemite Kingdom of Jordan. Phoenix Corporation.
- Plummer, L.N., Bubsy, J.F., Roger, W.L., and Hanshaw, 1990. Geochemical Modeling of the Madison Aquifer in Parts of Montana, Wyoming and South Dakota. Water Resources Research, Vol.26, No.9, pp.1981-2014.
- PRIDE, 1992. A water Management Study for Jordan. Report submitted to USAID/Jordan and Government of Jordan. Amman-Jordan, pp.218.
- Quennell, A. M., 1959. Handbook of the Geology of Jordan. Amman pp.82.
- Quennell, A. M., 1983. Evolution of the Dead Sea Rift - A review. Geology of Jordan, Proceeding of the first Jordanian Geological Conference, Jordan Geologist Association, Amman-Jordan, 460-482.
- Qura'an A., 1991. The gravitational studies of North Western Part of Jordan. M.Sc. Thesis, University of Jordan, Amman-Jordan.

- Rashdan, J., and Al-Momani, M., 1990. The effect of Irbed Sewage on the Groundwater in wadi Al-Arab area. Water Authority. Amman-Jordan.
- Reardon, E. J., and Fritz, P., 1978. Computer modelling of groundwater ^{13}C and ^{14}C isotope compositions. *J. Hydrol.* 36:201-224.
- Rimawi, O., 1985. Hydrochemistry and Isotope Hydrology of the Groundwater and Surface Water in North Jordan (North-Northeast of Mafraq, Dhuleil-Hallabat, Azraq-Basin). University of Munich. Ph.D. Thesis. pp.240.
- Rimawi, O., and Salameh, E., 1988. Hydrochemistry and Groundwater System of the Zarqa Ma'in-Zara Thermal Field, Jordan. *J. of hydrol.*, 98 pp. 147-163.
- Robert, P., 1980. The optical evolution of kerogen and geothermal histories applied to oil gas exploration, In: Durand, B., (ed.). kerogen-Insoluble Organic Matter from Sedimentary Rocks Editions Technip, Paris, pp.113-142.
- Rozanski, K., 1985. Deuterium and Oxygen-18 in European Groundwaters - Links to Atmospheric Circulation. *Chemical geology*, 52, 349-363.
- Sa'ad, A., 1986. Rainfall intensity duration-frequency in Jordan. Professional Paper No.3, WAJ, Amman-Jordan.
- Salameh, E., and Rimawi, O., 1984. Isotopic analyses and hydrochemistry of the thermal springs along the eastern side of the Jordan Dead Sea-Wadi Aqaba Rift Valley. *J. of Hydrol.*, 73.
- Salameh, E., 1992. Jordan's Water resources and the Future Potentials. Proceedings of the Symposium 27th and 28th October 1991. Organized by Friedrich Ebert Stiftung, Higher Council for Science and Technology, Water Research and Study

- Canter and University of Jordan. Amman-Jordan. pp.122.
- Salem, H.S., 1984. Hydrology and Hydrogeology of the area north of Zarqa River/Jordan. Unpublished M.Sc. Thesis. University of Jordan, Amman-Jordan.
- Saqqar, M., Matar, A., and Bajjali, W., 1989. Performance Evaluation of Wastewater Treatment Plants in Jordan and their Effect in Groundwater. Internal Report. WAJ, Amman-Jordan.
- Saqqar, M., 1992. Existing Situation for wastewater Treatment Plant in Jordan. Internal Report, Water Authority, Amman-Jordan.
- Sheppard, S.M.F., 1986. Characterization and Isotopic Variations in Natural Waters. In: Valley, J.W., Taylor, Jr., H.P., and O'Neil, J.R. (eds.). Stable Isotopes in High Temperature Geological Processes. Review in Mineralogy, Volume 16.
- Solmineq88: By Kharaka, Y., Gunter, W., Agarwal, P., Perkins, E., and DeBraal, J., 1989. A Computer Programm for Geochemical Modelling of Water-Rock Interactions. USGS, pp. 420.
- Sonntag, C., Klitzsch, E., Lohnert, E.P., El-Shazly, E.M., Munnich, K.O., Junghans, Ch., Thorweihe, U., Wesroffer, K., Swailem, F.M., 1979. Paleoclimatic information from deuterium and oxygen-18 in carbon-14 dated north saharian groundwaters: Groundwater formation in the past" Isotope Hydrology 1987 (Proc. Symp. Neuherberg, 1978) Vol.2, IAEA, Vienna, pp. 569-581.
- Sonntag, C., Thorweihe, U., Rudolf, J., Lohnert, E.P., Junghans, C., Munnich, K.O., Klitzch, E., El-Shazly, E.M., Swailem, F.M., 1980. Paleoclimatic evidence in apparent ^{14}C ages of Saharian groundwaters. Radiocarbon 22 (3):871-878.

- Strainsky, A., Katz, A., and Levitte, D., 1979. Temperature-composition-depth relationship in Rift Valley hot spring: Hammat Gader, northern Israel. *Chem. Geol.*, 27: 233-244.
- Stumm, W., and Morgan, J.J., 1970. *Aquatic Chemistry*: New York, Wiley Interscience, pp.788.
- Sunna' B., 1992. Geothermal Energy Project, Historical Account. Internal report, NRA Amman-Jordan, pp.11.
- Tamers, M.A., and Scharpenseel, H.W., 1970. Sequential sampling of radiocarbon in groundwater, in *Isotope Hydrology*, IAEA, Vienna, pp 241-256.
- Tamers, M.A., 1975. Validity of radiocarbon dates on groundwater. *Geophys. Surv. Vol.2* pp. 217-239
- Truesdell, A.H., 1979. Report on the chemistry and geothermal energy possibilities of the Zarqa Ma'in - Zara hot springs, USGS, Menlo Park California USA, pp.28.
- Truesdell, A.H., and Hulston, J.R., 1980. Isotopic evidence on environments of geothermal system. In: Fritz P., and Fontes, J-Ch., (Eds.). *Handbook of environmental isotope geochemistry, The terrestrial environment*, Elsevier Press.
- Urey, H., Brickwedde, I.G., and Murphy, G.M., 1932. A hydrogen isotope of mass 2 and its concentration. *Phys. Rev.*, 39: 1-15.
- Vogel, J.C., 1967. Investigation of groundwater flow with radiocarbon. *Isotope in Hydrology (proc. Sympos. Vienna, 1966)* IAEA, Vienna.
- Vogel, J.C., 1970. "Carbon-14 dating of groundwater" *Isotope Hydrology, Proc. Symp. Vienna, IAEA*.

- Vinegra, O.F., 1971. Age and evolution of salt basins of southeastern Mexico. *Am. Assoc. Pet. Geol., Bull.*, 55: 478-494.
- Wassenaar, L.I., Aravena, R., and Fritz, P., 1991. Radiocarbon content of dissolved organic and inorganic carbon in shallow groundwater systems: Implications for groundwater dating. *Isotope Techniques in Water resources Development*. IAEA, Vienna, 143-151.
- Water Authority of Jordan (WAJ), Annual Report 1991. Amman-Jordan.
- Water Authority of Jordan (WAJ-Files), Amman-Jordan, pp 88 (in arabic).
- Whelan, J.K., Carolyn, L., and Thompson-Rizer, 1993. Chemical Methods for Assessing Kerogen and Protokerogen Types and maturity. In: Engel, M.H., and Macko S.A. (eds.): *Organic Geochemistry, Principles and Applications*. Plenum Press, New York and London, 289-353.
- White, D.E., 1965. Saline waters of sedimentary rocks. In Young, A., and Galley, G.E., (eds.): *Fluids in Subsurface Environments*. American Association of Petroleum Geologists Memoir 4, pp. 342-366.
- White, D.E., 1970. Geochemistry applied to the discovery, evaluation, and exploitation of geothermal energy resources, *Geothermics*, 2, 1, 58-80.
- Wieseman, G., and Abdullatif, A.A., 1963. *Geology of the Yarmouk Area, North -Jordan*. German Geological Mission in Jordan, Amman-Jordan.
- Wieseman, G., and Abdullatif, A.A., 1991. Geological history of the Yarmouk River In: Goethe-Institute (ed.): *Geology of Jordan, Amman, Jordan*, pp.2.
- Williams, H.H., Sabbah, A., Faraj B., Ramini, H., 1990. *The Regional Petroleum*

- Geochemistry of Jordan. Petro-Canada and NRA, Amman-Jordan.
- Wilkinson, A.F., 1992. The hydrogeology of Jordan, with special reference to the North-Eastern 'Panhandle', M.Sc. Thesis. University of Permtingham, England.
- Winogard, I., and Farlekas, G.M., 1974. Problems in ^{14}C dating of groundwater from aquifers of deltaic origin in isotope techniques in groundwater hydrology: IAEA, Symp. SM-182/31, V.11 pp 69-76.
- Wishah, A., 1979. An Assessment of groundwater resources in Mughayer Jaber - Mughayer Sirhan - Um Essurab Area. NRA, Amman-Jordan, pp. 72.
- Wolf, A., 1993. The Jordan WaterShed: Past Attempts at Cooperation and Lessons for the future. Water International, Vol. 218 No.1 pp. 5-17.
- Yechieli, Y., Magaritz, M., Levy, Y., Weber, U., Kafri, U., Woelfli, W., and Bonani., 1993. Late Quaternary Geological History of the Dead Sea Area, Israel. Quaternary Research 39, 59-67.
- Yokoyama, Y., Reyss, J. L., Guichard, F., 1977. Production of radionuclides by cosmic rays at mountain altitudes, Earth Planet. Sci., Lett., 36, 44-50.
- Yurtsever, Y. and Gat, J.R. 1981. Atmospheric Waters. Stable Isotopes Hydrology, Deuterium and Oxygen-18 in the water cycle. Technical Reports Series No. 210. IAEA, Vienna.

Appendix A The residence time of the groundwater based on uncorrected and on various corrected models described in section II-V.

MODEL INPUT PARAMETERS		AGE CALCULATIONS IN YEARS BEFORE PRESENT															
MAP NO.	LOCATION	TRITIUM (TU)	RECHARGE SOIL PH PCO2	SOIL C-14	DIC C-14	SOIL C-13	ROCK C-13	DIC C-13	OPEN UNCOR.	CLOSED SYSTEMS		MIXED SYSTEMS		OPEN FONTES GARNIER	SYSTEM TAINERS		
										CARBONATE BY Ca	PEARSON	CALCITE LOSS	CHEMISTRY AND C-13			CARBONATE BY ALK	
Thermal Water																	
10	JRV1	0.4	0.037	6.99	100	22.9	-22	0	-9.4	12185	9712	5112	1560	7842	15152	3910	7626
10	JRV1	1.5	0.037	6.99	100	5.4	-22	0	-9.4	24190	23671	17117	7868	19847	26920	442	19630
9	Maqia	-	0.028	6.93	100	16.6	-22	0	-9.6	14855	11500	8017	5963	10649	14586	6810	10295
11	Mukhebeh 1	1.7	0.023	7.21	100	16.9	-22	0	-12.9	14717	11822	10278	11678	13308	16397	11274	10155
12	Mukhebeh 2	-	0.019	7.16	100	18.0	-22	0	-11.6	14176	10597	8906	9947	11876	13720	9383	9615
14	Mukhebeh 4	-	0.015	6.30	100	17.3	-22	0	-11.6	14504	4360	9198	8362	10509	1960	9831	9945
15	Mukhebeh 5	0.0	0.088	7.07	100	3.6	-22	0	-12.8	27480	26245	23029	22618	25879	36846	23887	22917
16	Mukhebeh 6	0.0	0.025	6.50	100	16.6	-22	0	-12.0	14865	8342	9861	10796	11619	7820	10506	10305
17	Mukhebeh 7	0.0	0.025	6.99	100	16.1	-22	0	-12.5	15118	11760	10458	11540	13189	15322	11324	10560
18	North Shuneh	0.0	0.093	6.75	100	8.0	-22	0	-10.2	20879	19138	14509	13340	16806	26896	13775	16318
19	S-90	-	0.102	6.66	100	4.7	-22	0	-9.5	25241	23545	18264	4201	20375	37216	22679	20695
24	Manshieh	0.8	0.317	6.30	100	3.8	-22	0	-	27143	25119	-	-	-	32166	-	22575
23	Sahasi 6	-	0.015	6.30	100	21.7	-22	0	-9.0	12630	3618	5232	2733	6543	1715	4184	8075
23	Mahasi 6	0.5	0.010	6.20	100	3.0	-22	0	-10.3	28878	16747	22580	20046	23678	13271	22196	24322
Non-Thermal Water																	
3	Buaimah 1	6.6	0.011	7.33	100	59.6	-22	0	-10.9	4278	885	-1527	956	1628	4949	-966	-277
4	Hama Farhan	9.2	0.012	7.14	100	63.1	-22	0	-11.3	3806	434	-1738	567	1427	4556	-999	-751
36	Jdeita	6.9	0.024	7.13	100	73.4	-22	0	-13.3	2556	-647	-1635	1468	1297	3651	-267	-2004
31	Wadi Arab 1	-	0.043	6.98	100	11.6	-22	0	-13.1	17829	15151	13544	13727	16258	19944	14439	13266
32	Wadi Arab 2	-	0.033	7.06	100	11.0	-22	0	-13.5	18269	15418	14220	15111	17056	19752	15236	13707
33	Wadi Arab 3	0.6	0.049	6.92	100	16.7	-22	0	-10.5	14795	12061	8665	10056	11280	17006	8513	10232
34	Wadi Arab 4	0.2	0.054	6.88	100	11.9	-22	0	-9.6	17597	14971	10698	10721	13243	19993	9679	13034
35	Wadi Arab 5	0.6	0.034	7.04	100	35.3	-22	0	-13.0	8608	5701	4265	5959	7072	10307	5349	4046
38	Walid Khazar	0.0	0.020	7.05	100	11.7	-22	0	-12.9	17737	13021	13305	14770	16126	14397	14300	13174
41	Ali samara	0.0	0.060	6.83	100	6.4	-22	0	-	22724	20005	-	-	-	24889	-	18161
42	Kamel Taba	1.6	0.087	7.06	100	1.2	-22	0	-11.5	36562	35357	31171	30578	34007	46145	31422	32000
43	H.Haji	0.7	0.024	7.15	100	9.8	-22	0	-11.8	19202	16420	14052	12909	17010	21405	14711	14543
44	M.samara	0.7	0.059	7.11	100	2.1	-22	0	-13.6	32015	30423	28033	25078	30939	39141	29176	27453
51	Taleb Masri	0.0	0.014	7.35	100	3.3	-22	0	-9.1	28250	25335	20952	21445	24126	29315	19170	23691

Appendix 1 Isotope data and deuterium excess of precipitation

Name	Date	Tritium ±1 T.U	O-18 ± 0.15 o/oo	Deuterium ± 1 o/oo	A.R mm	d o/oo
Ras Munif	Oct-87	8.6	-3.7	-11.2	15.3	18.4
Ras Munif	Nov-87	-	-5.9	-15.9	18.8	31.3
Ras Munif	Dec-87	7.2	-8.1	-36.4	184.1	28.3
Ras Munif	Jan-88	9.5	-9.1	-45.3	163.7	27.4
Ras Munif	Feb-88	9.1	-8.0	-40.3	187.8	24.0
Ras Munif	Mar-88	8.3	-5.3	-21.4	108.1	21.2
Ras Munif	Apr-88	12.9	-5.7	-27.6	21.7	17.6
Ras Munif	Nov-88	7.0	-6.9	-33.3	44.2	21.7
Ras Munif	Dec-88	6.7	-6.9	-28.8	195.6	26.1
Ras Munif	Jan-89	6.9	-7.2	-32.0	53.4	25.3
Ras Munif	Jun-89		-4.2	-22.3	52.4	11.5
Ras Munif	Feb-89	10.7	-5.7	-15.7	53.3	30.0
Ras Munif	Mar-89	16.0	-7.4	-41.1	88.8	17.9
Ras Munif	Oct-89		-4.9	-15.5	13.9	23.5
Ras Munif	Nov-89	5.8	-6.9	-32.4	80.0	22.6
Ras Munif	Dec-89	4.4	-7.6	-39.9	81.3	21.1
Ras Munif	Jan-90	4.7	-7.6	-36.5	149.1	24.2
Ras Munif	Feb-90	6.5	-6.4	-29.6	73.9	21.7
Ras Munif	Mar-90	8.1	-6.4	-27.7	107.7	23.7
Ras Munif	Apr-90	13.3	-7.2	-39.4	27.9	17.8
Ras Munif	Oct-90	4.3	-4.8	-15.3	6.6	23.4
Ras Munif	Dec-90	4.9	-4.1	-4.0	28.8	29.0
Ras Munif	Jan-91	4.7	-7.9	-38.9	169.5	24.5
Ras Munif	Feb-91	4.9	-6.4	-22.3	82.0	29.0
Ras Munif	Mar-91	6.2	-8.0	-40.8	133.6	23.1
Ras Munif	Apr-91	6.1	-5.7	-26.9	39.1	19.0
Irbed	Oct-87		-5.2	-36.8	15.6	4.8
Irbed	Nov-87	6.8	-5.9	-16.3	8.4	31.0
Irbed	Dec-87	5.3	-7.9	-37.9	126.6	25.2
Irbed	Jan-88	8.1	-7.8	-36.4	120.0	25.7
Irbed	Feb-88	8.5	-8.7	-43.0	147.3	26.4
Irbed	Mar-88	9.9	-4.3	-13.4	115.2	21.1
Irbed	Apr-88	21.7	-4.3	-17.9	16.7	16.6
Irbed	Oct-88		-4.2	-11.1	6.4	22.5
Irbed	Nov-88	8.1	-7.6	-36.8	35.1	23.9
Irbed	Dec-88	6.4	-5.9	-20.9	106.5	26.1
Irbed	Jun-89	11.9	-2.1	-13.9	48.2	3.2
Irbed	Jan-89	7.7	-6.3	-25.4	30.3	25.0
Irbed	Feb-89	8.8	-5.1	-13.3	46.9	27.6
Irbed	Mar-89	11.1	-6.5	-33.8	54.0	18.4
Irbed	Oct-89		-4.9	-18.1	2.5	20.9
Irbed	Nov-89	5.6	-6.5	-33.3	45.0	19.0
Irbed	Dec-89	5.5	-5.9	-29.0	50.3	18.3

Irbed	Jan-90	6.4	-7.5	-41.2	152.0	18.6
Irbed	Feb-90	6.9	-6.6	-34.5	67.5	18.5
Irbed	Mar-90	7.9	-4.9	-18.6	97.7	20.8
Irbed	Apr-90	10.4	-8.3	-44.6	29.7	22.0
Irbed	Oct-90		0.5	17.0	4.2	12.9
Irbed	Nov-90	3.8	-5.4	-12.0	22.9	31.1
Irbed	Dec-90	4.7	-3.8	-2.6	30.3	28.1
Irbed	Jan-91	4.9	-7.2	-34.8	165.7	23.0
Irbed	Feb-91	6.3	-7.3	-36.0	48.4	22.2
Irbed	Mar-91	7.9	-3.1	-10.8	116.5	14.1
Irbed	Apr-91	6.9	-5.2	-19.8	43.6	21.9
Der Alla	Dec-87	8.9	-4.8	-19.1	82.5	19.4
Der Alla	Jan-88	12.6	-6.0	-26.8	63.9	21.6
Der Alla	Feb-88	9.0	-6.2	-27.8	130.4	21.8
Der Alla	Mar-88	15.8	0.4	15.2	24.7	12.3
Der Alla	Oct-88		-0.2	8.7	2.0	10.3
Der Alla	Nov-88	7.1	-4.6	-21.9	21.3	15.2
Der Alla	Dec-88	8.7	-3.0	-8.3	45.0	15.8
Der Alla	Jan-89	11.5	-3.1	-7.5	44.0	17.0
Der Alla	Feb-89	11.7	-1.5	5.1	37.3	17.1
Der Alla	Oct-89		-1.1	6.0	9.1	15.0
Der Alla	Nov-89	6.0	-3.3	-8.2	64.4	18.2
Der Alla	Dec-89	5.0	-3.3	-8.5	62.6	18.0
Der Alla	Jan-90	6.7	-4.9	-28.3	79.2	11.1
Der Alla	Feb-90	6.8	-2.0	-0.6	31.9	15.2
Der Alla	Mar-90	13.4	-3.3	-13.3	45.1	12.9
Der Alla	Jan-91	5.4	-3.8	-15.9	93.0	14.5
Der Alla	Feb-91	7.2	-5.2	-29.7	121.3	11.8
Der Alla	Mar-91	7.9	-8.6	-53.7	113.2	15.4
Der Alla	Apr-91	8.7	-1.2	-0.5	10.0	8.8

A.R = Amount of Rain

d = Deuterium Excess

Appendix 2 General Hydrogeological Informations about Wells in the Study Area

Recharge Area							
NAME	D.D	N	E	Elev.	Depth	Aquifer	Yield
				m	m		
1 Rafad Farhan		202.850	237.200		302	B2/A7	44
2 Nuaimeh Well 2		203.350	236.128	705	337	B2/A7	
3 Nuaimeh Well 1	1980	203.575	235.495	717	196	B2/A7	59
4 Hamad Farhan	1976	206.178	237.883	646	334	B2/A7	20
5 Yarmouk University 2	1983	206.000	237.240	668	280	B2/A7	25
6 Yamoon Well	1974	200.679	235.884	783	267	B2/A7	22
7 Kitm Wel	1980	207.519	233.399	695	350	B2/A7	30
Side Wadies							
NAME	D.D	N	E	Elev.	Depth	Aquifer	Yield
				m	m		
25 Kufor Ubeh		215.550	224.300	475	287	A7	41
26 Kufr Assad		225.750	217.025	100	263	B2/A7	81
27 Deir Yusef 3	1987	209.800	227.120	651	320	A7	10
28 Juhfieh 1		210.650	226.800	628	300	A7	92
29 Abu said 2		213.000	215.600	180	284	B2/A7	176
30 Abu said 1	1983	212.600	216.300	200	226	B2/A7	176
36 Jdeita well		201.900	214.350	315	411	B2/A7	100
Wadi Araba							
NAME	D.D	N	E	Elev.	Depth	Aquifer	Yield
				m	m		
35 Wadi Arab 5	1983	222.550	212.850	50	375	B2	414
34 Wadi Arab 4	1982	226.500	213.300	27	750	B2/A7	702
33 Wadi Arab 3	1982	225.600	212.650	-20	257	B2	1486
32 Wadi Arab 2	1982	225.150	212.150	-26	407	B2/A7	1571
31 Wadi Arab 1	1982	224.188	211.947	11	703	B2/A7	640
37 R. Elhazaimh		221.375	220.245	357	341	B2/A7	55
38 Walid Khazar	1982	218.900	212.095	70	195	B2	46
39 Moh. Abdelwali	1982	216.900	212.800	250	341	B2	52
Adasyia Area							
NAME	D.D	N	E	Elev.	Depth	Aquifer	Yield
				m	m		
64 Adasyia 4		208.180	230.500	-209	80	Alluvium	162
65 Adasyia 5		207.720	229.900	-213	82	Alluvium	122
66 Adasyia 6		207.150	230.020	-215	80	Alluvium	151
69 Adasyia 8		207.550	228.860	-207	80	Alluvium	163
70 Adasyia 1B		207.560	230.900	-210	350	Alluvium	170
Adasyia Sp		230.000	207.900	-210			
Rimtha Area							
NAME	D.D	N	E	Elev.	Depth	Aquifer	Yield
				m	m		
40 Rahub Spring		223.600	237.600	450	0		36
Quelbeh		231.200	231.600	420			37

24	S-90	1968	211.326	248.790	566	2190	B2/A7,K,Z	
41	Ali Samara	1982	212.968	247.734	545	390	B2/A7	45
42	Kamel Tabah 2		211.620	249.820			B2/A7	
43	M.A.HAJI	1983	218.866	242.092	534	490	B2/A7	50
44	Muhamad Samara		214.609	241.644	541	480	B2/A7	65
23	Mahasi No. 6	1988	221.580	243.750	481	702	B2/A7	100
45	Ahmad Fares	1971	224.115	242.723	462	70	B4	30
46	Mahasi No. 4	1978	221.449	243.587	475	70	B4	19
47	Nahlawi Well	1983	228.950	244.070	438	300	B4	40
48	Kur Well	1983	229.585	243.669	435	250	B4	32
49	Mahasi No. 1	1971	221.258	243.742	482	85	B4	61

North Desert

NAME	D.D	N	E	Elev. m	Depth m	Aquifer	Yield m3/h	
50	Yusef Hmeidi	1983	203.059	253.219	691	405	A4	55
51	Taleb Masri	1982	212.150	261.960	582	213	B2/A7	82
52	Swelmeh Well	1983	211.765	258.860	631	385	B2/A7	59
53	Oraem Saket	1969	207.185	265.335	601	268	B2/A7	40
54	Qasem awjan	1980	208.335	261.040	610	225	A7	45
55	Muhamad S. Jalad	1981	202.170	274.725	678	293	B2/A7	52
56	M. Bechtian	1981	202.530	275.600	682	268	B2/A7	40
57	Ali Khashman	1980	206.675	273.900	657	323	B2/A7	40
58	Mohamad Arjani	1988	214.480	258.070	623	458	B2/A7	82
59	Muhamad Jahmani	1981	208.890	258.895	642	328	A7	43
60	Ali Ajian	1970	207.950	265.160	599	160	A7	73
61	Abdelhamid Zad 2	1979	205.365	272.120	653	310	B2/A7	5
62	Mousa Samara	1982	213.870	258.590	642	250	B2/A7	80

Mukhebeh Area

NAME	D.D	N	E	Elev. m	Depth m	Aquifer	Yield m3/h	
8	Balsam Spr.		234.500	214.500	-50		1969	
9	Maqla Spr.		234.500	214.500	-50		1969	
10	JRV1	1981	234.500	214.700	-70	1230	B2-A2	157
11	Mukhebeh 1	1982	235.000	216.000	-80	350	B2/A7	6000
12	Mukhebeh 2	1982	235.100	215.950	-110	488	B2	800
13	Mukhebeh 3	1983	235.020	216.000	-80	333	B2	2822
14	Mukhebeh 4	1983	235.100	215.980	-110	892	B2/A4	2200
15	Mukhebeh 5	1983	231.500	210.500	-118	900	B2/A7	200
16	Mukhebeh 6	1983	235.150	215.750	-95	475	B2	2000
17	Mukhebeh 7	1983	235.900	216.950	-115	500	B2	2100

JRV

NAME	D.D	N	E	Elev. m	Depth m	Aquifer	Yield m3/h	
18	North Shuneh	1981	224.360	208.141	-178	967	B2/A7	900
19	Manshieh	1989	220.700	207.700	-175	1150	B2/A7	200
21	Abu Ziad	1989	212.200	208.600	-120	1126	B2/A7	90
22	Waqas		216.200	209.160	-90	1300	B2/A7	60

D.D : Date Of Drilling

Elev : Elevation

Appendix 3 Chemical and Isotope Data for the area

NO.	DATE	O 18 ± 0.2	D ± 1.3	T.U ± 1	C-14 pmc	C-13 o/oo	EC	TDS ppm	pH	Ca meq/l	Mg meq/l	Na meq/l	K meq/l	Cl meq/l	SO4 meq/l	HCO3 meq/l	NO3 ppm	SiO2 ppm	Recharge Area	
																			EC	TDS
1	19-Jul-89	-6.4	-31.8	7.0			630	403	7.7	3.6	2.1	0.8	0.1	1.2	0.2	4.6	33.6			
2	09-Aug-88	-5.8	-32.3	10.5			610	390	7.3	3.3	1.8	0.9	0.1	1.0	0.3	4.2	36.0			
2	19-Jul-89	-6.4	-32.1	7.8			610	390	8.0	3.3	2.0	0.8	0.1	1.1	0.1	4.6	35.6			
2	11-Feb-91	-6.3	-29.7	6.4			630	403	7.3	3.5	2.0	1.0	0.1	1.2	0.2	4.5	47.8			
2	20-Oct-92	-6.2	-30.0	5.2			610	390	7.4	3.3	1.9	0.9	0.0	1.1	0.1	4.3	33.2			
2	30-Dec-92	-6.4	-30.4	7.0			690	435	7.4	4.0	2.2	1.0	0.1	1.4	0.3	4.6	52.0			
3	11-Jan-87	-5.5		6.2			560	358	7.3	3.3	1.5	0.8	0.1	1.0	0.0	4.4	20.2			
3	10-Mar-87	-5.5		6.0			540	346	7.3	3.2	1.5			0.9	0.2	4.4	20.9			
3	13-Feb-88	-7.0	-29.9	6.6	59.6 ± 0.7	-10.9	550	352	7.4	3.1	1.7	0.8	0.1	0.9	0.1	4.3	20.1			
3	09-Aug-88	-5.4	-32.5	8.4			540	346	7.4	3.0	1.6	0.6	0.1	0.9	0.1	3.9	23.0			
3	03-May-89	-5.9	-31.5	7.0			530	339	7.5	3.1	2.0			1.0	0.0	4.3	20.2			
3	22-May-89	-5.9	-30.8	5.5			540	346	7.5	3.0	1.4			0.9	0.9	4.1	20.1			
3	19-Jul-89	-6.1	-30.8	6.9			540	346	7.5	3.3	1.6	0.8	0.1	0.9	0.0	4.4	20.1			
3	02-Oct-89	-5.7	-31.2	5.3			560	353	7.5	3.3	1.5	0.8	0.1	0.9	0.3	4.2	20.0			
3	11-Feb-91	-6.0	-28.2	5.2			550	352	7.4	3.2	1.7	0.8	0.0	0.9	0.0	4.4	19.6			
3	30-Dec-92	-6.0	-29.3	4.5			560	353	7.5	3.1	2.0	0.9	0.0	1.1	0.1	4.2	24.7			
4	13-Feb-88	-7.2	-29.2	9.2	63.1 ± 0.7	-11.3	590	378	7.3	3.4	2.0	0.7	0.0	1.0	0.0	4.7	24.5			
4	09-Aug-88	-5.6	-32.7	10.1			570	365	7.4	3.2	1.7	0.7	0.1	0.9	0.1	4.3	23.2			
4	17-Jul-91	-6.3	-29.9	6.0			620	397	7.2	3.6	1.8	0.8	0.1	1.0	0.0	4.8	27.3			
4	20-Oct-92	-6.2	-30.4	7.2			600	378	7.5	3.5	1.7	0.8	0.0	1.0	0.0	4.6	24.3			
4	30-Dec-92	-6.2	-29.0	2.3			620	391	7.6	3.5	1.8	0.9	0.0	1.0	0.4	4.5	25.3			
5	11-Feb-91	-5.9	-28.5	7.1			620	397	7.4	3.7	1.8	0.9	0.0	1.1	0.3	4.7	27.5			

Side Wadies Wells

NO.	DATE	O 18 o/oo	D o/oo	T.U	C-14 pmc	C-13 o/oo	EC	TDS ppm	pH	Ca meq/l	Mg meq/l	Na meq/l	K meq/l	Cl meq/l	SO4 meq/l	HCO3 meq/l	NO3 ppm	SiO2 ppm	
																			25
25	19-Jul-89	-5.7	-25.5	4.1			490	314	7.8	2.9	1.8	0.6	0.1	0.7	0.3	4.0	22.8		
25	08-Apr-91	-5.6	-18.5	4.0			520	333	7.6	3.0	1.6	0.5	0.0	0.7	0.1	4.1	22.0		
26	16-Sep-92	-4.3	-19.0	6.3			1290	826	6.9	9.5	2.1	2.6	0.1	3.1	3.6	6.7	50.1		
26	23-May-91	-4.6	-20.0	4.2			1380	883	7.0	9.6	2.4	2.8	0.1	3.3	4.0	6.9	56.4		
27	06-Apr-88	-6.4	-28.8	9.9			430	275	7.8	2.9	1.1	0.4	0.1	0.4	0.1	3.7	26.8		
28	22-May-89	-6.1	-28.5	6.0			540	346	7.6	3.3	1.0			0.8	0.9	4.2	26.4		

28	19-Jul-89	-6.4	-28.8	6.1		540	346	7.6	3.5	1.8	0.6	0.1	0.7	0.3	4.5	26.2
28	02-Oct-89	-6.0	-29.8	5.1		550	352	7.5	3.5	1.7	0.5	0.1	0.7	0.7	4.5	26.0
28	13-May-90	-6.0	-28.0	6.4		560	353	7.6	3.6	1.6	0.6	0.1	0.8	0.1	4.5	27.7
28	08-Apr-91	-6.4	-20.9	2.9		600	384	7.6	3.7	1.6	0.6	0.1	0.8	0.0	4.6	28.6
29	14-Jan-87	-5.7		3.5		800	512	8.2	6.1	2.0	1.0	0.2	1.0	0.7	7.4	4.8
29	07-Aug-88	-5.3	-30.1	4.6		820	525	6.9	6.1	1.9	0.8	0.1	1.1	0.8	6.9	6.6
29	08-Apr-91	-5.6	-24.1	4.1		840	538	7.2	5.8	2.1	0.7	0.1	1.0	0.6	7.0	13.6
29	20-Oct-92	-5.6	-24.7	4.2		870	557	7.0	6.5	2.0	0.8	0.0	1.2	0.8	7.1	10.3
30	21-Mar-87	-5.9		5.5		850	544	7.0	6.1	2.3			1.0	0.7	6.9	12.8
30	17-Feb-88	-6.6	-26.2	4.6		840	538	6.8	6.2	2.4	1.0	0.1	1.1	0.9	7.3	17.5
30	07-Aug-88	-5.5	-29.7	0.4		820	525	6.9	5.4	2.4	1.0	0.1	1.1	0.7	6.8	17.0
30	08-Apr-91	-6.0	-27.3	4.1		820	525	7.3	4.9	2.6	0.9	0.1	1.0	0.4	6.8	20.7
30	20-Oct-92	-6.0	-26.3	3.7		1020	653	6.9	7.6	2.4	1.0	0.1	1.5	1.8	7.6	18.3
31	11-Jan-87	-4.9		0.0		880	563	7.0	5.5	3.2	1.0	0.1	1.1	1.6	7.2	0.8
31	10-Mar-87	-4.8		0.0		910	582	7.2	5.8	3.3			1.1	1.4	7.7	3.1
31	15-Feb-88	-5.7	-23.6	0.0		880	563	7.1	5.3	3.3	1.1	0.1	1.1	1.6	6.9	0.8
31	07-Aug-88	-4.7	-25.2	1.7		900	576	7.0	5.5	3.2	0.9	0.1	1.1	1.4	7.1	0.5
31	13-May-90	-5.5	-21.3	0.6		900	567	7.1	5.4	3.3	0.9	0.0	1.1	1.6	7.0	0.5
31	22-May-91	-5.1	-22.9	0.0		890	561	7.5	5.6	3.0	1.0	0.0	1.1	1.5	7.0	0.4
31	16-Sep-92	-5.5	-23.6	-		860	550	7.1	5.5	3.0	1.0	0.1	1.1	1.3	7.0	0.4
31	15-Oct-92	-5.4	-23.3	-	11.6 ± 0.8 -13.1	860	550	7.0	5.1	3.3	0.9	0.0	1.0	1.4	7.0	0.5
32	11-Jan-87	-4.7		0.0		870	556	7.0	5.6	3.0	1.0	0.1	1.1	1.6	7.2	1.2
32	10-Mar-87	-4.6		2.4		850	544	6.9	5.5	2.8			1.0	1.3	7.4	0.6
32	15-Feb-88	-5.6	-24.2	0.2		850	544	7.1	5.3	2.9	1.1	0.1	1.0	1.2	7.1	1.1
32	13-May-90	-5.2	-22.8	0.0		850	536	7.1	5.5	3.0	0.9	0.1	1.1	1.4	6.9	0.7
32	16-Sep-92	-5.5	-21.8	-		840	538	7.1	5.3	3.1	0.9	0.1	1.1	1.3	6.9	0.8
32	17-Oct-92	-5.4	-22.1	-	11.0 ± 0.9 -13.5	850	544	7.1	5.4	2.8	0.9	0.1	1.1	1.5	6.7	0.7
33	15-Feb-88	-5.6	-22.6	0.6	16.7 ± 0.6 -10.5	840	538	7.2	5.4	2.8	1.0	0.1	1.0	1.1	7.0	1.2
33	07-Aug-88	-4.6	-25.1	0.8		860	550	7.0	5.5	2.8	1.1	0.0	1.1	1.3	6.9	0.8
33	13-May-90	-5.3	-22.6	0.2		840	529	7.2	5.3	3.0	0.8	0.1	1.0	1.4	6.7	1.0
33	23-May-91	-5.3	-22.8	0.0		830	531	7.4	5.6	2.6	0.9	0.1	1.0	1.5	6.7	0.7
33	01-Aug-91	-5.2	-22.7	-		820	517	7.0	5.4	2.7	0.9	0.1	1.0	1.3	6.7	1.2
33	16-Sep-92	-5.5	-22.8	-		800	512	7.0	5.3	2.6	0.6	0.1	1.0	1.1	6.7	1.0
33	15-Oct-92	-5.3	-22.8	-		820	525	7.0	5.2	2.7	0.8	0.1	1.0	1.2	6.7	1.2
34	15-Feb-88	-5.8	-24.6	0.2	11.9 ± 0.6 -9.6	980	627	7.0	6.0	3.2	1.9	0.1	1.2	2.9	7.1	1.1
34	07-Aug-88	-4.8	-25.4	0.0		990	634	7.0	5.8	3.4	1.8	0.1	1.2	2.6	7.2	0.7
34	13-May-90	-5.1	-22.9	0.4		960	605	7.1	5.8	3.4	1.3	0.1	1.2	2.3	7.2	0.5
34	08-Nov-90	-4.9	-22.3	0.0		930	586	7.3	5.7	3.4	1.4	0.1	1.2	2.3	7.0	0.5

34	23-May-91	-5.0	-22.7	0.0					950	608	7.2	5.7	3.3	1.4	0.1	1.1	2.4	7.1	0.4
34	01-Aug-91	-5.3	-22.4	-					940	592	6.9	5.9	3.5	1.4	0.1	1.2	2.4	7.2	0.7
34	15-Oct-92	-5.2	-21.8	-					930	595	7.0	5.4	3.3	1.4	0.1	1.1	2.0	7.2	0.7
35	14-Feb-88	-5.9	-24.4	0.6	35.3 ± 0.7	-13.0			760	486	7.1	4.6	2.7	0.9	0.1	1.1	0.5	6.5	12.9
35	07-Aug-88	-5.1	-27.3	0.0					780	499	7.1	4.7	2.8	0.9	0.1	1.1	0.6	6.4	12.8
35	13-May-90	-5.2	-24.1	0.0					800	504	7.7	4.8	2.9	0.7	0.1	1.2	0.7	6.4	12.5
35	23-May-91	-5.4	-24.5	0.0					780	499	7.3	4.9	2.7	0.8	0.1	1.2	0.7	6.4	13.2
35	01-Aug-91	-5.4	-24.8	-					770	485	7.0	4.8	2.8	0.8	0.1	1.1	0.6	6.5	12.8
35	24-Mar-92	-5.8	-24.8	0.0					800	504	7.1	4.8	2.7	0.8	0.1	1.3	0.5	6.6	13.2
35	16-Sep-92	-5.5	-23.9	-					760	486	7.0	5.0	2.3	0.8	0.1	1.2	0.5	6.5	13.4
36	14-Feb-88	-6.4	-26.0	8.1					750	480	7.6	5.2	1.6	0.9	0.1	1.0	0.3	6.1	15.2
36	07-Aug-88	-5.1	-28.4	5.6					710	454	7.2	4.1	2.3	1.1	0.1	1.2	0.3	5.5	26.0
36	17-May-90	-5.7	-25.7	6.7					720	454	7.3	4.4	2.4	-	-	1.2	0.5	5.6	27.3
36	17-May-90	-5.7	-25.7	6.7					720	454	7.3	4.4	2.4	-	-	1.2	0.5	5.6	27.3
36	08-Apr-91	-6.0	-27.5	6.3					780	499	7.5	4.9	2.1	0.8	0.1	1.1	0.5	6.2	19.0
36	19-Oct-92	-6.2	-26.8	5.2					750	480	7.0	4.6	2.4	0.9	0.1	1.1	0.2	6.1	18.9
36	30-Mar-93			6.9	73.4 ± 1.7	-13.3													
37	19-Jul-89	-5.2	-22.3	0.5					630	403	7.6	3.6	2.2	0.8	0.1	0.9	0.0	5.2	27.0
38	19-Oct-92	-5.8							870	548	7.1	5.1	3.0	1.3	0.0	1.4	0.7	7.2	0.9
38	06-Apr-88	-6.0	-25.6	0.0					999	634	7.0	5.5	3.3	1.8	0.1	1.8	1.5	7.1	4.5
38	30-Mar-93			0.0	11.7 ± 0.7	-12.9													
39	06-Apr-88	-5.6	-22.5	0.0					910	582	7.0	6.1	2.2	1.6	0.1	1.4	1.6	6.8	1.8
39	25-Sep-90	-5.3	-23.7	0.1					960	605	7.0	6.2	2.8	1.5	0.1	1.6	1.7	7.2	0.9
W.A.	02-Dec-92	-5.4	-22.4						810	518	7.1	5.2	2.8	1.0	0.1	1.1	1.1	6.7	2.6

Adasyia Area

NO.	DATE	0 18	D	T.U	C-14	C-13	EC	TDS	pH	Ca	Mg	Na	K	Cl	SO4	HCO3	NO3	SiO2	
		o/oo	o/oo		pmc	o/oo		ppm		meg/1	meg/1	meg/1	meg/1	meg/1	meg/1	meg/1	ppm	ppm	
64	12-Nov-91	-3.4	-16.5	7.9				2640	1690	7.3	7.4	6.4	13.1	0.5	15.7	5.5	5.8	24.3	25.1
64	12-Nov-91	-3.5	-15.9	8.3				2640	1663	7.3	7.4	6.4	13.1	0.5	15.7	5.5	5.8	24.3	25.1
64	12-Nov-91	-3.6		9.1															
65	24-Mar-92	-3.2		10.7				3900	2457	7.2	10.2	16.8	12.4	0.6	28.7	7.4	3.7	2.2	
65	18-Jul-91	-3.5	-16.2	9.0				3500	2240	7.3	9.5	15.7	10.5	0.6	26.3	6.5	3.4	3.9	26.0
66	08-Mar-92	-3.7		5.3				6100	3843	7.7	8.4	28.2	24.8	1.5	53.0	5.7	3.4	2.3	17.5
69	06-Jul-91	-4.7	-23.6	0.0				3600	2304	7.9	1.8	9.2	22.6	1.4	28.7	2.8	3.8	1.2	24.9
70	18-Mar-92	-3.7		2.6				13800	8832	8.3	10.0	4.3	128.0	1.5	141	0.4	0.7	13.2	
A.S	14-Feb-88	-4.8	-22.4	8.3				2040	1326	7.1	5.9	5.2	9.0	0.2	10.0	3.8	6.1	36.2	

North-East Desert Area																		
NO.	DATE	0 18	D	T.U	C-14	C-13	EC	TDS	pH	Ca	Mg	Na	K	Cl	SO4	HCO3	NO3	SiO2
		o/oo	o/oo		pmc	o/oo	ppm	ppm		meq/l	meq/l	meq/l	meq/l	meq/l	meq/l	meq/l	ppm	ppm
50	07-Jun-88	-5.7	-32.4	0.3			1020	653	7.2	3.5	3.3	3.1	0.0	4.5	0.9	4.1	28.4	19.0
51	18-Mar-87	-6.0		0.0			940	602	7.4	2.8	2.7	2.2	0.2	3.6	1.0	4.7	2.7	
51	08-Jun-88	-6.4	-32.4	0.0			950	608	7.3	2.8	2.2	4.2	0.2	3.7	0.7	4.8	0.5	
51	04-Jul-89	-6.4	-32.2	0.0	3.3 ± 0.7	-9.1	970	621	7.4	2.8	2.8	4.2	0.2	3.8	1.0	5.4	0.2	
51	13-Jan-87	-6.2		0.0			950	608	7.4	2.9	2.4	4.0	0.1	3.7	0.4	5.1	1.2	
52	07-Jun-88	-6.0	-35.7	0.2			830	531	7.2	3.1	2.3	3.0	0.1	2.9	0.7	4.8	0.1	
52	15-Jul-91	-5.2	-30.4	0.0			830	531	7.2	3.6	2.0	2.7	0.2	2.8	0.7	4.9	0.3	
52	21-Oct-92	-5.8	-33.6	0.0			840	538	7.3	3.3	2.0	2.8	0.1	2.9	0.6	4.9	0.4	
53	08-Jun-88	-6.1	-30.7	0.3														
53	23-May-90	-6.0	-29.9	2.9			780	491	8.1	1.2	1.8	4.4	0.2	3.4	1.1	2.7	13.6	
53	15-Jul-91	-5.7	-26.8	0.5			810	518	7.8	1.3	1.7	4.3	0.2	3.7	1.0	2.8	14.1	
53	20-Oct-92	-6.0	-29.3	0.0			840	538	8.1	1.1	2.0	4.8	0.2	3.8	1.3	2.9	13.9	
54	07-Jun-88	-6.2	-31.6	1.5			760	486	7.7	1.5	1.9	4.0	0.1	3.0	1.0	3.3	9.6	
54	15-Jul-91	-6.3	-29.9	0.0			750	480	7.7	1.6	1.8	3.6	0.2	2.9	1.1	3.1	10.6	
55	08-Jun-88	-6.1	-30.3	0.0			850	544	8.1	1.1	2.2	4.7	0.1	4.0	1.4	2.4	19.6	
55	17-Jul-91	-6.1	-29.9	0.0			910	582	7.9	1.4	2.3	4.4	0.2	4.3	1.5	2.4	19.9	
56	23-May-90	-6.0	-30.8	0.0			720	454	8.0	1.0	1.8	3.9	0.1	2.8	1.0	2.9	12.9	
57	23-May-90	-5.9	-32.0	0.3			960	605	8.1	3.2	1.5	3.8	0.2	3.3	1.0	5.0	0.0	
58	21-Oct-92	-6.5	-32.6	0.0			770	429	7.6	2.3	2.1	2.1	0.1	2.0	0.8	4.0	0.3	
59	07-Jun-88	-6.1	-34.4	0.0			770	493	7.6	1.7	2.0	3.9	0.1	2.9	1.2	3.5	1.9	
59	15-Jul-91	-6.2	-28.5	0.0			790	506	8.1	2.1	1.9	3.6	0.2	2.9	1.2	3.7	1.9	
59	21-Oct-92	-6.2	-29.9	0.0			780	499	7.8	1.8	2.0	3.7	0.2	2.9	1.1	3.8	1.5	
60	07-Jun-88	-6.5	-29.6	1.1			890	570	7.8	1.3	1.9	5.0	0.1	4.3	1.1	3.0	10.9	
60	23-May-90	-6.1	-30.2	0.7			850	536	8.1	1.4	1.9	5.3	0.2	4.3	1.2	3.0	10.3	
60	15-Jul-91	-6.3	-30.5	0.6			920	589	8.0	1.6	1.9	4.9	0.3	4.3	1.3	3.0	10.7	
61	08-Jun-88	-6.1	-32.2	0.0			890	570	7.9	1.2	2.5	4.7	0.1	4.5	1.3	2.5	19.8	
61	21-Oct-92	-6.1	-31.5	0.0			1020	653	7.8	1.3	3.0	5.1	0.2	5.4	1.4	2.6	20.9	
62	21-Oct-92	-5.9	-31.7	0.0			790	506	8.0	3.0	2.0	2.8	0.1	2.7	0.5	4.7	0.4	

Thermal Water																		
NO.	DATE	0 18	D	T.U	C-14	C-13	EC	TDS	pH	Ca	Mg	Na	K	Cl	SO4	HCO3	NO3	SiO2
		o/oo	o/oo		pmc	o/oo	ppm	ppm		meq/l	meq/l	meq/l	meq/l	meq/l	meq/l	meq/l	ppm	ppm
8	11-Jan-87	-5.7		0.0			1000	640	7.0	5.0	5.0	2.7	2.8	0.2	2.7	2.0	6.0	0.5
8	10-Mar-87	-5.4		1.5			980	627	7.0	5.1	2.5			2.8	1.6	5.9	0.5	
8	05-Jul-87	-5.5	-26.9	1.6			1000	640	7.1	5.3	1.8	2.8	0.2	2.8	1.8	5.5	0.4	

8	09-Feb-88	-7.1	-28.7	1.6		1020	653	7.1	4.7	2.6	3.9	0.2	3.8	1.9	5.6	0.4	31.5	
8	17-Feb-88	-6.4	-29.3	1.3		980	627	7.0	4.3	3.1	3.9	0.1	3.8	2.0	5.6	0.4		
8	19-Jul-89	-6.0	-30.3	1.6		1020	653	7.1	5.0	2.8	2.9	0.2	2.9	2.0	5.9	0.5		
8	20-May-90	-5.8	-29.0	1.4		1050	662	7.2	5.2	2.8			2.8	2.0	5.8	0.5		
8	31-Jul-91	-6.1	-28.3															
8	29-Nov-92	-5.9	-28.0			1020	653	7.1	5.2	2.6	2.7	0.2	3.0	1.6	6.0	0.6	19.9	
9	11-Jan-87	-6.1		0.0		1380	883	7.0	5.8	2.9	5.2	0.0	5.6	2.9	5.5	3.2		
9	10-Mar-87	-5.9		0.0		1370	874	7.1	6.0	2.6			5.4	3.2	5.4	3.9		
9	05-Jul-87	-6.0	-28.9	0.8		1410	902	7.2	5.8	2.5	5.3	0.4	5.5	3.5	5.1	3.5		
9	09-Feb-88	-7.4	-30.7	0.8		1380	883	7.1	5.6	2.7	5.3	0.4	5.7	3.2	5.2	6.2	19.0	
9	17-Feb-88	-6.9	-31.5	0.9		1350	864	7.1	5.6	2.6	5.2	0.4	5.5	3.2	5.2	3.0		
9	19-Jul-89	-6.4	-32.9	1.5		1410	902	7.3	5.9	3.0	5.4	0.4	5.6	3.5	5.5	3.4	33.5	
9	20-May-90	-6.2	-31.7	1.6		1500	945	7.3	6.2	2.8			5.7	3.4	5.6	3.5		
9	31-Jul-91				16.6 ± 0.9	-9.6	1410	902	6.9	6.0	2.9	5.2	0.4	5.7	3.4	5.5	3.4	26.9
9	29-Nov-92	-6.4	-30.9			1410	902	7.4	6.2	2.8	5.4	0.4	5.9	3.4	5.5	3.8	33.5	
10	11-Jan-87	-6.1		1.0		1470	940	7.2	6.0	3.6	5.5	0.3	4.7	4.5	5.9	3.1		
10	21-Mar-87	-6.1		0.4		1410	902	7.2	5.9	3.6			4.9	4.5	5.7	19.0		
10	07-Apr-88	-5.9	-26.7			1500	960	7.0	6.1	3.5	5.7	0.3	5.5	4.5	5.5	3.5	13.6	
10	07-Apr-88	-6.6	-32.3	0.4	22.9 ± 0.6	1500	960	7.0	6.1	3.5	5.7	0.3	5.5	4.5	5.5	3.5		
10	19-Jul-89	-6.6	-32.4	1.5	5.36 ± 0.5	-9.4	1500	960	7.1	6.3	3.8	6.0	0.3	5.8	4.8	5.7	2.7	
10	20-May-90	-6.4	-32.1	0.0		1620	1021	7.4	6.6	3.6			5.7	5.1	5.3	0.6		
10	27-Nov-90	-6.7	-29.5	0.0		1620	1021	7.5	6.7	3.7	6.1	0.5	6.0	5.3	5.4	2.8		
10	23-May-91	-6.4	-32.1	0.0		1590	1018	7.6	6.5	3.6	5.8	0.4	6.6	5.0	4.9	0.3		
10	17-Sep-92	-6.6	-31.9			1560	998	7.1	6.5	3.5	5.8	0.4	6.2	4.5	5.3	1.0		
10	29-Nov-92	-6.8	-33.2			1650	1056	7.1	7.0	3.8	6.9	0.4	6.3	6.1	5.5	0.4	28.9	
11	14-Jan-87	-5.5		2.1		830	531	7.1	4.4	2.5	2.0	0.2	1.6	1.3	6.2	1.0		
11	21-Mar-87	-5.6		0.5		800	512	7.2	4.5	2.4			1.6	1.0	6.2	0.0		
11	20-Jul-89	-5.7	-27.8	1.7	16.8 ± 0.6	-12.9	820	525	7.4	4.9	2.6	1.8	0.1	1.7	1.3	6.2	0.7	
11	20-May-90	-5.7	-27.8	2.1		860	542	7.3	4.7	2.7			1.6	0.9	6.2	0.3		
11	27-Nov-90	-5.8	-26.9	0.3		810	510	7.3	4.6	2.8	1.6	0.1	1.7	1.3	6.2	0.6		
11	23-May-91	-6.1	-27.1	0.6		860	550	7.5	4.6	2.6	1.7	0.1	1.6	1.3	6.1	0.2		
11	17-Sep-92	-5.8	-27.2			830	531	7.0	4.7	2.5	1.7	0.1	1.7	1.0	6.3	0.4		
11	29-Nov-92	-5.9	-27.1			840	538	7.3	4.6	2.7	1.8	0.1	1.8	1.0	6.3	0.6	15.1	
12	23-May-91	-6.1	-27.3	1.1		830	531	7.3	4.4	2.7	1.7	0.1	1.5	1.3	6.0	0.1		
12	31-Jul-91					820	525	7.2	4.3	2.7	1.9	0.1	1.7	1.2	6.0	0.4	14.6	
12	08-Aug-91				18.0 ± 0.9	-11.6	820	517	7.2	4.3	2.7	1.9	0.1	1.7	1.2	6.0	0.4	14.6
12	17-Sep-92	-6.0	-27.4			800	512	7.2	4.4	2.3	1.8	0.1	1.7	0.9	6.0	0.4		
12	29-Nov-92	-5.9	-27.4			820	525	7.4	4.5	2.6	1.8	0.1	1.7	0.9	6.2	2.6	16.4	

13	23-May-91	-6.1	-27.1	0.1	860	550	7.3	4.7	2.6	1.8	0.1	1.7	1.2	6.3	0.0
13	17-Sep-92	-5.7	-27.3		830	531	7.2	4.6	2.6	1.8	0.1	1.8	1.1	6.1	0.4
13	29-Nov-92	-5.8	-27.0		850	544	7.3	4.6	2.7	1.7	0.1	1.7	1.0	6.3	1.7
13	08-Aug-91	-6.0	-27.0		830	531	7.2	4.6	2.6	1.9	0.1	1.8	1.2	6.1	0.2
14	20-Jul-89	-6.1	-27.7	1.1	780	499	7.7	3.9	2.6	2.1	0.1	1.8	1.1	5.5	3.2
14	23-May-91	-5.5	-27.4	0.0	840	538	7.4	4.5	2.7	1.7	0.1	1.6	1.4	6.1	0.2
14	17-Sep-92	-5.8	-27.5		790	506	7.2	4.1	2.4	1.8	0.1	1.6	1.0	5.8	0.4
14	29-Nov-92	-5.7	-26.5		840	538	7.4	4.6	2.7	1.8	0.1	1.7	1.1	6.2	1.4
14	31-Jul-91				820	525	7.2	4.5	2.6	1.8	0.1	1.7	1.1	6.1	0.4
15	14-Jan-87	-5.5		0.0	890	570	7.0	4.3	3.5	2.0	0.2	1.9	0.8	7.2	2.8
15	10-Mar-87	-5.5		0.0	900	576	6.9	4.3	3.5			1.7	1.3	7.1	2.0
15	17-Feb-88	-5.9	-26.6	0.0	870	557	7.0	4.0	3.8	1.9	0.1	1.7	0.9	7.0	3.0
15	19-Jul-89	-5.8	-26.2	0.0	890	570	7.1	4.2	3.9	1.9	0.1	1.7	1.4	7.1	2.5
15	20-May-90	-5.5	-26.1	0.7	930	586	7.1	4.3	3.6			1.6	0.9	7.0	1.8
15	27-Nov-90	-5.7	-24.7	0.9	860	542	7.2	4.4	3.5	1.6	0.1	1.7	1.2	6.7	3.8
15	08-Aug-91	-5.4	-25.2		880	563	7.0	4.1	3.7	1.9	0.1	1.5	1.3	6.7	3.6
15	18-Mar-92	-5.6		0.0	900	576	7.0	4.4	3.5	1.9	0.1	1.8	1.0	7.2	2.7
15	17-Sep-92	-5.5	-25.2		870	557	7.0	4.3	3.5	1.8	0.1	1.7	1.0	6.8	0.8
15	29-Nov-92	-5.6	-25.2		910	582	7.1	4.2	3.8	1.9	0.1	1.8	1.0	7.0	2.7
16	27-Nov-90	-6.1	-29.6	0.3	700	441	7.5	3.4	2.3	1.9	0.1	1.9	0.5	5.3	9.3
16	23-May-91	-6.1	-29.0	0.0	800	512	7.1	3.9	2.2	2.0	0.1	1.8	1.1	5.1	0.7
16	08-Aug-91														
16	17-Sep-92	-6.0	-28.1		770	493	7.2	4.0	2.2	2.0	0.1	1.8	1.1	5.3	0.7
16	29-Nov-92	-6.2	-28.0		790	506	7.4	3.9	2.3	2.1	0.1	1.8	0.6	5.8	2.5
16	31-Jul-91				790	506	6.9	4.0	2.2	2.0	0.2	1.9	0.6	5.6	3.7
17	20-Jul-89	-6.1	-29.3	0.0	730	467	7.5	3.6	2.3	2.0	0.1	1.7	1.0	5.2	3.0
17	20-May-90	-5.5	-26.7	0.7	770	485	7.8	3.6	2.0			1.8	0.8	5.2	1.5
17	23-May-91	-6.2	-28.6	0.0	760	486	7.3	3.7	2.1	1.8	0.1	1.6	1.2	4.9	0.1
17	31-Jul-91				740	474	7.4	3.5	2.2	2.0	0.1	1.6	0.8	5.2	4.0
17	17-Sep-92	-6.1	-28.7		720	461	7.2	3.6	2.0	1.9	0.1	1.6	0.4	5.6	4.6
17	29-Nov-92	-6.2	-28.7		740	474	7.4	3.7	2.2	2.0	0.1	1.5	0.5	5.6	4.5
18	11-Jan-87	-5.3		0.0	1000	640	6.9	3.9	3.8	2.9	0.1	2.7	1.4	6.6	2.3
18	10-Mar-87	-5.3		0.1	990	633	7.0	3.9	3.7			2.7	1.4	6.6	2.1
18	09-Feb-88	-6.9	-25.5	0.6	1020	653	7.3	3.9	3.4	3.2	0.2	2.6	2.1	6.0	0.6
18	14-Feb-88	-6.1	-26.8	0.0	1020	653	6.9	3.9	3.5	3.1	0.1	2.9	1.6	6.3	2.9
18	07-Aug-88	-5.1	-29.4	0.9	1000	640	7.0	4.0	3.7	3.2	0.1	2.8	1.7	6.4	0.9
18	17-May-90	-5.8	-27.4	1.2	1080	680	7.1	4.3	3.6			3.1	1.3	6.6	2.9
18	01-Aug-91	-5.9	-25.6												

